UNIVERSITY OF READING

DEPARTMENT OF MATHEMATICS AND STATISTICS

Instability and Regularization for Data Assimilation

Alexander J. F. Moodey

Thesis submitted for the degree of Doctor of Philosophy

April 2013

Abstract

The process of blending observations and numerical models is called in the environmental sciences community, data assimilation. Data assimilation schemes produce an analysis state, which is the best estimate to the state of the system. Error in the analysis state, which is due to errors in the observations and numerical models, is called the analysis error. In this thesis we formulate an expression for the analysis error as the data assimilation procedure is cycled in time and derive results on the boundedness of the analysis error for a number of different data assimilation schemes. Our work is focused on infinite dimensional dynamical systems where the equation which we solve is ill-posed. We present stability results for diagonal dynamical systems for a three-dimensional variational data assimilation scheme. We show that increasing the assumed uncertainty in the background state, which is an *a priori* estimate to the state of the system, leads to a bounded analysis error. We demonstrate for general linear dynamical systems that if there is uniform dissipation in the model dynamics with respect to the observation operator, then regularization can be used to ensure stability of many cycled data assimilation schemes. Under certain conditions we show that cycled data assimilation schemes that update the background error covariance in a general way remain stable for all time and demonstrate that many of these conditions hold for the Kalman filter. Our results are extended to dynamical system where the model dynamics are nonlinear and the observation operator is linear. Under certain Lipschitz continuous and dissipativity assumptions we demonstrate that the assumed uncertainty in the background state can be increased to ensure stability of cycled data assimilation schemes that update the background error covariance. The results are demonstrated numerically using the two-dimensional Eady model and the Lorenz 1963 model.

Declaration

I confirm that this is my own work and the use of all material from other sources has been properly and fully acknowledged.

Alexander Moodey

Acknowledgements

Firstly, I would like to thank my supervisors Dr. Amos Lawless, Prof. Roland Potthast and Prof. Peter Jan van Leeuwen for all the support they have provided me over the course of this PhD. I appreciate the opportunity they gave me and I am grateful for their enthusiasm, patience and guidance throughout the past three and a half years.

My thanks go to the staff and students of the Department of Mathematics and Statistics, with whom I have had many useful discussions. I particularly acknowledge the members of the Data Assimilation Research Centre (DARC) for their input in this project. I am also grateful to Prof. Nancy Nichols and Prof. Andrew Stuart for useful discussions during this work.

I would like to thank the Engineering and Physical Science Research Council (EPSRC) for the funding I have received. Without this funding I would not have been able to undertake this research.

Finally, I thank my family and friends that have supported me during this project. I thank my parents and girlfriend for always being there and believing in me. I would not have been able to complete this PhD without their love, encouragement and motivation.

Contents

Glossary of symbols

Sets and spaces

$\mathbb{N}$	Set of natural numbers $\{1, 2, \dots\}$
$\mathbb{N}_0$	Set of non-negative integers $\mathbb{N} \cup \{0\}$
$\mathbb{R}$	Set of real numbers
$\mathbb{R}^+$	Set of real positive numbers
$\mathbb{C}$	Set of complex numbers
$\lvert x \rvert$	Absolute value of real or complex numbers x
$\bar{x}$	Complex conjugate of x
$\mathscr{N}(H)$	Nullspace of an operator H
$\mathcal{S}(\mathbf{X})$	Range of an operator H
$L(\mathbf{X}, \mathbf{Y})$	Set of all bounded linear operators from $\mathbf{X}$ into $\mathbf{Y}$
$L(\mathbf{X})$	Set of all bounded linear operators from $\mathbf{X}$ into $\mathbf{X}$

Norms, operator and spectral notation

$\lVert \cdot \rVert_{\ell^2}$	Euclidean norm on a vector space
$\langle \cdot, \cdot \rangle$	Inner/scalar product on a vector space
I	Identity operator
H^*	Adjoint of an operator H
$H^{1/2}$	Square root of an operator H
$\sigma(H)$	Spectrum of an operator H
$r(H)$	Spectral radius of an operator H
$\kappa(H)$	Condition number of an operator H
λ	Eigenvalue
μ	Singular value

Data assimilation notation

$\mathbf{X}$	State space
$\mathbf{Y}$	Measurement or observation space
$\mathbf{x}$	State element
$\mathbf{x}^{(a)}$	Analysis element
$\mathbf{x}^{(b)}$	Background element
$\mathbf{y}$	Observation element
H	Linear observation operator
M	Linear model operator
$\mathcal{M}$	Nonlinear model operator
B	Background error covariance operator
R	Observation error covariance operator
$\mathscr{Q}$	Model error covariance operator
$\mathscr{K}$	Kalman gain operator
$\mathscr{R}$	Tikhonov-Phillips inverse
α	Regularization parameter
N	Reconstruction error operator
$\boldsymbol{\zeta}$	Model error
$\boldsymbol{\eta}$	Observation error
$\boldsymbol{\omega}$	Observation operator error
t	Time
$\mathbf{e}$	Analysis error

Miscellaneous

$\in$	Element inclusion
$\subset$	Set inclusion
$\circ$	Composition of mappings
$\oplus$	Direct sum
$\mathcal{O}(n)$	A quantity of order n

Chapter 1

Introduction

Making use of noisy observations and imperfect models to infer the state of a system is applicable to a wide range of scientific disciplines. The environmental sciences community call the incorporation of observational data into numerical models to produce the best estimate to the state of the system, *data assimilation*. Data assimilation methods make use of a background state, which is an *a priori* estimate to the state of the system. Techniques in data assimilation take account of the uncertainty in the initial conditions, physical model dynamics and observations by statistically weighting the influence of the prior estimate, dynamical model and the observations. The technique of data assimilation is widely used in many fields of science, such as numerical weather prediction (NWP), hydrology, oceanography, geophysics, image processing, chemistry and oil reservoir modelling. Many challenges arise from blending observational data with mathematical models in these scientific fields. The physical processes in each of these areas are governed usually by highly complex and nonlinear dynamical models which often employ a large number of unknown system parameters. Another significant challenge is that these dynamical systems work in spaces of very high dimension, for example in NWP the dimension of the state space currently ranges between orders $\mathcal{O}(10^8 - 10^9)$. The number of observations is currently between orders $\mathcal{O}(10^6 - 10^8)$ and they are often incomplete and always contain errors. In NWP the dimension of the state space is expected to increase as the dynamical models grow in complexity as they resolve physical processes on finer and finer scales. Also the number of observations is expected to increase as the atmospheric community improves its ability to observe the atmosphere.

Since data assimilation methods deal with such high dimension, it is natural to extend the analysis on the behaviour of data assimilation schemes into infinite dimensions to capture the key features of large-scale systems. Using an infinite dimensional approach, one is able to work within a framework that is best suited to analyse directly challenges that exist in high-dimensional data assimilation methods, such as ill-posedness. Hadamard [31] postulated that a mathematical problem is ill-posed if a solution does not exist, is not unique and/or does not depend continuously on the observational data. In practice, the data assimilation problem is an ill-posed problem, therefore errors in the observational data means that the errors can be amplified in the *analysis state*, which is the best estimate to the state of the system. This error in the analysis state which can be amplified, is called the *analysis error*.

1.1 Aims of the thesis

The task of this thesis is to investigate the instability of current data assimilation methods using tools from regularization theory and the theory of ill-posed problems. In particular, we study various variational and sequential data assimilation methods for a hierarchy of linear and nonlinear dynamical systems with the task to derive general results on the behaviour of the analysis error. Specifically, we aim to:

1. derive a general expression for the analysis error in cycled data assimilation, taking errors in model dynamics, observations, observation operators and cumulated errors from the previous assimilation cycle into account;

2. investigate using the regularization parameter to stabilise a class of cycled data assimilation schemes that employ static error covariances for a number of diagonal dynamical systems such as constant model dynamics, diagonal model dynamics with respect to the singular system of the observation operator and an observation operator that is diagonal with respect to the eigensystem of the model dynamics;

3. derive theoretical bounds on the behaviour of the analysis error for different classes of linear dynamical systems where the data assimilation scheme employs static error covariances, a multiplicative update to the background error covariance and a general update to the background error covariance;

4. develop results on the boundedness of the analysis error for a class of nonlinear dynamical systems, where the model dynamics are nonlinear and the observation operator is linear;

5. demonstrate the theoretical results using a variety of numerical experiments.

1.2 Outline of the thesis

This thesis is structured as follows.

In Chapter 2 we introduce tools from functional analysis which we require to carry out the analysis for the later chapters in this thesis. We introduce many definitions and results for linear operators on Hilbert spaces with infinite dimensional generalisations of well known finite dimensional results. We discuss how an operator equation is ill-posed. Finally, we introduce one classical regularization technique from the theory of inverse problems known as *Tikhonov-Phillips regularization*, which provides a well-posed solution.

In Chapter 3 we discuss two classes of data assimilation methods. Firstly, we present variational data assimilation, which is widely used operationally in many NWP centres around the world. Specifically we introduce two variational methods, three-dimensional variational data assimilation and four-dimensional variational data assimilation. Secondly, we introduce sequential data assimilation and present arguably the most famous method from filtering theory, the Kalman filter. We interpret these methods as a form of Tikhonov-Phillips regularization from the theory of inverse problems. This interpretation will guide us through the rest of this thesis.

In Chapter 4 we formulate our *linear analysis error evolution equation* which identifies terms arising from errors in the model equations, observational data, observation operator and cumulated errors from cycling the data assimilation scheme over time. We relate this form of the analysis error to the literature and discuss the state-of-the-art stability results for finite and infinite dimensional linear and nonlinear dynamical systems.

In Chapter 5 we introduce two dynamical models that will be used to test the developed theory. Firstly, we present the two-dimensional Eady model which is one of the simplest models of atmospheric instability. Secondly we present the Lorenz 1963 model, which is a

three dimensional system of ordinary differential equations that can exhibit chaotic behaviour. For the Lorenz 1963 model we introduce its deterministic and its stochastic form.

In Chapter 6 we present our first theoretical results on the *stability of data assimilation schemes*. Here we show that if the model dynamics are constant for all time then our stability result will only hold when the dimension of the state space and observation space is finite. We investigate the analysis error for two diagonal dynamical systems, where firstly the model dynamics are diagonal with respect to the observation operator and secondly the reverse case, where the observation operator is diagonal with respect to the model dynamics. We show that using the regularization parameter we can achieve a stable cycled data assimilation scheme that employs static error covariances. We present a numerical experiment for each of the diagonal cases to illustrate the behaviour of the analysis error. We observe that the regularization parameter must be chosen sufficiently small to keep the analysis error controlled in each step. However, we show that if the observation operator is ill-conditioned and the observations are noisy then the analysis error will become large again if the regularization parameter is chosen too small.

In Chapter 7 we derive new theoretical results for linear time-invariant dynamical systems that show the stability of cycled data assimilation schemes. We show that we can split the state space so that there is a contraction in the error dynamics leading to a stable cycled data assimilation scheme that employs static error covariances. We extend this result to the case of time-varying linear model dynamics for data assimilation schemes that employ a multiplicative update to the background error covariance. Finally, we show that a cycled data assimilation scheme that updates the background error covariance in a general way remains stable for all time. This result is under a number of assumptions and we demonstrate that many of these assumptions hold for the Kalman filter. We show that if we can artificially inflate the background error covariance for the Kalman filter then we can show asymptotic stability in the infinite dimensional setting. We illustrate our stability results using a cycled four-dimensional variational data assimilation scheme with a dynamical system comprised of the two-dimensional Eady model and a general observation operator.

In Chapter 8 we extend the linear results developed in Chapter 7 to the case where the dynamical model is *nonlinear*. We show that if the nonlinear model dynamics are Lipschitz continuous and dissipative on higher spectral modes of the linear time-invariant observation

operator then we can obtain a sufficient stability condition. We provide new theoretical bounds on the behaviour of the analysis error for data assimilation schemes that employ static error covariances, a multiplicative update to the background error covariance and a general update to the background error covariance. We illustrate the theoretical results with a numerical experiment for both the deterministic and the stochastic Lorenz 1963 equations using a cycled three-dimensional variational data assimilation scheme.

In Chapter 9 we summarise the work in this thesis. We present the main conclusions and discuss open questions in this field of research. We finish by providing suggestions on further work that could be done in this area.

Chapter 2

Operator and spectral theory

In this chapter we introduce key results from functional analysis, that will give us the necessary tools to carry out our analysis of data assimilation schemes. The aim of this chapter is to build the foundation for the research presented in future chapters. The majority of our analysis developed in future chapters will take place in a Hilbert space setting which we shall discuss. We then move onto the spectral representation of elements in a Hilbert space. Next we introduce compact operators with a discussion on their relevance to the data assimilation setting, and introduce linear projections onto a Hilbert space. Finally, this leads us to the concept of a well-posed problem, which can be guaranteed using the technique of Tikhonov-Phillips regularization.

2.1 Functional analysis

In this section we present important basic results and terminology from the field of functional analysis. We begin introducing terminology which will be used throughout this thesis.

2.1.1 Linear algebra

The following definition is taken from [46, p.9].

Definition 2.1.1. An inner product space is a pair $(\mathbf{X}, \langle \cdot, \cdot \rangle)$ consisting of a complex (or real) vector space, $\mathbf{X}$, and a function, $\langle \cdot, \cdot \rangle : \mathbf{X} \times \mathbf{X} \to \mathbb{C}$ (or $\mathbb{R}$), with the following four properties,

- positivity, $\langle \mathbf{x}, \mathbf{x} \rangle \geq 0$,
- definiteness, $\langle \mathbf{x}, \mathbf{x} \rangle = 0$ if and only if $\mathbf{x} = 0$,
- symmetry, $\langle \mathbf{x}^{(1)}, \mathbf{x}^{(2)} \rangle = \overline{\langle \mathbf{x}^{(2)}, \mathbf{x}^{(1)} \rangle}$,
- linearity, $\langle a\mathbf{x}^{(1)} + b\mathbf{x}^{(2)}, \mathbf{x}^{(3)} \rangle = a\langle \mathbf{x}^{(1)}, \mathbf{x}^{(3)} \rangle + b\langle \mathbf{x}^{(2)}, \mathbf{x}^{(3)} \rangle$,

for all $\mathbf{x}, \mathbf{x}^{(1)}, \mathbf{x}^{(2)}, \mathbf{x}^{(3)} \in \mathbf{X}$ and $a, b \in \mathbb{C}$ (or $\mathbb{R}$).

Now we are able to introduce a Hilbert space, which is of great importance to this work and its definition is taken from [46, p.10].

Definition 2.1.2. An inner product space, which is complete with respect to the norm

$$\|\mathbf{x}\| := \langle \mathbf{x}, \mathbf{x} \rangle^{1/2}, \tag{2.1}$$

for all $\mathbf{x} \in \mathbf{X}$, is called a Hilbert space.

We remark that a definition of *complete* can be found in [46, Definition 1.12]. Given two Hilbert spaces $\mathbf{X}$ and $\mathbf{Y}$, we denote a mapping from $\mathbf{X}$ into $\mathbf{Y}$ by, $H : \mathbf{X} \to \mathbf{Y}$. The space $\mathbf{X}$ is known as the domain of H. In this work we refer to $\mathbf{X}$ as the state space. The space $\mathbf{Y}$ is known as the codomain which we call the measurement or observation space.

Here we shall summarise terminology which will be used throughout this thesis and present the operator equation which we are interested in solving. We first remark that in this work we will only consider real Hilbert spaces. The following definition is taken from [46, p.1].

Definition 2.1.3. Let H be an operator mapping a Hilbert space $\mathbf{X}$ into a Hilbert space $\mathbf{Y}$. The nullspace of H is the subspace

$$\mathscr{N}(H) := \{\mathbf{x} \in \mathbf{X} : H\mathbf{x} = \mathbf{0}\}. \tag{2.2}$$

The range of H is the subspace

$$\mathcal{S}(\mathbf{X}) := \{H\mathbf{x} : \mathbf{x} \in \mathbf{X}\}. \tag{2.3}$$

The rank of H is the number

$$rk(H) = dim(\mathcal{S}(\mathbf{X})), \tag{2.4}$$

where *dim* denotes the dimension of a Hilbert space. The dimension of a Hilbert space $\mathbf{X}$ is the largest number of linearly independent vectors in the space. Given an operator equation

$$H\mathbf{x} = \mathbf{y}, \tag{2.5}$$

the operator H

- is injective if for any $\mathbf{y} \in \mathcal{S}(\mathbf{X})$ there is a unique element $\mathbf{x} \in \mathbf{X}$ such that (2.5) holds.
- is surjective if the codomain is equal to the range of the operator H.
- is bijective if it is injective and is surjective, that is if the inverse mapping $H^{-1} : \mathbf{Y} \to \mathbf{X}$ exists.

A useful property is the Cauchy-Schwarz inequality which we will use in our work.

Proposition 2.1.4 (Cauchy-Schwarz)**.** *Let* $\mathbf{X}$ *be a Hilbert space. Then*

$$\left|\left\langle \mathbf{x}^{(1)}, \mathbf{x}^{(2)} \right\rangle\right| \leq \left\|\mathbf{x}^{(1)}\right\| \cdot \left\|\mathbf{x}^{(2)}\right\| \tag{2.6}$$

for all $\mathbf{x}^{(1)}, \mathbf{x}^{(2)} \in \mathbf{X}$.

Proof. See Proposition 3.5 [22]. □

The following two definitions are taken from [46, p.10].

Definition 2.1.5. Given a Hilbert space $\mathbf{X}$, two elements $\mathbf{x}^{(1)}, \mathbf{x}^{(2)} \in \mathbf{X}$ are called orthogonal if

$$\left\langle \mathbf{x}^{(1)}, \mathbf{x}^{(2)} \right\rangle = 0. \tag{2.7}$$

Two subsets $\mathbf{X}^{(1)}$ and $\mathbf{X}^{(2)}$ of $\mathbf{X}$ are called orthogonal if each pair of elements $\mathbf{x}^{(1)} \in \mathbf{X}^{(1)}$ and $\mathbf{x}^{(2)} \in \mathbf{X}^{(2)}$ are orthogonal. A subset $\mathbf{X}^{(1)}$ of $\mathbf{X}$ is called an orthogonal system if $\langle \mathbf{x}^{(1)}, \mathbf{x}^{(2)} \rangle = 0$ for all $\mathbf{x}^{(1)}, \mathbf{x}^{(2)} \in \mathbf{X}^{(1)}$ with $\mathbf{x}^{(1)} \neq \mathbf{x}^{(2)}$.

Definition 2.1.6. An orthogonal system $\mathbf{X}^{(1)}$ is called an orthonormal system if $\|\mathbf{x}^{(1)}\| = 1$ for all $\mathbf{x}^{(1)} \in \mathbf{X}^{(1)}$. A *complete* orthonormal system is an orthonormal system such that there are enough elements in the system to span the space.

In the Hilbert space setting, orthogonality leads to the Fourier series and Parseval's equality, which we require for our analysis in future chapters.

Theorem 2.1.7. *Let $\{\boldsymbol{\varphi}_n : n \in \mathbb{N}\}$ be an orthonormal system in a Hilbert space $\mathbf{X}$. Then the following properties are equivalent,*

- *each $\mathbf{x} \in \mathbf{X}$ can be expanded in a Fourier series*
$$\mathbf{x} = \sum_{n=1}^{\infty} \langle \mathbf{x}, \boldsymbol{\varphi}_n \rangle \, \boldsymbol{\varphi}_n. \tag{2.8}$$
- *for each $\mathbf{x} \in \mathbf{X}$ we have Parseval's equality*
$$\|\mathbf{x}\|^2 = \sum_{n=1}^{\infty} |\langle \mathbf{x}, \boldsymbol{\varphi}_n \rangle|^2 . \tag{2.9}$$
- *$\mathbf{x} = \mathbf{0}$ is the only element in $\mathbf{X}$ with $\langle \mathbf{x}, \boldsymbol{\varphi}_n \rangle = 0$ for all $n \in \mathbb{N}$.*

Proof. See Theorem 1.28 [46]. □

Theorem 2.1.8 (Pythagorean/Parseval)**.** *Let $\{\boldsymbol{\varphi}_j : j \in \mathbb{N}\}$ be an orthogonal system in an inner product space $\mathbf{X}$, then*
$$\left\| \sum_{j=1}^{\infty} \boldsymbol{\varphi}_j \right\|^2 = \sum_{j=1}^{\infty} \left\| \boldsymbol{\varphi}_j \right\|^2 . \tag{2.10}$$
When the system $\{\boldsymbol{\varphi}_j\}$ is finite (2.10) degenerates to a finite sum, and is known as the Pythagorean theorem. The infinite dimensional form is an equivalent form of (2.9).

Proof. For a finite system $\{\boldsymbol{\varphi}_i\}$ see Proposition 3.10 in [22]. For an infinite system $\{\boldsymbol{\varphi}_i\}$ we begin with (2.9), normalising the orthogonal system
$$\|\mathbf{x}\|^2 = \sum_{i=1}^{\infty} \left| \left\langle \mathbf{x}, \frac{\boldsymbol{\varphi}_i}{\|\boldsymbol{\varphi}_i\|} \right\rangle \right|^2 = \sum_{i=1}^{\infty} \frac{|\langle \mathbf{x}, \boldsymbol{\varphi}_i \rangle|^2}{\|\boldsymbol{\varphi}_i\|^2}. \tag{2.11}$$
Now letting $\mathbf{x}$ be the orthogonal sum $\sum_{j=1}^{\infty} \boldsymbol{\varphi}_j$, we obtain
$$\left\| \sum_{j=1}^{\infty} \boldsymbol{\varphi}_j \right\|^2 = \sum_{i=1}^{\infty} \frac{\left| \left\langle \sum_{j=1}^{\infty} \boldsymbol{\varphi}_j, \boldsymbol{\varphi}_i \right\rangle \right|^2}{\|\boldsymbol{\varphi}_i\|^2} \tag{2.12}$$
$$= \sum_{i=1}^{\infty} \frac{\langle \boldsymbol{\varphi}_i, \boldsymbol{\varphi}_i \rangle^2}{\|\boldsymbol{\varphi}_i\|^2} \tag{2.13}$$
$$= \sum_{i=1}^{\infty} \|\boldsymbol{\varphi}_i\|^2 , \tag{2.14}$$
using the property of orthogonality in (2.7). We complete the proof by substituting the index i in (2.14) with j and obtain (2.10). □

Having introduced fundamental properties in a Hilbert space framework, which our analysis will use, we are now able to consider bounded linear operators.

2.1.2 Bounded linear operators

With the following definition taken from [46, p.15], we distinguish between linear and non-linear operators.

Definition 2.1.9. An operator $H : \mathbf{X} \to \mathbf{Y}$ mapping a space $\mathbf{X}$ into a space $\mathbf{Y}$ is called linear if

$$H\left(a\mathbf{x}^{(1)} + b\mathbf{x}^{(2)}\right) = aH\left(\mathbf{x}^{(1)}\right) + bH\left(\mathbf{x}^{(2)}\right) \tag{2.15}$$

for all $\mathbf{x}^{(1)}, \mathbf{x}^{(2)} \in \mathbf{X}$ and all $a, b \in \mathbb{R}$.

Here we introduce bounded linear operators, which leads us to the definition of operator norms.

Definition 2.1.10. A linear operator $H : \mathbf{X} \to \mathbf{Y}$ from a Hilbert space $\mathbf{X}$ into a Hilbert space $\mathbf{Y}$ is called bounded if there is a positive number C such that

$$\|H\mathbf{x}\| \leq C\|\mathbf{x}\| \tag{2.16}$$

for all $\mathbf{x} \in \mathbf{X}$.

Definition 2.1.10 is taken from [46, p.16]. The constant C in Definition 2.1.10 represents a bound on the operator H. The smallest constant C is known as the operator norm, which we will formally present next. Before considering the operator norm, we first introduce important notation.

Notation 2.1.11. Let $\mathbf{X}$ and $\mathbf{Y}$ be Hilbert spaces. We will denote the set of all bounded linear operators from $\mathbf{X}$ into $\mathbf{Y}$ by $L(\mathbf{X}, \mathbf{Y})$, and denote the set $L(\mathbf{X}, \mathbf{X})$ of all bounded linear operators from $\mathbf{X}$ into $\mathbf{X}$ by $L(\mathbf{X})$.

It is well known that properties of boundedness and continuity are equivalent for linear operators $H : \mathbf{X} \to \mathbf{Y}$ from a Hilbert space $\mathbf{X}$ into a Hilbert space $\mathbf{Y}$; see [73, Lemma 4.1] for further details. Therefore, we can use the words bounded and continuous interchangeably for linear operators. The following definition is taken from [73, p.98].

Definition 2.1.12. Let $\mathbf{X}$ and $\mathbf{Y}$ be Hilbert spaces and let $H \in L(\mathbf{X}, \mathbf{Y})$. The operator norm of H is defined as

$$\|H\| := \sup\{\|H\mathbf{x}\| : \mathbf{x} \in \mathbf{X}, \|\mathbf{x}\| \leq 1\}. \tag{2.17}$$

Operator norms are important, since they bring the idea of size to linear operators. In the following chapters, we will make extensive use of the operator norm in our estimates of the stability of particular data assimilation schemes. Operator norms are a generalisation of matrix norms from the finite dimensional setting; see [28] for further details. The adjoint operator applies further structure to a Hilbert space and gives us a different concept of invertibility.

Theorem 2.1.13. *Let* $\mathbf{X}$ *and* $\mathbf{Y}$ *be Hilbert spaces and let* $H \in L(\mathbf{X}, \mathbf{Y})$ *be a bounded linear operator. Then there exists a unique linear operator* $H^* \in L(\mathbf{Y}, \mathbf{X})$ *such that*

$$\langle H\mathbf{x}, \mathbf{y} \rangle = \langle \mathbf{x}, H^*\mathbf{y} \rangle \tag{2.18}$$

for all $\mathbf{x} \in \mathbf{X}$ *and* $\mathbf{y} \in \mathbf{Y}$*. We call the operator* H^* *the adjoint of the operator* H *where* $\|H^*\| = \|H\|$*.*

Proof. See Theorem 4.9 [46]. □

In the real finite dimensional case the adjoint operator is equivalent to the matrix transpose for a Euclidean inner product; see [28] for further details on the matrix transpose. Self-adjoint operators are useful and we explore their properties in Section 2.2. The following definition is taken from [46, p.272].

Definition 2.1.14. Let $\mathbf{X}$ be a Hilbert space and $H \in L(\mathbf{X})$. H is called self-adjoint if $H = H^*$ such that

$$\left\langle H\mathbf{x}^{(1)}, \mathbf{x}^{(2)} \right\rangle = \left\langle \mathbf{x}^{(1)}, H\mathbf{x}^{(2)} \right\rangle \tag{2.19}$$

for all $\mathbf{x}^{(1)}, \mathbf{x}^{(2)} \in \mathbf{X}$.

Self-adjoint operators generalise Hermitian matrices from the finite dimensional setting; see [28] for further details on Hermitian matrices. Before introducing the inverse operator, it is necessary to define operator products and necessary notation. The following definition is taken from [73, p.106].

Definition 2.1.15. Let $\mathbf{X}$ and $\mathbf{Y}$ be Hilbert spaces and $M \in L(\mathbf{X})$ and $H \in L(\mathbf{X}, \mathbf{Y})$. The composition $H \circ M$ of H and M will be denoted HM, and called the product of H and M.

Notation 2.1.16. Let $\mathbf{X}$ be a Hilbert space and let $M \in L(\mathbf{X})$. The product of M with itself n times will be denoted by M^n.

The following definition is taken from [73, p.109].

Definition 2.1.17. Let $\mathbf{X}$ and $\mathbf{Y}$ be Hilbert spaces. An operator $H \in L(\mathbf{X}, \mathbf{Y})$ is said to be invertible if there exists $J \in L(\mathbf{Y}, \mathbf{X})$, such that $JH = I_{\mathbf{X}}$, $HJ = I_{\mathbf{Y}}$, where $I_{\mathbf{X}}$ and $I_{\mathbf{Y}}$ are the identity operators in the respective spaces. It is conventional to denote the inverse $J \in L(\mathbf{Y}, \mathbf{X})$ by H^{-1}.

Here we have introduced the inverse operator, which will be used to solve (2.5). However, as we will see in Section 2.3, it is not possible in general to simply apply the inverse operator to (2.5).

We now introduce the condition number. The condition number is a key measure in numerical analysis that determines the sensitivity of the solution of an operator equation to errors in the data. We will discuss the condition number further in Section 2.3 and in future chapters in numerical experiments. The following definition is taken from [46, p.248].

Definition 2.1.18. Let $\mathbf{X}$ and $\mathbf{Y}$ be Hilbert spaces and let $H \in L(\mathbf{X}, \mathbf{Y})$ with a bounded inverse $H^{-1} \in L(\mathbf{Y}, \mathbf{X})$. Then

$$\kappa(H) := \|H\| \cdot \left\|H^{-1}\right\| \tag{2.20}$$

is called the condition number of H.

In future chapters, we will make use of the following results.

Lemma 2.1.19. *If $\mathbf{X}, \mathbf{Y}$ and $\mathbf{Z}$ are Hilbert spaces and $H^{(1)} \in L(\mathbf{X}, \mathbf{Y})$, $H^{(2)} \in L(\mathbf{Y}, \mathbf{Z})$ are invertible, then $H^{(2)}H^{(1)}$ is invertible with inverse $H^{(1)-1}H^{(2)-1}$.*

Proof. See Lemma 4.35 [73]. □

Lemma 2.1.20. *Let $\mathbf{X}$ and $\mathbf{Y}$ be Hilbert spaces.*

(a) *If $M, N \in L(\mathbf{X})$ then $M + N \in L(\mathbf{X})$ and*

$$\|M + N\| \leq \|M\| + \|N\| . \tag{2.21}$$

(b) *If* $c \in \mathbb{R}$ *and* $M \in L(\mathbf{X})$ *then* $cM \in L(\mathbf{X})$ *and*

$$\|cM\| = |c| \cdot \|M\| . \tag{2.22}$$

(c) *If* $H \in L(\mathbf{X}, \mathbf{Y})$ *and* $M \in L(\mathbf{X})$ *then* $HM \in L(\mathbf{X}, \mathbf{Y})$ *and*

$$\|HM\| \leq \|H\| \cdot \|M\| . \tag{2.23}$$

Proof. See Proposition 1.2 [14]. □

The following definition is taken from [27, p.49].

Definition 2.1.21. A sequence (a_n) is bounded if there exists numbers $m_{(1)}, m_{(2)} \in \mathbb{R}$ such that $m_{(1)} \leq a_n \leq m_{(2)}$ for all n.

We finish this section with a key property in operator theory, which is taken from [73, p.205].

Definition 2.1.22. Let $\mathbf{X}$ and $\mathbf{Y}$ be Hilbert space. An operator $H \in L(\mathbf{X}, \mathbf{Y})$ is compact if, for any bounded sequence $(\mathbf{x}_n)$ in $\mathbf{X}$, the sequence $(H\mathbf{x}_n)$ in $\mathbf{Y}$ contains a convergent subsequence.

Compact operators arise when solving operator equations. Here we now introduce the Hilbert-Schmidt operator, which we will use in subsequent chapters for our norm estimates.

2.1.3 Hilbert-Schmidt operator

One class of compact operators which has an interesting property is the Hilbert-Schmidt operator. The following definition is taken from [85, p.326].

Definition 2.1.23. Let $M \in L(\mathbf{X})$ be a linear operator on a Hilbert space $\mathbf{X}$ and $\{\boldsymbol{\varphi}_i : i \in \mathbb{N}\}$, $\{\boldsymbol{\psi}_j : j \in \mathbb{N}\}$ a pair of complete orthonormal systems. M is called a Hilbert-Schmidt operator if the following norm is finite,

$$\|M\|^2 = \sum_{i=1}^{\infty} \|M\boldsymbol{\varphi}_i\|^2 = \sum_{i=1}^{\infty} \sum_{j=1}^{\infty} \left|\langle M\boldsymbol{\varphi}_i, \boldsymbol{\psi}_j \rangle\right|^2 . \tag{2.24}$$

The interesting property of the Hilbert-Schmidt operator is that its definition is independent of the choice of orthonormal system. This is reflected in the following theorem, which we will use in subsequent chapters.

Theorem 2.1.24. *Let* $\mathbf{X}$ *be a Hilbert space and let* $\{\boldsymbol{\varphi}_i^{(1)} : i \in \mathbb{N}\}$ *and* $\{\boldsymbol{\varphi}_i^{(2)} : i \in \mathbb{N}\}$ *be complete orthonormal systems for* $\mathbf{X}$*. Then for a Hilbert-Schmidt operator* $M \in L(\mathbf{X})$*,*

$$\sum_{i=1}^{\infty} \left\| M\boldsymbol{\varphi}_i^{(1)} \right\|^2 = \sum_{i=1}^{\infty} \left\| M\boldsymbol{\varphi}_i^{(2)} \right\|^2. \tag{2.25}$$

Hence the norm of the Hilbert-Schmidt operator is independent of the orthonormal system.

Proof. See Theorem 7.16 [73]. □

We next consider projection operators, which will be useful in our analysis.

2.1.4 Projections

We now introduce projection operators. These are important since we will project elements onto particular subspaces in our work. In order to introduce the subsequent projection result, we require the definitions of complementary subspaces and projection operators. The following two definitions are taken from [73, p.155].

Definition 2.1.25. Let $\mathbf{X}$ be a Hilbert space. Then two subspaces $\mathbf{X}^{(1)}, \mathbf{X}^{(2)} \subset \mathbf{X}$ are called complementary if $\mathbf{X} = \mathbf{X}^{(1)} \oplus \mathbf{X}^{(2)}$, such that if for any $\mathbf{x} \in \mathbf{X}$ there is a unique decomposition of the form

$$\mathbf{x} = \mathbf{x}^{(1)} + \mathbf{x}^{(2)}, \tag{2.26}$$

where $\mathbf{x}^{(1)} \in \mathbf{X}^{(1)}$ and $\mathbf{x}^{(2)} \in \mathbf{X}^{(2)}$.

Definition 2.1.26. Let $\mathbf{X}$ be a Hilbert space. A projection on $\mathbf{X}$ is a linear operator $P \in L(\mathbf{X})$ such that $P^2 = P$.

Now we are able to present the following result, which we will require to decompose our state space in future chapters.

Lemma 2.1.27. *Suppose* $\mathbf{X}^{(1)}, \mathbf{X}^{(2)}$ *are complementary subspaces in a Hilbert space* $\mathbf{X}$ *and let* $P_1 : \mathbf{X} \to \mathbf{X}^{(1)}$*,* $P_2 : \mathbf{X} \to \mathbf{X}^{(2)}$ *be linear operators, such that*

$$P_1\mathbf{x} = \mathbf{x}^{(1)}, \quad P_2\mathbf{x} = \mathbf{x}^{(2)}, \tag{2.27}$$

for $\mathbf{x} \in \mathbf{X}$*, where* $\mathbf{x}^{(1)}$ *and* $\mathbf{x}^{(2)}$ *satisfy (2.26). Then* P_1 *and* P_2 *are projections on* $\mathbf{X}$ *and* $P_1 + P_2 = I$*.*

Proof. See Lemma 5.61 [73]. □

In our work we will be concerned with *orthogonal projection operators* and their definition is taken from [73, p.194].

Definition 2.1.28. Let $\mathbf{X}$ be a Hilbert space. An orthogonal projection on $\mathbf{X}$ is an operator $P \in L(\mathbf{X})$ such that

$$P = P^* = P^2. \tag{2.28}$$

The following result demonstrates the representation of orthogonal projection operators.

Corollary 2.1.29. *If* $\mathbf{X}$ *is a Hilbert space,* $\mathbf{X}^{(1)}$ *is a closed linear subspace of* $\mathbf{X}$*,* $\{\boldsymbol{\varphi}_1, \ldots, \boldsymbol{\varphi}_n\}$ *is a complete orthonormal system for* $\mathbf{X}^{(1)}$*, where* n *is a positive integer or* ∞*, and* P *is the orthogonal projection of* $\mathbf{X}$ *onto* $\mathbf{X}^{(1)}$*, then*

$$P\mathbf{x} = \sum_{i=1}^{n} \langle \mathbf{x}, \boldsymbol{\varphi}_i \rangle \, \boldsymbol{\varphi}_i. \tag{2.29}$$

Proof. See Lemma 6.53 [73]. □

Positive and *strictly positive* operators in a Hilbert space have useful properties, some of which we will require in this work. The following definition is taken from [17, p.69]

Definition 2.1.30. Let $\mathbf{X}$ be a Hilbert space. A positive operator is a self-adjoint operator $H \in L(\mathbf{X})$ such that

$$\langle H\mathbf{x}, \mathbf{x} \rangle \geq 0 \tag{2.30}$$

for all $\mathbf{x} \in \mathbf{X}$. A positive operator is called strictly positive if

$$\langle H\mathbf{x}, \mathbf{x} \rangle = 0 \tag{2.31}$$

only if $\mathbf{x} = \mathbf{0}$. We call a sequence of self-adjoint operators $H_k \in L(\mathbf{X})$ *uniformly strictly positive* if there exists a constant $a > 0$, such that

$$\langle H_k\mathbf{x}, \mathbf{x} \rangle \geq a\|\mathbf{x}\|^2 \tag{2.32}$$

for all $\mathbf{x} \in \mathbf{X}$ and $k \in \mathbb{N}$.

Lemma 2.1.31. *Let* $\mathbf{X}$ *be a Hilbert space. If* $H \in L(\mathbf{X})$ *is a positive operator then there exists a positive constant* $a > 0$ *and a constant* $b \geq 0$*, such that*

$$a\|\mathbf{x}\|^2 \geq \langle H\mathbf{x}, \mathbf{x}\rangle \geq b\|\mathbf{x}\|^2 \tag{2.33}$$

for all $\mathbf{x} \in \mathbf{X}$*. If* H *is strictly positive then* $b > 0$ *and in this case* H *has a bounded inverse* H^{-1}*, such that*

$$\frac{1}{b}\|\mathbf{x}\|^2 \geq \left\langle H^{-1}\mathbf{x}, \mathbf{x}\right\rangle \geq \frac{1}{a}\|\mathbf{x}\|^2 \tag{2.34}$$

for all $\mathbf{x} \in \mathbf{X}$*.*

Proof. See [17, p.70]. □

In the following chapters we will require the square root of an operator.

Theorem 2.1.32. *Let* $\mathbf{X}$ *be a Hilbert space and let* $H \in L(\mathbf{X})$ *be a positive operator. Then there exists a unique positive square root* $H^{1/2} \in L(\mathbf{X})$*, such that*

$$H^{1/2}H^{1/2} = H. \tag{2.35}$$

Proof. See Theorem 23.2 [3]. □

We now explore spectral theory for compact operators, which is important since we will analyse in Chapter 6 the data assimilation schemes in Chapter 3 spectrally.

2.2 Spectral theory

In this section, we introduce important results on the underlying structure of operators acting on Hilbert spaces. We first introduce the spectrum and the spectral radius of a bounded linear operator. Here we also consider the singular system of a compact linear operator on a Hilbert space.

2.2.1 Spectral representation

In this thesis we use the spectrum of bounded linear operators. The following definition is taken from [46, p.35].

Definition 2.2.1. Let $\mathbf{X}$ be a Hilbert space and let $H \in L(\mathbf{X})$. Then $\lambda \in \mathbb{C}$ is called an eigenvalue of H if there exists an element $\mathbf{x} \in \mathbf{X}$, such that

$$H\mathbf{x} = \lambda\mathbf{x}, \tag{2.36}$$

where $\mathbf{x} \neq \mathbf{0}$. Here $\mathbf{x}$ is known as an eigenelement. A complex number λ is called a regular value of H if the resolvent operator of H, $(\lambda I - H)^{-1} \in L(\mathbf{X})$. We call the set of regular values of H the resolvent set. The complement of the resolvent set is called the spectrum $\sigma(H)$ of H, and the constant

$$r(H) := \sup_{\lambda \in \sigma(H)} |\lambda| \tag{2.37}$$

is called the spectral radius of H.

Two useful result from spectral theory, which we will use in later chapters, are as follows.

Theorem 2.2.2. *Let $\mathbf{X}$ be a Hilbert space and let $H \in L(\mathbf{X})$ be a self-adjoint compact linear operator (where $H \neq 0$). Then the spectrum $\sigma(H) = \{0\} \cup \{\lambda_n\}$ where λ_n are distinct real nonzero eigenvalues of H. There exists a complete orthonormal system of eigenelements corresponding to eigenvalues of H.*

Proof. Theorem 7.44 [25]. □

Theorem 2.2.3. *The spectral radius of a bounded self-adjoint operator H satisfies*

$$r(H) = \|H\|. \tag{2.38}$$

If H is compact then there exists at least one eigenvalue with $|\lambda| = \|H\|$.

Proof. Theorem 15.11 [46]. □

In the following chapters, we will represent our data assimilation scheme in accordance with the following result.

Theorem 2.2.4. *Let $\mathbf{X}$ be a Hilbert space and let $H \in L(\mathbf{X})$ be a self-adjoint compact linear operator (where $H \neq 0$). Then all eigenvalues of H are real. H has at least one eigenvalue different from zero and at most a countable set of eigenvalues accumulating only at zero. All nullspaces $\mathcal{N}(\lambda I - H)$ for nonzero eigenvalues λ have finite dimension and nullspaces of*

different eigenvalues are orthogonal. Assume the sequence (λ_n) *of the nonzero eigenvalues to be ordered such that*

$$|\lambda_1| \geq |\lambda_2| \geq |\lambda_3| \geq \dots. \tag{2.39}$$

Let the sequence of eigenvalues (λ_n) *be repeated according to the dimension of the nullspace* $\mathscr{N}(\lambda_n I - H)$*. Then there exists a sequence* $(\boldsymbol{\varphi}_n)$ *of corresponding orthonormal eigenelements, such that*

$$H\mathbf{x} = \sum_{n=1}^{\infty} \lambda_n \langle \mathbf{x}, \boldsymbol{\varphi}_n \rangle \boldsymbol{\varphi}_n \tag{2.40}$$

and

$$\mathbf{x} = \sum_{n=1}^{\infty} \langle \mathbf{x}, \boldsymbol{\varphi}_n \rangle \boldsymbol{\varphi}_n + Q\mathbf{x} \tag{2.41}$$

for each $\mathbf{x} \in \mathbf{X}$ *where* $Q : \mathbf{X} \to \mathscr{N}(H)$ *denote the orthogonal projection operator onto the nullspace* $\mathscr{N}(H)$*. We call each system* $(\lambda_n, \boldsymbol{\varphi}_n), n \in \mathbb{N}$*, the eigensystem of* H*.*

Proof. Theorem 15.12 [46]. □

We now consider the singular system of a compact linear operator.

2.2.2 Singular system

In this work we will need the singular values of a compact operator. The definition of a singular value is taken from [46, p.277].

Definition 2.2.5. Let $\mathbf{X}$ and $\mathbf{Y}$ be Hilbert spaces, $H \in L(\mathbf{X}, \mathbf{Y})$ be a compact linear operator, and $H^* \in L(\mathbf{Y}, \mathbf{X})$ be its adjoint. The non-negative square roots of the eigenvalues of the positive self-adjoint compact operator $H^*H \in L(\mathbf{X})$ are called the singular values of H.

We will carry out our analysis of the data assimilation scheme spectrally, and require the following decomposition, which is known as the singular value decomposition.

Theorem 2.2.6. *Let* (μ_n) *denote the sequence of the positive singular values of the compact linear operator* H *(where* $H \neq 0$*) ordered such that*

$$\mu_1 \geq \mu_2 \geq \mu_3 \dots \tag{2.42}$$

and repeated according to the dimension of the nullspaces $\mathscr{N}(\mu_n^2 I - H^*H)$*. Then there exists orthonormal sequences* $(\boldsymbol{\varphi}_n)$ *in* $\mathbf{X}$ *and* $(\mathbf{g}_n)$ *in* $\mathbf{Y}$ *such that,*

$$H\boldsymbol{\varphi}_n = \mu_n \mathbf{g}_n, \quad H^*\mathbf{g}_n = \mu_n \boldsymbol{\varphi}_n, \tag{2.43}$$

for all $n \in \mathbb{N}$*. For each* $\mathbf{x} \in \mathbf{X}$ *we have the following singular value decomposition,*

$$\mathbf{x} = \sum_{n=1}^{\infty} \langle \mathbf{x}, \boldsymbol{\varphi}_n \rangle \, \boldsymbol{\varphi}_n + Q\mathbf{x}, \tag{2.44}$$

with the orthogonal projection operator $Q : \mathbf{X} \to \mathscr{N}(H)$ *and*

$$H\mathbf{x} = \sum_{n=1}^{\infty} \mu_n \langle \mathbf{x}, \boldsymbol{\varphi}_n \rangle \, \mathbf{g}_n. \tag{2.45}$$

We call each system $(\mu_n, \boldsymbol{\varphi}_n, \mathbf{g}_n), n \in \mathbb{N}$*, with these properties, the singular system of* H*.*

Proof. See Theorem 15.16 [46]. □

The singular value decomposition also applies to the finite dimensional setting, where the infinite sums in (2.44) and (2.45) degenerate into finite summations; see [45] for further details. The following result will be useful when we carry out the norm estimates in the following chapters.

Theorem 2.2.7. *Let* $H \in L(\mathbf{X}, \mathbf{Y})$ *be a compact operator. Then given the singular system* $(\mu_n, \boldsymbol{\varphi}_n, \mathbf{g}_n), n \in \mathbb{N}$ *of* H *we have*

$$\|\mathbf{x}\|^2 = \sum_{n=1}^{\infty} |\langle \mathbf{x}, \boldsymbol{\varphi}_n \rangle|^2 + \|Q\mathbf{x}\|^2 \tag{2.46}$$

and

$$\|H\mathbf{x}\|^2 = \sum_{n=1}^{\infty} \mu_n^2 \, |\langle \mathbf{x}, \boldsymbol{\varphi}_n \rangle|^2 \tag{2.47}$$

for all $\mathbf{x} \in \mathbf{X}$*. Furthermore*

$$\|H\| = \sup_{\|\mathbf{x}\|=1} \|H\mathbf{x}\| = \mu_1. \tag{2.48}$$

Proof. See Theorem 15.17 [46]. □

We now move to the final section in this chapter, where we introduce the concept of a well-posed problem.

2.3 Well-posedness

In this section we introduce the concept of a well-posed problem. When solving operator equations, it is important to check that the equation satisfies certain properties. If these properties are not satisfied, then the operator equation might not be be physically relevant to the process it is modelling. We now consider the aspect of a well-posed problem.

In 1923 Jacques Hadamard defined what is known as a properly-posed or well-posed problem. This consisted of three properties which must be satisfied, see [42]:

1. There exists a solution to the problem (existence).

2. There is at most one solution to the problem (uniqueness).

3. The solution depends continuously on the data (stability).

If a problem does not satisfy at least one of these condition, it is known as *ill-posed* [31].

We now present a formal definition of a well-posed problem. This definition is taken from [46, p.266].

Definition 2.3.1. Let $\mathbf{X}$ and $\mathbf{Y}$ be Hilbert spaces and let $H : \mathbf{X}^{(1)} \to \mathbf{Y}^{(1)}$ be an operator from $\mathbf{X}^{(1)} \subset \mathbf{X}$ into $\mathbf{Y}^{(1)} \subset \mathbf{Y}$. The operator equation,

$$H\mathbf{x} = \mathbf{y} \tag{2.49}$$

is called well-posed if H is bijective and the inverse operator $H^{-1} : \mathbf{Y}^{(1)} \to \mathbf{X}^{(1)}$ is continuous.

With this understanding of ill-posed problems, we can now present a fundamental theorem, which demonstrates when the operator equation is ill-posed.

Theorem 2.3.2. *Let $\mathbf{X}$ and $\mathbf{Y}$ be Hilbert spaces and $H \in L(\mathbf{X}, \mathbf{Y})$ be a compact operator. If $\mathbf{X}$ has infinite dimension then H cannot have a bounded inverse and the operator equation is ill-posed.*

Proof. See Corollary 7.7 [73] or Theorem 15.4 [46]. □

As we have seen in Theorem 2.3.2, compact operators in an infinite dimensional setting cannot have a bounded inverse. This lack of boundedness in the inverse operator leads to an

ill-posed operator equation. It is well known that the singular values of an injective compact linear operator decay to zero, such that $\mu_n \to 0$ as $n \to \infty$ [46]. The singular values will not decay to zero for a finite dimensional injective linear operator, although they might be very close to zero. The condition number from Definition 2.1.18 will be very large for an operator with singular values that lie close to zero [45], [46]. An operator with a large condition number is called ill-conditioned. When numerically solving an operator equation by matrix inversion, an ill-conditioned matrix will affect the numerical results. In numerical analysis the condition number can be seen as a measure of stability for linear operator equations. There exists methods that provide stable approximates to an ill-posed operator equation. These are called *regularization methods*, which we now consider.

2.3.1 Regularization

Many regularization methods have been developed. However, we shall only introduce arguably the most famous, *Tikhonov-Phillips regularization* named after Andrey Tikhonov and David Phillips.

Theorem 2.3.3 (Tikhonov-Phillips regularization)**.** *Let $H \in L(\mathbf{X}, \mathbf{Y})$ be a compact operator. Then for each parameter $\alpha > 0$ the operator $\alpha I + H^*H \in L(\mathbf{X})$ is bijective and has a bounded inverse. Furthermore, if H is injective then*

$$\mathscr{R}_\alpha := (\alpha I + H^*H)^{-1} H^* \tag{2.50}$$

describes a regularization scheme with $\|\mathscr{R}_\alpha\| \leq 1/(2\sqrt{\alpha})$. We call the operator $\mathscr{R}_\alpha$ the Tikhonov-Phillips inverse of H and the parameter α the regularization parameter. In the finite dimensional setting for an invertible operator H as $\alpha \to 0$ then $\mathscr{R}_\alpha = H^{-1}$.

Proof. See Theorem 15.23 [46]. □

Here Tikhonov-Phillips regularization shifts the eigenvalues of H^*H away from zero by the regularization parameter α. This means that the problem is no longer ill-posed in the infinite dimensional setting, or ill-conditioned in the finite dimensional setting. Of course, replacing the unbounded inverse operator with this Tikhonov-Phillips family of bounded inverses, means that we are not solving the original operator equation in (2.5). Instead we

solve a slightly different problem. However, we are able to solve it now correctly. This of course incurs an error, which is dependent on how far we shift the eigenvalues of H^*H. We shall discuss this further in future chapters. We now present another formulation of Tikhonov-Phillips regularization, which is considered as a penalised residual minimisation, that we will parallel to the data assimilation algorithms introduced in Chapter 3.

Theorem 2.3.4 (Tikhonov-Phillips regularization)**.** *Let $H \in (\mathbf{X}, \mathbf{Y})$ be a compact linear operator and let $\alpha > 0$ be the regularization parameter. Then for each $\mathbf{y}^{(1)} \in \mathbf{Y}$ there exists a unique element $\tilde{\mathbf{x}} \in \mathbf{X}$ such that*

$$\left\|H\tilde{\mathbf{x}} - \mathbf{y}^{(1)}\right\|^2 + \alpha \left\|\tilde{\mathbf{x}}\right\|^2 = \inf_{\mathbf{x}^{(1)} \in \mathbf{X}} \left\{ \left\|H\mathbf{x}^{(1)} - \mathbf{y}^{(1)}\right\|^2 + \alpha \left\|\mathbf{x}^{(1)}\right\|^2 \right\}. \tag{2.51}$$

The minimiser $\tilde{\mathbf{x}}$ is given by the unique solution of the equation

$$\alpha\tilde{\mathbf{x}} + H^*H\tilde{\mathbf{x}} = H^*\mathbf{y}^{(1)} \tag{2.52}$$

and depends continuously on $\mathbf{y}^{(1)}$.

Proof. See Theorem 16.1 [46]. □

The equation in (2.52) is known as the *normal equation*. We will explore the impact of Tikhonov-Phillips regularization and its association with the data assimilation schemes, which we consider in the following chapters.

2.4 Summary

In this chapter we have introduced key definitions and theorems, which we shall use throughout this thesis. We began with important aspects from functional analysis, which led to the spectral approach in a Hilbert space setting. We finished this chapter introducing well-posedness, and how it can be ensured with regularization methods. Our main focus was to provide the necessary tools with which to carry out the analysis in the following chapters. In the next chapter we will introduce popular data assimilation schemes and show their link with Tikhonov-Phillips regularization.

Chapter 3

Data assimilation schemes

In this chapter we introduce two variational data assimilation methods and one sequential data assimilation method. These different approaches are widely used in many areas of science. We demonstrate how these methods are a form of Tikhonov-Phillips regularization, which we introduced in Chapter 2. We shall begin with a brief introduction to data assimilation and its applications in the NWP community.

3.1 Data assimilation

The process of data assimilation is the incorporation of observational data into a numerical model to produce a model state. This model state gives the most accurate depiction of the observed reality. In the data assimilation community we call this model state the *analysis*. In many areas of science, in particular NWP, the analysis can be used with a numerical model to produce a forecast of the state of the system.

Mathematically, we can interpret the data assimilation task for a linear time-invariant observation operator, as seeking the analysis $\mathbf{x}_k^{(a)}$ at every assimilation step $k \in \mathbb{N}_0$ to solve an operator equation

$$H\mathbf{x}_k^{(a)} = \mathbf{y}_k, \tag{3.1}$$

where $\mathbf{y}_k$ represents the measurements, and H is a mapping from the state space into the measurement space. In this work we will assume that our observation operator H is compact. This is an adequate mathematical assumption since operators associated with remote sensing

measurements are compact; see [71] and [49]. It has long been known that the problem of solving operator equations is ill-posed; see [46] and [73]. Here we work with compact operators to represent an ill-posed operator equation in a classical mathematical framework. We present a formal definition of the data assimilation task.

Definition 3.1.1. Given observations $\mathbf{y}_k \in \mathbf{Y}$ at times k then the data assimilation task for a linear time-invariant observation operator is to determine the states $\mathbf{x}_k \in \mathbf{X}$ from the operator equation

$$H\mathbf{x}_k = \mathbf{y}_k, \tag{3.2}$$

for $k \in \mathbb{N}$.

Here we remark that H, which is known as the observation operator, is assumed for the majority of this work to be a compact time-invariant linear operator, $H \in L(\mathbf{X}, \mathbf{Y})$. Also we consider linear and nonlinear time-varying model dynamics denoted by M_k and $\mathcal{M}_k$ respectively. The absence of the time index k shall denote a time-invariant linear and nonlinear model operator. In data assimilation we also employ knowledge from some given prior or *background* state $\mathbf{x}_k^{(b)}$.

It is important to discuss our mathematical approach in this work. From Definition 3.1.1 we interpret the data assimilation task as solving an operator equation. However, the data assimilation problem can be introduced from a Bayesian viewpoint, where one combines prior knowledge (background) of the state of the system with a likelihood, to produce a posterior estimate to the state of the system. In data assimilation the likelihood arises from the probability density function (PDF) of the errors in the observations. Further details on data assimilation from a Bayesian perspective can be found in [47]. In this work we provide deterministic analysis of data assimilation schemes which aim to solve an operator equation, in accordance with Definition 3.1.1. Results on analysing data assimilation schemes from a stochastic perspective can be found in [79].

In this research we focus on practical methods which can be successfully applied in operational NWP centres. Many approaches have been developed in science to estimate the state of the system. However, most of these are limited because of the difficulties to make operational for weather forecasting. Monte Carlo methods, such as the particle filter are not yet practical in NWP since the dimension of the state space means that a large number

of particles are required to produce a posterior PDF. Currently this is not computationally feasible. Further details on Monte Carlo methods can be found in [41] and results on particle filters in the field of geophysical sciences can be found in [83] and [84]. We later explore in Section 3.1.2 the problem of computing matrix operations in a high-dimensional setting. This is a major challenge that the NWP community would face when trying to implement one particular sequential data assimilation method. First we present an introduction to a popular class of data assimilation methods used operationally in NWP, variational data assimilation.

3.1.1 Variational data assimilation

In the 1980's, variational data assimilation methods appeared in the NWP community. The UK Meteorological Office was the first operational NWP centre to propose the variational data assimilation method of *three-dimensional variational data assimilation* (3DVar) in 1986 [50]. However, 3DVar did not become operational in NWP centres until the 1990's; see [16] and [51] for further details.

In this section we will present the data assimilation method of 3DVar under the following assumption.

Assumption 3.1.2. *The observation operator $H \in L(\mathbf{X}, \mathbf{Y})$ is a linear time-invariant operator. The model dynamics $\mathcal{M}_k : \mathbf{X} \to \mathbf{X}$ is a discrete time-varying nonlinear operator.*

We remark that the 3DVar method can be defined for a more general setting than Assumption 3.1.2. Under the assumptions in Assumption 3.1.2, the objective of 3DVar is to minimise the following functional,

$$\begin{aligned} \mathcal{J}^{(3D)}\left(\mathbf{x}_k\right) &:= \mathcal{J}^{(b)} + \mathcal{J}^{(o)} \\ &= \left\langle B^{-1}\left(\mathbf{x}_k - \mathbf{x}_k^{(b)}\right), \mathbf{x}_k - \mathbf{x}_k^{(b)} \right\rangle_{\ell^2} \\ &+ \left\langle R^{-1}\left(\mathbf{y}_k - H\mathbf{x}_k\right), \mathbf{y}_k - H\mathbf{x}_k \right\rangle_{\ell^2}, \end{aligned} \tag{3.3}$$

with respect to $\mathbf{x}_k$ for an ℓ^2 inner product, where the resultant minimiser to the functional in (3.3) is the analysis $\mathbf{x}_k^{(a)}$. The 3DVar functional in (3.3) is then subject to the discrete-time evolution

$$\mathbf{x}_{k+1}^{(b)} = \mathcal{M}_k\left(\mathbf{x}_k^{(a)}\right), \tag{3.4}$$

for $k \in \mathbb{N}_0$, in accordance with Definition 3.1.1. In NWP the background state at $k = 0$ can come from a previous forecast or climatological data. Since we observe measurements in a different space to the state space, we need an operation that passes from $\mathbf{X}$ into $\mathbf{Y}$. This is represented by the operator $H : \mathbf{X} \to \mathbf{Y}$ which maps elements in the state space $\mathbf{X}$, into the measurement space $\mathbf{Y}$. Finally, all data assimilated into the scheme is uncertain. Therefore, we have weights $B : \mathbf{X}^* \to \mathbf{X}$ and $R : \mathbf{Y}^* \to \mathbf{Y}$ which represent our uncertainty in the background state and observations respectively. Here $\mathbf{X}^*$ and $\mathbf{Y}^*$ respectively denote the dual spaces of $\mathbf{X}$ and $\mathbf{Y}$. The dual space is defined as a space of all continuous linear functionals on a vector space; see [46] for further details on the dual space. Since we restrict our analysis to the Hilbert space framework, which is reflexive by construction, the background and observation weights map $B : \mathbf{X} \to \mathbf{X}$ and $R : \mathbf{Y} \to \mathbf{Y}$. Under the assumption that the errors on both the background state and the observations come from some probability distribution, then we can construct these weights to be covariances of these errors. If the noises are modelled as Gaussian then from a Bayesian perspective it is natural to choose the weights as covariance operators. In the finite dimensional setting, such that $\mathbf{X} = \mathbb{R}^n$ and $\mathbf{Y} = \mathbb{R}^m$, the weights $B \in \mathbb{R}^{n \times n}$ and $R \in \mathbb{R}^{m \times m}$ are covariance matrices, see [20, p.38] for further details. In an infinite dimensional setting, for Hilbert space $\mathbf{X}$ and $\mathbf{Y}$, the weights $B \in L(\mathbf{X})$ and $R \in L(\mathbf{Y})$ are covariance operators, see [79] for further details.

In operational NWP centres, the process of data assimilation is repeated over time to assimilate more and more measurements. Therefore, we can consider this approach of repeating 3DVar as cycling the data assimilation scheme, which we present in the following definition.

Definition 3.1.3. Let Assumption 3.1.2 hold. Given an initial background state $\mathbf{x}_0^{(b)}$ at time t_0. Cycled 3DVar is defined as follows:
For $k = 0, 1, \ldots$

1. *Analysis step.* Using the observation $\mathbf{y}_k$ calculate an analysis $\mathbf{x}_k^{(a)}$ at time k by minimising the functional in (3.3).

2. *Forecast step.* Using the model dynamics $\mathcal{M}_k$, calculate the background state $\mathbf{x}_{k+1}^{(b)}$ at time $k + 1$ using (3.4).

The analysis step in Definition 3.1.3 can also be performed using other data assimilation schemes such as four-dimensional variational data assimilation, which we now present.

Towards the end of the 1990's *four-dimensional variational data assimilation* (4DVar) appeared operationally in the data assimilation community; see [68] for further details. The objective of strong-constraint 4DVar is to minimise a functional over an assimilation window of size L, with respect to the state element $\mathbf{x}_{\hat{k},0}$ located at the start of each assimilation window $\hat{k}$. The resultant minimiser to the functional in (3.5) is the analysis $\mathbf{x}^{(a)}_{\hat{k},0}$. For clarity, we remark that the index $\hat{k}$ represents the assimilation cycle. Observations $\mathbf{y}_{\hat{k},l}$ in 4DVar are located at discrete observation times l where $l = 1, \ldots, L$, each with error covariances R_l, within an assimilation cycle $\hat{k}$. We adopt the notation $\hat{k}$ in order to not clash with the previous notation for assimilation time. In 4DVar assimilation time refers to an assimilation window L over which observations are assimilated, whereas in 3DVar assimilation time refers to only assimilating observations at time k.

We will present the data assimilation method of 4DVar under the following assumption.

Assumption 3.1.4. *The observation operator $H \in L(\mathbf{X}, \mathbf{Y})$ is a linear time-invariant operator. The model dynamics $\mathcal{M}_{\hat{k}} : \mathbf{X} \to \mathbf{X}$ is a nonlinear time-varying operator.*

We remark that the 4DVar method can be defined for a more general setting than Assumption 3.1.4. Under the assumption in Assumption 3.1.4 the 4DVar functional is as follows,

$$\begin{aligned}\mathcal{J}^{(4D)}\left(\mathbf{x}_{\hat{k},0}\right) &:= \mathcal{J}^{(b)}_{\hat{k},0} + \mathcal{J}^{(o)}_{\hat{k},L:1} \\ &= \left\langle B^{-1}\left(\mathbf{x}_{\hat{k},0} - \mathbf{x}^{(b)}_{\hat{k},0}\right), \mathbf{x}_{\hat{k},0} - \mathbf{x}^{(b)}_{\hat{k},0}\right\rangle_{\ell^2} \\ &+ \sum_{l=1}^{L}\left\langle R_l^{-1}\left(\mathbf{y}_{\hat{k},l} - H\mathbf{x}_{\hat{k},l}\right), \mathbf{y}_{\hat{k},l} - H\mathbf{x}_{\hat{k},l}\right\rangle_{\ell^2}. \end{aligned} \tag{3.5}$$

As we see, 4DVar seeks an analysis $\mathbf{x}^{(a)}_{\hat{k},0}$ at the beginning of each assimilation window. Then the next background state at assimilation cycle $\hat{k}+1$ is obtained using the model dynamics such that,

$$\mathbf{x}^{(b)}_{\hat{k}+1,0} = \mathcal{M}_{\hat{k}}\left(\mathbf{x}^{(a)}_{\hat{k},0}\right). \tag{3.6}$$

The 4DVar functional in (3.5) is subject to the discrete-time evolution

$$\mathbf{x}_{\hat{k},l+1} = \mathcal{M}_{\hat{k},l+1:l}\left(\mathbf{x}_{\hat{k},l}\right), \tag{3.7}$$

for $\hat{k}, l \in \mathbb{N}_0$. Again for clarity, the index $\hat{k}$ in $\mathcal{M}_{\hat{k},l+1:l}(\cdot)$ represents the assimilation cycle, and $l+1:l$ represents the transition between discrete points l and $l+1$. We can see that 4DVar considers measurements across an assimilation window, and seeks to find an analysis at the start of the assimilation window, which when mapped forward using the model dynamics, best fits through the data across the assimilation window. Reformulating the problem, we are able to display (3.5) in a similar form to (3.3), which will be important to connect both with Tikhonov-Phillips regularization. We store all observations across the assimilation window in a new vector as follows,

$$\hat{\mathbf{y}}_{\hat{k}} := \begin{pmatrix} \mathbf{y}_{\hat{k},1} \\ \mathbf{y}_{\hat{k},2} \\ \vdots \\ \mathbf{y}_{\hat{k},L} \end{pmatrix}. \tag{3.8}$$

We redefine the observation operator to include compositions with the possibly nonlinear model dynamics operator $\mathcal{M}_{\hat{k}}$ as follows,

$$\hat{\mathcal{H}}_{\hat{k}} := \begin{bmatrix} H\mathcal{M}_{\hat{k},1:0} \\ H\mathcal{M}_{\hat{k},2:0} \\ \vdots \\ H\mathcal{M}_{\hat{k},L:0} \end{bmatrix} \tag{3.9}$$

and we redefine the observation error covariance operator as follows

$$\hat{R} := \begin{bmatrix} R_1 & & & \\ & R_2 & & \\ & & \ddots & \\ & & & R_L \end{bmatrix}. \tag{3.10}$$

Using (3.8), (3.9) and (3.10), we can rewrite (3.5) as follows,

$$\begin{aligned} \mathcal{J}^{(4D)}\left(\mathbf{x}_{\hat{k},0}\right) = &\left\langle B^{-1}\left(\mathbf{x}_{\hat{k},0} - \mathbf{x}_{\hat{k},0}^{(b)}\right), \mathbf{x}_{\hat{k},0} - \mathbf{x}_{\hat{k},0}^{(b)} \right\rangle_{\ell^2} \\ &+ \left\langle \hat{R}^{-1}\left(\hat{\mathbf{y}}_{\hat{k}} - \hat{\mathcal{H}}_{\hat{k}}(\mathbf{x}_{\hat{k},0})\right), \hat{\mathbf{y}}_{\hat{k}} - \hat{\mathcal{H}}_{\hat{k}}(\mathbf{x}_{\hat{k},0}) \right\rangle_{\ell^2}, \end{aligned} \tag{3.11}$$

subject to (3.6). Further details for rewriting 4DVar in the form of (3.11) can be found in [36] in the finite dimensional setting. Here we now see the similarity between (3.3) and (3.11). However, for a nonlinear model operator $\mathcal{M}_{\hat{k}}$, the functional in (3.11) has now a nonlinear

term $\hat{\mathcal{H}}_{\hat{k}}$. For a linear model operator $M_{\hat{k}}$ we shall write $\hat{H}_{\hat{k}}$ instead of $\hat{\mathcal{H}}_{\hat{k}}$. We are now able to consider cycling 4DVar, in a similar way to cycling 3DVar in Definition 3.1.3.

However, since the nonlinear model dynamics $\mathcal{M}_{\hat{k}}$ is dependent on $\hat{k}$ this means that the operator $\hat{\mathcal{H}}_{\hat{k}}$ as defined in (3.9) is time-varying. This means that we are unable to connect 4DVar with cycled Tikhonov-Phillips regularization that we will introduce in Section 3.1.3. Instead we will make the following assumption for the 4DVar method.

Assumption 3.1.5. *The observation operator $H \in L(\mathbf{X}, \mathbf{Y})$ is a linear time-invariant operator. The model dynamics $M \in L(\mathbf{X})$ is a linear time-invariant operator.*

Under the assumptions in Assumption 3.1.5 (3.11) becomes

$$\begin{aligned}\mathcal{J}^{(4DLIN)}\left(\mathbf{x}_{\hat{k},0}\right) = &\left\langle B^{-1}\left(\mathbf{x}_{\hat{k},0} - \mathbf{x}_{\hat{k},0}^{(b)}\right), \mathbf{x}_{\hat{k},0} - \mathbf{x}_{\hat{k},0}^{(b)}\right\rangle_{\ell^2} \\ &+ \left\langle \hat{R}^{-1}\left(\hat{\mathbf{y}}_{\hat{k}} - \hat{H}(\mathbf{x}_{\hat{k},0})\right), \hat{\mathbf{y}}_{\hat{k}} - \hat{H}(\mathbf{x}_{\hat{k},0})\right\rangle_{\ell^2},\end{aligned} \tag{3.12}$$

where

$$\hat{H} := \begin{bmatrix} HM \\ HM^2 \\ \vdots \\ HM^L \end{bmatrix}. \tag{3.13}$$

We can minimise the functional in (3.12) to seek an analysis, then we use the linear time-invariant model dynamics M^L to calculate a background state at the next assimilation window. Therefore, cycling 4DVar means that we cycle over the assimilation windows $\hat{k}$. Both data assimilation algorithms, 3DVar and 4DVar introduced here employ no update to the background error covariance operator. However, one such algorithm that does make use of an updated background error covariance operator is the Kalman filter. We now explore the Kalman filter, which is a sequential data assimilation algorithm.

3.1.2 The Kalman filter

The Kalman filter [40], [21] as introduced by Rudolf E. Kalman in 1960, differs from the variational approach in the way it includes information from previous observational data. 3DVar assimilates present observations and 4DVar considers observations over an assimilation window. Now we consider a sequential approach; the Kalman filter which includes

information from past measurements in the update covariance operators. There exist many different versions of the Kalman filter. Here we only consider the linear Kalman filter which applies to our theory developed later in this thesis. In this work we do not consider the extended Kalman filter [47] which is a nonlinear extension to the linear Kalman filter. We will introduce the standard discrete Kalman filter under the following assumption.

Assumption 3.1.6. *The observation operator is a linear time-invariant observation operator* $H \in L(\mathbf{X}, \mathbf{Y})$. *The model dynamics is a linear time-varying operator* $M_k \in L(\mathbf{X})$.

We remark that the Kalman filter can be defined for a more general setting than Assumption 3.1.6.

Definition 3.1.7. Let Assumption 3.1.6 hold. Let $\mathbf{x}_0^{(b)}$ be an initial background state with error covariance $B_0^{(b)}$. Let $\mathbf{y}_k$ be a set observations with error covariance R_k for all time $k \in \mathbb{N}_0$. Let $M_k : \mathbf{X} \to \mathbf{X}$ be a modelled linear model operator such that

$$M_k \mathbf{x}_k^{(t)} = M_k^{(t)} \mathbf{x}_k^{(t)} + \boldsymbol{\zeta}_{k+1}, \tag{3.14}$$

where t in $\mathbf{x}_k^{(t)}$ and $M_k^{(t)}$ denotes the true state and operator respectively, and $\boldsymbol{\zeta}_{k+1}$ represents the model error with error covariance $\mathscr{Q}_k$, for all time $k \in \mathbb{N}_0$. Then the Kalman filter under the assumption of a linear time-invariant observation operator $H \in L(\mathbf{X}, \mathbf{Y})$ is as follows:
For $k = 0$

$$\mathscr{K}_0 = B_0^{(b)} H^* \left(H B_0^{(b)} H^* + R_0 \right)^{-1}, \tag{3.15}$$

$$\mathbf{x}_0^{(a)} = \mathbf{x}_0^{(b)} + \mathscr{K}_0 \left(\mathbf{y}_0 - H \mathbf{x}_0^{(b)} \right), \tag{3.16}$$

and

$$B_0^{(a)} = \left(I - \mathscr{K}_0 H \right) B_0^{(b)}. \tag{3.17}$$

Then for $k = 1, 2, \ldots$

1. Forecast the analysis to obtain a new background state,

$$\mathbf{x}_k^{(b)} = M_{k-1} \mathbf{x}_{k-1}^{(a)}. \tag{3.18}$$

2. Update the background error covariance,

$$B_k^{(b)} = M_{k-1} B_{k-1}^{(a)} M_{k-1}^* + \mathscr{Q}_k. \tag{3.19}$$

3. Calculate a new observer (Kalman) gain

$$\mathscr{K}_k = B_k^{(b)} H^* \left(H B_k^{(b)} H^* + R_k \right)^{-1}, \tag{3.20}$$

where H^* is the adjoint of the operator H.

4. Update the state estimate using the measurements,

$$\mathbf{x}_k^{(a)} = \mathbf{x}_k^{(b)} + \mathscr{K}_k \left(\mathbf{y}_k - H \mathbf{x}_k^{(b)} \right). \tag{3.21}$$

5. Update the analysis error covariance,

$$B_k^{(a)} = \left(I - \mathscr{K}_k H \right) B_k^{(b)}. \tag{3.22}$$

The Kalman filter differs from 3DVar and 4DVar in many ways. Most importantly, it provides a framework to update the background error covariance operator over time. In operational NWP this update in (3.19) is computationally not feasible. Currently in NWP the dimension of the state space ranges between orders of $\mathcal{O}(10^8 - 10^9)$, therefore it is not possible to compute (3.19). Despite this, many current data assimilation algorithms popular in the NWP community use the approach of Kalman filtering with ensembles; see [47] for data assimilation schemes in this direction. Therefore, it is important to study the original Kalman filter in Definition 3.1.7, since it has practical relevance to the NWP community. We also note that ensemble Kalman filtering is more general than the Kalman filter because it accounts for nonlinear model dynamics. Furthermore, there is a nonlinear extension to the Kalman filter, which is known as the extended Kalman filter. Details on the extended Kalman filter can be found in [47]. However, in this work we will only study the Kalman filter as introduced in Definition 3.1.7.

To streamline the presentation we now present cycled Tikhonov-Phillips regularization. Presenting this method will enable us to focus the analysis on one method, which under a number of assumptions is then equivalent to the data assimilation schemes introduced in this chapter. For a particular specification of the observation operator H we can align cycled

Tikhonov-Phillips regularization with 3DVar and 4DVar. We now consider cycled Tikhonov-Phillips regularization, demonstrate its equivalence with 3DVar and 4DVar, and we shall discuss its relevance to the Kalman filter.

3.1.3 Tikhonov-Phillips regularization

We will introduce the method of cycled Tikhonov-Phillips regularization under the following assumption.

Assumption 3.1.8. *The observation operator is a linear time-invariant observation operator $H \in L(\mathbf{X}, \mathbf{Y})$. The model dynamics is a nonlinear time-varying operator $\mathcal{M}_k : \mathbf{X} \to \mathbf{X}$.*

We remark that cycled Tikhonov-Phillips regularization can be defined for a more general setting than Assumption 3.1.8. The following definition is taken from [57, p.2].

Definition 3.1.9. Let Assumption 3.1.8 hold. Given measurements $\mathbf{y}_k \in \mathbf{Y}$ for $k \in \mathbb{N}$ and an initial guess $\mathbf{x}_k^{(b)}$, the objective of cycled Tikhonov-Phillips regularization is to seek an estimate, $\mathbf{x}_k^{(a)}$ that minimises the functional,

$$\mathcal{J}^{(CTP)}\left(\mathbf{x}_k\right) := \alpha \left\| \mathbf{x}_k - \mathbf{x}_k^{(b)} \right\|_{\mathbf{X}}^2 + \left\| \mathbf{y}_k - H\mathbf{x}_k \right\|_{\mathbf{Y}}^2, \tag{3.23}$$

with respect to $\mathbf{x}_k$ for Hilbert spaces $(\mathbf{X}, \|\cdot\|_{\mathbf{X}})$ and $(\mathbf{Y}, \|\cdot\|_{\mathbf{Y}})$, where $\mathbf{x}_k^{(b)} = \mathcal{M}_{k-1}(\mathbf{x}_{k-1}^{(a)})$ and $\alpha > 0$.

Cycled Tikhonov-Phillips regularization features in the literature in many different forms, often called dynamic or iterated regularization. One form of cycled Tikhonov-Phillips regularization can be found in [70], which precedes the work of Tikhonov and Phillips. An extensive review of the literature behind cycled Tikhonov-Phillips regularization can be found in [56]. With the following result we will be able to present cycled Tikhonov-Phillips regularization in an update form, which will suit our analysis in subsequent chapters.

Theorem 3.1.10. *Let $H \in L(\mathbf{X}, \mathbf{Y})$ be a linear time-invariant observation operator and let $\mathcal{M}_k : \mathbf{X} \to \mathbf{X}$ be a time-varying nonlinear model operator. Then the minimiser $\mathbf{x}_k^{(a)}$ to (3.23) is given by*

$$\mathbf{x}_k^{(a)} = \mathcal{M}_{k-1}\mathbf{x}_{k-1}^{(a)} + \mathscr{R}_\alpha\left(\mathbf{y}_k - H\mathcal{M}_{k-1}\left(\mathbf{x}_{k-1}^{(a)}\right)\right), \tag{3.24}$$

given $\mathbf{x}_k^{(b)} = \mathcal{M}_{k-1}(\mathbf{x}_{k-1}^{(a)})$*, where*

$$\mathscr{R}_\alpha = (\alpha I + H^*H)^{-1}H^* \tag{3.25}$$

is known as the Tikhonov-Phillips inverse, with an adjoint H^* *to the linear time-invariant observation operator* $H \in L(\mathbf{X}, \mathbf{Y})$ *and a regularization parameter* α*. Here (3.24) is what we characterise as cycled Tikhonov-Phillips regularization.*

Proof. The proof is obtained using Theorem 2.3.4. We rewrite (2.51) for $\mathbf{x}^{(1)} := \mathbf{x}_k - \mathbf{x}_k^{(b)}$ and $\mathbf{y}^{(1)} := \mathbf{y}_k - H\mathbf{x}_k^{(b)}$. Then the minimiser, $\mathbf{x}_k^{(a)}$ to the functional in (3.23) is given by (2.52) rewritten such that,

$$\alpha\left(\mathbf{x}_k^{(a)} - \mathbf{x}_k^{(b)}\right) + H^*H\left(\mathbf{x}_k^{(a)} - \mathbf{x}_k^{(b)}\right) = H^*\left(\mathbf{y}_k - H\mathbf{x}_k^{(b)}\right). \tag{3.26}$$

Rearranging (3.26) and substituting $\mathbf{x}_k^{(b)} = \mathcal{M}_{k-1}(\mathbf{x}_{k-1}^{(a)})$, we obtain (3.24) which completes the proof. □

We can adapt the proof in Theorem 3.1.10 by replacing $\mathscr{R}_\alpha$ with two variations of the Kalman gain, $\mathscr{K}$ and $\hat{\mathscr{K}}$ as defined in (3.28) and (3.30), to obtain the following two results.

Theorem 3.1.11. *Let* $H \in L(\mathbf{X}, \mathbf{Y})$ *be a linear time-invariant observation operator. Let* $B \in L(\mathbf{X})$ *and* $R \in L(\mathbf{Y})$ *be a time-invariant linear background error covariance operator and a time-invariant linear observation error covariance operator respectively. Then the minimiser* $\mathbf{x}_k^{(a)}$ *to (3.3) is given by*

$$\mathbf{x}_k^{(a)} = \mathbf{x}_k^{(b)} + \mathscr{K}\left(\mathbf{y}_k - H\mathbf{x}_k^{(b)}\right), \tag{3.27}$$

where

$$\mathscr{K} := BH'(HBH' + R)^{-1} \tag{3.28}$$

is known as the Kalman gain and H' *is the adjoint of* H *with respect to the Euclidean inner product.*

Theorem 3.1.12. *Let* $H \in L(\mathbf{X}, \mathbf{Y})$ *be a linear time-invariant observation operator and let* $M \in L(\mathbf{X})$ *be a time-invariant linear model operator. Let* $B \in L(\mathbf{X})$ *and* $R \in L(\mathbf{Y})$ *be a time-invariant linear background error covariance operator and a time-invariant linear*

observation error covariance operator respectively. Then the minimiser $\mathbf{x}_k^{(a)}$ *to (3.12) is given by*

$$\mathbf{x}_k^{(a)} = \mathbf{x}_k^{(b)} + \hat{\mathscr{K}} \left(\hat{\mathbf{y}}_k - \hat{H}\mathbf{x}_k^{(b)} \right), \tag{3.29}$$

where

$$\hat{\mathscr{K}} := B\hat{H}'(\hat{H}B\hat{H}' + \hat{R})^{-1} \tag{3.30}$$

is known as the Kalman gain, with $\hat{R}$ *defined in (3.10),* $\hat{H}$ *defined in (3.13) and where* $\hat{H}'$ *is the adjoint of* $\hat{H}$ *with respect to the Euclidean inner product.*

We can now state the equivalence between 3DVar and 4DVar under the assumptions respectively in Assumption 3.1.2 and Assumption 3.1.5, and cycled Tikhonov-Phillips regularization. When the model dynamics is nonlinear then we cannot show equivalence between 4DVar and cycled Tikhonov-Phillips regularization.

Theorem 3.1.13. *Let* $\mathbf{X}$ *and* $\mathbf{Y}$ *be Hilbert spaces. Let Assumption 3.1.2 and Assumption 3.1.5 hold for the 3DVar method with its cost functional as defined in (3.3) and the 4DVar method with its cost functional as defined in (3.12) respectively.*

For the Euclidean inner product and the weighted norms

$$\langle \cdot, \cdot \rangle_{B^{-1}} := \left\langle \cdot, B^{-1} \cdot \right\rangle_{\ell^2} \text{ on } \mathbf{X} \quad \text{and} \quad \langle \cdot, \cdot \rangle_{R^{-1}} := \left\langle \cdot, R^{-1} \cdot \right\rangle_{\ell^2} \text{ on } \mathbf{Y} \tag{3.31}$$

for self-adjoint, strictly positive operators B *and* R*, the Kalman gain in (3.28) for 3DVar corresponds to the Tikhonov-Phillips inverse, (3.25) where its adjoint is given by*

$$H^* = \alpha B H' R^{-1} \tag{3.32}$$

for $\alpha = 1$*.*

For the Euclidean inner product and the weighted norms

$$\langle \cdot, \cdot \rangle_{B^{-1}} := \left\langle \cdot, B^{-1} \cdot \right\rangle_{\ell^2} \text{ on } \mathbf{X} \quad \text{and} \quad \langle \cdot, \cdot \rangle_{\hat{R}^{-1}} := \left\langle \cdot, \hat{R}^{-1} \cdot \right\rangle_{\ell^2} \text{ on } \mathbf{Y} \tag{3.33}$$

for self-adjoint, strictly positive operators, B *and* $\hat{R}$*, the Kalman gain in (3.30) for 4DVar corresponds to the Tikhonov-Phillips inverse, (3.25) where its adjoint is given by*

$$H^* = \alpha B \hat{H}' \hat{R}^{-1} \tag{3.34}$$

for $\alpha = 1$*.*

Proof. See Theorem 2.1 [57]. □

The result in Theorem 3.1.13 is important, since it shows that for weighted norms according to (3.31) and (3.33), studying cycled Tikhonov-Phillips regularization in (3.24) is equivalent to studying 3DVar and 4DVar respectively. Furthermore, in Theorem 3.1.13 we see the appearance of the regularization parameter α for both 3DVar and 4DVar.

We remark that the cycled Tikhonov-Phillips functional (3.23) in Definition 3.1.9 can be defined for a linear time-varying observation operator $H_k \in L(\mathbf{X}, \mathbf{Y})$. It then follows that the results in Theorem 3.1.10, Theorem 3.1.11, Theorem 3.1.12 and Theorem 3.1.13 can be adapted for a linear time-varying observation operator $H_k \in L(\mathbf{X}, \mathbf{Y})$. In this case the operators in (3.25), (3.28), (3.30), (3.32) and (3.34) are time-varying. In most of this thesis we will assume that $H \in L(\mathbf{X}, \mathbf{Y})$ is a linear time-invariant observation operator. However, in Section 7.3 we consider the case where the observation operator $H_k \in L(\mathbf{X}, \mathbf{Y})$ is time-varying.

From (3.23) we can see that reducing the regularization parameter has the effect of increasing the weight on the term involving the initial guess $\mathbf{x}_k^{(b)}$ in (3.23). We can parallel this with the 3DVar functional in (3.3) by including a regularization parameter $\alpha = 1$, such that

$$\begin{aligned} \mathcal{J}^{(3D)}(\mathbf{x}_k) &:= \alpha \mathcal{J}^{(b)} + \mathcal{J}^{(o)} \\ &= \left\langle \alpha B^{-1} \left(\mathbf{x}_k - \mathbf{x}_k^{(b)} \right), \mathbf{x}_k - \mathbf{x}_k^{(b)} \right\rangle_{\ell^2} \\ &+ \left\langle R^{-1} \left(\mathbf{y}_k - H\mathbf{x}_k \right), \mathbf{y}_k - H\mathbf{x}_k \right\rangle_{\ell^2}. \end{aligned} \tag{3.35}$$

From (3.35) we see that reducing the regularization parameter has the effect of increasing the uncertainty in the background, which means the data assimilation scheme trusts the observation term more. Conversely, increasing the regularization parameter has the effect of decreasing the uncertainty in the background which means the data assimilation scheme trusts the background term more. Therefore the regularization parameter can be understood as a form of *multiplicative variance inflation* we apply to each data assimilation scheme. If the regularization parameter α_k can be chosen in each assimilation step k then this can be seen as *adaptively* applying multiplicative variance inflation. In particular, multiplicative variance inflation is used in ensemble Kalman filtering where the variance on the background state is inflated to reduce filter error and avoid filter divergence. Ensemble Kalman filters

are beyond the scope of this work however, further details on filter error and divergence for ensemble Kalman filters can be found in [1] and [59]. We will discuss our use of variance inflation in the following chapters.

Interpreting the Kalman filter as a form of cycled Tikhonov-Phillips regularization is more difficult since the Kalman filter provides a framework to update the background error covariance operator. In this case, using the approach of weighted norms from Theorem 3.1.13 does not yield any benefit, since the measure associated with the state space $\mathbf{X}$, changes in each assimilation step. We shall discuss this in more depth in Chapter 7.

3.2 Summary

In this chapter we introduced three data assimilation schemes. In the following chapters we will present our theoretical and numerical results which relate to these data assimilation schemes. We began introducing 3DVar, a popular variational data assimilation scheme, which finds the best state to fit between the background and the observations. We then discussed a similar method to 3DVar, which aims to seek the best trajectory through an assimilation window of observations, 4DVar. We also presented one sequential data assimilation scheme, the Kalman filter. Finally, we introduced cycled Tikhonov-Phillips regularization, which will form the basis for our research. We demonstrated how cycled Tikhonov-Phillips is equivalent to 3DVar and 4DVar under weighted norms. Our main focus was to introduce each assimilation scheme, and present it so that our results in the following chapters can be applicable to each method. In the next chapter, we consider the stability of each data assimilation scheme introduced in this chapter, and the relevant literature associated with each method.

Chapter 4

Instability in data assimilation schemes

We saw in Chapter 2 and Chapter 3 that we are interested in solving an operator equation. In Chapter 2 it was shown that in the infinite dimensional setting, a compact linear operator does not have a bounded inverse, and hence the operator equation is ill-posed. Therefore we replace H^{-1} with a family of bounded operators $\mathscr{R}_\alpha$. Regularization provides a stable solution to an ill-posed problem. In this chapter we will introduce our definition of a stable and unstable data assimilation scheme. We will present the error evolution for the cycled Tikhonov-Phillips regularization scheme and relate its form to the literature. We will see that the error evolution for the cycled Tikhonov-Phillips scheme has been investigated extensively for the finite dimensional linear setting. Furthermore, there has been extensive research in the finite dimensional nonlinear setting. However as we will see, the theory developed for nonlinear systems relies on linearisations. In this chapter we will identify key open questions for infinite dimensional systems, which we begin to answer in this thesis. We start with our definition of the stability in the context of cycled data assimilation schemes.

4.1 Instability

We will be concerned with what we call the analysis error. In this section we will introduce the analysis error for the cycled data assimilation scheme, discussed in Chapter 3. We will

then derive an explicit form for the evolution of the analysis error of a cycled data assimilation scheme. We present this evolution equation so that it can be paralleled with the literature.

For this section we want to introduce a general form for the linear analysis error evolution equation. We will return to the nonlinear analysis error evolution equation later in Chapter 8 and derive similar results. We collect all the assumptions that we will make in this section.

Assumption 4.1.1. *Let* $\mathbf{X}$ *and* $\mathbf{Y}$ *be Hilbert spaces. Let* $H_k \in L(\mathbf{X}, \mathbf{Y})$ *be a time-varying linear observation operator. Let* $M_k \in L(\mathbf{X})$ *be a time-varying linear model operator.*

As a first step we shall define what is known as the true state of the system. We consider that the dynamical system is comprised of a linear dynamical flow equation and let $M_k^{(t)} \in L(\mathbf{X})$ be a true linear time-varying model operator which maps a state $\mathbf{x}_k^{(t)} \in \mathbf{X}$ onto the state $\mathbf{x}_{k+1}^{(t)}$ for $k \in \mathbb{N}_0$, where $\mathbf{X}$ represents a Hilbert space. The mapping is a discrete-time evolution where the true state is defined as,

$$\mathbf{x}_{k+1}^{(t)} = M_k^{(t)} \mathbf{x}_k^{(t)}, \tag{4.1}$$

for $\mathbf{x}_k^{(t)} \in \mathbf{X}$ for $k \in \mathbb{N}_0$. Here we have used the notation $M_k^{(t)}$ and $\mathbf{x}_k^{(t)}$, whereby we remark that t here refers to the true linear system operator and true state respectively.

With this definition of the true state we are now able to consider the analysis error. The analysis error and the notion of stability in the context of cycled data assimilation schemes are defined as follows.

Definition 4.1.2. The analysis error $\mathbf{e}_k$ is defined as the difference between the analysis $\mathbf{x}_k^{(a)}$ and the true state of the system $\mathbf{x}_k^{(t)}$, such that

$$\mathbf{e}_k := \mathbf{x}_k^{(a)} - \mathbf{x}_k^{(t)} \tag{4.2}$$

at time $k \in \mathbb{N}_0$.

Definition 4.1.3. We call the data assimilation scheme stable if the analysis error $\mathbf{e}_k$ from (4.2) is bounded, such that

$$\limsup_{k \to \infty} \|\mathbf{e}_k\| = c < \infty, \tag{4.3}$$

given some positive constant c. We call the data assimilation scheme unstable if the analysis error $\mathbf{e}_k$ from (4.2) is unbounded, such that

$$\limsup_{k \to \infty} \|\mathbf{e}_k\| = \infty. \tag{4.4}$$

We now consider the evolution of the analysis error. In Section 3 we showed that the data assimilation schemes which we consider, take the form of cycled Tikhonov-Phillips regularization in Theorem 3.1.10. We assume that we have a modelled linear model operator $M_k : \mathbf{X} \to \mathbf{X}$ such that,

$$\left(M_k - M_k^{(t)}\right) \mathbf{x}_k^{(t)} = \boldsymbol{\zeta}_{k+1}, \tag{4.5}$$

where $\boldsymbol{\zeta}_k$ is some additive noise which we call *model error* for $k \in \mathbb{N}_0$. We require that the noise $\boldsymbol{\zeta}_k$ be bounded by some constant $\upsilon > 0$ for $k \in \mathbb{N}_0$.

We assume that we have a true linear observation operator $H_k^{(t)}$, such that $H_k^{(t)} : \mathbf{X} \to \mathbf{Y}$ maps elements in the Hilbert space $\mathbf{X}$ into a Hilbert space $\mathbf{Y}$. Here we state that the true observations $\mathbf{y}_k^{(t)} \in \mathbf{Y}$ are located at discrete-times k, linearly such that

$$\mathbf{y}_k^{(t)} = H_k^{(t)} \mathbf{x}_k^{(t)}, \tag{4.6}$$

for $k \in \mathbb{N}_0$, where $\mathbf{x}_k^{(t)}$ represents the true state of the system. In addition, we assume that we have a modelled linear time-varying observation operator $H_k : \mathbf{X} \to \mathbf{Y}$ such that

$$\left(H_k - H_k^{(t)}\right) \mathbf{x}_k^{(t)} = \boldsymbol{\omega}_k, \tag{4.7}$$

where $\boldsymbol{\omega}_k$ is some additive noise, which we call the *observation operator error*. We also require that the noise $\boldsymbol{\omega}_k$ be bounded by some constant $\gamma > 0$ for $k \in \mathbb{N}_0$. We assume that the given observations $\mathbf{y}_k \in \mathbf{Y}$ take the form

$$\mathbf{y}_k = \mathbf{y}_k^{(t)} + \boldsymbol{\eta}_k, \tag{4.8}$$

where $\boldsymbol{\eta}_k$ is some additive noise which we call the *observation error* for $k \in \mathbb{N}_0$. Similarly to the model error, we require that the noise $\boldsymbol{\eta}_k$ is bounded by some constant $\delta > 0$ for $k \in \mathbb{N}_0$.

Throughout this work, the noise terms that we have described in (4.5), (4.7) and (4.8) are only assumed to be bounded by the respective constants υ, γ and δ. There are no more assumptions on these noise terms. We remark that we can follow through our same analysis in Chapter 6, Chapter 7 and Chapter 8 assuming that the additive noise terms in (4.5), (4.7) and (4.8) are constant in time. This approach can be found in [57] and is less general than what we consider in this thesis.

In order to obtain an estimate for the analysis error at time k, we subtract the true state of the system $\mathbf{x}_k^{(t)}$ from both sides of (3.24) and substitute for linear model dynamics M_{k-1},

such that

$$\mathbf{x}_k^{(a)} - \mathbf{x}_k^{(t)} = M_{k-1}\mathbf{x}_{k-1}^{(a)} + \mathscr{R}_{\alpha,k}\left(\mathbf{y}_k - H_k M_{k-1}\mathbf{x}_{k-1}^{(a)}\right) - \mathbf{x}_k^{(t)}, \tag{4.9}$$

where $\mathscr{R}_{\alpha,k} = (\alpha I + H_k^* H_k)^{-1} H_k^* \in L(\mathbf{Y}, \mathbf{X})$. We substitute (4.8) into (4.9)

$$\mathbf{x}_k^{(a)} - \mathbf{x}_k^{(t)} = M_{k-1}\mathbf{x}_{k-1}^{(a)} + \mathscr{R}_{\alpha,k}\left(\mathbf{y}_k^{(t)} + \boldsymbol{\eta}_k - H_k M_{k-1}\mathbf{x}_{k-1}^{(a)}\right) - \mathbf{x}_k^{(t)}. \tag{4.10}$$

Now we can input (4.6) into (4.10)

$$\mathbf{x}_k^{(a)} - \mathbf{x}_k^{(t)} = M_{k-1}\mathbf{x}_{k-1}^{(a)} + \mathscr{R}_{\alpha,k}\left(H_k^{(t)}\mathbf{x}_k^{(t)} + \boldsymbol{\eta}_k - H_k M_{k-1}\mathbf{x}_{k-1}^{(a)}\right) - \mathbf{x}_k^{(t)}. \tag{4.11}$$

Then we rewrite the model state using (4.1)

$$\begin{aligned}\mathbf{x}_k^{(a)} - \mathbf{x}_k^{(t)} = {} & M_{k-1}\mathbf{x}_{k-1}^{(a)} + \mathscr{R}_{\alpha,k}\left(H_k^{(t)} M_{k-1}^{(t)}\mathbf{x}_{k-1}^{(t)} + \boldsymbol{\eta}_k - H_k M_{k-1}\mathbf{x}_{k-1}^{(a)}\right) \\ & - M_{k-1}^{(t)}\mathbf{x}_{k-1}^{(t)}.\end{aligned} \tag{4.12}$$

Using the substitution

$$\begin{aligned}H_k^{(t)} M_{k-1}^{(t)}\mathbf{x}_{k-1}^{(t)} - H_k M_{k-1}\mathbf{x}_{k-1}^{(a)} = {} & \left(H_k^{(t)} - H_k\right) M_{k-1}^{(t)}\mathbf{x}_{k-1}^{(t)} \\ & + H_k\left(M_{k-1}^{(t)}\mathbf{x}_{k-1}^{(t)} - M_{k-1}\mathbf{x}_{k-1}^{(a)}\right),\end{aligned} \tag{4.13}$$

we can rearrange (4.12) so that

$$\begin{aligned}\mathbf{x}_k^{(a)} - \mathbf{x}_k^{(t)} = {} & M_{k-1}\mathbf{x}_{k-1}^{(a)} - M_{k-1}^{(t)}\mathbf{x}_{k-1}^{(t)} + \mathscr{R}_{\alpha,k}\boldsymbol{\eta}_k \\ & + \mathscr{R}_{\alpha,k}\left(\left(H_k^{(t)} - H_k\right) M_{k-1}^{(t)}\mathbf{x}_{k-1}^{(t)}\right. \\ & \left. + H_k\left(M_{k-1}^{(t)}\mathbf{x}_{k-1}^{(t)} - M_{k-1}\mathbf{x}_{k-1}^{(a)}\right)\right).\end{aligned} \tag{4.14}$$

In a similar way to (4.13), we can use the substitution

$$\begin{aligned}M_{k-1}\mathbf{x}_{k-1}^{(a)} - M_{k-1}^{(t)}\mathbf{x}_{k-1}^{(t)} = {} & M_{k-1}\left(\mathbf{x}_{k-1}^{(a)} - \mathbf{x}_{k-1}^{(t)}\right) \\ & + \left(M_{k-1} - M_{k-1}^{(t)}\right)\mathbf{x}_{k-1}^{(t)},\end{aligned} \tag{4.15}$$

so that (4.14) becomes

$$\begin{aligned}\mathbf{x}_k^{(a)} - \mathbf{x}_k^{(t)} = {} & M_{k-1}\left(\mathbf{x}_{k-1}^{(a)} - \mathbf{x}_{k-1}^{(t)}\right) + \left(M_{k-1} - M_{k-1}^{(t)}\right)\mathbf{x}_{k-1}^{(t)} + \mathscr{R}_{\alpha,k}\boldsymbol{\eta}_k \\ & + \mathscr{R}_{\alpha,k}\left(\left(H_k^{(t)} - H_k\right) M_{k-1}^{(t)}\mathbf{x}_{k-1}^{(t)} - H_k M_{k-1}\left(\mathbf{x}_{k-1}^{(a)} - \mathbf{x}_{k-1}^{(t)}\right)\right. \\ & \left. - H_k\left(M_{k-1} - M_{k-1}^{(t)}\right)\mathbf{x}_{k-1}^{(t)}\right).\end{aligned} \tag{4.16}$$

We rearrange (4.16) and input (4.5) and (4.7) so that

$$\mathbf{x}_k^{(a)} - \mathbf{x}_k^{(t)} = (I - \mathscr{R}_{\alpha,k} H_k)\, M_{k-1} \left(\mathbf{x}_{k-1}^{(a)} - \mathbf{x}_{k-1}^{(t)} \right) + \mathscr{R}_{\alpha,k} \boldsymbol{\eta}_k + (I - \mathscr{R}_{\alpha,k} H_k)\, \boldsymbol{\zeta}_k - \mathscr{R}_{\alpha,k} \boldsymbol{\omega}_k. \tag{4.17}$$

Using (4.2) in Definition 4.1.2, we rewrite (4.17) such that

$$\mathbf{e}_k = (I - \mathscr{R}_{\alpha,k} H_k)\, M_{k-1} \mathbf{e}_{k-1} + \mathscr{R}_{\alpha,k} \boldsymbol{\eta}_k + (I - \mathscr{R}_{\alpha,k} H_k)\, \boldsymbol{\zeta}_k - \mathscr{R}_{\alpha,k} \boldsymbol{\omega}_k. \tag{4.18}$$

Here in (4.18) we see the errors in each term which are classified as follows:

A. error from the *Tikhonov-Phillips inverse* $\mathscr{R}_{\alpha,k}$ which is not identical to H_k^{-1};

B. cumulated errors from *previous iterations/cycling*;

C. error in the *observational data* $\mathbf{y}_k$;

D. error in the *model dynamics* M_k;

E. error in the *observation operator* H_k.

We identify the role of these different types of errors,

$$\mathbf{e}_k = \underbrace{(I - \mathscr{R}_{\alpha,k} H_k)}_{\text{A.}}\, M_{k-1} \underbrace{\mathbf{e}_{k-1}}_{\text{B.}} + \mathscr{R}_{\alpha,k} \underbrace{\boldsymbol{\eta}_k}_{\text{C.}} + (I - \mathscr{R}_{\alpha,k} H_k) \underbrace{\boldsymbol{\zeta}_k}_{\text{D.}} - \mathscr{R}_{\alpha,k} \underbrace{\boldsymbol{\omega}_k}_{\text{E.}}. \tag{4.19}$$

For convenience we will often write

$$\Lambda_k := (I - \mathscr{R}_{\alpha,k} H_k) M_{k-1}. \tag{4.20}$$

The form we have obtained in (4.19) has been investigated in the control/systems theory community since the 1960s. We now discuss the literature on the analysis error in the case of finite dimensional linear dynamical systems.

4.2 Finite dimensional linear systems

In this section we present the literature associated with the cycled Tikhonov-Phillips regularization in (3.24) and its error evolution in (4.19). As we described in Chapter 3, we consider in this work both linear and nonlinear model dynamics. Here we first consider the analysis error in the case of linear finite dimensional dynamical systems.

4.2.1 Time-invariant observer system

In a finite dimensional setting, control and systems theory call the method of data assimilation *state estimation*. The analysis error has many names in the literature such as state reconstruction error, observer error and estimation error. As we discussed in Chapter 3, the data assimilation schemes take the form of cycled Tikhonov-Phillips regularization. Therefore, from Theorem 3.1.10 we saw that cycled Tikhonov-Phillips regularization can be written as (3.24). In the control theory community, the form (3.24), is a variant of a *Luenberger observer*, named after David Luenberger; see [54] and [55]. For a deterministic system, an observer reconstructs the state ensuring that the analysis error is stable for all time. For a noise-free system, an observer will reconstruct the current state of the system. We shall begin with the most simple case of a time-invariant linear system. Let us introduce a discrete time-invariant finite dimensional linear system of the following form,

$$\mathbf{x}_k^{(t)} = M\mathbf{x}_{k-1}^{(t)} \tag{4.21}$$

$$\mathbf{y}_k = H\mathbf{x}_k^{(t)}, \tag{4.22}$$

where $\mathbf{x}_k^{(t)} \in \mathbf{X} = \mathbb{R}^n$, $\mathbf{y}_k \in \mathbf{Y} = \mathbb{R}^m$ with $n, m \in \mathbb{N}$ and $M \in L(\mathbf{X})$, $H \in L(\mathbf{X}, \mathbf{Y})$. Much theory has been developed for this system in terms of stability due to its simplicity. We now present one definition and one theorem, which is important to explain Luenberger's stability result in Theorem 4.2.3. For a linear finite dimensional system the notion of asymptotic stability is as follows and is taken from [6, p.170].

Definition 4.2.1. The discrete-time linear time-invariant system

$$\mathbf{x}_k = \Lambda\mathbf{x}_{k-1}, \tag{4.23}$$

where $\Lambda \in L(\mathbf{X} = \mathbb{R}^n)$ is a real $n \times n$ matrix is called *asymptotically stable* if $\mathbf{x}_k \to \mathbf{0}$ as $k \to \infty$ for all $\mathbf{x}_0 \in \mathbf{X} = \mathbb{R}^n$.

The following theorem give a necessary condition to ensure asymptotic stability. Here we present the finite dimensional form, which we will require for the infinite dimensional case later on.

Theorem 4.2.2. *The discrete-time linear time-invariant system*

$$\mathbf{x}_k = \Lambda \mathbf{x}_{k-1}, \tag{4.24}$$

where $\Lambda \in L(\mathbf{X} = \mathbb{R}^n)$ is a real matrix is asymptotically stable if and only if the eigenvalues of Λ lie in the open unit disc.

Proof. See Theorem 5.8 [6] or Lemma D.3.1 [38] or Theorem 4.1.2 [34]. □

To reconstruct the state $\mathbf{x}_k^{(a)}$ from the observations $\mathbf{y}_k$ for the system in (4.21) and (4.22), we have the Luenberger observer, which takes the following form,

$$\mathbf{x}_k^{(a)} = M\mathbf{x}_{k-1}^{(a)} + \mathscr{R}_\alpha \left(\mathbf{y}_{k-1} - H\mathbf{x}_{k-1}^{(a)} \right), \tag{4.25}$$

where $\mathscr{R}_\alpha$ is the known as the observer gain.

Before presenting the important stability result, we first observe several differences between the Luenberger observers in (4.25) and (3.24). The system in (4.21) and (4.22), which the Luenberger observer reconstructs, assumes no additive noise on the observations, model or observation operator. Often in the literature the Luenberger observer is referred to as a deterministic device to reconstruct the state of the system [64]. Furthermore, the Luenberger observer assimilates observations at a different time-step to that of the cycled Tikhonov-Phillips scheme. This mismatch in observations and model state is known as a *delay* in the control theory community, and leads to a slightly different error equation formulation as we will see. From (4.25) we substitute the observation $\mathbf{y}_{k-1}$ for the true observations $H\mathbf{x}_{k-1}^{(t)}$ such that,

$$\mathbf{x}_k^{(a)} = M\mathbf{x}_{k-1}^{(a)} + \mathscr{R}_\alpha \left(H\mathbf{x}_{k-1}^{(t)} - H\mathbf{x}_{k-1}^{(a)} \right). \tag{4.26}$$

Now subtracting the true state $\mathbf{x}_k^{(t)}$ from both sides, from (4.26) we obtain

$$\mathbf{x}_k^{(a)} - \mathbf{x}_k^{(t)} = M\mathbf{x}_{k-1}^{(a)} - \mathbf{x}_k^{(t)} + \mathscr{R}_\alpha \left(H\mathbf{x}_{k-1}^{(t)} - H\mathbf{x}_{k-1}^{(a)} \right). \tag{4.27}$$

Substituting $\mathbf{x}_k^{(t)}$ for $M\mathbf{x}_{k-1}^{(t)}$ and defining $\mathbf{e}_k := \mathbf{x}_k^{(a)} - \mathbf{x}_k^{(t)}$ we obtain the error equation for the time-invariant Luenberger observer as follows,

$$\mathbf{e}_k = (M - \mathscr{R}_\alpha H)\, \mathbf{e}_{k-1}. \tag{4.28}$$

We briefly mention the difference between (4.28) and (4.18). (4.28) does not have any noise terms. This is expected since the Luenberger observer is a noise-free deterministic reconstructor of the state of the system. Furthermore we observe that the operator evolving the previous error in (4.28) is different from that in (4.18). This is due to the Luenberger assimilating observations at a different time-step to the cycled Tikhonov-Phillips scheme, which we have already mentioned. Therefore, the error evolution of our cycled data assimilation scheme is slightly different and hence the stability result for the Luenberger observer does not directly apply to the problem we are interested in solving.

In control theory the observer gain in (4.25) is chosen such that the error equation for the Luenberger observer in (4.28) is asymptotically stable. The stability result in Theorem 4.2.3 relies on the dynamical system in (4.21) and (4.22) being completely observable. A dynamical system is called completely observable if all initial states can be uniquely determined given the observed data [6]. As we will see in future chapters, our analysis does not follow the direction of observability for the following two reasons. Firstly, it is difficult to ascertain observability conditions in an infinite dimensional linear setting [12]. Secondly, observability conditions are less established for infinite dimensional nonlinear dynamical systems [65]. Therefore, in this work we do not focus on the control theory approach of seeking an observability condition on the dynamical system. However for completeness, a formal definition of observability can be found in [6].

The following stability result is fundamental part of linear control theory and is due to Luenberger [54], [55]. This approach to show stability is known as *eigenvalue assignment*. This means that the eigenvalues can be placed not only to ensure stability, but also to determine the rate of the decay in (4.28). Here we present the following theorem formally, since we will parallel our work with this important result in future chapters.

Theorem 4.2.3. *Given linear time-invariant operators $M \in L(\mathbf{X} = \mathbb{R}^n)$ and $H \in L(\mathbf{X} = \mathbb{R}^n)$ from (4.21) and (4.22) respectively, then there exists an observer gain $\mathscr{R}_\alpha$ such that the eigenvalues of $M - \mathscr{R}_\alpha H$ can be arbitrarily assigned if and only if the system in (4.21) and (4.22) is completely observable.*

Proof. See Theorem 1.16 [64] or Theorem 28.10 [72] or Theorem 9.3.2 [15]. □

As we have seen, the concept of observability is crucial in assigning the eigenvalues of the

operator $M - \mathscr{R}_\alpha H$, so that asymptotic stability can be assured according to Theorem 4.2.2. We now move to the more interesting situation of a time-varying linear system.

4.2.2 Time-varying observer system

Similar to the system in (4.21) and (4.22), the discrete time-varying finite dimensional linear system takes the following form,

$$\mathbf{x}_k^{(t)} = M_{k-1}\mathbf{x}_{k-1}^{(t)} \tag{4.29}$$

$$\mathbf{y}_k = H_k\mathbf{x}_k^{(t)}, \tag{4.30}$$

where now the linear operators have a time dependence. The work of [11] has showed that if the model operator is invertible for all time and the finite dimensional time-varying linear system is uniformly completely observable then an observer gain can be chosen so that the time-varying observer system is stable. This result can be found here in [11, Theorem D.1]. The work of [61] has relaxed the assumption that the model operator must be invertible. A definition of of uniform complete observability can be found in [72].

It is often mentioned in the literature that an observer system can be seen as a deterministic representation of the Kalman filter [15]. We now discuss this statistically optimal observer.

4.2.3 Optimal time-varying observer system

In the previous section we discussed observer systems. Now we turn our attention to systems which are optimal in some statistical sense. The Kalman filter is an observer system that has been optimised with respect to errors in both the model dynamics and observations. Let the discrete time-varying finite dimensional linear system take the following form,

$$\mathbf{x}_k^{(t)} = M_{k-1}\mathbf{x}_{k-1}^{(t)} + \Gamma_{k-1}\boldsymbol{\zeta}_{k-1} \tag{4.31}$$

$$\mathbf{y}_k = H\mathbf{x}_k^{(t)} + \boldsymbol{\eta}_k \tag{4.32}$$

where $\mathbf{x}_k^{(t)} \in \mathbf{X} = \mathbb{R}^n$, $\mathbf{y}_k \in \mathbf{Y} = \mathbb{R}^m$ with $n, m \in \mathbb{N}$, M_{k-1} is an $n \times n$ matrix, Γ_{k-1} is a time dependent $n \times o$ matrix for $n, o \in \mathbb{N}$ and $H \in L(\mathbf{X}, \mathbf{Y})$. We note that here we only consider the time-invariant observation operator $H \in L(\mathbf{X}, \mathbf{Y})$ despite the Kalman filter being more

general. Both $\boldsymbol{\zeta}_{k-1} \in \mathbb{R}^o$ and $\boldsymbol{\eta}_k \in \mathbb{R}^m$ are normally distributed elements with mean zero and covariance operators $\mathscr{Q}_{k-1}$ and R_k respectively. It is well known that under these statistical assumptions, the Kalman filter is optimal [40]. Here optimal means that the Kalman filter mean produces an analysis which is closest to the truth in a root mean square (RMS) sense, such that it is a *minimum variance estimator*. Therefore, the analysis covariance matrix $B_k^{(a)}$ at time k from (3.22) will have the smallest trace. A definition of RMS error can be found in [5, p.7]. In 1960, Kalman showed under certain conditions that for a finite dimensional state space, the continuous-time Kalman filter is stable [39, Theorem 6.10 and 7.2] or [40, Theorem 4]. Soon after, it was shown that the finite dimensional discrete-time Kalman filter is also stable under certain conditions ([21], [35, Theorem 7.4]). This stability result was under a number of conditions, such that:

1. the system in (4.31) and (4.32) must be uniformly completely observable and uniformly completely controllable; see [35, p.232-233] for details on uniform complete controllability;

2. the state transition matrix in (4.31) must be bounded with bounded inverse;

3. the errors in the observations and model must be normally distributed with respective bounded error covariance matrices for all time k;

4. the initial background error covariance matrix, $B_0^{(a)}$ in Definition 3.1.7 must be positive.

This stability result has been generalised by relaxing the assumption that state transition matrix in (4.31) must have a bounded inverse [61]. We now move onto discussing the literature associated with nonlinear finite dimensional systems.

4.3 Finite dimensional nonlinear systems

Here we consider work related to finite dimensional nonlinear systems. With the added complexity of nonlinear dynamics comes a difficulty in establishing rigorous analytical theory on the stability of observer systems. Previous work from the literature used the technique of linearisation to overcome the challenge of analysing nonlinear observers. When linearising,

one must argue that higher order terms are somehow negligible in the estimates of the behaviour of the analysis error. This of course is not true of highly nonlinear systems.

The work of [2] showed that employing a first order Taylor expansion and neglecting higher order terms, they could obtain a stable evolution of the analysis error in accordance with linear observer theory developed previously by [54], [40] and [21].

The work of [44] considered a nonlinear time-invariant continuous-time dynamical system of the following form,

$$\dot{\mathbf{x}}^{(t)}(k) = \tilde{\mathcal{M}}\left(\mathbf{x}^{(t)}(k)\right) \tag{4.33}$$

$$\mathbf{y}(k) = \tilde{\mathcal{H}}\left(\mathbf{x}^{(t)}(k)\right) \tag{4.34}$$

with $\mathbf{x}^{(t)}(k) \in \mathbb{R}^n$, $\mathbf{y}(k) \in \mathbb{R}^m$ where $\tilde{\mathcal{M}} : \mathbb{R}^n \to \mathbb{R}^n$ and $\tilde{\mathcal{H}} : \mathbb{R}^n \to \mathbb{R}^m$ are continuous nonlinear operators. They showed that if the nonlinear operator $\tilde{\mathcal{M}}$ is comprised of nonlinear perturbations to a linear operator, then an observer gain can be chosen so that the nonlinear observer is asymptotically stable [44, Theorem 2]. It is stated in [64] that the conditions for [44, Theorem 2] to hold are conservative. Moreover, [64] states that the work of [44] does not demonstrate a constructive procedure for choosing such an observer gain to ensure stability. This highlights the difficulty in analysing general nonlinear systems [64]. The work of [4] has generalised the work of [44] by considering an operator $\tilde{\mathcal{M}}$ that is comprised of nonlinear perturbations to a particular nonlinear operator. The nonlinear perturbations are assumed to be Lipschitz continuous, which is the assumption we make in Chapter 8.

The work of [82] showed stability for a nonlinear stochastic observer system. Let a stochastic discrete time-invariant finite dimensional nonlinear system be defined as follows,

$$\mathbf{x}_k^{(t)} = \mathcal{M}\left(\mathbf{x}_{k-1}^{(t)}\right) + A^{(1)}\left(\mathbf{x}_{k-1}^{(t)}\right)\boldsymbol{\zeta}_{k-1}, \tag{4.35}$$

$$\mathbf{y}_k = \mathcal{H}\left(\mathbf{x}_k^{(t)}\right) + A^{(2)}\left(\mathbf{x}_k^{(t)}\right)\boldsymbol{\eta}_k, \tag{4.36}$$

where $\mathbf{x}_k \in \mathbb{R}^n$, $\mathbf{y}_k \in \mathbb{R}^m$, $\mathcal{M}(\cdot), \mathcal{H}(\cdot)$ are continuously differentiable nonlinear operators, $\boldsymbol{\zeta}_{k-1}$, $\boldsymbol{\eta}_k$ are normalised, mean zero, uncorrelated Gaussian random variables for $k \in \mathbb{N}$ and $A^{(1)}(\mathbf{x}_{k-1})$, $A^{(2)}(\mathbf{x}_k)$ are error covariance matrices of an appropriate dimension. Their main result in [82, Theorem 4] showed that if the error covariance matrices $A^{(1)}(\mathbf{x}_{k-1})$ and $A^{(2)}(\mathbf{x}_k)$ are bounded for $k \in \mathbb{N}$ then an observer gain exists and the nonlinear stochastic observer is stable.

In the data assimilation literature, the work of [81] considered the convergence of a particular type of 4DVar scheme for a weakly nonlinear dynamical system. They considered a criterion for convergence using the amplification matrix, which arose from a linearisation of the nonlinear model dynamics. The work of [33] extended this criterion to sequential data assimilation schemes from the variational setting in [81], and provided numerical experiments of the behaviour of the analysis error. Their work again assumed that the error evolution can be adequately represented using a linearisation of the nonlinear dynamics.

Finally, the work in [77] considered the stability of an observer for a general discrete-time nonlinear system. They provided an alternative proof to that of [21], for the finite dimensional Kalman filter. Furthermore, they extended their stability result for the Kalman filter and showed that the extended Kalman filter may be stable under given conditions [77, Theorem 3.2]. This stability result showed convergence of the nonlinear observer under the following assumptions:

1. the nonlinearity in the system must be weak such that higher order terms from a Taylor expansion are negligible;

2. the linearised nonlinear system must satisfy an observability rank condition to ensure the error covariance matrices remain bounded over time;

3. the states of the system must behave in an appropriate way; further details on this behaviour can be found in [77, Assumption 3.1].

Details on the extended Kalman filter can be found in [35]. Now we consider stability results for infinite dimensional linear systems.

4.4 Infinite dimensional linear systems

Work on infinite dimensional linear dynamical systems has proved stability of observer systems using the semigroup approach. For a detailed introduction to semigroups see [19]. Notably [18] developed many results from the finite dimensional setting into the infinite dimensional setting. They considered the system dynamics in terms of a strongly continuous semigroup on an appropriate Banach space. Their work, like others, including [9] and [48]

focused on the continuous stochastical derivation, with particular attention to optimal state estimation, the Kalman filter. Here we state a significant deterministic result from [19] in the continuous-time setting, given the following class of deterministic infinite dimensional systems,

$$\dot{\mathbf{x}}(k) = \tilde{M}\mathbf{x}(k) \tag{4.37}$$

$$\mathbf{y}(k) = \tilde{H}\mathbf{x}(k), \tag{4.38}$$

where $\tilde{M}$ is an infinitesimal generator of the strongly continuous semigroup $T(k)$ on a Hilbert space $\mathbf{X}$ and $\tilde{H} \in L(\mathbf{X}, \mathbf{Y})$ such that $\mathbf{Y}$ is also a Hilbert space. See [19] for the definition of an infinitesimal generator. An infinite dimensional Luenberger observer for this system is given by,

$$\dot{\mathbf{x}}^{(a)}(k) = \tilde{M}\mathbf{x}^{(a)}(k) + \mathscr{R}_\alpha \left(\mathbf{y}(k) - \tilde{H}\mathbf{x}^{(a)}(k)\right), \tag{4.39}$$

where $\mathscr{R}_\alpha \in L(\mathbf{X}, \mathbf{Y})$. Here we state the following result which shows that if an observer gain can be chosen in a particular way, then the analysis error will asymptotically tend to zero.

Lemma 4.4.1. *Consider the linear system in (4.37), (4.38) and a corresponding Luenberger observer given by (4.39). If $\mathscr{R}_\alpha$ is such that*

$$\hat{\Lambda} := \tilde{M} - \mathscr{R}_\alpha \tilde{H} \tag{4.40}$$

generates an exponentially stable strongly continuous semigroup, then the approximation error $\mathbf{e}(k) := \mathbf{x}(k) - \mathbf{x}^{(t)}(k)$ converges exponentially to zero as $k \to \infty$.

Proof. See Lemma 5.3.2 in [19]. □

In Section 7.1 we will show that we can choose an observer gain $\mathscr{R}_\alpha$ so that the analysis error of a linear discrete time-invariant observer system is asymptotically stable. Our stability result in Section 7.1 will show that for a particular choice of observer gain, the bound on the analysis error consists of error terms arising from the dynamical system.

The generalisations of finite dimensional results for assumed controllable and observable Gramians, into an infinite dimensional setting can be found in [32]. Their main stability result in [32, Theorem 4] showed stability of the infinite dimensional time-invariant observer

$$\mathbf{x}_k^{(a)} = M\mathbf{x}_{k-1}^{(a)} + \mathscr{K}\left(\mathbf{y}_k - H\mathbf{x}_{k-1}^{(a)}\right), \tag{4.41}$$

where $\mathscr{K} \in L(\mathbf{Y}, \mathbf{X})$ is the time-invariant Kalman gain operator from (3.28). This result is under certain positivity conditions, see [32, Section 3] for further details. Their work is an infinite dimensional extension of the finite dimensional results in [21]. The work of [32] also extends their stability result to time-varying systems, and can be found in [32, Appendix A].

The work of [74] has generalised the infinite dimensional results of [32] by relaxing strong conditions on the controllability. Their main result showed that the no-noise analysis error equation,

$$\mathbf{e}_k = (I - \mathscr{K}_k H_k) M_{k-1} \mathbf{e}_{k-1}, \tag{4.42}$$

where $\mathscr{K}_k = B_k^{(b)} H_k^* \left(H_k B_k^{(b)} H_k^* + R_k \right)^{-1}$ is the time-varying Kalman gain operator, is asymptotically stable in the sense that $\limsup_{k\to\infty} \|\mathbf{e}_k\| = 0$. Their main result, [74, Theorem 5.1], assumes bounds on the model dynamics M_k, a linear time-varying observation operator H_k, a time-varying linear background error covariance operator B_k, bounds on the observation error covariance and uniform complete observability. In Chapter 7 we extend this result by relaxing the observability condition in [74], allowing for noise in the dynamical system and assuming a number of positivity conditions on the covariance operators.

Most recently, the work of [57] has considered linear observers for time-invariant linear systems with constant observation noise. The linear time-invariant system takes the following form

$$\mathbf{x}_k = M \mathbf{x}_{k-1} \tag{4.43}$$

$$\mathbf{y}_k = H \mathbf{x}_k + \boldsymbol{\eta} \tag{4.44}$$

given a constant observation error $\boldsymbol{\eta} \in \mathbf{Y}$, where $M \in L(\mathbf{X})$ and $H \in L(\mathbf{X}, \mathbf{Y})$ for Banach spaces $\mathbf{X}$ and $\mathbf{Y}$. Then the linear observer takes the following form

$$\mathbf{x}_k^{(a)} = M \mathbf{x}_{k-1}^{(a)} + \mathscr{R}_\alpha \left(\mathbf{y}_k - H M \mathbf{x}_{k-1}^{(a)} \right) \tag{4.45}$$

where $\mathscr{R}_\alpha = (\alpha I + H^* H)^{-1} H^* \in L(\mathbf{Y}, \mathbf{X})$ is the observer gain. They considered the convergence of the linear observer for constant model dynamics, $M = I$. They showed in [57, Lemma 3.3] that given an injective linear observation operator H, if the constant observation error lies in the range of the observation operator, then the observer in (4.45) converges as time tends to infinity. Conversely, if the constant observation error does not lie in the range of the observation operator, then the observer in (4.45) diverges as time tends to infinity.

The work of [57] went further and represented the linear observer system spectrally in a Hilbert space setting. They suggested how the observer would asymptotically behave for spectrally expanding and damping diagonal dynamics, with respect to the observation operator. We formally present our results in this direction later in Chapter 6.

4.5 Infinite dimensional nonlinear systems

In this section we discuss one of the most recent results in infinite dimensional nonlinear filtering. Closely related to our work, [7] have considered the stability of observers for infinite dimensional nonlinear systems, developing theoretical results for the 2D incompressible Navier-Stokes equations.

In their work, [7] developed theory for the particular Navier-Stokes system, where the observation operator and the Stokes operator commute. They consider two types of observations, complete and partial. Here we focus on the partial observations case since it is most relevant to the work in this thesis. We state their result explicitly since we derive similar results in Chapter 6 and Chapter 8. Let $\mathbf{X}$ be a Hilbert space and let $H^{(1)} : \mathbf{X} \to \mathbf{X}$ and $H^{(2)} : \mathbf{X} \to \mathbf{X}$ be orthogonal projection operators, where $H^{(2)} = I - H^{(1)}$, and $H^{(1)}$ projects an element $\mathbf{x} \in \mathbf{X}$ onto a space spanned by the lower spectral modes of H in accordance with Section 2.1.4. The discrete time-invariant infinite dimensional nonlinear system takes the following form,

$$\mathbf{x}_k = \mathcal{M}(\mathbf{x}_{k-1}) \tag{4.46}$$

$$\mathbf{y}_k = H^{(1)}\mathbf{x}_k + \boldsymbol{\eta}_k \tag{4.47}$$

where $\mathbf{x} \in \mathbf{X}$ and $\boldsymbol{\eta}_k$ is some sequence satisfying $\sup_{k\geq 1} \|\boldsymbol{\eta}_k\| \leq \delta$. The observer gain takes the form,

$$\mathscr{R}_{\alpha,k} := B_k H^{(1)*} \left(H^{(1)} B_k H^{(1)*} + \alpha R_k\right)^{-1} \tag{4.48}$$

where B_k and R_k are two sequences of operators that weight the background state and observations respectively and $\alpha = 1$. Both sequences of operators are assumed to be strictly positive. The nonlinear observer then becomes,

$$\mathbf{x}_k^{(a)} = N_{\alpha,k}\mathcal{M}\left(\mathbf{x}_{k-1}^{(a)}\right) + \mathscr{R}_{\alpha,k}\mathbf{y}_k \tag{4.49}$$

where $N_{\alpha,k} := I - \mathscr{R}_{\alpha,k}H^{(1)}$. The following assumption on the family of operators $N_{\alpha,k}$ is necessary to present the main result of [7].

Assumption 4.5.1. *The family of positive operators $\{N_{\alpha,k}\}$ commutes with the Stokes operator A, $\sup_{k\geq 1}\|N_{\alpha,k}\| \leq 1$, $\sup_{k\geq 1}\|\mathscr{R}_{\alpha,k}\| \leq c$ for some $c \in \mathbb{R}^+$, uniformly with respect to α. Furthermore $\mathscr{R}_{\alpha,k}H^{(2)} = 0$ and there is a constant $d > 0$ such that $\sup_{k\geq 1}\|H^{(1)}N_{\alpha,k}\| \leq d\alpha^2$.*

Theorem 4.5.2. *Under Assumption 4.5.1, there is an α sufficiently small such that there exists a constant $0 < a < 1$, where*

$$\|\mathbf{e}_k\| \leq a^k + 2c\delta\sum_{j=0}^{k-1} a^j \tag{4.50}$$

and

$$\limsup_{k\to\infty}\|\mathbf{e}_k\| \leq \frac{2c\delta}{1-a}. \tag{4.51}$$

Proof. See Theorem 3.3 [7]. □

It was shown in [7] that the data assimilation scheme 3DVar satisfies Assumption 4.5.1, for static operators B and R which are fractional powers of the Stokes operator, and for an observation operator that commutes with the Stokes operator. Hence, they showed asymptotic stability for a cycled 3DVar scheme where the nonlinear model dynamics were governed by the 2D incompressible Navier-Stokes equations. In Chapter 6 we will show that if the observation operator H has the same orthonormal system as a compact linear self-adjoint model operator M then we can obtain a similar asymptotic result to [7, Theorem 3.3]. Our work in Chapter 8 will show the asymptotic stability of a cycled 3DVar scheme with a nonlinear dynamical model operator and a linear observation operator that are more general than considered in [7]. However, our result will depend upon a global dissipative assumption in the nonlinear model dynamics. A local dissipative assumption has been shown to hold for the Navier-Stokes equations in [7] for a particular observation operator. Moreover, in Chapter 7 and Chapter 8 we will show that we can satisfy similar bounds on the operators $N_{\alpha,k}$ and $\mathscr{R}_{\alpha,k}$ from Assumption 4.5.1 in the linear and nonlinear setting, for the data assimilation algorithms which we consider in Chapter 3.

4.6 Summary

In this chapter we have discussed the literature associated with the stability of the data assimilation schemes introduced in Chapter 3. We have seen that finite dimensional linear and nonlinear systems have been extensively studied since the 1960s. Stability results for the finite dimensional linear setting assume that the system satisfies various observability and controllability conditions. The finite dimensional nonlinear results assume that the nonlinear behaviour is locally linear in the sense that it can be adequately represented by a low order Taylor expansion. Therefore, this removes any nonlinearity in the error equations and results from the linear setting can be applied to show stability.

Stability results are less known in the infinite dimensional setting. This has led to more recent and ongoing research into the convergence of the analysis error and norm estimates. The work of both [57] and [7] showed rigorous mathematical results for specific dynamical systems. It was shown in [57] that a linear observer with constant model dynamics will converge in the infinite dimensional linear setting if the set of observations $\mathbf{y}_k \in \mathcal{S}(\mathbf{X})$. In the infinite dimensional nonlinear setting the work of [7] used norm estimates to show that the analysis error of a cycled 3DVar is bounded for all time in the case where the observation operator and the Stokes operator commute.

Our work in this thesis will develop original stability results for a wider class of infinite dimensional linear and nonlinear systems using norm estimates. Throughout this chapter we saw that various stability results have been obtained in the finite dimensional setting for systems which are observable and controllable. Our interest lies in the infinite dimensional setting. We discussed the work of [32], where the authors generalised results from the finite setting into the infinite setting under the assumption that the system remains observable and controllable. More recently, the work of [74] has investigated the evolution of the analysis error equation for infinite dimensional linear dynamical systems under observability and controllability assumptions. Furthermore, stability results have recently emerged for finite dimensional nonlinear observers that are Lipschitz continuous and satisfy nonlinear observability and controllability conditions; see [10], [75] and [58].

In this work we focus on developing stability results with norm estimates for infinite dimensional linear and nonlinear dynamical systems. We seek to develop stability results for

dynamical systems which are more general than those considered in [57] and [7]. However, in seeking stability results for general dynamical systems, we expect our results to be weaker compared with [57] in the linear setting and [7] in the nonlinear setting. In Chapter 6 and Chapter 7 we will study linear systems where the model dynamics are amplifying a finite number of modes and damping all sufficiently high modes. In Chapter 8 we will study nonlinear model dynamics that are Lipschitz continuous and dissipative on higher spectral modes. In particular, for both the linear and nonlinear setting we will derive new conditions on the regularization under which the cycled data assimilation schemes from Chapter 3 will remain stable over time. In the next chapter we introduce the dynamical models, which will be used to demonstrate numerically the theory developed in later chapters.

Chapter 5

Dynamical models

In this chapter we introduce two dynamical models which we will use to numerically demonstrate the theory developed in future chapters. The focus of this chapter is to provide the necessary details on the dynamical models that we have chosen, and the numerical schemes used to discretise them. We provide a brief overview of firstly a linear model, the two-dimensional Eady model which will be used to illustrate the linear results we develop in Chapter 6 and Chapter 7. Secondly, we provide a brief overview of a nonlinear model, the Lorenz 1963 model which will be used to illustrate the nonlinear results we develop in Chapter 8.

5.1 Two-dimensional Eady model

In this section, we consider a linear dynamical model where the model operator M arises from the discretisation of a system of partial differential equations. The system we consider is the two-dimensional Eady (2D Eady) model, a simple model of atmospheric instability; see [23] for a detailed introduction. The model is defined in the $x - z$ plane, with periodic boundary conditions in x and $z \in [-1/2, 1/2]$. The state vector consists of the nondimensional buoyancy b on the upper and lower boundaries and the nondimensional potential vorticity in the interior of the domain. For this work we restrict ourselves to the situation where the interior potential vorticity is zero. Therefore it is only necessary to consider the dynamics on the boundaries. The buoyancy is advected along the boundaries forced by the nondimensional

streamfunction ψ according to the following equation,

$$\frac{\partial b}{\partial t} + z\frac{\partial b}{\partial x} = \frac{\partial \psi}{\partial x} \tag{5.1}$$

on $z = \pm 1/2$, where the streamfunction satisfies,

$$\frac{\partial^2 \psi}{\partial x^2} + \frac{\partial^2 \psi}{\partial z^2} = 0 \tag{5.2}$$

in $z \in [-1/2, 1/2]$, with the Neumann boundary condition

$$\frac{\partial \psi}{\partial z} = b \tag{5.3}$$

on $z = \pm 1/2$. The equations are discretised with a leap-frog advection scheme as described in [36] and [37] using 40 grid points in the horizontal, giving 80 degrees of freedom. We acknowledge in this work that the code for the discretisation of the two-dimensional Eady model was developed by Dr. Christine Johnson, Prof. Nancy Nichols and Prof. Brian Hoskins. In our experiment we choose $\Delta x = 0.1$ and $\Delta t = 0.1728$, which corresponds to $\Delta x = 100$km and $\Delta t = 4320$s in its dimensionalised form. We run the model for 5 time-steps, giving us an 80×80 matrix M that corresponds to a 6 hour forecast of the Eady model. In Chapter 2 we introduced the singular system of a linear operator. The singular values of the 2D Eady model range as follows,

$$\mu(M) \approx (1.4293, \ldots, 0.6975) \tag{5.4}$$

with spectral radius $r(M) \approx 1.3066$. Here in Figure 5.1 and Figure 5.2 we plot the singular values and eigenvalues of M respectively.

We observe that the 2D Eady model has growing and damping spectral modes. Now we introduce the following nonlinear dynamical model.

5.2 Lorenz 1963 model

In this section we consider the Lorenz 1963 (Lorenz '63) system [52], which presents chaotic behaviour under the classical parameters; see [78] for further details. Even though these equations are finite dimensional they will still allow us to show the behaviour of the analysis error. Lorenz derived these equations from a Fourier truncation of the flow equations that

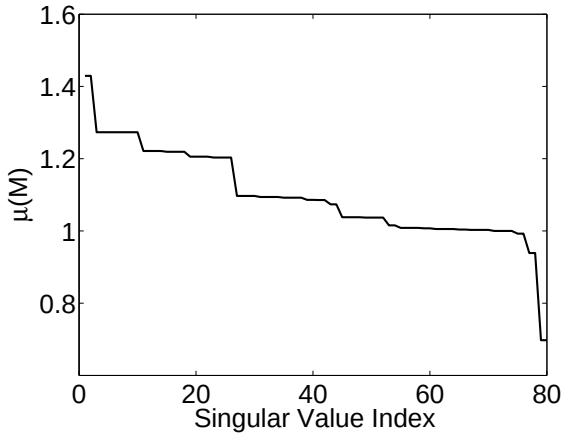

Figure 5.1: Singular values of the operator M.

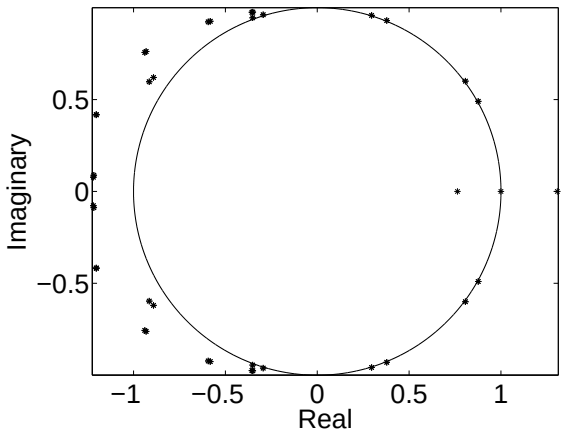

Figure 5.2: Eigenvalues of the operator M.

govern thermal convection. Despite their limited practical use, these equations present an excellent foundation for our numerical experiments due to their simplicity. We consider two formulations of the Lorenz equations, firstly, the deterministic form and, secondly, the stochastic form. As discussed previously in Chapter 4 we consider the effect of model error on the data assimilation schemes introduced in Chapter 3. Therefore, we aim to represent additional unresolved processes (from the atmosphere), as a stochastical noise term. This noise term will be the model error discussed in Chapter 4 and is assumed to be an additive Wiener process; further details on the Wiener process can be found in [43]. Firstly, we present the deterministic Lorenz equations which will be used for our experiments where model error does not appear.

5.2.1 Deterministic formulation

The deterministic Lorenz '63 equations are as follows,

$$\frac{\mathrm{d}x}{\mathrm{d}t} = -\sigma(x - y), \tag{5.5}$$

$$\frac{\mathrm{d}y}{\mathrm{d}t} = \rho x - y - xz, \tag{5.6}$$

$$\frac{\mathrm{d}z}{\mathrm{d}t} = xy - \beta z, \tag{5.7}$$

where typically σ, ρ and β are known as the Prandtl number, the Rayleigh number and a non-dimensional wave number respectively. In this work we will use the classical parameters, $\sigma = 10$, $\rho = 28$ and $\beta = 8/3$. We discretise the system using a fourth order Runge-Kutta approximation with a step-size $h = 0.01$; see [80] for further details on the Runge-Kutta scheme. Secondly, we consider the stochastic Lorenz equations.

5.2.2 Stochastic formulation

We seek to present the stochastic Lorenz '63 equations in the form of a stochastic differential equation as follows,

$$\mathrm{d}\Psi = a(\Psi)\mathrm{d}t + b(\Psi)\mathrm{d}W. \tag{5.8}$$

Therefore the stochastic Lorenz '63 equations are as follows,

$$\mathrm{d}x = -\sigma(x-y)\mathrm{d}t + c^{(1)}\mathrm{d}W^{(1)}, \tag{5.9}$$

$$\mathrm{d}y = (\rho x - y - xz)\,\mathrm{d}t + c^{(2)}\mathrm{d}W^{(2)}, \tag{5.10}$$

$$\mathrm{d}z = (xy - \beta z)\,\mathrm{d}t + c^{(3)}\mathrm{d}W^{(3)}, \tag{5.11}$$

where x, y, z all represent random variables, σ, ρ, β are the same parameters chosen as before, and $\mathrm{d}W^{(1)}$, $\mathrm{d}W^{(2)}$, $\mathrm{d}W^{(3)}$ represent values from independent Wiener processes. Here the constants $c^{(1)}$, $c^{(2)}$, $c^{(3)}$ can be altered to increase or decrease the level of stochastic noise. We discretise the stochastic Lorenz equations using an Euler-Maruyama approximation with a step-size $h = 0.01$. Further details of the Euler-Maruyama scheme can be found in [43].

5.3 Summary

In this chapter we have introduced two dynamical models, which will be used to illustrate numerically the theoretical results developed in the following chapters. We began introducing the linear system which we will use, the 2D Eady model. Next, we considered two formulations of the Lorenz '63 equations. Firstly, the deterministic form which will be used for our numerical experiments where we do not consider model error, and secondly, the stochastic form for our numerical experiments with model error. In the following chapters, we will explicitly discuss all numerical details, such as initial conditions, parameters, variables, *et cetera*; for each individual experiment we produce. We now move onto the main part of this thesis where we consider the stability of cycled data assimilation schemes.

Chapter 6

Constant and diagonal operators

In this chapter we develop new theoretical results for the stability of cycled 3DVar as introduced in Chapter 3 for simple dynamical systems. This will act as the foundation for more advanced results in the following chapters. We first consider the case where we have a linear observation operator and constant dynamics. We then consider diagonal model dynamics with respect to linear observation operators, such that the model dynamics are constructed using the same orthonormal system as the observation operator. Finally, we consider the reverse and explore diagonal observation operators with respect to linear model dynamics.

For the theory in this chapter we will make a number of assumptions. For clarity we now list these assumptions so that we can refer to them clearly later on.

Assumption 6.0.1. *The model error $\boldsymbol{\zeta}_k$ for $k \in \mathbb{N}_0$ is bounded by $\upsilon > 0$. The observation error $\boldsymbol{\eta}_k$ for $k \in \mathbb{N}_0$ is bounded by $\delta > 0$. The observation operator error $\boldsymbol{\omega}_k$ for $k \in \mathbb{N}_0$ is bounded by $\gamma > 0$.*

Assumption 6.0.2. *The observation operator $H \in L(\mathbf{X}, \mathbf{Y})$ is a time-invariant linear injective compact operator.*

Assumption 6.0.3. *The model dynamics $M \in L(\mathbf{X})$ is constant in time, such that $M = I$, where I is the identity operator.*

Assumption 6.0.4. *The model dynamics $M \in L(\mathbf{X})$ is a time-invariant linear operator that decomposes with respect to the singular system of the observation operator in Assumption 6.0.2. Therefore, given the singular system $(\mu_i, \boldsymbol{\varphi}_i, \mathbf{g}_i)$, $i \in \mathbb{N}$ of the observation operator H,*

we have that

$$M = UDU^{-1}, \tag{6.1}$$

where $U = \{\boldsymbol{\varphi}_i : i \in \mathbb{N}\}$ *is an orthonormal transformation such that* $U : \mathbf{X} \to \mathbf{X}$ *and* D *is a diagonal operator. We define a diagonal operator as follows,*

$$D\boldsymbol{\varphi}_i = d_i\boldsymbol{\varphi}_i \tag{6.2}$$

for $i \in \mathbb{N}$*, where* $\{\boldsymbol{\varphi}_i : i \in \mathbb{N}\}$ *is the same orthonormal system in* $\mathbf{X}$ *and* (d_i) *is a bounded sequence of real numbers. Therefore, we say that the model dynamics are diagonal with respect to the observation operator, since they have the same orthonormal system.*

Assumption 6.0.5. *The model dynamics* $M \in L(\mathbf{X})$ *is an injective linear time-invariant self-adjoint compact model operator. The observation operator* H *is a linear time-invariant operator that decomposes with respect to the eigensystem of the model dynamics* M*. Therefore, given the eigensystem,* $(\tilde{\lambda}_i, \tilde{\boldsymbol{\varphi}}_i)$*, for* $i \in \mathbb{N}$ *of the model dynamics* M*, we have that*

$$H = \tilde{U}\tilde{D}\tilde{U}^{-1}, \tag{6.3}$$

where $\tilde{U} = \{\tilde{\boldsymbol{\varphi}}_i : i \in \mathbb{N}\}$ *is an orthonormal transformation such that* $\tilde{U} : \mathbf{X} \to \mathbf{X}$ *and* $\tilde{D}$ *is a diagonal operator. We define a diagonal operator as follows,*

$$\tilde{D}\tilde{\boldsymbol{\varphi}}_i = \tilde{d}_i\tilde{\boldsymbol{\varphi}}_i, \tag{6.4}$$

for $i \in \mathbb{N}$*, where* $\{\tilde{\boldsymbol{\varphi}}_i : i \in \mathbb{N}\}$ *is the same orthonormal system in* $\mathbf{X}$ *and* $(\tilde{d}_i)$ *is a bounded sequence of real numbers.*

In this work we will refer to an operator being diagonal with respect to either the observation operator or the model dynamics. These two situations relate to Assumption 6.0.4 and Assumption 6.0.5 respectively and we use the term *diagonal system* to relate to both Assumption 6.0.4 and Assumption 6.0.5.

6.1 Linear observation operators with constant model dynamics

In this section we develop theory on the analysis error for cycled Tikhonov-Phillips regularization as introduced in Theorem 3.1.10. We first explore the simple case of constant model

dynamics, such that $M = I$ where I is the identity operator. We found in Chapter 4 that the work of [57] has looked at the pointwise convergence of the analysis error for this situation. They showed that for constant model dynamics if the observations lie in the range of the observation operator then the linear observer converges as time tends to infinity. It was further shown in [57] that if the observations did not lie in the range of the observation operator then the linear observer diverges. However, they did not consider the evolution of the analysis error in the form of norm estimates, which we will now present. Given Hilbert spaces $(\mathbf{X}, \|\cdot\|_{B^{-1}})$ and $(\mathbf{Y}, \|\cdot\|_{R^{-1}})$ from (4.19) we substitute M_k for the identity operator I so that

$$\mathbf{e}_k = (I - \mathscr{R}_\alpha H_k)\,\mathbf{e}_{k-1} + \mathscr{R}_\alpha \boldsymbol{\eta}_k + (I - \mathscr{R}_\alpha H_k)\,\boldsymbol{\zeta}_k - \mathscr{R}_\alpha \boldsymbol{\omega}_k, \tag{6.5}$$

where $\mathscr{R}_\alpha = (\alpha I + H^*H)^{-1}H^* \in L(\mathbf{Y}, \mathbf{X})$. Let us assume that the observation operator is time-invariant and let us define $N := I - \mathscr{R}_\alpha H \in L(\mathbf{X})$. We shall refer to this operator N as the reconstruction error operator, since it reflects how much we regularize (2.5). Therefore, (6.5) now becomes

$$\mathbf{e}_k = N\mathbf{e}_{k-1} + \mathscr{R}_\alpha \boldsymbol{\eta}_k + N\boldsymbol{\zeta}_k - \mathscr{R}_\alpha \boldsymbol{\omega}_k. \tag{6.6}$$

This equation in (6.6) shows the evolution of the analysis error equation. From this form there are two natural directions with which to analyse this equation, stochastic and deterministic. In this work we will focus on deterministic analysis since we assume that the distributions that the errors are drawn from are unknown. Therefore, we take norms on both sides, such that

$$\|\mathbf{e}_k\| = \|N\mathbf{e}_{k-1} + \mathscr{R}_\alpha \boldsymbol{\eta}_k + N\boldsymbol{\zeta}_k - \mathscr{R}_\alpha \boldsymbol{\omega}_k\|\,. \tag{6.7}$$

Using the triangle inequality and the properties of homogeneity we have that

$$\|\mathbf{e}_k\| \leq \|N\mathbf{e}_{k-1}\| + \|\mathscr{R}_\alpha \boldsymbol{\eta}_k\| + \|N\boldsymbol{\zeta}_k\| + \|-\mathscr{R}_\alpha \boldsymbol{\omega}_k\| \tag{6.8}$$

$$\leq \|N\mathbf{e}_{k-1}\| + \|\mathscr{R}_\alpha \boldsymbol{\eta}_k\| + \|N\boldsymbol{\zeta}_k\| + |-1| \cdot \|\mathscr{R}_\alpha \boldsymbol{\omega}_k\| \tag{6.9}$$

$$\leq \|N\mathbf{e}_{k-1}\| + \|\mathscr{R}_\alpha \boldsymbol{\eta}_k\| + \|N\boldsymbol{\zeta}_k\| + \|\mathscr{R}_\alpha \boldsymbol{\omega}_k\|\,. \tag{6.10}$$

We now make use of the property induced by Definition 2.1.10 and rearrange, such that

$$\|\mathbf{e}_k\| \leq \|N\| \cdot \|\mathbf{e}_{k-1}\| + \|\mathscr{R}_\alpha\| \cdot \|\boldsymbol{\eta}_k\| + \|N\| \cdot \|\boldsymbol{\zeta}_k\| + \|\mathscr{R}_\alpha\| \cdot \|\boldsymbol{\omega}_k\| \tag{6.11}$$

$$e_k \leq \|N\|\,(e_{k-1} + \|\boldsymbol{\zeta}_k\|) + \|\mathscr{R}_\alpha\|\,(\|\boldsymbol{\eta}_k\| + \|\boldsymbol{\omega}_k\|)\,, \tag{6.12}$$

where we define $e_k := \|\mathbf{e}_k\|$ for all $k \in \mathbb{N}_0$. We now use the bounds on the model error, observation error and the observation operator error from Section 4.1, such that

$$e_k \leq \|N\| \left(e_{k-1} + \upsilon\right) + \|\mathscr{R}_\alpha\| \left(\delta + \gamma\right). \tag{6.13}$$

Before we present the next result we should mention our approach of norm estimates. We know from Theorem 4.2.2 that the stability according to Definition 4.2.1 is determined by the eigenvalues of the relevant operator. However, we deal with an error evolution equation that comprises of many noise terms as seen in (4.19), which we bound as seen in (6.7) through to (6.13). In general, the operator that governs the error evolution from (4.20) is not self-adjoint. This means that in taking these bounds we no longer deal with the eigenvalues, instead we explore the singular values through the norms of these operators in (4.19); see (2.48) in Theorem 2.2.7. Since the largest singular value bounds the spectral radius, then by ensuring that the largest singular value is less than one we can derive a sufficient stability condition. In general, we will only be able to derive a sufficient condition for stability. However, in this chapter the operator that governs the behaviour of the error dynamics is self-adjoint, which allows us to derive necessary and sufficient stability conditions. We have the following definition of asymptotic stability for discrete-time linear time-invariant systems.

Definition 6.1.1. Let $(\mathbf{X}, \|\cdot\|_{\ell^2})$ be a Hilbert space. Then the discrete-time linear time-invariant system

$$\mathbf{x}_{k+1} = \Lambda \mathbf{x}_k, \tag{6.14}$$

where $\Lambda \in L(\mathbf{X})$ is called *asymptotically stable* if for all $\mathbf{x}_0 \in \mathbf{X}$, $\|\mathbf{x}_k\| \to 0$ for $k \to \infty$.

Definition 6.1.1 can be considered as an infinite dimensional version of Definition 4.2.1. We now present the following stability theorem which will be used throughout this work and can be considered as an infinite dimensional extension to Theorem 4.2.2.

Theorem 6.1.2. *The discrete-time linear time-invariant system*

$$\mathbf{x}_{k+1} = \Lambda \mathbf{x}_k, \tag{6.15}$$

where $\Lambda \in L(\mathbf{X})$, is asymptotically stable according to Definition 6.1.1 if $\|\Lambda\| < 1$.

Proof. Using (6.15) we write

$$\mathbf{x}_k = \Lambda^k \mathbf{x}_0, \tag{6.16}$$

according to Notation 2.1.16. Using the property induced in Definition 2.1.10 and (c) in Lemma 2.1.20 we obtain

$$\|\mathbf{x}_k\| = \left\|\Lambda^k \mathbf{x}_0\right\| \leq \left\|\Lambda^k\right\| \cdot \|\mathbf{x}_0\| \leq \underbrace{\|\Lambda\| \cdots \|\Lambda\|}_{k \text{ times}} \|\mathbf{x}_0\| = \|\Lambda\|^k \cdot \|\mathbf{x}_0\| . \tag{6.17}$$

Since $\|\Lambda\| < 1$ then as $k \to \infty$, $\|\mathbf{x}_k\| \to 0$ for all $\mathbf{x}_0 \in \mathbf{X}$, which completes the proof. □

In Theorem 6.1.2 we only derive a sufficient condition compared to the necessary and sufficient condition in Theorem 4.2.2. This is important and we will later explore in detail this property in our numerical experiment in Section 7.1.1. Given Definition 6.1.1 and Theorem 6.1.2 we can now present the following stability result on the asymptotic behaviour of the analysis error for cycled data assimilation schemes.

Theorem 6.1.3. *For the Hilbert space $(\mathbf{X}, \|\cdot\|_{B^{-1}})$, let Assumption 6.0.1, Assumption 6.0.2 and Assumption 6.0.3 hold. Then the error evolution in (6.13) and the error term $\mathbf{e}_k \in \mathbf{X}$ for $k \in \mathbb{N}_0$, where $\mathbf{e}_k := \mathbf{x}_k^{(a)} - \mathbf{x}_k^{(t)}$ and $N := I - \mathscr{R}_\alpha H$ is estimated by*

$$\|\mathbf{e}_k\| \leq \|N\|^k \cdot \|\mathbf{e}_0\| + \sum_{l=0}^{k-1} \|N\|^l \left(\|N\| \, \upsilon + \|\mathscr{R}_\alpha\| \, (\delta + \gamma)\right), \tag{6.18}$$

for $k \in \mathbb{N}_0$. If $\|N\| \neq 1$ then

$$\|\mathbf{e}_k\| \leq \|N\|^k \cdot \|\mathbf{e}_0\| + \frac{1 - \|N\|^k}{1 - \|N\|} \left(\|N\| \, \upsilon + \|\mathscr{R}_\alpha\| \, (\delta + \gamma)\right), \tag{6.19}$$

for $k \in \mathbb{N}_0$. If $\|N\| < 1$ then

$$\limsup_{k \to \infty} \|\mathbf{e}_k\| \leq \frac{\|N\| \, \upsilon + \|\mathscr{R}_\alpha\| \, (\delta + \gamma)}{1 - \|N\|}. \tag{6.20}$$

Proof. We prove by induction. For the base case we set $k = 1$ and using (6.13) we obtain

$$e_1 \leq \|N\| \, (e_0 + \upsilon) + \|\mathscr{R}_\alpha\| \, (\delta + \gamma) , \tag{6.21}$$

where $e_k := \|\mathbf{e}_k\|$ such that (6.21) is equal to (6.18). We continue with the inductive step. From (6.13) rewriting step $k + 1$ we have that

$$e_{k+1} \leq \|N\| \, (e_k + \upsilon) + \|\mathscr{R}_\alpha\| \, (\delta + \gamma) . \tag{6.22}$$

Now we bound e_k using (6.18), such that

$$e_{k+1} \leq \|N\| \left(\|N\|^k e_0 + \sum_{l=0}^{k-1} \|N\|^l \left(\|N\| \upsilon + \|\mathscr{R}_\alpha\| (\delta + \gamma) \right) + \upsilon \right) + \|\mathscr{R}_\alpha\| (\delta + \gamma) . \tag{6.23}$$

Expanding and reordering the summation we obtain

$$e_{k+1} \leq \|N\|^{k+1} e_0 + \sum_{l=0}^{k-1} \|N\|^{l+1} \left(\|N\| \upsilon + \|\mathscr{R}_\alpha\| (\delta + \gamma) \right) + \|N\| \upsilon + \|\mathscr{R}_\alpha\| (\delta + \gamma) \tag{6.24}$$

$$\leq \|N\|^{k+1} e_0 + \sum_{l=0}^{k} \|N\|^l \left(\|N\| \upsilon + \|\mathscr{R}_\alpha\| (\delta + \gamma) \right), \tag{6.25}$$

which is equal to (6.18) if we replace k with $k+1$ and hence by induction (6.18) is proved. If $\|N\| \neq 1$ then we can use the geometric series, such that

$$\sum_{l=0}^{k-1} \|N\|^l = \frac{1 - \|N\|^k}{1 - \|N\|}. \tag{6.26}$$

The geometric series can be found in [66, Theorem 5.3]. Replacing the summation in (6.18) with (6.26) we obtain (6.19). If $\|N\| < 1$ then we ensure convergence of the infinite geometric series and taking the limit in accordance with the *Theorem for Convergence of a Geometric Sequence*, which can be found in [66, Theorem 2.34], we have that

$$\|N\|^k \to 0 \tag{6.27}$$

as $k \to \infty$. Therefore, we obtain (6.20) which completes the proof. □

Theorem 6.1.3 shows a sufficient condition for asymptotic stability of the analysis error. If $\|N\| < 1$ then the analysis error will remain bounded for all time and has the asymptotic limit given by (6.20). We now investigate under what conditions can we make the reconstruction error operator contract, such that $\|N\| < 1$. It is useful to rearrange the reconstruction

operator as follows,

$$N = I - \mathscr{R}_\alpha H \tag{6.28}$$
$$= I - (\alpha I + H^*H)^{-1} H^*H \tag{6.29}$$
$$= (\alpha I + H^*H)^{-1} (\alpha I + H^*H) - (\alpha I + H^*H)^{-1} H^*H \tag{6.30}$$
$$= (\alpha I + H^*H)^{-1} ((\alpha I + H^*H) - H^*H) \tag{6.31}$$
$$= \alpha (\alpha I + H^*H)^{-1} \tag{6.32}$$
$$= \left(I + \alpha^{-1} H^*H\right)^{-1}. \tag{6.33}$$

Before presenting the following finite dimensional result, we must first remark on the operator N. We saw in Theorem 6.1.3 that to show stability it is sufficient that $\|N\| < 1$, and we have discussed that this is only a sufficient condition for stability. We know from Theorem 4.2.2 that in the finite dimensional setting the necessary and sufficient stability condition from Definition 4.2.1 is determined by the spectral radius of the relevant operator. From Theorem 2.2.3 we know that the spectral radius is equal to the norm of a compact self-adjoint operator. For this case of constant model dynamics, the condition of $\|N\| < 1$ is actually a necessary and sufficient condition for asymptotic stability. This is because for any $\alpha > 0$ the operator N, which governs the error evolution, is a self-adjoint operator. This can directly be seen in (6.33) using the property $(N^*)^{-1} = (N^{-1})^*$, given $N \in L(\mathbf{X})$ for a Hilbert space $\mathbf{X}$. From Theorem 2.2.4 we can carry out our analysis using the eigenvalues of N.

We now present the following finite dimensional stability result using Theorem 2.2.4. Here we consider the finite dimensional setting since it demonstrates challenges which exist in the infinite dimensional setting. Moreover, we will use this finite dimensional results in Chapter 7 and Chapter 8.

Lemma 6.1.4. *Let $\mathbf{X}, \mathbf{Y}$ be finite dimensional Hilbert spaces and let Assumption 6.0.2 and Assumption 6.0.3 hold. Given a parameter $0 < \rho < 1$ and a regularization parameter $\alpha > 0$ chosen sufficiently small then we can always achieve $\|N\| \leq \rho < 1$.*

Proof. Let us introduce the operator $G := H^*H$, which by construction is a self-adjoint compact linear operator. From the spectral theorem for compact self-adjoint linear operators in Theorem 2.2.4, we know that $\mathbf{X}$ has an orthonormal system consisting of eigenvectors

$\{\varphi_1, \ldots, \varphi_n\}$ with real eigenvalues $\{\lambda_1, \ldots, \lambda_n\}$ of G. We choose α and ρ such that

$$\alpha\left(\frac{1}{\rho} - 1\right) = \inf_{j=1,\ldots,n} |\lambda_j| > 0. \tag{6.34}$$

Now

$$\|N\| = \sup_{j\in\{1,\ldots,n\}} \left|\frac{1}{1+\frac{\lambda_j}{\alpha}}\right| \leq \frac{\alpha}{\alpha + \alpha\left(\frac{1}{\rho} - 1\right)} = \rho < 1, \tag{6.35}$$

which completes the proof. □

Here we can parallel this result with the literature. We saw in Chapter 4 that Luenberger's main result in Theorem 4.2.3 involved choosing an observer gain to move the eigenvalues of $M - \mathscr{R}_\alpha H$ to obtain stability. Here we have a similar result for the finite dimensional setting, where we use the regularization parameter to shift the eigenvalues of $I - \mathscr{R}_\alpha H$. From Lemma 6.1.4 to obtain a stable cycled data assimilation scheme, we must choose the regularization parameter sufficiently small so that the norm of the reconstruction error operator is less one.

We now present an important result for the infinite dimensional setting, which will be used throughout this thesis.

Lemma 6.1.5. *Let* $\mathbf{X}$ *and* $\mathbf{Y}$ *be Hilbert spaces and let Assumption 6.0.2 and Assumption 6.0.3 hold. Then the operator norm of the reconstruction error operator is given by*

$$\|N\| = \|I - \mathscr{R}_\alpha H\| = 1. \tag{6.36}$$

Proof. Since H is compact, we have that $G := H^*H$ is also compact ([73, Theorem 7.3]). Therefore, the eigenvalues $\{\lambda_1, \lambda_2, \ldots\}$ of G decay, such that $\lambda_i \to 0$ for $i \to \infty$ ([46, p.280]). This means that

$$\|N\| = \sup_{i=1,\ldots,\infty} \left|\frac{\alpha}{\alpha + \lambda_i}\right| = 1 \tag{6.37}$$

for all $\alpha > 0$, which completes the proof. □

This result will determine our ability to achieve stability for the cycled data assimilation scheme. We have the following remark.

Remark 6.1.6. In an infinite dimensional space, if Assumption 6.0.2 and Assumption 6.0.3 hold then we are unable to obtain the limit in Theorem 6.1.3, since the proof of Theorem 6.1.3 uses the sufficient condition for stability $\|N\| < 1$.

Of course this set up of constant model dynamics has limited practical use and hence this result is somewhat artificial. However, this result does highlight that in the infinite dimensional setting we require some contraction in the model dynamics to seek stability. As we will see later in this chapter and the next two chapters, it is necessary for the model dynamics to behave in a particular way to ensure stability for the cycled data assimilation scheme.

In the next section we consider diagonal model dynamics with respect to the observation operator, such that the model dynamics are constructed using the same orthonormal system as the observation operator. Again this situation has limited practical use. However, we will use it as a stepping stone towards a more realistic set-up.

6.2 Linear observation operators with diagonal model dynamics

In this section we consider a model dynamics operator that is constructed using the same orthonormal system as the observation operator in accordance with Assumption 6.0.4. Again we explore the observation operator spectrally and demonstrate how we can achieve a stable cycled 3DVar with particular model dynamics. We also present a numerical experiment which will confirm the theory developed in this section.

Since we work in a Hilbert space we can use Theorem 2.1.7 to expand each element of $\mathbf{X}$ in a Fourier series in a similar way to (2.44). Given an injective linear compact observation operator H we have that

$$\mathbf{x}_k = \sum_{i=1}^{\infty} \langle \mathbf{x}_k, \boldsymbol{\varphi}_i \rangle \, \boldsymbol{\varphi}_i, \tag{6.38}$$

for $k \in \mathbb{N}_0$. The inner product $\langle \mathbf{x}_k, \boldsymbol{\varphi}_i \rangle$ is called the spectral coefficient. From (2.43) we see that the application of the operator H and H^* corresponds to the spectral multiplication by μ_i for $i \in \mathbb{N}$ and applying H^{-1} corresponds to the multiplication by $1/\mu_i$ for $i \in \mathbb{N}$. Therefore, for any element $\mathbf{x} \in \mathbf{X}$ we have from (2.45)

$$H\mathbf{x} = \sum_{i=1}^{\infty} \mu_i \, \langle \mathbf{x}, \boldsymbol{\varphi}_i \rangle \, \mathbf{g}_i. \tag{6.39}$$

Similarly the application of the Tikhonov-Phillips inverse operator $\mathscr{R}_\alpha = (\alpha I + H^*H)^{-1}H^* \in L(\mathbf{Y}, \mathbf{X})$ to any measurement $\mathbf{y}_k \in \mathbf{Y}$ we have from (2.45)

$$\mathscr{R}_\alpha \mathbf{y}_k = \sum_{i=1}^{\infty} \frac{\mu_i}{\alpha + \mu_i^2} \langle \mathbf{y}_k, \mathbf{g}_i \rangle \boldsymbol{\varphi}_i. \tag{6.40}$$

Finally, applying the reconstruction error operator N to any element $\mathbf{x}_k \in \mathbf{X}$ we have from (2.45)

$$N\mathbf{x}_k = \sum_{i=1}^{\infty} \frac{\alpha}{\alpha + \mu_i^2} \langle \mathbf{x}_k, \boldsymbol{\varphi}_i \rangle \boldsymbol{\varphi}_i. \tag{6.41}$$

From (4.19) substituting for time-invariant model dynamics and observation operator we have that

$$\mathbf{e}_k = (I - \mathscr{R}_\alpha H)\, M\mathbf{e}_{k-1} + \mathscr{R}_\alpha \boldsymbol{\eta}_k + (I - \mathscr{R}_\alpha H)\, \boldsymbol{\zeta}_k - \mathscr{R}_\alpha \boldsymbol{\omega}_k. \tag{6.42}$$

Applying the steps from (6.7) through to (6.13) then

$$e_k \leq \|\Lambda\|\, e_{k-1} + \|N\|\, \upsilon + \|\mathscr{R}_\alpha\|\, (\delta + \gamma)\,, \tag{6.43}$$

where $e_k := \|\mathbf{e}_k\|$, $\Lambda := NM$, $N := I - \mathscr{R}_\alpha H$, with noise terms υ, δ and γ in accordance with Section 4.1. In a similar way to (6.13) and Theorem 6.1.3, we must show for a sufficient condition that $\|\Lambda\|$ must be kept less than one in each assimilation step to asymptotically control the error dynamics. We present the following result.

Theorem 6.2.1. *For the Hilbert space $(\mathbf{X}, \|\cdot\|_{B^{-1}})$, let Assumption 6.0.1, Assumption 6.0.2 and Assumption 6.0.4 hold. Defining $\Lambda := (I - \mathscr{R}_\alpha H)M$ then the error evolution in (6.43) and the error term, $\mathbf{e}_k \in \mathbf{X}$ for $k \in \mathbb{N}_0$, where $\mathbf{e}_k := \mathbf{x}_k^{(a)} - \mathbf{x}_k^{(t)}$ is estimated by*

$$\|\mathbf{e}_k\| \leq \|\Lambda\|^k \cdot \|\mathbf{e}_0\| + \sum_{l=0}^{k-1} \|\Lambda\|^l \left(\|N\|\, \upsilon + \|\mathscr{R}_\alpha\|\, (\delta + \gamma)\right), \tag{6.44}$$

for $k \in \mathbb{N}_0$. If $\|\Lambda\| \neq 1$ then

$$\|\mathbf{e}_k\| \leq \|\Lambda\|^k \cdot \|\mathbf{e}_0\| + \frac{1 - \|\Lambda\|^k}{1 - \|\Lambda\|} \left(\|N\|\, \upsilon + \|\mathscr{R}_\alpha\|\, (\delta + \gamma)\right), \tag{6.45}$$

for $k \in \mathbb{N}_0$. If $\|\Lambda\| < 1$ then

$$\limsup_{k \to \infty} \|\mathbf{e}_k\| \leq \frac{\|N\|\, \upsilon + \|\mathscr{R}_\alpha\|\, (\delta + \gamma)}{1 - \|\Lambda\|}. \tag{6.46}$$

Proof. The proof is same as that of Theorem 6.1.3 for a different constant $\|\Lambda\|$. □

We briefly remark as follows.

Remark 6.2.2. Since Assumption 6.0.2 holds then using Lemma 6.1.4 and Lemma 6.1.5 we have that for any $\alpha > 0$ then $\|N\| \leq 1$. From Theorem 2.3.3, since H is injective then the Tikhonov-Phillips inverse is bounded by

$$\|\mathscr{R}_\alpha\| \leq \frac{1}{2\sqrt{\alpha}}. \tag{6.47}$$

Therefore, from (6.46) we have that

$$\limsup_{k\to\infty} \|\mathbf{e}_k\| \leq \frac{\upsilon + \frac{\delta+\gamma}{2\sqrt{\alpha}}}{1 - \|\Lambda\|}. \tag{6.48}$$

From Theorem 6.2.1 we see that we must keep the norm of the operator Λ less than one for the analysis error to remain bounded for all time, such that we obtain the limit in (6.46). We now investigate under what conditions can we ensure stability of cycled data assimilation schemes. Since our model dynamics are constructed using the same orthonormal system as the observation operator, given any element $\mathbf{x}_k \in \mathbf{X}$ we have from (2.45)

$$\Lambda \mathbf{x}_k = \sum_{i=1}^{\infty} \frac{\alpha d_i}{\alpha + \mu_i^2} \langle \mathbf{x}_k, \boldsymbol{\varphi}_i \rangle \boldsymbol{\varphi}_i. \tag{6.49}$$

Since M is diagonal with respect to the singular system of H and N is self-adjoint, then Λ which governs the evolution of the analysis error is also self-adjoint. Therefore, in the same way as in Section 6.1, the stability results we develop in this section are necessary and sufficient in the sense of Theorem 4.2.2. We have the following spectral result.

Lemma 6.2.3. *Let Assumption 6.0.2 and Assumption 6.0.4 hold. Then if M is uniformly damping on all spectral modes then $\|\Lambda\| < 1$.*

Proof. From (6.49) we know that the application of Λ to $\boldsymbol{\varphi}_i$, with respect to a singular system $(\mu_i, \boldsymbol{\varphi}_i, \mathbf{g}_i)$ of H, is given by the multiplication

$$\frac{\alpha d_i}{\alpha + \mu_i^2}. \tag{6.50}$$

Given that M is uniformly damping on all spectral modes, which means that there exists a constant $0 < \rho < 1$, such that

$$\sup_{i\in\mathbb{N}} |d_i| = \rho. \tag{6.51}$$

From (6.37) for any $\alpha > 0$ then

$$\frac{\alpha}{\alpha + \mu_i^2} \leq 1, \tag{6.52}$$

where using Definition 2.2.5 we have that $\mu_i^2 = \lambda_i$ for all $i \in \mathbb{N}$. Therefore, using the multiplicative property of absolute values we have that

$$\left| \frac{\alpha d_i}{\alpha + \mu_i^2} \right| = \left| \frac{\alpha}{\alpha + \mu_i^2} \right| |d_i| \leq \rho < 1, \tag{6.53}$$

for all $i \in \mathbb{N}$. Hence, we have that $\|\Lambda\| = \sup_{i \in \mathbb{N}} |\alpha d_i / (\alpha + \mu_i^2)| < 1$, which completes the proof. □

Both Lemma 6.2.3 and Lemma 6.1.5 highlight the difficulty in generalising these stability results to more realistic systems. Our interest is with ill-posed observation operators and therefore from Lemma 6.1.5, for any positive choice of regularization parameter, we have that the norm of the reconstruction error operator is always one. Hence, in Lemma 6.2.3 we required contractive model dynamics to ensure stability for the cycled data assimilation scheme. The following result demonstrates how the model dynamics do not need to be strictly contractive.

Lemma 6.2.4. *Let Assumption 6.0.2 and Assumption 6.0.4 hold. If M is uniformly damping on higher spectral modes, then there is a regularization parameter α sufficiently small, such that $\|\Lambda\| < 1$.*

Proof. From (6.49) we know that the application of Λ to $\boldsymbol{\varphi}_i$, with respect to a singular system $(\mu_i, \boldsymbol{\varphi}_i, \mathbf{g}_i)$ of H, is given by the multiplication

$$\frac{\alpha d_i}{\alpha + \mu_i^2}. \tag{6.54}$$

Given that M is uniformly damping on higher spectral modes, which means that there exists a constant $0 < \rho < 1$ and an $n \in \mathbb{N}$ such that $\sup_{i=n+1,\ldots,\infty} |d_i| = \rho$.

From the previous result in Lemma 6.2.3, given any regularization parameter $\alpha > 0$ we have that

$$\sup_{i=n+1,\ldots,\infty} \left| \frac{\alpha d_i}{\alpha + \mu_i^2} \right| \leq \rho < 1. \tag{6.55}$$

So for $i \leq n$, we require for some constant $0 < \epsilon < 1$ that

$$\left| \frac{\alpha d_i}{\alpha + \mu_i^2} \right| \leq \epsilon. \tag{6.56}$$

We choose

$$d = \sup_{i=1,\ldots,n} |d_i| < \infty, \tag{6.57}$$

then we require that

$$\frac{\alpha}{\alpha + \mu_i^2} \leq \frac{\epsilon}{d}, \tag{6.58}$$

where we drop the absolute value signs since the inequality is positive on both sides. We can now choose α accordingly

$$\frac{\alpha}{\alpha + \mu_i^2} \leq \frac{\epsilon}{d} \tag{6.59}$$

$$\frac{\alpha + \mu_i^2}{\alpha} \geq \frac{d}{\epsilon} \tag{6.60}$$

$$\frac{\mu_i^2}{\alpha} \geq \frac{d - \epsilon}{\epsilon} \tag{6.61}$$

$$\frac{1}{\alpha} \geq \frac{d - \epsilon}{\mu_i^2 \epsilon} \tag{6.62}$$

$$\alpha \leq \frac{\mu_i^2 \epsilon}{d - \epsilon}. \tag{6.63}$$

Since the singular values of H are ordered such that $\mu_1 \geq \cdots \geq \mu_n > 0$, then if we choose $\alpha \leq \mu_n^2 \epsilon/(d - \epsilon)$, then $\|\Lambda\| \leq \epsilon < 1$. □

Of course this result has limited practicality since the situation of diagonal model dynamics with respect to the observation operator rarely occurs. However, we observe in Lemma 6.2.4 an interesting result which we can carry through to more realistic situations. If we can split the state space into two parts, one part where the regularization parameter could be chosen to control any expansion in the model dynamics, and another part where the model dynamics are strictly contracting, then we would be able to stabilise the cycled data assimilation scheme. Another observation we make is that the regularization parameter must be chosen sufficiently small to obtain stability in the cycled data assimilation scheme. The stability which we consider here is in the sense of cycling the data assimilation scheme in time. We know from regularization theory that the regularization parameter must be chosen sufficiently large so that the solution of the regularization problem is stable. This type of stability is in the sense of the inversion at a fixed time as we discussed in Section 2.3. This leads to contradictory properties of α such that we expect a region for α where the error is smallest which we will observe numerically in the next section. Our results in this section also

apply to the finite dimensional setting where the proofs are the same but the singular system becomes finite as discussed in Section 2.2.2. Since our approach is to use norm estimate our results are not as strong as the necessary and sufficient finite dimensional stability conditions discussed in Chapter 4.

6.2.1 Numerical experiment

In this section we will set up one simple numerical experiment. Even though our theoretical results do not apply to this numerical experiment we still can illustrate one aspect of the theoretical results from Section 6.2. Our theoretical results in Lemma 6.2.4 apply to the infinite dimensional setting. Therefore, our theoretical results do not apply directly to the finite dimensional numerical experiments in this section. Despite this we can still observe the evolution of the linear analysis error in Theorem 6.2.1 for a finite dimensional system. We concluded from Section 6.2 that the regularization parameter can be chosen sufficiently small so that the analysis error will remain stable. We will see this demonstrated numerically in this experiment. In our work our approach is to use the same noise realisations when comparing experiments.

We choose a random 3×3 observation operator H, drawn from the standard normal distribution, using the *randn* command in Matlab. Here we remark that the distribution with mean 0 and standard deviation 1 is called the standard normal distribution. We then decompose H in terms of its singular system in accordance with Theorem 2.2.6. We set the last singular value $\mu_3 = 10^{-5}$ to create an ill-conditioned observation operator, such that

$$H = \begin{pmatrix} 0.4268 & 0.5220 & 0.5059 \\ 0.8384 & -0.7453 & 1.6690 \\ 0.4105 & 1.6187 & 0.0610 \end{pmatrix} \tag{6.64}$$

to four decimal places. Therefore, the condition number from Definition 2.1.18 of the observation operator $\kappa(H) \approx 2.1051 \times 10^5$ with respect to the matrix 2-norm. We choose the following diagonal spectral operator for the model dynamics randomly, such that

$$D = \begin{pmatrix} 1.28 & 0 & 0 \\ 0 & 0.956 & 0 \\ 0 & 0 & 0.286 \end{pmatrix}. \tag{6.65}$$

Now we formulate the model dynamics according to (6.1) using the right singular vectors of H, such that

$$M = \begin{pmatrix} 0.5167 & 0.0488 & 0.3624 \\ 0.0488 & 1.0416 & -0.2074 \\ 0.3624 & -0.2074 & 0.9638 \end{pmatrix} \tag{6.66}$$

to four decimal places. We have a model operator with one growing mode and two damping modes, which is consistent with the setting in Lemma 6.2.4.

It is natural to set up the noise in these experiments to be Gaussian, since the 3DVar functional can be viewed as a maximum *a posteriori* probability Bayesian estimator of the state of the system under Gaussian statistics, see [47]. However, as we have discussed we require for our analysis that the noise be bounded for all time. We have tested different type of noise and they illustrate the same behaviour as seen here. Therefore, we shall choose normally distributed noise and note that for a finite sample the noise is bounded and hence is consistent with the theory developed in Section 6.2. Throughout this work we shall use the terms Gaussian and normally distributed synonymously. We draw the noise terms from the following distributions,

$$\boldsymbol{\eta}_k \sim \mathcal{N}(\mathbf{0}, R), \;\; \boldsymbol{\zeta}_k \sim \mathcal{N}(\mathbf{0}, \mathscr{Q}) \;\text{ and }\; \boldsymbol{\omega}_k \sim \mathcal{N}(\mathbf{0}, W), \tag{6.67}$$

for $k = 1, \ldots, 1000$. We remark for notational purposes that $\boldsymbol{\eta}_k \sim \mathcal{N}(\mathbf{0}, R)$ means we draw $\boldsymbol{\eta}_k$ from a normal distribution with zero mean and covariance matrix R. Further details on the Gaussian distribution can be found in [5]. In order to connect the cycled Tikhonov-Phillips scheme from (3.24) with 3DVar we must formulate covariance matrices to weight the errors on the background and observations.

We saw in Theorem 3.1.13 that with weighted norms, 3DVar is equivalent to cycled Tikhonov-Phillips for $\alpha = 1$. In this experiment we set up simple covariance matrices, such that

$$B = \sigma_{(b)}^2 I, \;\; R = \sigma_{(o)}^2 I, \;\; \mathscr{Q} = \sigma_{(q)}^2 I \;\text{ and }\; W = \sigma_{(w)}^2 I, \tag{6.68}$$

where $\sigma_{(b)}^2$, $\sigma_{(o)}^2$, $\sigma_{(q)}^2$ and $\sigma_{(w)}^2$ are the variances of the noise on the background, observations, model and observation operator respectively. In this case if we choose $\alpha = \sigma_{(o)}^2/\sigma_{(b)}^2$ then 3DVar is equivalent to cycled Tikhonov-Phillips with respect to the Euclidean norm. For this experiment we choose the standard deviation on the noise as follows, $\sigma_{(b)} = 0.06$, $\sigma_{(o)} = 0.3$,

$\sigma_{(q)} = 0.25$ and $\sigma_{(w)} = 0.2$. Since this is a toy system these standard deviations are not necessarily representative of the expected errors in this system. However, these values are chosen in order to illustrate the unstable behaviour as the regularization parameter α is changed. We choose $\sigma_{(b)}$ smaller than the standard deviation of the other noise terms so that the initial error, $\mathbf{e}_1 \sim \mathcal{N}(\mathbf{0}, B)$ is small. The standard deviations of the other noise terms are chosen so that they are almost equal. Of course changing the level of noise will affect the analysis error evolution. In this experiment we will not consider the impact of the noise level and postpone this investigation to later experiments. For $\alpha = \sigma_{(o)}^2/\sigma_{(b)}^2 = 0.3^2/0.06^2 = 25$ we connect 3DVar with cycled Tikhonov-Phillips regularization. In the following chapters we will construct more realistic covariance matrices for our experiments, but for this experiment the covariance matrices in (6.68) will be sufficient.

Since we deal with linear operators in this chapter, we can explicitly calculate the error evolution using (6.42). Furthermore, we also want to explore the bound on the error evolution in (6.43). This bound in (6.43) can be considered as a worst case scenario and all our theory is restricted to this bound. Therefore, it is necessary to compare this bound with the actual error evolution. In this experiment we want to demonstrate that choosing the regularization parameter sufficiently small means that the analysis error evolution is stable for all assimilation time.

Before we present the results we must discuss the implications of these numerical experiments. As we have discussed our interest is with the infinite dimensional setting. However, all numerical experiment work is in the finite dimensional setting. In this experiment we work with a very low-dimensional toy system to illustrate and understand behaviour of the analysis error evolution. Later in this thesis we will carry out numerical experiments with more complicated systems, whereby our finite dimensional numerical experiments parallel with our infinite dimensional results. This numerical experiment is useful since we can take its findings to more realistic numerical experiments later in this work.

We draw an initial analysis error using the standard deviation of the background state, therefore $\mathbf{e}_1 \sim \mathcal{N}(\mathbf{0}, B)$ and calculate the analysis error for $k = 2, \ldots, 1000$ using (6.42) and calculate its bound in (6.43). Varying the regularization parameter α we can study the time-averaged error over the integration period. The time-averaged error is defined by the integrated normalised total analysis error calculated by the sum of $\|\mathbf{e}_k\|$ from $k = 1, \ldots, 1000$,

renormalised with division by 1000. In Figure 6.1 we plot the error integral for both (6.42) and (6.43), against the regularization parameter. Here we observe that choosing a small regularization parameter leads to a smaller averaged error. We see that there is a small difference between the bound on the analysis error and the actual analysis error. We see that for a wide range of regularization parameters the analysis error is stable, but as we increase α to around 10 then the analysis error begins to grow.

We can also investigate the analysis error evolution for individual regularization parameters. We plot in Figure 6.2 the evolution of (6.42) and (6.43) for $\alpha = 25$, which corresponds to 3DVar for given covariances in (6.68). We see that both (6.42) and (6.43) are unstable for this choice of regularization parameter. From the theory developed in Section 6.2 and from observing Figure 6.1, to stabilise our data assimilation scheme we must reduce the regularization parameter. By changing the regularization parameter α we carry out an inflation to the background error variance. Therefore, using Figure 6.1 we choose the regularization parameter which corresponds to the smallest time-averaged error. In Figure 6.3 we plot the evolution of (6.42) and (6.43) for $\alpha = 1$ (the regularization parameter with the smallest time-averaged error). We see that the actual analysis error remains stable for all assimilation time with random oscillations dependent on realisations of the noise chosen at each time-step. Furthermore, we can investigate the behaviour of the analysis error at the point where it becomes unstable. We plot the analysis error from (6.42) and the bound from (6.43) for $\alpha = 15$ in Figure 6.4 and for $\alpha = 16$ in Figure 6.5. Comparing both figures we see that the evolution of the analysis error is similar up until $k = 10^2$ but then in Figure 6.5 the trajectory of the analysis error becomes unstable whereas in Figure 6.4 it remains stable.

This work is interested in developing theoretical results for data assimilation algorithms in the NWP setting. Therefore, it seems unnatural in this section to investigate model dynamics which arise from the observation operator. Instead we could consider an observation operator that arises from the model dynamics. In the next section we investigate this situation where the observation operator is diagonalisable with respect the linear model dynamics.

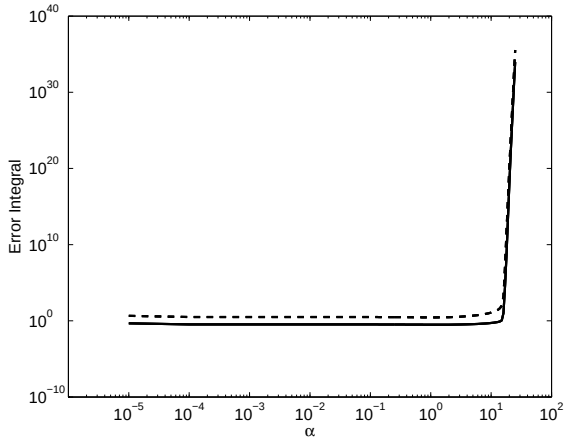

Figure 6.1: ℓ^2 norm of the time-averaged analysis error, $\|\mathbf{e}_k\|_{\ell^2}$ integrated for all assimilation time $k = 1, \ldots, 1000$, varying the regularization parameter, α. Solid: Analysis error governed by the actual error in (6.42). Dashed: Theoretical bound from (6.43).

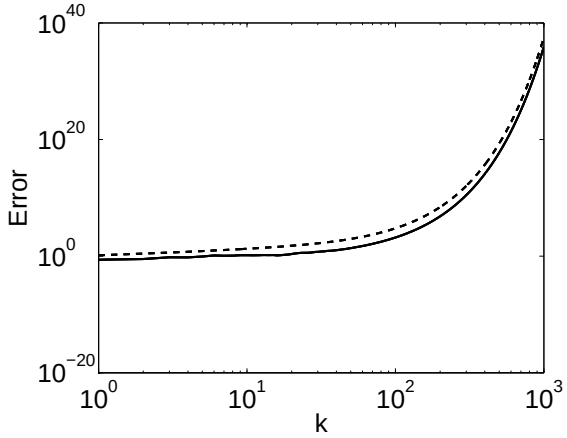

Figure 6.2: ℓ^2 norm of the analysis error, $\|\mathbf{e}_k\|_{\ell^2}$ as the scheme is cycled for index k with regularization parameter, $\alpha = 25$. Solid: Analysis error governed by the actual error in (6.42). Dashed: Theoretical bound from (6.43).

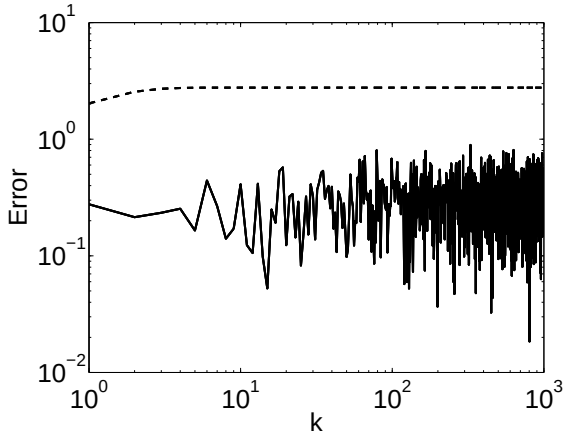

Figure 6.3: ℓ^2 norm of the analysis error, $\|\mathbf{e}_k\|_{\ell^2}$ as the scheme is cycled for index k with regularization parameter, $\alpha = 1$. Solid: Analysis error governed by the actual error in (6.42). Dashed: Theoretical bound from (6.43).

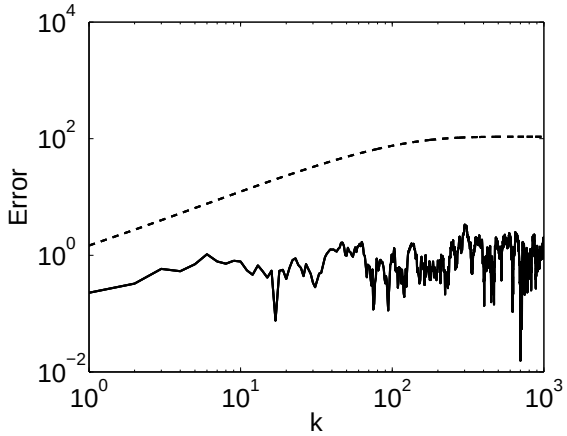

Figure 6.4: ℓ^2 norm of the analysis error, $\|\mathbf{e}_k\|_{\ell^2}$ as the scheme is cycled for index k with regularization parameter, $\alpha = 15$. Solid: Analysis error governed by the actual error in (6.42). Dashed: Theoretical bound from (6.43).

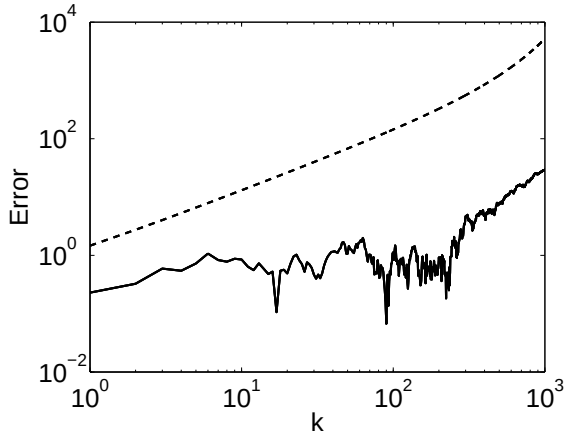

Figure 6.5: ℓ^2 norm of the analysis error, $\|\mathbf{e}_k\|_{\ell^2}$ as the scheme is cycled for index k with regularization parameter, $\alpha = 16$. Solid: Analysis error governed by the actual error in (6.42). Dashed: Theoretical bound from (6.43).

6.3 Linear model dynamics with diagonal observation operators

In this section we develop stability results for the situation where the observation operator is diagonalisable with respect the linear model dynamics in accordance with Assumption 6.0.5. This is the reverse situation to the previous chapter and in some ways is more important. We aim to investigate if given some dynamical flow then can we create an observation operator so that the cycled data assimilation scheme is stable over all time.

Here we remark that we adopt *tilde* notation for the eigensystem of M. This is necessary so as not to clash notation with the previous singular system of H in Section 6.2. Since the model operator is self-adjoint such that $M : \mathbf{X} \to \mathbf{X}$, we cannot construct an operator $H \in L(\mathbf{X}, \mathbf{Y})$. Instead we must restrict ourselves to the situation of direct measurements such that the observation operator $H \in L(\mathbf{X})$ and therefore will only act on the state space and amplify or contract spectral modes of M. Given an injective linear self-adjoint compact model operator M, for any element $\mathbf{x} \in \mathbf{X}$ from (2.40) we have

$$M\mathbf{x} = \sum_{i=1}^{\infty} \tilde{\lambda}_n \langle \mathbf{x}, \tilde{\boldsymbol{\varphi}}_i \rangle \, \tilde{\boldsymbol{\varphi}}_i. \tag{6.69}$$

The application of the operator H^*H corresponds to the spectral multiplication

$$H^*H\mathbf{x} = \sum_{i=1}^{\infty} \tilde{d}_i^2 \langle \mathbf{x}, \tilde{\boldsymbol{\varphi}}_i \rangle \tilde{\boldsymbol{\varphi}}_i. \tag{6.70}$$

With this set-up we have the following spectral result which is similar to Lemma 6.2.3.

Lemma 6.3.1. *Let Assumption 6.0.2 and Assumption 6.0.5 hold. If M is uniformly damping on all spectral modes then $\|\Lambda\| < 1$.*

Proof. Using Section 6.2 we can follow through the same process to find that the application of Λ to $\tilde{\boldsymbol{\varphi}}_i$, with respect to an eigensystem $(\tilde{\lambda}_i, \tilde{\boldsymbol{\varphi}}_i)$ of M, is given by the multiplication

$$\frac{\alpha\tilde{\lambda}_i}{\alpha + \tilde{d}_i^2}. \tag{6.71}$$

Given that M is uniformly damping on all spectral modes then there exists a constant $0 < \rho < 1$, such that

$$\sup_{i\in\mathbb{N}} \left|\tilde{\lambda}_i\right| = \rho. \tag{6.72}$$

By construction, given any $\alpha > 0$,

$$\frac{\alpha}{\alpha + \tilde{d}_i^2} \leq 1 \tag{6.73}$$

for $i \in \mathbb{N}$. Hence, using the multiplicative property of absolute values

$$\left|\frac{\alpha\tilde{\lambda}_i}{\alpha + \tilde{d}_i^2}\right| = \left|\frac{\alpha}{\alpha + \tilde{d}_i^2}\right| \cdot \left|\tilde{\lambda}_i\right| \leq \rho < 1 \tag{6.74}$$

for all $i \in \mathbb{N}$. Therefore we have that $\|\Lambda\| < 1$ which completes the proof. □

Using the regularization parameter we can relax the need for contractive model dynamics in Lemma 6.3.1 and formulate the following result, which is similar to Lemma 6.2.4.

Lemma 6.3.2. *Let Assumption 6.0.2 and Assumption 6.0.5 hold. If M is uniformly damping on higher spectral modes then there exists a regularization parameter α sufficiently small, such that $\|\Lambda\| < 1$.*

Proof. From (6.71) we know that the application of Λ to $\tilde{\boldsymbol{\varphi}}_i$, with respect to an eigensystem $(\tilde{\lambda}_i, \tilde{\boldsymbol{\varphi}}_i)$ of M, is given by the multiplication

$$\frac{\alpha\tilde{\lambda}_i}{\alpha + \tilde{d}_i^2}. \tag{6.75}$$

Given that M is uniformly damping on higher spectral modes, which means that there exists a constant $0 < \rho < 1$ and an $n \in \mathbb{N}$ such that $\sup_{i=n+1,\ldots,\infty} \left|\tilde{\lambda}_i\right| = \rho$.

From the previous result in Lemma 6.3.1, given any regularization parameter $\alpha > 0$ we have that

$$\sup_{i=n+1,\ldots,\infty} \left|\frac{\alpha\tilde{\lambda}_i}{\alpha + \tilde{d}_i^2}\right| \leq \rho < 1. \tag{6.76}$$

So for $i \leq n$ we require for some constant $0 < \epsilon < 1$ that

$$\left|\frac{\alpha\tilde{\lambda}_i}{\alpha + \tilde{d}_i^2}\right| \leq \epsilon. \tag{6.77}$$

Since the eigenvalues of M are assumed to be ordered according to their absolute size then we require that

$$\frac{\alpha}{\alpha + \tilde{d}_i^2} \leq \frac{\epsilon}{\left|\tilde{\lambda}_1\right|}, \tag{6.78}$$

where we drop the absolute value sign on the left hand side since the inequality is positive. We can now choose α accordingly,

$$\frac{\alpha}{\alpha + \tilde{d}_i^2} \leq \frac{\epsilon}{\left|\tilde{\lambda}_1\right|} \tag{6.79}$$

$$\frac{\alpha + \tilde{d}_i^2}{\alpha} \geq \frac{\left|\tilde{\lambda}_1\right|}{\epsilon} \tag{6.80}$$

$$\frac{\tilde{d}_i^2}{\alpha} \geq \frac{\left|\tilde{\lambda}_1\right| - \epsilon}{\epsilon} \tag{6.81}$$

$$\frac{1}{\alpha} \geq \frac{\left|\tilde{\lambda}_1\right| - \epsilon}{\tilde{d}_i^2\epsilon} \tag{6.82}$$

$$\alpha \leq \frac{\tilde{d}_i^2\epsilon}{\left|\tilde{\lambda}_1\right| - \epsilon} \tag{6.83}$$

We define

$$\tilde{d} = \inf_{i=1,\ldots,n} \left|\tilde{d}_i\right| < \infty. \tag{6.84}$$

Therefore, if we choose $\alpha \leq \tilde{d}^2\epsilon/(|\tilde{\lambda}_1| - \epsilon)$ then $\|\Lambda\| \leq \epsilon < 1$. □

As we saw in Lemma 6.2.4, the regularization parameter can be chosen sufficiently small to ensure that $\|\Lambda\| < 1$ which then implies stability in accordance with Theorem 6.2.1. In this case we have set up the observation operator so that it has the same orthonormal system

as the model dynamics operator. It is well known that if two linear compact self-adjoint operators commute then they have a complete orthogonal set of common eigenelements [29, Theorem 9.7]. This result can be paralleled with the work of [7] whereby they assume that the observation operator and Stokes operator commute, as seen in Chapter 4. We will investigate these results numerically in the next section.

6.3.1 Numerical experiment

Here in this section we set up a numerical experiment. In this experiment we take a significant step forward numerically from Section 6.2.1. We are able to apply our theoretical results to the experimental problem. Here we take a well known linear partial differential equation for our model dynamics and form an observation operator from its discretisation. The model we use for this experiment is the 2D Eady model as introduced in Chapter 5. Therefore, we can relate our numerical experiment with our infinite dimensional results in Section 6.2.1. Of course no numerical experiment could ever work in an infinite dimensional space. However, for a convergent numerical scheme, the discretisation of the partial differential equation would match with our theory. Therefore, in the limit of small step-size the infinite dimensional partial differential equation would match with the numerical discretisation. A formal definition of convergence can be found in [62, p.157]. In Chapter 5, we mentioned that we discretise the 2D Eady model using the leap-frog scheme as detailed in [36, Appendix A]. Further details on the leap-frog scheme can be found in [62].

In particular we show that a cycled 3DVar scheme is stable over time. Our result in Lemma 6.3.2 is under the condition that Assumption 6.0.2 and Assumption 6.0.5 hold. Therefore, in this experiment the observation operator is a time-invariant linear injective compact operator and decomposes with respect to the eigensystem of the time-invariant linear model operator M that is damping on higher spectral modes.

We saw previously that the regularization parameter chosen sufficiently small led to a stable cycled data assimilation scheme. Here in this experiment we will investigate choosing the regularization too small. In this case we will see that the analysis error gets worse and we can explain the theoretical reason for this.

We begin with the discretised Eady model, which is an 80×80 non-Hermitian matrix.

Since our theoretical result require that M be a self-adjoint (Hermitian) matrix, we multiply the 80×80 non-Hermitian matrix with its transpose. Changing the model dynamics in this way means that the model M no longer has any physical meaning, however, this is not a problem since we view this experiment as a stepping stone to more realistic numerical experiments in Chapter 7 and Chapter 8.

We decompose M into its eigensystem according to Theorem 2.2.4. We choose a random uniformly distributed vector of length 80 from the closed interval $[0, 2]$ using the Matlab command *rand*. This vector will be the spectrum of H in the form of the diagonal matrix $\tilde{D}$ from (6.3) and ranges as follows,

$$\lambda(H) \approx (1.9821, \ldots, 0.0317). \tag{6.85}$$

We set the last eigenvalue $\lambda_{80} = 3.16 \times 10^{-6}$ to create an ill-conditioned observation operator. Now we use the eigenvectors of M with $\tilde{D}$ to form the matrix H in accordance with (6.3). H has condition number $\kappa(H) \approx 6.2724 \times 10^5$ with respect to the matrix 2-norm in accordance with Definition 2.1.18.

We again set up the noise in this experiment to be Gaussian but only draw the following noise term,

$$\boldsymbol{\eta}_k \sim \mathcal{N}(\mathbf{0}, R), \tag{6.86}$$

for $k = 1, \ldots, 1000$ where R is defined in (6.68) with $\sigma_{(o)} = 8$. We have chosen only to have noise on the observations and not on the observation operator to emphasise the consequence of choosing the regularization parameter too small. We can see from (6.42) and (6.43) that with noise only on the observations the analysis error will evolve such that

$$\mathbf{e}_k = \Lambda \mathbf{e}_{k-1} + \mathscr{R}_\alpha \boldsymbol{\eta}_k, \tag{6.87}$$

and the bound on the analysis error will evolve such that

$$e_k \leq \|\Lambda\| \, e_{k-1} + \|\mathscr{R}_\alpha\| \, \delta. \tag{6.88}$$

With an ill-conditioned observation operator we expect $\|\mathscr{R}_\alpha\| \to \infty$ as $\alpha \to 0$. Therefore, as we decrease α, the analysis error will be controlled in each step. However, error in the observations means that the analysis error will be amplified due to the Tikhonov-Phillips inverse being large in norm.

In the same way as Section 6.2.1, we set up simple error covariance matrices in accordance with (6.68). For this experiment we choose the standard deviation on the background state and observations to be $\sigma_{(b)} = 0.5$ and $\sigma_{(o)} = 8$, hence for $\alpha = \sigma^2_{(o)}/\sigma^2_{(b)} = 8^2/0.5^2 = 256$ we connect 3DVar with cycled Tikhonov-Phillips regularization.

Again, since we deal with linear operators in this chapter we can explicitly calculate the error evolution using (6.87). Furthermore, we also want to explore the bound on the error evolution in (6.88). This bound in (6.88) can be considered as a worst case scenario and all our theory is restricted to this bound. Therefore, it is necessary to compare this bound with the actual error evolution. In this experiment we want to demonstrate that choosing the regularization parameter too small means that the analysis error evolution becomes worse despite remaining stable for all assimilation time.

We draw an initial analysis error using the background error statistics, such that $\mathbf{e}_1 \sim \mathcal{N}(\mathbf{0}, B)$ and calculate the analysis error for $k = 2, \ldots, 1000$ using both (6.87) and (6.88). Varying the regularization parameter α we can study the time-averaged error, the same way as Section 6.2.1. In Figure 6.6 we plot the error integral for (6.87) against the regularization parameter. Here in Figure 6.6 we do not plot the error integral for (6.88), since we want to capture the behaviour of (6.87). Including (6.88) in Figure 6.6 rescales the image so that the growth in the error integral is not as clear. We see in Figure 6.6 that as the regularization parameter is reduced, the analysis improves significantly, but then very quickly begins to grow. This growth is due to the ill-conditioned observation operator. We know that the Tikhonov-Phillips inverse will grow in norm as the regularization parameter is reduced, which affects the observation noise. Therefore, if we had perfect observations we would not see this growth in the analysis error for a small regularization parameter.

Similarly to Section 6.2.1 we can investigate the analysis error evolution for individual regularization parameters. We plot in Figure 6.7 the evolution of (6.87) and (6.88) for $\alpha = 256$, which corresponds to 3DVar for given covariances in (6.68). We see that both (6.87) and (6.88) are unstable for this choice of regularization parameter. Now we investigate inflating the background error statistics. Using Figure 6.6 we choose the regularization parameter which corresponds to the smallest time-averaged error. In Figure 6.8 we plot the evolution of (6.87) and (6.88) for $\alpha = 3$ (the regularization with the smallest time-averaged error). Now we choose the regularization parameter which corresponds to the largest time-

averaged error. In Figure 6.9 we observe stable evolutions for both (6.87) and (6.88) with a regularization parameter $\alpha = 10^{-10}$. Despite the evolution of (6.87) in Figure 6.9 being stable, we observe that the analysis error is much larger compared with Figure 6.8. This is reflected in what we observe in Figure 6.6. We take conclusions from this experiment and those developed in Section 6.2.1 forward into more realistic experiments carried out later in Chapter 7 and Chapter 8.

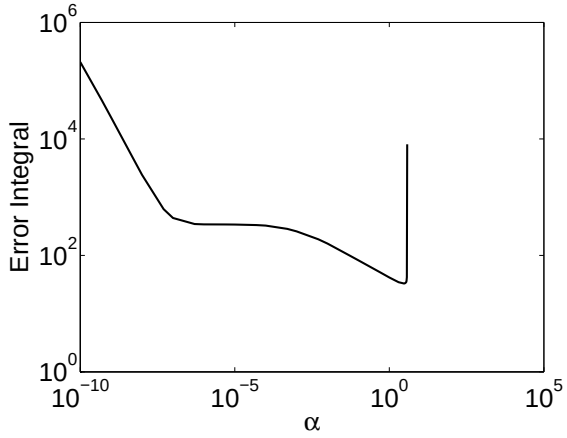

Figure 6.6: ℓ^2 norm of the time-averaged analysis error, $\|\mathbf{e}_k\|_{\ell^2}$ integrated for all assimilation time $k = 1, \ldots, 1000$, varying the regularization parameter, α. Solid: Analysis error governed by the actual error in (6.87).

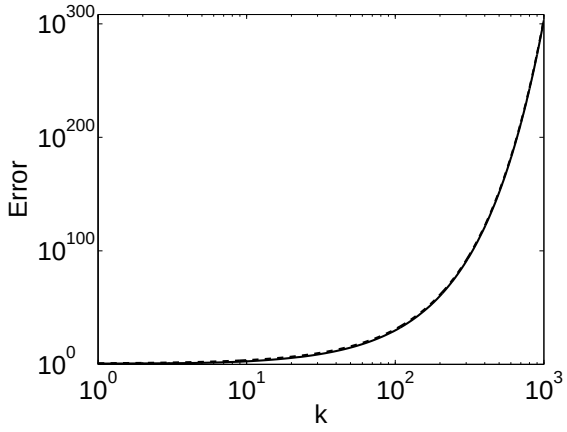

Figure 6.7: ℓ^2 norm of the analysis error, $\|\mathbf{e}_k\|_{\ell^2}$ as the scheme is cycled for index k with regularization parameter, $\alpha = 256$. Solid: Analysis error governed by the actual error in (6.87). Dashed: Theoretical bound from (6.88).

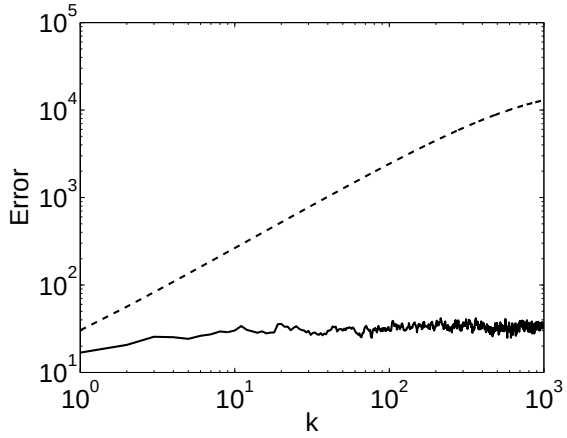

Figure 6.8: ℓ^2 norm of the analysis error, $\|\mathbf{e}_k\|_{\ell^2}$ as the scheme is cycled for index k with regularization parameter, $\alpha = 3$. Solid: Analysis error governed by the actual error in (6.87). Dashed: Theoretical bound from (6.88).

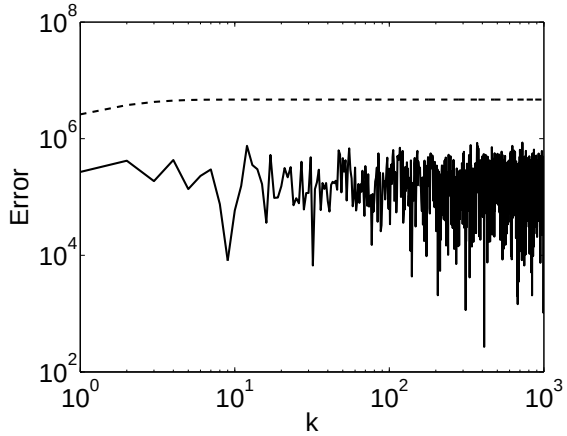

Figure 6.9: ℓ^2 norm of the analysis error, $\|\mathbf{e}_k\|_{\ell^2}$ as the scheme is cycled for index k with regularization parameter, $\alpha = 10^{-10}$. Solid: Analysis error governed by the actual error in (6.87). Dashed: Theoretical bound from (6.88).

6.4 Summary

In this chapter new theoretical results for the stability of cycled 3DVar were presented. We saw in three simple situations that stability can be guaranteed using the regularization parameter. Most notably we saw in Remark 6.1.6 that we were unable to obtain a stability result for the case of constant model dynamics when the dimension of the state space was infinite. Moreover, it was seen that we require some contractive modes of the model dynamics in the case where either the observation operator arose from the model operator or *vice versa*. Lemma 6.1.5 demonstrated an additional challenge, which was that the norm of the reconstruction error operator is always equal to one when the operator equation is ill-posed in an infinite dimension setting. However, we saw that this can be resolved by splitting the state space. Let us assume that the model dynamics are contractive on higher modes of the observation operator. Then splitting the state space means that the norm estimate in Lemma 6.1.5 can be controlled by the contractive part of the model operator and we can use the regularization parameter to control growth in the model dynamics on the lower modes of the observation operator.

We also investigated the evolution of the analysis error numerically. We found that the regularization parameter must be chosen to balance the growth in each cycled assimilation step with the growth in the Tikhonov-Phillips inverse. We take these conclusions forward into the following two chapters and develop theory and numerical experiments for more realistic and practical systems.

Chapter 7

Linear model dynamics

In this chapter we develop new theoretical results for the stability of the data assimilation schemes introduced in Chapter 3 for more realistic dynamical systems compared with Chapter 6. We first consider the case of time-invariant linear model dynamics for cycled data assimilation schemes which employ static error covariances. We present theoretical results and a numerical experiment using the 4DVar scheme introduced in Chapter 3. Next we present results for time-varying linear model dynamics for cycled data assimilation schemes that use a multiplicative update to the background error covariance. Finally, we present results for time-varying model dynamics for cycled data assimilation schemes that update the background error covariance in a general way. Under a number of conditions we can connect one of our stability results with the Kalman filter from Chapter 3. We have submitted separately some of the results of this chapter for publication in [67].

For the theory in this chapter we will make a number of assumptions. For clarity we now list these assumptions so that we can refer to them clearly later on.

Assumption 7.0.1. *The observation operator $H_k \in L(\mathbf{X}, \mathbf{Y})$ is a time-varying linear injective compact operator.*

Assumption 7.0.2. *The time-invariant linear model dynamics $M \in L(\mathbf{X})$ is strictly contractive, such that $\|M\| < 1$.*

Assumption 7.0.3. *The model dynamics $M \in L(\mathbf{X})$ is a time-invariant Hilbert-Schmidt operator.*

Assumption 7.0.4. *The model dynamics $M_k \in L(\mathbf{X})$ is a time-varying linear operator.*

7.1 Time-invariant linear dynamics

In this section we develop theory on the analysis error for cycled Tikhonov-Phillips regularization as introduced in Theorem 3.1.10. Here we move to a more realistic scenario where the model dynamics are independent of the observation operator. This is a more general situation compared with the results obtained in Chapter 6. We assume that the model dynamics is a time-invariant Hilbert-Schmidt operator in accordance with Assumption 7.0.3. The observation operator is assumed to be a time-invariant compact linear operator in accordance with Assumption 6.0.2. From (4.19) substituting for time-invariant model dynamics and observation operator we have that

$$\mathbf{e}_k = (I - \mathscr{R}_\alpha H)\, M\mathbf{e}_{k-1} + \mathscr{R}_\alpha \boldsymbol{\eta}_k + (I - \mathscr{R}_\alpha H)\, \boldsymbol{\zeta}_k - \mathscr{R}_\alpha \boldsymbol{\omega}_k, \tag{7.1}$$

where $\mathscr{R}_\alpha = (\alpha I + H^*H)^{-1}H^* \in L(\mathbf{Y}, \mathbf{X})$. Repeating the step from (6.7) through to (6.13) we have the following bound on the analysis error,

$$e_k \leq \|\Lambda\|\, e_{k-1} + \|N\|\, \upsilon + \|\mathscr{R}_\alpha\|\, (\delta + \gamma)\,, \tag{7.2}$$

where $e_k := \|\mathbf{e}_k\|$, $\Lambda := NM$, $N := I - \mathscr{R}_\alpha H$, with noise terms υ, δ and γ in accordance with Section 4.1. This is the same form as that in (6.42) and (6.43). Therefore, we can formulate Theorem 6.2.1 and ensure asymptotic stability of the cycled scheme by demonstrating that $\|\Lambda\| < 1$. In this case, this condition means that the model dynamics M is not increasing the error stronger than the reconstruction error operator N can reduce it.

As a first attempt we use (c) in Lemma 2.1.20 to split the operator Λ as follows

$$\|\Lambda\| = \|NM\| \leq \|N\| \cdot \|M\|\,. \tag{7.3}$$

The following result follows directly from (7.3).

Lemma 7.1.1. *Let* $\mathbf{X}$ *and* $\mathbf{Y}$ *be Hilbert spaces and let Assumption 6.0.2 hold. If Assumption 7.0.2 holds then* $\|\Lambda\| < 1$.

Proof. From Lemma 6.1.5 we have that $\|N\| = 1$. Therefore from (7.3) we have

$$\|\Lambda\| \leq \|N\| \cdot \|M\| = \|M\| < 1, \tag{7.4}$$

since M is strictly contractive. □

The result in Lemma 7.1.1 has limited practicality since it requires that the model dynamics are strictly contractive for stability. However, as indicated by the work in Chapter 6, if we can split the state space into two parts, one part where the growth in the model can be controlled and another part where a contraction in the model dynamics appears, then we would be able to generalise the result in Lemma 7.1.1 to more realistic systems.

We use the singular system of the observation operator to split the state space. Let $(\mu_i, \boldsymbol{\varphi}_i, \mathbf{g}_i)$ be the singular system of H in accordance with Theorem 2.2.6. We define orthogonal projection operators $P^{(1)}$ and $P^{(2)}$, such that

$$P^{(1)} : \mathbf{X} \to \operatorname{span}\{\boldsymbol{\varphi}_i, i \leq n\} \text{ and } P^{(2)} : \mathbf{X} \to \operatorname{span}\{\boldsymbol{\varphi}_i, i > n\}, \tag{7.5}$$

for $i, n \in \mathbb{N}$. For convenience we define the following orthogonal subspaces

$$\mathbf{X}^{(1)} := \operatorname{span}\{\boldsymbol{\varphi}_1, \ldots, \boldsymbol{\varphi}_n\} \text{ and } \mathbf{X}^{(2)} := \operatorname{span}\{\boldsymbol{\varphi}_{n+1}, \boldsymbol{\varphi}_{n+2}, \ldots\}. \tag{7.6}$$

Using Theorem 2.1.7, Lemma 2.1.27 and Corollary 2.1.29 we can expand any element $\mathbf{x}_k \in \mathbf{X}$ in a Fourier series as follows,

$$\mathbf{x}_k = \left(P^{(1)} + P^{(2)}\right)\mathbf{x}_k = P^{(1)}\mathbf{x}_k + P^{(2)}\mathbf{x}_k \tag{7.7}$$

$$= \sum_{i=1}^{n} \langle \mathbf{x}_k, \boldsymbol{\varphi}_i \rangle \boldsymbol{\varphi}_i + \sum_{i=n+1}^{\infty} \langle \mathbf{x}_k, \boldsymbol{\varphi}_i \rangle \boldsymbol{\varphi}_i \tag{7.8}$$

for $k \in \mathbb{N}_0$.

Using the orthogonal projection operators $P^{(1)}$ and $P^{(2)}$ we define operators $M^{(1)} : \mathbf{X} \to \mathbf{X}^{(1)}$ and $M^{(2)} : \mathbf{X} \to \mathbf{X}^{(2)}$, such that

$$M^{(1)} := P^{(1)}M \text{ and } M^{(2)} := P^{(2)}M. \tag{7.9}$$

Using the reconstruction error operator $N = I - \mathscr{R}_\alpha H$ we split Λ as follows,

$$\Lambda = N|_{\mathbf{X}^{(1)}} M^{(1)} + N|_{\mathbf{X}^{(2)}} M^{(2)}, \tag{7.10}$$

in which $N|_{\mathbf{X}^{(1)}}$ means the operator N is restricted to the subspace $\mathbf{X}^{(1)}$, such that N maps $\mathbf{X}^{(j)}$ for $j = 1, 2$ into itself. This is possible because the operator N is diagonal with respect to the singular system of the observation operator H as seen in (6.41). This leads to the norm estimate

$$\|\Lambda \mathbf{x}_k\|^2 = \left\| \left(N|_{\mathbf{X}^{(1)}} M^{(1)} + N|_{\mathbf{X}^{(2)}} M^{(2)}\right) \mathbf{x}_k \right\|^2 \tag{7.11}$$

$$= \left\| N|_{\mathbf{X}^{(1)}} M^{(1)} \mathbf{x}_k \right\|^2 + \left\| N|_{\mathbf{X}^{(2)}} M^{(2)} \mathbf{x}_k \right\|^2, \tag{7.12}$$

for all $\mathbf{x}_k \in \mathbf{X}$ where equality comes from Theorem 2.1.8, since the subspaces $\mathbf{X}^{(1)}$ and $\mathbf{X}^{(2)}$ in (7.6) are orthogonal. Applying (a) and (c) in Lemma 2.1.20 we have that

$$\|\Lambda\|^2 \leq \|N|_{\mathbf{X}^{(1)}}\|^2 \cdot \left\|M^{(1)}\right\|^2 + \|N|_{\mathbf{X}^{(2)}}\|^2 \cdot \left\|M^{(2)}\right\|^2. \tag{7.13}$$

The following result estimates $\|N|_{\mathbf{X}^{(1)}}\|$ and is similar to Lemma 6.1.4.

Lemma 7.1.2. *For the Hilbert space $(\mathbf{X}, \|\cdot\|_{B^{-1}})$, the regularised reconstruction error operator N restricted to the subspace $\mathbf{X}^{(1)}$ has the following norm estimate,*

$$\|N|_{\mathbf{X}^{(1)}}\| = \sup_{i=1,\ldots,n} \left|\frac{\alpha}{\alpha + \mu_i^2}\right| \tag{7.14}$$

where μ_i are the singular values of the operator H ordered according to their size and multiplicity. Then for some constant $0 < \rho < 1$ we can choose $\alpha > 0$ sufficiently small such that

$$\|N|_{\mathbf{X}^{(1)}}\| \leq \rho. \tag{7.15}$$

Proof. We use (6.33) to obtain (7.14). Since $\mathbf{X}^{(1)}$ is spanned by a finite number of spectral modes of the operator H, we can use Lemma 6.1.4 to show (7.15), which completes the proof. □

The following result is similar to Lemma 6.1.5 and is a consequence of a compact linear operator in an infinite dimensional Hilbert space.

Lemma 7.1.3. *For the Hilbert space $(\mathbf{X}, \|\cdot\|_{B^{-1}})$, the reconstruction error operator N restricted to the subspace $\mathbf{X}^{(2)}$ has the norm estimate*

$$\|N|_{\mathbf{X}^{(2)}}\| = 1. \tag{7.16}$$

Proof. Since H is compact, the singular values $\mu_i \to 0$ for $i \to \infty$. This means that

$$\|N|_{\mathbf{X}^{(2)}}\| = \sup_{i=n+1,\ldots,\infty} \left|\frac{\alpha}{\alpha + \mu_i^2}\right| = 1 \tag{7.17}$$

for all $\alpha > 0$, which completes the proof. □

The sufficient condition for stability of the cycled data assimilation scheme requires that $\|\Lambda\| < 1$. Applying our norm estimates from Lemma 7.1.2 and Lemma 7.1.3 to (7.13) we obtain

$$\|\Lambda\|^2 \leq \rho^2 \cdot \left\|M^{(1)}\right\|^2 + \left\|M^{(2)}\right\|^2. \tag{7.18}$$

Here we directly see how the linear growth in $\mathbf{X}^{(1)}$ can be controlled by the regularization parameter $\alpha > 0$. It is seen that the linear system M has to be damping in $\mathbf{X}^{(2)}$ for $\|\Lambda\| < 1$. Therefore, only if M is strictly damping on higher spectral modes of H, will we be able to stabilise the cycled data assimilation scheme. Instead of assuming this damping on higher spectral modes we can go further and show that if we split the state space in a particular way then for a particular class of compact model operators we can obtain a contraction in the error dynamics. The following result is restricted to Hilbert-Schmidt operators as introduced in Section 2.1.3.

Lemma 7.1.4. *If Assumption 7.0.3 holds then given $0 < \epsilon < 1$ there is an $n \in \mathbb{N}$, such that on $\mathbf{X}^{(2)}$*

$$\left\|M^{(2)}\right\|^2 \leq \epsilon. \tag{7.19}$$

Proof. We begin with expressing the operator $M^{(2)}$ applied to any element $\mathbf{x}_k \in \mathbf{X}$ as

$$\left\|M^{(2)}\mathbf{x}_k\right\|^2 = \sum_{i=n+1}^{\infty} \left|\langle M\mathbf{x}_k, \boldsymbol{\varphi}_i\rangle\right|^2 \tag{7.20}$$

$$= \sum_{i=n+1}^{\infty} \left|\left\langle M \sum_{j=1}^{\infty} \left\langle \mathbf{x}_k, \boldsymbol{\varphi}_j \right\rangle \boldsymbol{\varphi}_j, \boldsymbol{\varphi}_i \right\rangle\right|^2, \tag{7.21}$$

by expanding $\mathbf{x}_k$ in a Fourier series according to (2.8). Rearranging we obtain

$$\left\|M^{(2)}\mathbf{x}_k\right\|^2 = \sum_{i=n+1}^{\infty} \left|\sum_{j=1}^{\infty} \left\langle \mathbf{x}_k, \boldsymbol{\varphi}_j \right\rangle \left\langle M\boldsymbol{\varphi}_j, \boldsymbol{\varphi}_i \right\rangle\right|^2 \tag{7.22}$$

$$\leq \sum_{i=n+1}^{\infty} \left(\sum_{j=1}^{\infty} \left|\left\langle \mathbf{x}_k, \boldsymbol{\varphi}_j \right\rangle\right|^2\right) \left(\sum_{j=1}^{\infty} \left|\left\langle M\boldsymbol{\varphi}_j, \boldsymbol{\varphi}_i \right\rangle\right|^2\right), \tag{7.23}$$

where we have applied the Cauchy-Schwarz inequality from Proposition 2.1.4. Reordering and applying Parseval's equality in (2.9), we have

$$\left\|M^{(2)}\mathbf{x}_k\right\|^2 \leq \left(\sum_{i=n+1}^{\infty} \sum_{j=1}^{\infty} \left|\left\langle M\boldsymbol{\varphi}_j, \boldsymbol{\varphi}_i \right\rangle\right|^2\right) \cdot \left\|\mathbf{x}_k\right\|^2. \tag{7.24}$$

From Definition 2.1.23 we know that the norm of a Hilbert-Schmidt operator is finite. This means that

$$|a_i|^2 := \sum_{j=1}^{\infty} \left|\left\langle M\boldsymbol{\varphi}_j, \boldsymbol{\varphi}_i \right\rangle\right|^2 \tag{7.25}$$

is a sequence where

$$\sum_{i=1}^{\infty} |a_i|^2 < \infty. \tag{7.26}$$

Let b_l be the partial sum such that

$$b_l := \sum_{i=1}^{l} |a_i|^2 . \tag{7.27}$$

Then we know that the sequence (b_l) is monotonically increasing and from (7.26) we know that the sequence is bounded from above. Then from [27, Proposition 2.8] we have that (b_l) is convergent. This means that given $0 < \epsilon < 1$ there is an $n \in \mathbb{N}$, such that

$$\sum_{i=n+1}^{\infty} \sum_{j=1}^{\infty} \left| \langle M\boldsymbol{\varphi}_j, \boldsymbol{\varphi}_i \rangle \right|^2 = \sum_{i=n+1}^{\infty} |a_i|^2 \leq \epsilon. \tag{7.28}$$

This completes the proof. □

The result in Lemma 7.1.4 is interesting since it demonstrates how we can ensure stability in an infinite dimensional setting for a Hilbert-Schmidt operator. It shows that we can split the state space $\mathbf{X}$ so that there is a contraction in the error dynamics over the higher spectral modes of H. Then using the result in Lemma 7.1.2 we can use the regularization parameter to control any expansion in the lower spectral modes of H. We are now able to collect all parts of our analysis to show asymptotic stability for cycled data assimilation schemes with a compact observation operator.

Theorem 7.1.5. *For the Hilbert spaces $(\mathbf{X}, \|\cdot\|_{B^{-1}})$ and $(\mathbf{Y}, \|\cdot\|_{R^{-1}})$, let both Assumption 6.0.2 and Assumption 7.0.3 hold. Then, for regularization parameter $\alpha > 0$ sufficiently small we have $\|\Lambda\| < 1$. If Assumption 6.0.1 holds then the analysis error is bounded over time by*

$$\limsup_{k\to\infty} \|\mathbf{e}_k\| \leq \frac{\|N\|\,\upsilon + \|\mathscr{R}_\alpha\|\,(\delta+\gamma)}{1-\|\Lambda\|} \leq \frac{\upsilon + \frac{\delta+\gamma}{2\sqrt{\alpha}}}{1-\|\Lambda\|}. \tag{7.29}$$

Proof. Given that M is a time-invariant Hilbert-Schmidt operator, we first show that we can achieve $\|\Lambda\| < 1$. From (7.13) we let $\|M^{(1)}\|$ be an arbitrary constant c and $\|N|_{\mathbf{X}^{(2)}}\| = 1$ in accordance with Lemma 7.1.3. We use Lemma 7.1.4 to choose n such that $\|M^{(2)}\|^2 < 1/2$. With n fixed, according to Lemma 7.1.2, the norm $\|N|_{\mathbf{X}^{(1)}}\|$ can be made arbitrarily small by choosing α small enough. We choose α such that

$$c^2 \cdot \|N|_{\mathbf{X}^{(1)}}\|^2 \leq \frac{1}{2}. \tag{7.30}$$

Then we obtain $\|\Lambda\| < 1$ from (7.13). The bound for the analysis error is then given by Theorem 6.2.1, which also provides the estimate in (7.29). The inequality completes the proof in accordance with Remark 6.2.2. □

The result in Theorem 7.1.5 demonstrates the stability of cycled data assimilation schemes in an infinite dimensional setting. The result shows for a regularization parameter that is chosen sufficiently small, we are in a stable range for the data assimilation scheme, that is the analysis error remains bounded for all time. We can relate our result in Theorem 7.1.5 with other results in the literature. In Lemma 4.4.1 it was stated that for a noise-free continuous-time dynamical system, if an observer gain can be chosen so that (4.40) generates an exponentially stable strongly continuous semigroup, then the analysis error asymptotically tends to zero. However, they did not show how an observer gain can be chosen. Here we show that for the discrete-time dynamical system in (4.5) and (4.7) we can find an observer gain so that the norm of Λ from (7.2) is less than one, which means from Theorem 7.1.5 that we obtain a bounded analysis error for all time. In the next section we set-up a realistic numerical experiment using the 2D Eady model as introduced in Chapter 5.

7.1.1 Numerical experiment

In this section we set up a numerical experiment that will demonstrate the behaviour of the analysis error in cycled data assimilation schemes. In the same way as Section 6.3.1 we are able to apply our theoretical results in Section 7.1 to the experimental problem. This is because we can relate a well known linear partial differential equation with its finite dimensional discretisation. Here we again take the 2D Eady model for the model dynamics and use a random linear injective compact observation operator that satisfies Assumption 6.0.2. In particular we show that a cycled 3DVar scheme is stable over time for a model dynamics operator that satisfies Assumption 7.0.3. Using bounded noise in accordance with Assumption 6.0.1 we are therefore able to apply the result in Theorem 7.1.5 since Assumption 6.0.2 and Assumption 7.0.3 hold.

We illustrate numerically the result from Theorem 7.1.5, that the regularization parameter can be chosen sufficiently small such that the analysis error remains bounded for all time. Previously in Section 6.3.1 we observed that choosing the regularization parameter sufficiently

small led to a stable cycled data assimilation scheme. We consider that the model operator M is the discretised Eady model from Chapter 5 and H is a general injective linear ill-conditioned operator. Here the model dynamics operator M, the discretised Eady model is a time-invariant linear Hilbert-Schmidt operator.

We begin with the discretised Eady model, such that M is an 80×80 matrix. For the observation operator we create a random 80×80 matrix using the *rand* function in Matlab. Similar to Section 6.3.1 we change the singular values of H by drawing from the closed interval $[0, 2]$. Therefore, the singular values of H range as follows,

$$\mu(H) \approx (1.9740, \ldots, 0.0224). \tag{7.31}$$

Hence, H has growing and damping modes of a similar size to that of M as was discussed in Chapter 5. We set the last singular value $\mu_{80} = 6.6 \times 10^{-14}$ to create an ill-conditioned observation operator. Therefore H has condition number $\kappa(H) \approx 2.9967 \times 10^{13}$ with respect to the matrix 2-norm in accordance with Definition 2.1.18. The observation operator is a linear time-invariant compact operator which satisfies the theory we have developed in Section 7.1.

Using (3.13) we formulate the matrix $\hat{H}$ for an assimilation window of length $L = 5$. We again set up the noise in this experiment to be Gaussian and draw the following noise terms,

$$\boldsymbol{\eta}_{k_l} \sim \mathcal{N}(\mathbf{0}, R), \;\; \boldsymbol{\zeta}_{k_l} \sim \mathcal{N}(\mathbf{0}, \mathscr{Q}) \;\text{ and }\; \boldsymbol{\omega}_{k_l} \sim \mathcal{N}(\mathbf{0}, W), \tag{7.32}$$

for $k_l = 1, \ldots, 1000$. In a similar way to Section 6.2.1 we set up simple covariance matrices as follows,

$$R = \sigma^2_{(o)} I, \;\; \mathscr{Q} = \sigma^2_{(q)} I \;\text{ and }\; W = \sigma^2_{(w)} I, \tag{7.33}$$

where $\sigma^2_{(o)}$, $\sigma^2_{(q)}$ and $\sigma^2_{(w)}$ are the variances of the noise on the observations, model and observation operator respectively. However, in this experiment we shall formulate a realistic background error covariance matrix using a Laplacian correlation matrix. The inverse of the Laplacian correlation matrix for a periodic parameter is

$$C^{-1} = \gamma^{-1} \left(I + \frac{\hat{L}^4}{2\Delta x^4} L^2_{xx} \right). \tag{7.34}$$

Here $\hat{L}$ is the lengthscale, Δx is the great circle distance between grid points, I is an identity matrix of appropriate size and $\gamma > 0$ is a scaling factor that ensures that the maximum

element of C is equal to one. The matrix L_{xx} is the second order derivative matrix, such that

$$L_{xx} = \begin{pmatrix} -2 & 1 & 0 & \dots & 0 & 1 \\ 1 & -2 & 1 & 0 & \dots & 0 \\ 0 & \ddots & \ddots & \ddots & \ddots & \vdots \\ \vdots & \ddots & \ddots & \ddots & \ddots & 0 \\ 0 & \dots & 0 & 1 & -2 & 1 \\ 1 & 0 & \dots & 0 & 1 & -2 \end{pmatrix}. \tag{7.35}$$

The continuous limit of the covariance operator is as follows,

$$C = \gamma \left(I + \hat{L}^4 \Delta^2 \right)^{-1} \tag{7.36}$$

where Δ is the Laplacian with periodic boundary conditions [79]. Further details of the Laplacian correlation matrix can be found in [36, p.50], [37] and [30, p.53]. We assume that the background error variances are equal to $\sigma^2_{(b)}$ at every grid point, therefore the background error covariance matrix is

$$B = \sigma^2_{(b)} C, \tag{7.37}$$

where C is the inverse of the matrix defined in (7.34).

We choose a similar lengthscale to the experiments in [37], which corresponds to 500km in its dimensionalised form. We assume that errors of the buoyancy on the top and bottom boundaries are uncorrelated. This is a reasonable assumption to make and is consistent with the experiments in [37]. We choose the standard deviation on the background to be $\sigma_{(b)} = 0.06$. In Figure 7.1 and Figure 7.2 we plot the background error covariance matrix and its inverse respectively. Since we assume that the error in the buoyancy on the upper boundary is uncorrelated with the error in the buoyancy on the lower boundary, the matrix in Figure 7.1 is block diagonal. We use the matrix in Figure 7.2 to calculate the weighted norms of the error evolution. If we choose $\alpha = \sigma^2_{(o)}$ then 4DVar is equivalent to cycled Tikhonov-Phillips regularization with respect to the weighted norm in Theorem 3.1.13. For this experiment we choose the standard deviation on the noise as follows, $\sigma_{(o)} = 4$, $\sigma_{(q)} = 1.3$ and $\sigma_{(w)} = 0.6$. Therefore, for $\alpha = \sigma^2_{(o)} = 4^2 = 16$ we connect 4DVar with cycled Tikhonov-Phillips regularization.

Again, since we deal with linear operators in this chapter, we can explicitly calculate the error evolution using (7.1). Furthermore, we also want to explore the bound on the error

evolution in (7.2). We draw an initial analysis error using the background statistics, such that $\mathbf{e}_1 \sim \mathcal{N}(\mathbf{0}, B)$ and calculate the analysis error for $k = 2, \ldots, 200$ using (7.1) and the bound in (7.2). This corresponds to cycling 4DVar over 1000 time-steps since the assimilation window is $L = 5$. Varying the regularization parameter α we can study the time-averaged error in the same way as Section 6.2.1 and Section 6.3.1. In Figure 7.3 we plot the error integral for (7.1) and (7.2) against the regularization parameter. We see in Figure 7.3 that as the regularization parameter is reduced the analysis improves significantly. We do not observe an increase in the error evolution as the regularization parameter is further reduced, which we observed in Section 6.3.1. This can be explained if we calculate the condition number of $\hat{H}$, as $\kappa(\hat{H}) \approx 7.3398$. We see that despite H being ill-conditioned, the resulting matrix $\hat{H}$ which we formulate is reasonably well-conditioned. Therefore, we do not expect the analysis error to grow as we reduce the regularization parameter.

We also see in Figure 7.3 that the bound from (7.2) on the analysis error is unstable for a smaller regularization parameter compared with the actual analysis error from (7.1). Our theoretical understanding of the behaviour of the analysis error is confirmed by the numerical result. It demonstrates the sufficient stability condition which we obtain through our approach of norm estimates. Therefore, we cannot say that if $\|\Lambda\| \geq 1$ then the analysis error evolution will be unstable. Instead we must restrict ourselves and say that if $\|\Lambda\| < 1$ then the analysis error will be stable.

In order to observe the impact of the weighted norm, we plot in Figure 7.4 the time-averaged error for both an ℓ^2 norm and the weighted norm. We see that the only difference is a rescaling of the y axis. We expect this since the weight B^{-1} is constant in time and as such is only scaling the error evolution. Here in Figure 7.4 we do not plot the time-averaged error for the bound in (7.2) since it rescales the image so that it is not clear to observe the difference in the y axis between the ℓ^2 norm and the weighted norm.

In Figure 7.5 we plot the evolution of (7.1) and (7.2) with regularization parameter $\alpha = 1$, which is the value of the regularization parameter that leads to the smallest time-averaged error in Figure 7.3. Here we observe the stable error evolution from (7.1) and unstable growth in (7.2). This directly demonstrates the sufficient stability condition, which we previously discussed, such that for this choice of regularization parameter $\|\Lambda\| \geq 1$ but $r(\Lambda) < 1$. In Figure 7.6 we plot the error evolution for $\alpha = 16$, which corresponds to 4DVar for the

weighted norm. We see that for cycled 4DVar, both evolutions in (7.1) and (7.2) are unstable.

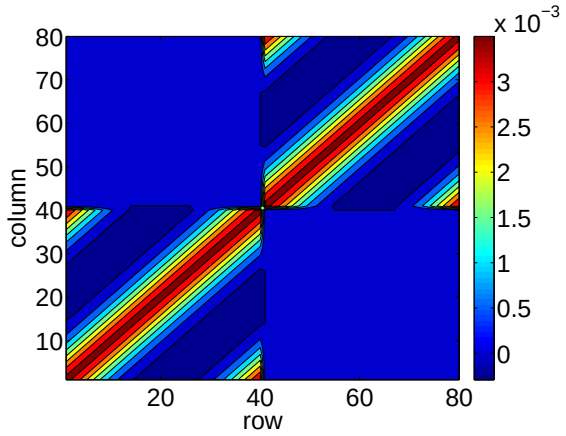

Figure 7.1: The background error covariance matrix, B for a lengthscale of 500km

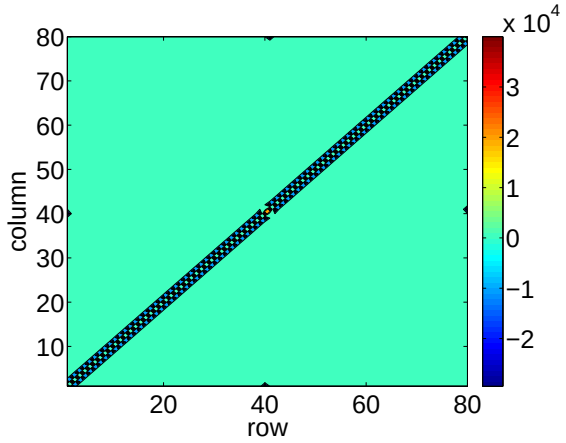

Figure 7.2: The inverse background error covariance matrix, B^{-1} for a lengthscale of 500km

In this section we restricted our analysis to a time-invariant model operator M. However, in the next section we take a further step forward and consider time variant model dynamics.

7.2 Time-varying linear dynamics with a multiplicative update to the background error covariance

In this section we assume that the model dynamics is a time-varying linear operator in accordance with Assumption 7.0.4. However, the observation operator will remain time-invariant in accordance with Assumption 6.0.2. Furthermore, we consider a class of data

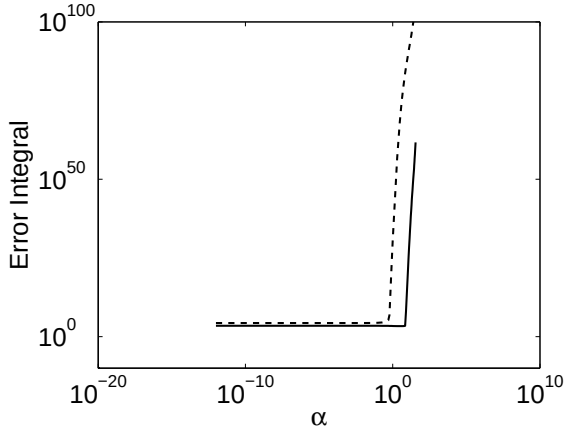

Figure 7.3: Weighted norm of the time-averaged analysis error, $\|\mathbf{e}_k\|_{B^{-1}}$ integrated for all assimilation time $k = 1, \ldots, 200$, varying the regularization parameter, α. Solid: Analysis error governed by (7.1). Dashed: Theoretical bound from (7.2).

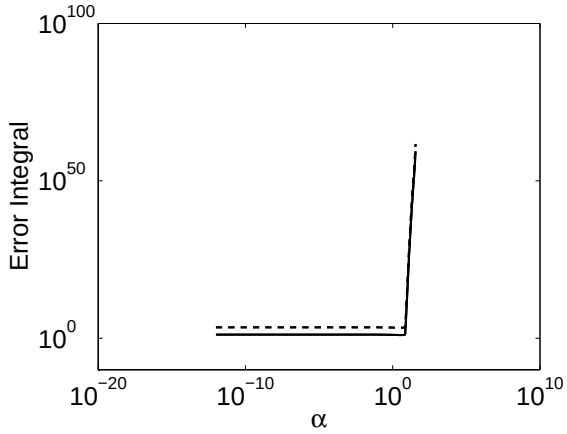

Figure 7.4: ℓ^2 norm of the time-averaged analysis error, $\|\mathbf{e}_k\|_{\ell^2}$ and weighted norm of the analysis error, $\|\mathbf{e}_k\|_{B^{-1}}$, integrated for all assimilation time $k = 1, \ldots, 200$, varying the regularization parameter, α. Solid: ℓ^2 norm of analysis error governed by (7.1). Dashed: Weighted norm of analysis error governed by (7.1).

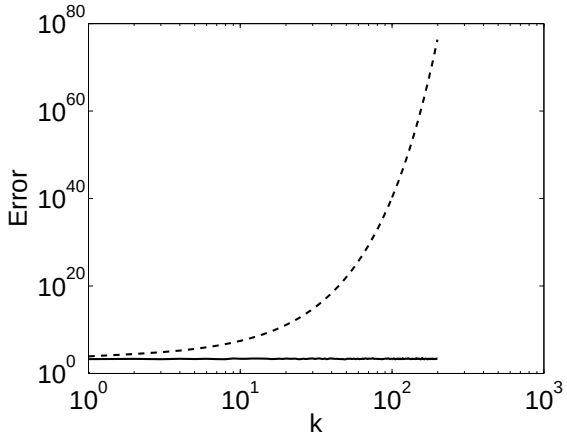

Figure 7.5: Weighted norm of the analysis error, $\|\mathbf{e}_k\|_{B^{-1}}$ as the scheme is cycled for index k with regularization parameter, $\alpha = 1$. Solid: Analysis error governed by (7.1). Dashed: Theoretical bound from (7.2).

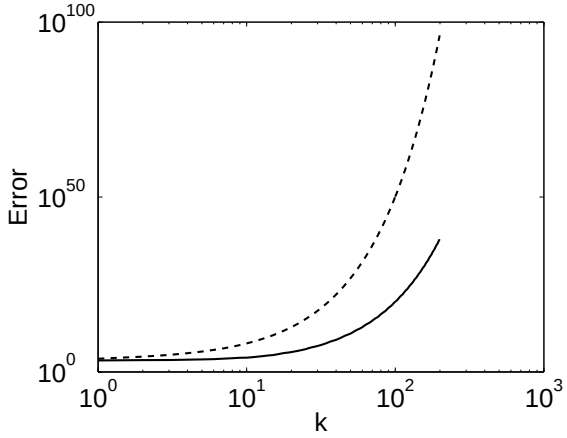

Figure 7.6: Weighted norm of the analysis error, $\|\mathbf{e}_k\|_{B^{-1}}$ as the scheme is cycled for index k with regularization parameter, $\alpha = 16$. Solid: Analysis error governed by (7.1). Dashed: Theoretical bound from (7.2).

assimilation schemes that perform an update to the background error covariance operator. Here we consider a time-dependent regularization parameter α_k. Previously in Section 7.1 we chose a regularization parameter $\alpha > 0$ for all time that inflated the background covariance operator as in (3.32) and (3.34). Now we are interested in changing $\alpha > 0$ in each step such that given an initial background error covariance operator $B_0 \in L(\mathbf{X})$, then

$$B_k = \alpha_k B_0, \tag{7.38}$$

for a given positive time-dependent regularization parameter $\alpha_k > 0$. We are interested in choosing a regularization parameter adaptively in order to extend our previous time-invariant result in Theorem 7.1.5 to dynamical systems where the model dynamics are time-varying. We call this set-up in (7.38) a multiplicative update in the background error statistics and it can be seen as applying *adaptive variance inflation* as discussed in Section 3.1.3. We now weight the state space using the initial background error covariance operator B_0 in (7.38) in accordance with Theorem 3.1.13 and represent a multiplicative update in the background error statistics with a time-dependent regularization parameter α_k in the Tikhonov-Phillips inverse, such that

$$\mathscr{R}_{\alpha_k} = \left(\alpha_k I + H^* H\right)^{-1} H^*. \tag{7.39}$$

Here we clarify that $H \in L(\mathbf{X}, \mathbf{Y})$ remains a time-invariant linear compact operator in accordance with Assumption 6.0.2. However, now α_k is dependent on k therefore, we write $\mathscr{R}_{\alpha_k}$ since the Tikhonov-Phillips inverse operator is dependent on a changing regularization parameter α_k. It directly follows from Theorem 3.1.13 that if $\alpha_k = 1$ for all $k \in \mathbb{N}_0$ in (7.39) then the cycled Tikhonov-Phillips scheme would correspond to 3DVar for the weighted norms $\|\cdot\|_{B_0^{-1}}$ on $\mathbf{X}$ and $\|\cdot\|_{R^{-1}}$ on $\mathbf{Y}$.

From (4.19) we substitute $\mathscr{R}_\alpha$ for a time-dependent $\mathscr{R}_{\alpha_k}$ and H_k for a time-invariant observation operator H, such that

$$\mathbf{e}_k = \left(I - \mathscr{R}_{\alpha_k} H\right) M_{k-1} \mathbf{e}_{k-1} + \mathscr{R}_{\alpha_k} \boldsymbol{\eta}_k + \left(I - \mathscr{R}_{\alpha_k} H\right) \boldsymbol{\zeta}_k - \mathscr{R}_{\alpha_k} \boldsymbol{\omega}_k. \tag{7.40}$$

Repeating the step from (6.7) through to (6.13), we have the following bound on the analysis error

$$e_k \leq \|\Lambda_k\| \, e_{k-1} + \|N_{\alpha_k}\| \, \upsilon + \|\mathscr{R}_{\alpha_k}\| \left(\delta + \gamma\right), \tag{7.41}$$

where $e_k := \|\mathbf{e}_k\|$, $\Lambda_k := N_{\alpha_k} M_{k-1}$, $N_{\alpha_k} := I - \mathscr{R}_{\alpha_k} H$, with noise terms υ, δ and γ in accordance with Section 4.1. This form in (7.40) and (7.41) does not allow us to formulate a similar result on the error evolution as in Theorem 6.2.1. This is because now the operators $N_{\alpha_k} \in L(\mathbf{X})$ and $\mathscr{R}_{\alpha_k} \in L(\mathbf{Y})$ are time-varying. Therefore, it is necessary to take a further bound on the behaviour of the analysis error. From Lemma 6.1.4 and Lemma 6.1.5 we know that $\|N_{\alpha_k}\| \leq 1$ for any regularization parameter $\alpha > 0$. Also if we substitute α_k into (6.47) we have that $\|\mathscr{R}_{\alpha_k}\| \leq 1/(2\sqrt{\alpha_k})$. Therefore, we can bound (7.41) such that

$$e_k \leq \|\Lambda_k\| \, e_{k-1} + \upsilon + \frac{\delta + \gamma}{2\sqrt{\alpha_k}} \tag{7.42}$$

$$\leq \|\Lambda_k\| \, e_{k-1} + \upsilon + \frac{\delta + \gamma}{2\sqrt{\alpha^*}}, \tag{7.43}$$

where $0 < \alpha^* \leq \inf_{k \in \mathbb{N}_0} \alpha_k$. We can now formulate the following result that is similar to Theorem 6.2.1.

Theorem 7.2.1. *For the Hilbert space $(\mathbf{X}, \|\cdot\|_{B_0^{-1}})$, let Assumption 6.0.1 hold. If there exists a constant $\chi > 0$ such that $\sup_{k \in \mathbb{N}_0} \|\Lambda_k\| := \sup_{k \in \mathbb{N}_0} \|(I - \mathscr{R}_{\alpha_k} H) M_{k-1}\| \leq \chi$, then the error evolution in (7.43) and the error term, $\mathbf{e}_k \in \mathbf{X}$ for $k \in \mathbb{N}_0$ where $\mathbf{e}_k := \mathbf{x}_k^{(a)} - \mathbf{x}_k^{(t)}$ is bounded by*

$$\|\mathbf{e}_k\| \leq \chi^k \|\mathbf{e}_0\| + \sum_{l=0}^{k-1} \chi^l \left(\upsilon + \frac{\delta + \gamma}{2\sqrt{\alpha^*}} \right), \tag{7.44}$$

for $k \in \mathbb{N}_0$. If $\chi \neq 1$ then

$$\|\mathbf{e}_k\| \leq \chi^k \|\mathbf{e}_0\| + \frac{1 - \chi^k}{1 - \chi} \left(\upsilon + \frac{\delta + \gamma}{2\sqrt{\alpha^*}} \right), \tag{7.45}$$

for $k \in \mathbb{N}_0$. If $\chi < 1$ then

$$\limsup_{k \to \infty} \|\mathbf{e}_k\| \leq \frac{\upsilon + \frac{\delta + \gamma}{2\sqrt{\alpha^*}}}{1 - \chi}. \tag{7.46}$$

Proof. Given that there exists some constant $\chi > 0$ such that $\sup_{k \in \mathbb{N}_0} \|\Lambda_k\| \leq \chi$ then from (7.43) we have

$$e_k \leq \chi e_{k-1} + \upsilon + \frac{\delta + \gamma}{2\sqrt{\alpha^*}}, \tag{7.47}$$

where $e_k := \|\mathbf{e}_k\|$. The form in (7.47) is similar to that in (6.13). Therefore, we can complete the proof using Theorem 6.1.3 for a different constant χ. □

This result in Theorem 7.2.1 is important since it demonstrates the reverse situation of the previous work we have presented so far. The difference between Theorem 6.1.3, Theorem 6.2.1 and Theorem 7.2.1 is subtle. In Theorem 6.1.3 and Theorem 6.2.1 we were able to present a stability result which was not conditioned on Λ being bounded by a particular constant. However, in Theorem 7.2.1 the operator Λ_k is time-varying, therefore we must first assume that it is bounded by some constant χ before we present our stability result. Instead we could have expressed the error evolution in (7.44) using a state transition matrix, although in this case it would be more difficult to produce as asymptotic result similar to (7.46).

To ensure asymptotic stability of the cycled scheme we must demonstrate that the operator Λ_k is uniformly bounded for all time, such that there exists a constant $0 < \chi < 1$ with $\sup_{k\in\mathbb{N}_0} \|\Lambda_k\| \leq \chi$. In this case we must show that the model dynamics M_{k-1} is not increasing the error in each assimilation step stronger than the reconstruction error operator N_k can reduce it. We have seen previously in this work in Section 7.1 that if there is an expansion in the model dynamics, then we can choose a small regularization parameter to control the error in each step. Now in this section the model dynamics are time-varying therefore, if M_{k-1} was to grow uniformly with respect to k, such that $\|M_{k-1}\| \to \infty$ as $k \to \infty$, then α_k would have to be chosen smaller and smaller, such that $\alpha_k \to 0$ as $k \to \infty$. This cannot be allowed therefore we make the following assumption.

Assumption 7.2.2. *The sequence of linear model operators M_k is bounded for all time, such that*

$$\sup_{k\in\mathbb{N}_0} \|M_k\| = c < \infty, \tag{7.48}$$

for some constant $c > 0$.

It is unclear whether Assumption 7.2.2 holds and if there exists a constant χ such that $\sup_{k\in\mathbb{N}_0} \|\Lambda_k\| \leq \chi$ for realistic models. If Assumption 7.2.2 holds then we can formulate the following finite dimensional result using Lemma 6.1.4.

Lemma 7.2.3. *Let $\mathbf{X}$ and $\mathbf{Y}$ be finite dimensional spaces with the weighted norm $\|\cdot\|_{B_0^{-1}}$ on $\mathbf{X}$ and let Assumption 6.0.2 hold. Let the model dynamics M_{k-1} satisfy Assumption 7.2.2 for all $k \in \mathbb{N}$. Given some constant $0 < \rho < 1$, then using the regularization parameter $\alpha_k > 0$ we can make $\sup_{k\in\mathbb{N}_0} \|\Lambda_k\| = \rho$.*

Proof. We split the operator Λ_k according to (7.3), so that $\|\Lambda_k\| \leq \|N_{\alpha_k}\| \cdot \|M_{k-1}\|$. Using Lemma 6.1.4 we can choose α_k on each assimilation step sufficiently small, so that if $\|M_{k-1}\| \geq 1$, then we choose α_k so that $\|N_{\alpha_k}\| < 1/\|M_{k-1}\|$, else if $\|M_{k-1}\| < 1$, then we choose any $\alpha_k > 0$. This ensures that $\sup_{k\in\mathbb{N}_0} \|\Lambda_k\| = \rho < 1$. By Assumption 7.2.2 we ensure that $\alpha_k > 0$ for all time $k \in \mathbb{N}_0$. □

Similar to Lemma 7.1.1, if $\mathbf{X}$ is of infinite dimension, then M_{k-1} must be uniformly damping for all time to ensure that there exists a constant $0 < \rho < 1$, such that $\sup_{k\in\mathbb{N}_0} \|\Lambda_k\| = \rho$.

Lemma 7.2.4. *For the Hilbert space* $(\mathbf{X}, \|\cdot\|_{B_0^{-1}})$*, let Assumption 6.0.2 hold. If there exists a constant* $0 < \rho < 1$ *such that* $\sup_{k\in\mathbb{N}} \|M_{k-1}\| = \rho$ *then* $\|\Lambda_k\| < 1$ *for all* $k \in \mathbb{N}_0$*.*

Proof. Since H is compact and $\mathbf{X}$ has infinite dimension then from Lemma 6.1.5 $\|N_{\alpha_k}\| = 1$ for any $\alpha_k > 0$. Using (7.3) and Lemma 7.1.1 we complete the proof. □

These two results are limited since they are for the situation of a well-posed observation operator in Lemma 7.2.3 and contractive model dynamics in Lemma 7.2.4. However, splitting the space in a similar way to Section 7.1, we can show that for a sequence of time-varying Hilbert-Schmidt model operators the cycled data assimilation scheme is asymptotically stable.

As in Section 7.1 we define the orthogonal projection operators $P_{n_k}^{(1)}$ and $P_{n_k}^{(2)}$, such that

$$P_{n_k}^{(1)} : \mathbf{X} \to \{\boldsymbol{\varphi}_i, i \leq n_k\} \text{ and } P_{n_k}^{(2)} : \mathbf{X} \to \{\boldsymbol{\varphi}_i, i > n_k\}, \tag{7.49}$$

with respect to the singular system $(\mu_i, \boldsymbol{\varphi}_i, \mathbf{g}_i)$ of H and $n_k \in \mathbb{N}$. We define the following orthogonal spaces

$$\mathbf{X}_{n_k}^{(1)} := \text{span}\{\boldsymbol{\varphi}_1, \ldots, \boldsymbol{\varphi}_{n_k}\} \text{ and } \mathbf{X}_{n_k}^{(2)} := \text{span}\{\boldsymbol{\varphi}_{n_{k+1}}, \boldsymbol{\varphi}_{n_{k+2}}, \ldots\}. \tag{7.50}$$

Using the orthogonal projection operators $P_{n_k}^{(1)}$ and $P_{n_k}^{(2)}$ we define time-dependent operators $M_{k-1}^{(1)} : \mathbf{X} \to \mathbf{X}_{n_k}^{(1)}$ and $M_{k-1}^{(2)} : \mathbf{X} \to \mathbf{X}_{n_k}^{(2)}$, such that

$$M_{k-1}^{(1)} := P_{n_k}^{(1)} M_{k-1} \text{ and } M_{k-1}^{(2)} := P_{n_k}^{(2)} M_{k-1}. \tag{7.51}$$

From (7.43) we apply the steps from (7.7) through to (7.10) so that

$$e_k \leq \left(\left\| N_{\alpha_k}|_{\mathbf{X}_{n_k}^{(1)}} M_{k-1}^{(1)} \right\| + \left\| N_{\alpha_k}|_{\mathbf{X}_{n_k}^{(2)}} M_{k-1}^{(2)} \right\| \right) e_{k-1} + \upsilon + \frac{\delta + \gamma}{2\sqrt{\alpha^*}}. \tag{7.52}$$

Applying (c) in Lemma 2.1.20 we have that

$$e_k \leq \left(\left\| N_{\alpha_k}|_{\mathbf{X}_{n_k}^{(1)}} \right\| \cdot \left\| M_{k-1}^{(1)} \right\| + \left\| N_{\alpha_k}|_{\mathbf{X}_{n_k}^{(2)}} \right\| \cdot \left\| M_{k-1}^{(2)} \right\| \right) e_{k-1} + \upsilon + \frac{\delta + \gamma}{2\sqrt{\alpha^*}}. \tag{7.53}$$

Given some constant $0 < \rho_k < 1$ for all $k \in \mathbb{N}_0$, we can use Lemma 7.2.3 and Lemma 7.1.3 to choose α_k so that

$$e_k \leq \left(\rho_k \cdot \left\| M_{k-1}^{(1)} \right\| + \left\| M_{k-1}^{(2)} \right\| \right) e_{k-1} + \upsilon + \frac{\delta + \gamma}{2\sqrt{\alpha^*}}. \tag{7.54}$$

Before we present our next stability result we must present the following definition.

Definition 7.2.5. Let M_k be a sequence of Hilbert-Schmidt operators on a Hilbert space $\mathbf{X}$ and let $\{\boldsymbol{\varphi}_i : i \in \mathbb{N}\}$ be a complete orthonormal system in $\mathbf{X}$. We call M_k a *uniform sequence of Hilbert-Schmidt operators*, if for every $d > 0$ there is an $n \in \mathbb{N}$ such that

$$\sum_{i=n+1}^{\infty} \|M_k \boldsymbol{\varphi}_i\|^2 \leq d \tag{7.55}$$

for all $k \in \mathbb{N}_0$.

We are now in a position to collect all parts of our analysis to show asymptotic stability for cycled data assimilation schemes with ill-posed observation operators and time-varying model dynamics.

Theorem 7.2.6. *For the Hilbert space $(\mathbf{X}, \|\cdot\|_{B_0^{-1}})$, let M_k be a uniform sequence of Hilbert-Schmidt operators in accordance with Definition 7.2.5 that satisfies Assumption 7.2.2. Then for any constant $0 < d < 1$ there exists an $n_k \in \mathbb{N}$ in each assimilation step k such that*

$$\sup_{k \in \mathbb{N}} \left\| M_{k-1}^{(2)} \right\| = d. \tag{7.56}$$

Let Assumption 6.0.2 hold. Then using the regularization parameter $\alpha_k > 0$ we can ensure for some constant $0 < \rho < 1$ that

$$\left\| N_{\alpha_k}|_{\mathbf{X}_{n_k}^{(1)}} \right\| \leq \frac{\rho - \left\| M_{k-1}^{(2)} \right\|}{\left\| M_{k-1}^{(1)} \right\|}, \tag{7.57}$$

for all $k \in \mathbb{N}$. Then under the conditions of Theorem 6.2.1, there exists a constant $0 < \chi < 1$, such that the analysis error is bounded over time by

$$\limsup_{k\to\infty} \|\mathbf{e}_k\| \leq \frac{\upsilon + \frac{\delta+\gamma}{2\sqrt{\alpha^*}}}{1-\chi}, \tag{7.58}$$

where $0 < \alpha^* \leq \inf_{k\in\mathbb{N}_0} \alpha_k$.

Proof. From Lemma 7.1.4, given any $0 < \epsilon_k < 1$, there exists an $n_k \in \mathbb{N}$ in each step k such that

$$\sum_{i=n_k+1}^{\infty} \|M_{k-1}\boldsymbol{\varphi}_i\|^2 \leq \epsilon_k^2. \tag{7.59}$$

Since M_{k-1} is a uniform sequence of Hilbert-Schmidt operators, it then follows from Definition 7.2.5 that there exists a constant $\epsilon_k \leq d < 1$ and an $n_k \in \mathbb{N}$ such that

$$\sup_{k\in\mathbb{N}} \sqrt{\sum_{i=n_k+1}^{\infty} \|M_{k-1}\boldsymbol{\varphi}_i\|^2} = d, \tag{7.60}$$

which satisfies (7.56).

Now n_k is changing in each step k. Hence we must choose a regularization parameter $\alpha_k > 0$ in each step so that (7.57) holds. Since n_k is finite this means that $\mathbf{X}_{n_k}^{(1)}$ is finite dimensional and we have the following norm estimate in each assimilation step k, such that

$$\left\| N_{\alpha_k}|_{\mathbf{X}_{n_k}^{(1)}} \right\| = \sup_{j\in\{1,\ldots,n_k\}} \left| \frac{\alpha_k}{\alpha_k + \lambda_j} \right|, \tag{7.61}$$

where λ_j are the eigenvalues of the self-adjoint compact operator H^*H. We now show that we can choose a constant $0 < \alpha^* \leq \alpha_k$ for all $k \in \mathbb{N}_0$ so that

$$\sup_{j\in\{1,\ldots,n_k\}} \left| \frac{\alpha^*}{\alpha^* + \lambda_j} \right| \leq \frac{\rho - \left\| M_{k-1}^{(2)} \right\|}{\left\| M_{k-1}^{(1)} \right\|}. \tag{7.62}$$

Since the eigenvalues of H^*H are assumed to be ordered then from (7.61) we have that

$$\sup_{j\in\{1,\ldots,n_k\}} \left| \frac{\alpha_k}{\alpha_k + \lambda_j} \right| \leq \frac{\alpha_k}{\alpha_k + \lambda_{n_k}}. \tag{7.63}$$

Under Assumption 7.2.2 there exists a constant $c > 0$ such that $\sup_{k\in\mathbb{N}} \|M_{k-1}^{(1)}\| = c$. Since the model dynamics are assumed not to be globally damping then we have that $c \geq 1$. From (7.60) there exists a constant $0 < d < 1$ such that $\sup_{k\in\mathbb{N}} \|M_{k-1}^{(2)}\| = d$. Hence,

$$f := \frac{\rho - d}{c} \leq \frac{\rho - \left\| M_{k-1}^{(2)} \right\|}{\left\| M_{k-1}^{(1)} \right\|}. \tag{7.64}$$

We choose α^* such that

$$\alpha^* = \frac{\lambda^* f}{1-f}, \tag{7.65}$$

where $\lambda^* := \inf_{k\in\mathbb{N}_0} \lambda_{n_k} > 0$ since n_k is finite. Then rearranging we have that

$$\frac{\alpha^*}{\alpha^* + \lambda^*} = f. \tag{7.66}$$

Therefore, we have found an $\alpha^* > 0$ such that (7.62) is satisfied, which means that there exists an $\alpha_k \geq \alpha^*$ in each step k such that (7.57) is satisfied. Then from (7.54) there exists a constant $0 < \chi < 1$ such that a bound for the analysis error is given by

$$e_k \leq \chi e_{k-1} + \upsilon + \frac{\delta + \gamma}{2\sqrt{\alpha^*}}. \tag{7.67}$$

Then we can apply Theorem 7.2.1 to (7.67) and complete the proof to satisfy (7.58). □

This result in Theorem 7.2.6 is substantial since it extends the previous result in Theorem 7.1.5. We see that choosing the regularization parameter on each assimilation step means that we can control the time-varying model dynamics. This result is restricted to cycled data assimilation schemes where we can perform a multiplicative update to the background error covariance. Therefore, using the regularization parameter in each step enables us to control any growth in the time-varying model dynamics. We see in (7.58) that the asymptotic bound on the analysis error depends on a lower bound for the regularization parameter chosen over time. It was necessary to bound the error evolution in (7.43) by α^* to remove the time dependence in the noise term. This is a trade off, since as we extend our results to more general realistic systems, we must relax the bounds on the analysis error. In the next section we move to a more complicated situation where there is a general update to the background error covariance operator. This is a more interesting situation since we can parallel our theoretical work with the Kalman filter as introduced in Chapter 3.

7.3 Time-varying linear dynamics with a general update to the background error covariance

In this section we consider an update to the background covariance operator in a more general way compared with Section 7.2. In this case it does not make sense to weight the state space

$\mathbf{X}$ with respect to the background covariance operator as in Theorem 3.1.13. A general update to the background covariance operator means the norm on the state space $\mathbf{X}$ will be changing in each assimilation step. Therefore, we must include the covariances B and R in the Tikhonov-Phillips inverse directly. Despite this we will see that the Tikhonov-Phillips inverse can be transformed into a symmetric form similar to (3.25).

This approach will allow us to develop results for a more general setting compared with Section 7.1 and Section 7.2. However, unlike before these bounds will be dependent on the condition number of the square root of the background error covariance operator. We use the square root of the background error covariance operator to transform the Tikhonov-Phillips inverse into a symmetric form. This approach can be seen as using a transformation of variables and then transforming back. The control variable transform is a technique used operationally in NWP centres such as the UK Meteorological Office ([51], [69]) and the European Centre for Medium-Range Weather Forecasts ([16]). These centres like many others use a change of variable, such that

$$\mathbf{z}_k = B_k^{-1/2}\mathbf{x}_k, \tag{7.68}$$

as a preconditioning tool for all $\mathbf{z}_k, \mathbf{x}_k \in \mathbf{X}$, given an invertible square root of the background covariance operator B_k for $k \in \mathbb{N}_0$. Here we drop the index (b) from $B_k^{(b)}$ to keep this work clear and note that B_k here will refer to the background covariance operator at time k. This change of variable through the use of the background covariance operator is known as the control variable transform technique. Operationally speaking, the control variable transform is only currently applied for a static square root of the background error covariance matrix. However, here we assume that we can calculate $B_k^{-1/2}$ for all time k. Preconditioning improves the conditioning of the problem in accordance with Definition 2.1.18.

We begin with the Kalman filter update equation in (3.21) and substitute for (7.68) as follows,

$$B_k^{1/2}\mathbf{z}_k^{(a)} = M_{k-1}B_{k-1}^{1/2}\mathbf{z}_{k-1}^{(a)} + \mathscr{K}_k\left(\mathbf{y}_k - HM_{k-1}B_{k-1}^{1/2}\mathbf{z}_{k-1}^{(a)}\right), \tag{7.69}$$

given a discrete time-varying linear model operator $M_{k-1} : \mathbf{X} \to \mathbf{X}$, such that

$$\mathbf{x}_k^{(b)} = M_{k-1}\mathbf{x}_{k-1}^{(a)}, \tag{7.70}$$

for $k \in \mathbb{N}$ and the Kalman gain $\mathscr{K}_k$ from (3.20).

We assume that there exists unique square roots $B_k^{1/2}, B_k^{-1/2} \in L(\mathbf{X})$ for all time $k \in \mathbb{N}$. Later in Lemma 7.3.6 we show under a number of conditions that this assumption holds for the Kalman filter. Multiplying through by $B_k^{-1/2}$ we obtain,

$$\mathbf{z}_k^{(a)} = B_k^{-1/2} M_{k-1} B_{k-1}^{1/2} \mathbf{z}_{k-1}^{(a)} + B_k^{-1/2} \mathscr{K}_k \left(\mathbf{y}_k - H M_{k-1} B_{k-1}^{1/2} \mathbf{z}_{k-1}^{(a)} \right). \tag{7.71}$$

We use Lemma 2.1.19 and rearrange the Kalman gain as follows,

$$\begin{aligned}
B_k^{-1/2} \mathscr{K}_k &= B_k^{-1/2} B_k H^* \left(H B_k H^* + R_k \right)^{-1} && (7.72)\\
&= B_k^{-1/2} \left(B_k^{-1} + H^* R_k^{-1} H \right)^{-1} \left(B_k^{-1} + H^* R_k^{-1} H \right) \\
&\quad \cdot B_k H^* \left(H B_k H^* + R_k \right)^{-1} && (7.73)\\
&= B_k^{-1/2} \left(B_k^{-1} + H^* R_k^{-1} H \right)^{-1} \left(H^* + H^* R_k^{-1} H B_k H^* \right) \\
&\quad \cdot \left(H B_k H^* + R_k \right)^{-1} && (7.74)\\
&= B_k^{-1/2} \left(B_k^{-1} + H^* R_k^{-1} H \right)^{-1} H^* R_k^{-1} \left(R_k + H B_k H^* \right) \\
&\quad \cdot \left(H B_k H^* + R_k \right)^{-1} && (7.75)\\
&= B_k^{-1/2} \left(B_k^{-1} + H^* R_k^{-1} H \right)^{-1} H^* R_k^{-1} && (7.76)\\
&= \left(B_k^{-1/2} + H^* R_k^{-1} H B_k^{1/2} \right)^{-1} H^* R_k^{-1} && (7.77)\\
&= \left(I + B_k^{1/2} H^* R_k^{-1} H B_k^{1/2} \right)^{-1} B_k^{1/2} H^* R_k^{-1} && (7.78)\\
&= \left(I + \mathscr{G}_k^* R_k^{-1} \mathscr{G}_k \right)^{-1} \mathscr{G}_k^* R_k^{-1}, && (7.79)
\end{aligned}$$

where $\mathscr{G}_k := H B_k^{1/2}$. We now assume that the observation error covariance takes the diagonal form

$$R_k = rI, \tag{7.80}$$

for all $k \in \mathbb{N}_0$ with $r \in \mathbb{R}^+$. If there exists unique bounded square roots $R_k^{-1/2} \in L(\mathbf{Y})$ for all k then it is possible to avoid assuming R_k is defined by (7.80). However, we will make this assumption to simplify our bounds later in this section. Hence (7.79) becomes

$$B_k^{-1/2} \mathscr{K}_k = \left(I + r^{-1} \mathscr{G}_k^* \mathscr{G}_k \right)^{-1} r^{-1} \mathscr{G}_k^*, \tag{7.81}$$

and therefore

$$\mathscr{K}_k = B_k^{1/2} \left(rI + \mathscr{G}_k^* \mathscr{G}_k \right)^{-1} \mathscr{G}_k^*. \tag{7.82}$$

From (7.82) we include a time-dependent regularization parameter α_k so that the Tikhonov-Phillips inverse is

$$\mathscr{R}_{\alpha_k,k} := B_k^{1/2} \left(r\alpha_k I + \mathscr{G}_k^* \mathscr{G}_k\right)^{-1} \mathscr{G}_k^* \tag{7.83}$$

and is equivalent to the Kalman gain for $\alpha_k = 1$ for all $k \in \mathbb{N}_0$. We see that this form in (7.83) is similar to that of (3.25), although here in (7.83) we have an extra term $B_k^{1/2} \in L(\mathbf{X})$. Furthermore, the operator $\mathscr{G}_k$ is time-varying, which is different to the previous set-up. This means that if we span the space with respect to a singular system of $\mathscr{G}_k$, in a similar way to (7.6) and (7.50), then the singular system would be time-varying. Hence, the subspaces $\mathbf{X}_1$ and $\mathbf{X}_2$ would be changing in each assimilation step since the orthonormal system $\{\boldsymbol{\varphi}_i : i \in \mathbb{N}\}$ is changing in each step. We must keep this in mind when carrying out our analysis. In addition, since now $\mathscr{G}_k$ is time-varying we can generalise our results even further and assume that the observation operator is time-varying, such that $\mathscr{G}_k := H_k B_k^{1/2}$. In this section we assume that the observation operators $H_k \in L(\mathbf{X}, \mathbf{Y})$ are a sequence of injective linear time-varying compact operators and the inverse square root background error covariance operator $B_k^{-1/2} \in L(\mathbf{X})$ is injective for all time. Then it follows directly that $\mathscr{G}_k$ is injective for all time. Later in Lemma 7.3.6 we show that under a number of assumptions, the Kalman filter will produce an injective square root background error covariance operator for all time.

From (4.19) we replace $\mathscr{R}_\alpha$ with (7.83) so that

$$\begin{aligned}\mathbf{e}_k = &\left(I - \mathscr{R}_{\alpha_k,k} H_k\right) M_{k-1} \mathbf{e}_{k-1} + \mathscr{R}_{\alpha_k,k} \boldsymbol{\eta}_k + \left(I - \mathscr{R}_{\alpha_k,k} H_k\right) \boldsymbol{\zeta}_k \\ &- \mathscr{R}_{\alpha_k,k} \boldsymbol{\omega}_k.\end{aligned} \tag{7.84}$$

We rearrange the new reconstruction error operator in a similar way as seen from (6.28) through to (6.33) as follows,

$$\begin{aligned} I - \mathscr{R}_{\alpha_k,k} H_k &= I - B_k^{1/2} \left(r\alpha_k I + \mathscr{G}_k^* \mathscr{G}_k\right)^{-1} \mathscr{G}_k^* H_k && (7.85)\\ &= B_k^{1/2} \left(r\alpha_k I + \mathscr{G}_k^* \mathscr{G}_k\right)^{-1} \cdot \\ &\quad \left(\left(r\alpha_k I + \mathscr{G}_k^* \mathscr{G}_k\right) B_k^{-1/2} - \mathscr{G}_k^* H_k\right) && (7.86)\\ &= B_k^{1/2} \left(r\alpha_k I + \mathscr{G}_k^* \mathscr{G}_k\right)^{-1} r\alpha_k B_k^{-1/2} && (7.87)\\ &= B_k^{1/2} \left(I + r^{-1}\alpha_k^{-1} \mathscr{G}_k^* \mathscr{G}_k\right)^{-1} B_k^{-1/2} && (7.88)\\ &= B_k^{1/2} N_{\alpha_k,k} B_k^{-1/2}, && (7.89) \end{aligned}$$

where

$$N_{\alpha_k,k} := (I + r^{-1}\alpha_k^{-1}\mathscr{G}_k^*\mathscr{G}_k)^{-1}. \tag{7.90}$$

Therefore, we can rewrite (7.84) so that

$$\mathbf{e}_k = \hat{\Lambda}_k \mathbf{e}_{k-1} + \mathscr{R}_{\alpha_k,k}(\boldsymbol{\eta}_k - \boldsymbol{\omega}_k) + B_k^{1/2} N_{\alpha_k,k} B_k^{-1/2} \boldsymbol{\zeta}_k, \tag{7.91}$$

where $\hat{\Lambda}_k := B_k^{1/2} N_{\alpha_k,k} B_k^{-1/2} M_{k-1}$. Taking norms we have

$$e_k \leq \left\|\hat{\Lambda}_k\right\| e_{k-1} + \|\mathscr{R}_{\alpha_k,k}\|(\delta + \gamma) + \left\|B_k^{1/2} N_{\alpha_k,k} B_k^{-1/2}\right\| \upsilon, \tag{7.92}$$

where $e_k := \|\mathbf{e}_k\|$ and noise terms δ, γ and υ in accordance with Section 4.1.

We define the time-dependent orthogonal projection operators $P_k^{(1)}$ and $P_k^{(2)}$, such that

$$P_k^{(1)} : \mathbf{X} \to \operatorname{span}\{\boldsymbol{\varphi}_{i,k}, i \leq n_k\} \text{ and } P_k^{(2)} : \mathbf{X} \to \operatorname{span}\{\boldsymbol{\varphi}_{i,k}, i > n_k\}, \tag{7.93}$$

with respect to the singular system $(\mu_{i,k}, \boldsymbol{\varphi}_{i,k}, \mathbf{g}_{i,k})$ of $\mathscr{G}_k$ for $i \in \mathbb{N}$ and $k \in \mathbb{N}_0$. We define the following orthogonal subspaces,

$$\mathbf{X}_k^{(1)} := \operatorname{span}\{\boldsymbol{\varphi}_{1,k}, \ldots, \boldsymbol{\varphi}_{n_k,k}\} \text{ and } \mathbf{X}_k^{(2)} := \operatorname{span}\{\boldsymbol{\varphi}_{n_{k+1},k}, \boldsymbol{\varphi}_{n_{k+2},k}, \ldots\}. \tag{7.94}$$

Using the orthogonal projection operators $P_k^{(1)}$ and $P_k^{(2)}$ we define time-dependent operators $M_{k-1}^{(1)} : \mathbf{X} \to \mathbf{X}^{(1)}$ and $M_{k-1}^{(2)} : \mathbf{X} \to \mathbf{X}^{(2)}$, such that

$$M_{k-1}^{(1)} := P_k^{(1)} M_{k-1} \text{ and } M_{k-1}^{(2)} := P_k^{(2)} M_{k-1}. \tag{7.95}$$

In the same way as (7.10), we write

$$\hat{\Lambda}_k = \left(B_k^{1/2} N_{\alpha_k,k} B_k^{-1/2}\right)|_{\mathbf{X}_k^{(1)}} M_{k-1}^{(1)} + \left(B_k^{1/2} N_{\alpha_k,k} B_k^{-1/2}\right)|_{\mathbf{X}_k^{(2)}} M_{k-1}^{(2)}. \tag{7.96}$$

Taking norms and applying (a) and (c) in Lemma 2.1.20 we obtain

$$\begin{aligned}
\left\|\hat{\Lambda}_k\right\| &= \left\|\left(B_k^{1/2} N_{\alpha_k,k} B_k^{-1/2}\right)|_{\mathbf{X}_k^{(1)}} M_{k-1}^{(1)} + \left(B_k^{1/2} N_{\alpha_k,k} B_k^{-1/2}\right)|_{\mathbf{X}_k^{(2)}} M_{k-1}^{(2)}\right\| && (7.97)\\
&\leq \left\|\left(B_k^{1/2} N_{\alpha_k,k} B_k^{-1/2}\right)|_{\mathbf{X}_k^{(1)}} M_{k-1}^{(1)}\right\| + \left\|\left(B_k^{1/2} N_{\alpha_k,k} B_k^{-1/2}\right)|_{\mathbf{X}_k^{(2)}} M_{k-1}^{(2)}\right\| && (7.98)\\
&\leq \left\|B_k^{1/2}|_{\mathbf{X}_k^{(1)}}\right\| \cdot \left\|N_{\alpha_k,k}|_{\mathbf{X}_k^{(1)}}\right\| \cdot \left\|B_k^{-1/2}|_{\mathbf{X}_k^{(1)}}\right\| \cdot \left\|M_{k-1}^{(1)}\right\| \\
&\quad + \left\|B_k^{1/2}|_{\mathbf{X}_k^{(2)}}\right\| \cdot \left\|N_{\alpha_k,k}|_{\mathbf{X}_k^{(2)}}\right\| \cdot \left\|B_k^{-1/2}|_{\mathbf{X}_k^{(2)}}\right\| \cdot \left\|M_{k-1}^{(2)}\right\|. && (7.99)
\end{aligned}$$

Using Definition 2.1.18 we have

$$\begin{aligned}\left\|\hat{\Lambda}_k\right\| \leq \kappa\left(B_k^{1/2}|_{\mathbf{X}_k^{(1)}}\right) \cdot \left\|N_{\alpha_k,k}|_{\mathbf{X}_k^{(1)}}\right\| \cdot \left\|M_{k-1}^{(1)}\right\| \\ + \kappa\left(B_k^{1/2}|_{\mathbf{X}_k^{(2)}}\right) \cdot \left\|N_{\alpha_k,k}|_{\mathbf{X}_k^{(2)}}\right\| \cdot \left\|M_{k-1}^{(2)}\right\|,\end{aligned} \tag{7.100}$$

where $\kappa(\cdot)$ denotes the condition number. We can now bound the operators acting on the noise terms. Since $\mathscr{G}_k$ is injective then

$$\left\|\mathscr{R}_{\alpha_k,k}\right\| = \left\|B_k^{1/2}\left(r\alpha_k I + \mathscr{G}_k^*\mathscr{G}_k\right)^{-1}\mathscr{G}_k^*\right\| \tag{7.101}$$

$$\leq \frac{\left\|B_k^{1/2}\right\|}{2\sqrt{r\alpha_k}}, \tag{7.102}$$

using Theorem 2.3.3 and

$$\left\|B_k^{1/2}\left(I + r^{-1}\alpha_k^{-1}\mathscr{G}_k^*\mathscr{G}_k\right)^{-1}B_k^{-1/2}\right\| \leq \kappa\left(B_k^{1/2}\right) \cdot \left\|N_{\alpha_k,k}\right\|, \tag{7.103}$$

using (c) in Lemma 2.1.20 and Remark 6.2.2. Applying (7.100), (7.102) and (7.103) to (7.92) we obtain

$$\begin{aligned}e_k \leq \Big(\kappa\left(B_k^{1/2}|_{\mathbf{X}_k^{(1)}}\right) \cdot \left\|N_{\alpha_k,k}|_{\mathbf{X}_k^{(1)}}\right\| \cdot \left\|M_{k-1}^{(1)}\right\| \\ + \kappa\left(B_k^{1/2}|_{\mathbf{X}_k^{(2)}}\right) \cdot \left\|N_{\alpha_k,k}|_{\mathbf{X}_k^{(2)}}\right\| \cdot \left\|M_{k-1}^{(2)}\right\|\Big) e_{k-1} \\ + \frac{\left\|B_k^{1/2}\right\|(\delta+\gamma)}{2\sqrt{r\alpha_k}} + \kappa\left(B_k^{1/2}\right) \cdot \left\|N_{\alpha_k,k}\right\| \upsilon.\end{aligned} \tag{7.104}$$

The following remark explains that we can further bound (7.104) and highlights why it was necessary to split the state space with respect to the singular system of $\mathscr{G}_k$.

Remark 7.3.1. Directly from Lemma 6.1.5 we have

$$\left\|N_{\alpha_k,k}\right\| = \left\|\left(I + r^{-1}\alpha_k^{-1}\mathscr{G}_k^*\mathscr{G}_k\right)^{-1}\right\| = 1, \tag{7.105}$$

and from Lemma 7.1.3 we have

$$\left\|N_{\alpha_k,k}|_{\mathbf{X}_k^{(2)}}\right\| = \left\|\left(I + r^{-1}\alpha_k^{-1}\mathscr{G}_k^*\mathscr{G}_k\right)^{-1}|_{\mathbf{X}_k^{(2)}}\right\| = 1, \tag{7.106}$$

for all $\alpha_k > 0$ for $k \in \mathbb{N}_0$.

Using Remark 7.3.1 we have from (7.104) that

$$e_k \leq \left(\kappa\left(B_k^{1/2}|_{\mathbf{X}_k^{(1)}}\right)\cdot\left\|N_{\alpha_k,k}|_{\mathbf{X}_k^{(1)}}\right\|\cdot\left\|M_{k-1}^{(1)}\right\|+\kappa\left(B_k^{1/2}|_{\mathbf{X}_k^{(2)}}\right)\cdot\left\|M_{k-1}^{(2)}\right\|\right)e_{k-1}$$
$$+\frac{\left\|B_k^{1/2}\right\|(\delta+\gamma)}{2\sqrt{r\alpha_k}}+\kappa\left(B_k^{1/2}\right)\upsilon. \tag{7.107}$$

In order to achieve a bound on the analysis error, it is necessary to make the following assumption on the behaviour of the background error covariance operator.

Assumption 7.3.2. *The square root background error covariance and its inverse are uniformly bounded, such that*

$$\sup_{k\in\mathbb{N}_0}\left\|B_k^{-1/2}\right\|\leq a \tag{7.108}$$

and

$$\sup_{k\in\mathbb{N}_0}\left\|B_k^{1/2}\right\|\leq b, \tag{7.109}$$

for constants $a, b\in\mathbb{R}^+$.

If Assumption 7.3.2 holds then we can satisfy the following bounds on the square root of the background error covariance operator and its inverse restricted to the subspaces $\mathbf{X}_k^{(1)}$ and $\mathbf{X}_k^{(2)}$, such that

$$\sup_{k\in\mathbb{N}_0}\left\|B_k^{-1/2}|_{\mathbf{X}_k^{(1)}}\right\|\leq a^{(1)}\ ,\ \sup_{k\in\mathbb{N}_0}\left\|B_k^{1/2}|_{\mathbf{X}_k^{(1)}}\right\|\leq b^{(1)}, \tag{7.110}$$

$$\sup_{k\in\mathbb{N}_0}\left\|B_k^{-1/2}|_{\mathbf{X}_k^{(2)}}\right\|\leq a^{(2)}\ \text{ and }\ \sup_{k\in\mathbb{N}_0}\left\|B_k^{1/2}|_{\mathbf{X}_k^{(2)}}\right\|\leq b^{(2)}, \tag{7.111}$$

for constants $a^{(1)}, a^{(2)}, b^{(1)}, b^{(2)}\in\mathbb{R}^+$. Later in this chapter we will show under certain positivity conditions that the Kalman filter satisfies (7.108) in Assumption 7.3.2. If Assumption 7.3.2 holds, then from (7.107) using (7.110) and (7.111) we have that

$$e_k \leq \left(a^{(1)}b^{(1)}\cdot\left\|N_{\alpha_k,k}|_{\mathbf{X}_k^{(1)}}\right\|\cdot\left\|M_{k-1}^{(1)}\right\|+a^{(2)}b^{(2)}\cdot\left\|M_{k-1}^{(2)}\right\|\right)e_{k-1}$$
$$+\frac{b\,(\delta+\gamma)}{2\sqrt{r\alpha^*}}+ab\upsilon, \tag{7.112}$$

where $0<\alpha^*\leq\inf_{k\in N_0}\alpha_k$. Before we present our next stability result we must present the following definition.

Definition 7.3.3. Let $\mathscr{G}_k\in L(\mathbf{X},\mathbf{Y})$ be a sequence of injective linear compact operators mapping a Hilbert space $\mathbf{X}$ into a Hilbert space $\mathbf{Y}$ and let $(\mu_{i,k},\boldsymbol{\varphi}_{i,k},\mathbf{g}_{i,k})$ be the singular

system of $\mathscr{G}_k$ for $i \in \mathbb{N}$ and $k \in \mathbb{N}_0$. We call $\mathscr{G}_k$ a *uniform spectral sequence of injective linear compact operators* if there exists a sequence $\hat{\mu}_i > 0$ such that

$$\mu_{i,k} \geq \hat{\mu}_i, \tag{7.113}$$

for all $i \in \mathbb{N}$ and $k \in \mathbb{N}_0$.

As we will see, Definition 7.3.3 is necessary to achieve uniformity in the bounds on the analysis error. We are now in a position to state the main result for cycled data assimilation schemes that employ a general update to the background error covariance.

Theorem 7.3.4. *For the Hilbert space $(\mathbf{X}, \|\cdot\|_{\ell^2})$, let M_k be a uniform sequence of Hilbert-Schmidt operators in accordance with Definition 7.2.5 that satisfies Assumption 7.2.2. Let Assumption 7.3.2 hold. Then for any constant $0 < d < 1$ there exists an $n_k \in \mathbb{N}$ in each assimilation step k, such that*

$$\sup_{k\in\mathbb{N}} \left\| M_{k-1}^{(2)} \right\| = \frac{d}{a^{(2)}b^{(2)}}, \tag{7.114}$$

with positive constants $a^{(2)}b^{(2)} \in \mathbb{R}^+$ from (7.111). Let $\mathscr{G}_k$ be a uniform spectral sequence of injective linear compact operators in accordance with Definition 7.3.3. Then using the regularization parameter $\alpha_k > 0$, we can always ensure for some constant $0 < \rho < 1$ that

$$\left\| N_{\alpha_k,k}|_{\mathbf{X}_k^{(1)}} \right\| \leq \frac{\rho - a^{(2)}b^{(2)} \left\| M_{k-1}^{(2)} \right\|}{a^{(1)}b^{(1)} \left\| M_{k-1}^{(1)} \right\|}, \tag{7.115}$$

for all $k \in \mathbb{N}$ where $N_{\alpha_k,k}$ is defined in (7.90) and for positive constants $a^{(1)}b^{(1)} \in \mathbb{R}^+$ from (7.110). Under the conditions of Theorem 6.2.1, there exists some constant $0 < \chi < 1$, such that the analysis error is bounded over time by

$$\limsup_{k\to\infty} \|\mathbf{e}_k\| \leq \frac{ab\upsilon + \frac{b(\delta+\gamma)}{2\sqrt{r\alpha^*}}}{1-\chi}, \tag{7.116}$$

where $0 < \alpha^* \leq \inf_{k\in\mathbb{N}_0} \alpha_k$.

Proof. From Lemma 7.1.4, given any $0 < \epsilon_k < 1/(a^{(2)}b^{(2)})$, there exists an $n_k \in \mathbb{N}$ in each step k such that

$$\sum_{i=n_k+1}^{\infty} \left\| M_{k-1}\boldsymbol{\varphi}_{i,k} \right\|^2 \leq \epsilon_k^2, \tag{7.117}$$

given the singular system $(\mu_{i,k}, \boldsymbol{\varphi}_{i,k}, \mathbf{g}_{i,k})$ of the sequence of compact operators $\mathscr{G}_k$ for $i \in \mathbb{N}$. Since M_{k-1} is a uniform sequence of Hilbert-Schmidt operators, it then follows from Definition 7.2.5 that there exists a constant $\epsilon_k \leq d/(a^{(2)}b^{(2)}) < 1/(a^{(2)}b^{(2)})$ and an $n_k \in \mathbb{N}$ such that

$$\sup_{k\in\mathbb{N}} \sqrt{\sum_{i=n_k+1}^{\infty} \left\| M_{k-1}\boldsymbol{\varphi}_{i,k} \right\|^2} = \frac{d}{a^{(2)}b^{(2)}}, \tag{7.118}$$

which satisfies (7.114).

Now n_k and the orthonormal system $\{\boldsymbol{\varphi}_{i,k} : i \in \mathbb{N}\}$ are changing in each step k. Hence we must choose a regularization parameter $\alpha_k > 0$ in each step so that (7.115) holds. Since n_k is finite this means that $\mathbf{X}_k^{(1)}$ from (7.93) is finite dimensional and we have the following norm estimate in each assimilation step k, such that

$$\left\| N_{\alpha_k,k}|_{\mathbf{X}_k^{(1)}} \right\| = \sup_{j\in\{1,\dots,n_k\}} \left| \frac{r\alpha_k}{r\alpha_k + \lambda_{j,k}} \right|, \tag{7.119}$$

where $\lambda_{j,k}$ are the eigenvalues of the sequence of self-adjoint compact operators $\mathscr{G}_k^*\mathscr{G}_k$. We now show that we can choose a constant $0 < \alpha^* \leq \alpha_k$ for all $k \in \mathbb{N}_0$ so that

$$\sup_{j\in\{1,\dots,n_k\}} \left| \frac{r\alpha^*}{r\alpha^* + \lambda_{j,k}} \right| \leq \frac{\rho - a^{(2)}b^{(2)} \left\| M_{k-1}^{(2)} \right\|}{a^{(1)}b^{(1)} \left\| M_{k-1}^{(1)} \right\|}. \tag{7.120}$$

Since the eigenvalues of $\mathscr{G}_k^*\mathscr{G}_k$ are assumed to be ordered then from (7.119) we have that

$$\sup_{j\in\{1,\dots,n_k\}} \left| \frac{r\alpha_k}{r\alpha_k + \lambda_{j,k}} \right| = \frac{r\alpha_k}{r\alpha_k + \lambda_{n_k,k}}. \tag{7.121}$$

Under Assumption 7.2.2 there exists a constant $c > 0$ such that $\sup_{k\in\mathbb{N}} \|M_{k-1}^{(1)}\| = c$. Since the model dynamics are assumed not to be globally damping then we have that $c \geq 1$. From (7.118) there exists a constant $0 < d < 1$ such that $\sup_{k\in\mathbb{N}} \|M_{k-1}^{(2)}\| = d/(a^{(2)}b^{(2)})$. Hence,

$$f := \frac{\rho - d}{a^{(1)}b^{(1)}c} \leq \frac{\rho - a^{(2)}b^{(2)} \left\| M_{k-1}^{(2)} \right\|}{a^{(1)}b^{(1)} \left\| M_{k-1}^{(1)} \right\|}. \tag{7.122}$$

From Definition 7.3.3 there exists a real positive constant $0 < \lambda^* \leq \lambda_{n_k,k}$ for all $k \in \mathbb{N}_0$ such that we can choose α^* so that

$$\alpha^* = \frac{\lambda^* f}{r - rf}. \tag{7.123}$$

Then rearranging we have that

$$\frac{r\alpha^*}{r\alpha^* + \lambda^*} = f. \tag{7.124}$$

Therefore, we have found an $\alpha^* > 0$ such that (7.120) is satisfied, which means that there exists an $\alpha_k \geq \alpha^*$ in each assimilation step k such that (7.115) is satisfied. Then from (7.112) there exists a constant $0 < \chi < 1$ such that the bound for the analysis error is then given by

$$e_k \leq \chi e_{k-1} + \frac{b\,(\delta + \gamma)}{2\sqrt{r\alpha^*}} + abv. \tag{7.125}$$

Therefore, we can apply Theorem 7.2.1 to (7.125) and complete the proof to satisfy (7.116). □

The result in Theorem 7.3.4 shows that splitting the state space in a particular way and choosing the regularization parameter sufficiently small, means that the cycled data assimilation scheme can be kept stable for all time. We have shown that if Assumption 7.3.2 holds then the operator bounds in Assumption 4.5.1 from [7] can be satisfied in a more general setting. With the added challenge of an updated background error covariance, it was necessary to bound our expression for the analysis error by the condition number of the square root of the background error covariance operator. Of course in generalising the set-up, we expect the bounds to become weaker. Including the background error covariance directly in the analysis error evolution means that it was necessary to satisfy Assumption 7.3.2. We now show that under certain positivity conditions that the Kalman filter produces unique square roots $B_k^{(b)1/2}, B_k^{(b)-1/2} \in L(\mathbf{X})$ for all time $k \in \mathbb{N}_0$ and satisfies (7.108) in Assumption 7.3.2.

Reducing the regularization parameter α here can be related to assuming that the observations are more accurate. The work of [30] has showed that having more accurate observations or a less accurate background (which both correspond to a reduction in the weight to the background term, i.e. a smaller regularization parameter α) means that the Tikhonov-Phillips inverse at a fixed time is more ill-conditioned. Furthermore, we see that as the condition number of the square root background error covariance operator gets larger then our bound in (7.116) gets worse. Similar results can be seen in [30, Section 6.1.1] in the finite dimensional setting where the upper and lower bounds on the condition number of the Hessian matrix of the 3DVar cost functional get worse as the background error covariance operator became more ill-conditioned.

7.3.1 The Kalman filter

Here we show that the Kalman filter produces unique square roots $B_k^{(b)1/2}, B_k^{(b)-1/2} \in L(\mathbf{X})$ for all time $k \in \mathbb{N}_0$ and satisfies the uniformity condition in (7.108). If (7.109) holds then the Kalman filter is asymptotically stable by Theorem 7.3.4 for an appropriate choice of regularization parameter. We first show that given a perfect model Kalman filter with constant model dynamics and a time-invariant observation operator, then the background error covariance asymptotically collapses in at least one direction. This result can be seen indirectly embedded in [26, Section 7].

Lemma 7.3.5. *Let* $\mathbf{X}$ *and* $\mathbf{Y}$ *be Hilbert spaces. Let* $B_0 \in L(\mathbf{X})$ *be the initial background error covariance operator and let Assumption 6.0.3 hold. Let Assumption 6.0.2 hold and let* $R \in L(\mathbf{Y})$ *be a static observation error covariance operator. Then given the perfect model Kalman filter update equations, the background error covariance operators behave such that*

$$\left\|B_k^{-1}\right\| \to \infty, \tag{7.126}$$

as $k \to \infty$.

Proof. Using (3.19) and (3.22) we have that

$$B_k = (I - \mathscr{K}_{k-1}H)\, B_{k-1}, \tag{7.127}$$

given constant model dynamics $M_k = I$ and $\mathscr{Q}_k = 0$, for all $k \in \mathbb{N}_0$. Here we note that B_k represents the background error covariance $B_k^{(b)}$ where we drop the index (b) in order to read better. Following a similar process from (6.28) through to (6.33), we have that

$$\begin{aligned} B_k &= \left(I - \left(B_{k-1}^{-1} + H^*R^{-1}H\right)^{-1} H^*R^{-1}H\right) B_{k-1} && (7.128)\\ &= \left(B_{k-1}^{-1} + H^*R^{-1}H\right)^{-1} \left(\left(B_{k-1}^{-1} + H^*R^{-1}H\right) - H^*R^{-1}H\right) B_{k-1} && (7.129)\\ &= \left(B_{k-1}^{-1} + H^*R^{-1}H\right)^{-1}. && (7.130) \end{aligned}$$

We invert both sides and obtain

$$B_k^{-1} = B_{k-1}^{-1} + H^*R^{-1}H. \tag{7.131}$$

We use induction to show that

$$B_k^{-1} = B_0^{-1} + \sum_{i=0}^{k-1} H^*R^{-1}H. \tag{7.132}$$

We begin with the base case for $k = 1$ and obtain from (7.132) that

$$B_1^{-1} = B_0^{-1} + H^* R^{-1} H, \tag{7.133}$$

which is equivalent to (7.131) for $k = 1$. Now we proceed with the inductive step. From (7.131) we have that

$$B_k^{-1} = B_{k-1}^{-1} + H^* R^{-1} H \tag{7.134}$$

$$= B_0^{-1} + \sum_{i=0}^{k-2} H^* R^{-1} H + H^* R^{-1} H \tag{7.135}$$

$$= B_0^{-1} + \sum_{i=0}^{k-1} H^* R^{-1} H, \tag{7.136}$$

which satisfies (7.132). This completes the induction. We rearrange (7.132) as follows,

$$B_k^{-1} - B_0^{-1} = \sum_{i=0}^{k-1} H^* R^{-1} H. \tag{7.137}$$

We now take norms and use (a) and (b) in Lemma 2.1.20 to obtain

$$\left\| \sum_{i=0}^{k-1} H^* R^{-1} H \right\| = \left\| B_k^{-1} - B_0^{-1} \right\| \tag{7.138}$$

$$\leq \left\| B_k^{-1} \right\| + \left\| -B_0^{-1} \right\| = \left\| B_k^{-1} \right\| + \left\| B_0^{-1} \right\| \tag{7.139}$$

$$\left\| B_k^{-1} \right\| \geq \left\| \sum_{i=0}^{k-1} H^* R^{-1} H \right\| - \left\| B_0^{-1} \right\|. \tag{7.140}$$

Since the operator composition $H^* R^{-1} H$ is time-invariant we can replace $\sum_{i=0}^{k-1} H^* R^{-1} H$ with $k H^* R^{-1} H$. Therefore, from (7.140) using (b) in Lemma 2.1.20 we have

$$\left\| B_k^{-1} \right\| \geq k \left\| H^* R^{-1} H \right\| - \left\| B_0^{-1} \right\|. \tag{7.141}$$

Taking the limit $k \to \infty$ we complete the proof. □

This result, which also holds in the finite dimensional setting, shows that the background error covariance collapses in at least one direction in the limit. Of course this is a very particular set-up where the model dynamics are constant in time. However, it does highlight that the model error operator $\mathscr{Q}_k$ is important to ensure that the background error covariance does not collapse. Furthermore, it was necessary to again restrict to the case where the observation operator is time-invariant. Here we now show for a more realistic scenario that with a

particular choice of model error operator $\mathscr{Q}_k$, we can connect the Kalman filter with (7.108) in Assumption 7.3.2. We note that we reintroduce the index (b) on the background error covariance operator and (a) on the analysis error covariance operator so that a distinction can be made between the two operators.

Lemma 7.3.6. *Let* $\mathbf{X}$ *and* $\mathbf{Y}$ *be Hilbert spaces. Let* $B_0^{(b)} \in L(\mathbf{X})$ *be an initial strictly positive background error covariance operator and let Assumption 7.0.4 hold. Let Assumption 7.0.1 hold and let* $R_k \in L(\mathbf{Y})$ *be a strictly positive time-varying observation error covariance operators for all time* $k \in \mathbb{N}_0$*. Let* $\mathscr{Q}_k \in L(\mathbf{X})$ *be a sequence of strictly positive model error covariance operators for all time* $k \in \mathbb{N}_0$*. Then there exists unique square roots*

$$B_k^{(b)1/2} \in L(\mathbf{X}) \text{ and } B_k^{(b)-1/2} \in L(\mathbf{X}) \tag{7.142}$$

for all time $k \in \mathbb{N}_0$*.*

If the sequence of model error covariance operator $\mathscr{Q}_k \in L(\mathbf{X})$ *is uniformly strictly positive for all time* $k \in \mathbb{N}_0$*, then there exists a positive real number* $a^* \in \mathbb{R}^+$ *such that*

$$\sup_{k\in\mathbb{N}_0} \left\| B_k^{(b)-1/2} \right\| \leq a^*. \tag{7.143}$$

Proof. We first show an obvious result from the background error covariance update in the Kalman filter. Given that $B_k^{(b)} \in L(\mathbf{X})$, $R_k \in L(\mathbf{Y})$ and $\mathscr{Q}_{k+1} \in L(\mathbf{X})$ are self-adjoint operators, then

$$\begin{aligned} B_k^{(a)*} &= \left(B_k^{(b)} - K_k H_k B_k^{(b)} \right)^* && (7.144)\\ &= B_k^{(b)} - B_k^{(b)} H_k^* \left(\left(H_k B_k^{(b)} H_k^* + R_k \right)^{-1} \right)^* H_k B_k^{(b)} && (7.145)\\ &= B_k^{(b)} - B_k^{(b)} H_k^* \left(H_k B_k^{(b)} H_k^* + R_k \right)^{-1} H_k B_k^{(b)} && (7.146)\\ &= \left(I - K_k H_k \right) B_k^{(b)} = B_k^{(a)}, && (7.147) \end{aligned}$$

which shows that $B_k^{(a)}$ is self-adjoint. Hence,

$$\begin{aligned} B_{k+1}^{(b)*} &= \left(M_k B_k^{(a)} M_k^* + \mathscr{Q}_{k+1} \right)^* && (7.148)\\ &= M_k B_k^{(a)} M_k^* + \mathscr{Q}_{k+1} = B_{k+1}^{(b)}, && (7.149) \end{aligned}$$

which shows that $B_{k+1}^{(b)}$ is self-adjoint. Therefore, the Kalman filter will always produce a self-adjoint operator. We now show that the Kalman filter produces a strictly positive operator in each assimilation step.

We prove by induction. Since the initial $B_0^{(b)} \in L(\mathbf{X})$ is strictly positive then there exists constants $c_0, d_0 > 0$ such that

$$d_0\|\mathbf{x}\|^2 \geq \left\langle B_0^{(b)}\mathbf{x}, \mathbf{x}\right\rangle \geq c_0\|\mathbf{x}\|^2 \tag{7.150}$$

and therefore from Lemma 2.1.31

$$\frac{1}{c_0}\|\mathbf{x}\|^2 \geq \left\langle B_0^{(b)-1}\mathbf{x}, \mathbf{x}\right\rangle \geq \frac{1}{d_0}\|\mathbf{x}\|^2. \tag{7.151}$$

Hence, from Theorem 2.1.32 there exists unique square roots $B_0^{(b)1/2}, B_0^{(b)-1/2} \in L(\mathbf{X})$. Now for the inductive step we show that if there exists constants $a_k, b_k > 0$, such that

$$b_k\|\mathbf{x}\|^2 \geq \left\langle B_k^{(b)}\mathbf{x}, \mathbf{x}\right\rangle \geq a_k\|\mathbf{x}\|^2, \tag{7.152}$$

then $B_{k+1}^{(b)1/2}, B_{k+1}^{(b)-1/2} \in L(\mathbf{X})$. From (7.152) using Lemma 2.1.31 we have that

$$\frac{1}{a_k}\|\mathbf{x}\|^2 \geq \left\langle B_k^{(b)-1}\mathbf{x}, \mathbf{x}\right\rangle \geq \frac{1}{b_k}\|\mathbf{x}\|^2. \tag{7.153}$$

Since $R_k \in L(\mathbf{Y})$ is strictly positive then $R_k^{-1} \in L(\mathbf{Y})$ is strictly positive such that from Theorem 2.1.32 there exists a unique square root $R_k^{-1/2} \in L(\mathbf{Y})$. Therefore,

$$\begin{aligned}
\left\langle B_k^{(a)-1}\mathbf{x}, \mathbf{x}\right\rangle &= \left\langle \left(B_k^{(b)-1} + H_k^* R_k^{-1} H_k\right)\mathbf{x}, \mathbf{x}\right\rangle && (7.154)\\
&= \left\langle B_k^{(b)-1}\mathbf{x}, \mathbf{x}\right\rangle + \left\langle H_k^* R_k^{-1} H_k\mathbf{x}, \mathbf{x}\right\rangle && (7.155)\\
&= \left\langle B_k^{(b)-1}\mathbf{x}, \mathbf{x}\right\rangle + \left\langle R_k^{-1/2} H_k\mathbf{x}, R_k^{-1/2} H_k\mathbf{x}\right\rangle && (7.156)\\
&= \left\langle B_k^{(b)-1}\mathbf{x}, \mathbf{x}\right\rangle + \left\|R_k^{-1/2} H_k\mathbf{x}\right\|^2 \geq \frac{1}{b_k}\|\mathbf{x}\|^2, && (7.157)
\end{aligned}$$

since $\|R_k^{-1/2} H_k\mathbf{x}\|^2 \geq 0$ for all $\mathbf{x} \in \mathbf{X}$. Since $H_k \in L(\mathbf{X}, \mathbf{Y})$, $H_k^* \in L(\mathbf{Y}, \mathbf{X})$ and $R_k^{-1} \in L(\mathbf{Y})$ then from property (b) in Lemma 2.1.20 we have that $H_k^* R_k^{-1} H_k \in L(\mathbf{X})$. From (7.153) we know that $B_k^{(b)-1} \in L(\mathbf{X})$ and since $H_k^* R_k^{-1} H_k \in L(\mathbf{X})$ then from property (a) in Lemma 2.1.20 we have that $B_k^{(a)-1} = B_k^{(b)-1} + H_k^* R_k^{-1} H_k \in L(\mathbf{X})$. Hence, $B_k^{(a)-1}$ is a strictly positive operator and there exists a constant $e_k > 0$, such that

$$e_k\|\mathbf{x}\|^2 \geq \left\langle B_k^{(a)-1}\mathbf{x}, \mathbf{x}\right\rangle \geq \frac{1}{b_k}\|\mathbf{x}\|^2. \tag{7.158}$$

From Lemma 2.1.31 we have that

$$b_k\|\mathbf{x}\|^2 \geq \left\langle B_k^{(a)}\mathbf{x}, \mathbf{x}\right\rangle \geq \frac{1}{e_k}\|\mathbf{x}\|^2. \tag{7.159}$$

Therefore, $B_k^{(a)}$ is strictly positive and from Theorem 2.1.32 there exists a unique square root $B_k^{(a)1/2} \in L(\mathbf{X})$. Then there exists a constant $c_{k+1} > 0$, such that

$$\left\langle B_{k+1}^{(b)}\mathbf{x}, \mathbf{x} \right\rangle = \left\langle \left(M_k B_k^{(a)} M_k^* + \mathscr{Q}_{k+1} \right) \mathbf{x}, \mathbf{x} \right\rangle \tag{7.160}$$

$$= \left\langle M_k B_k^{(a)} M_k^* \mathbf{x}, \mathbf{x} \right\rangle + \langle \mathscr{Q}_{k+1}\mathbf{x}, \mathbf{x} \rangle \tag{7.161}$$

$$= \left\langle B_k^{(a)1/2} M_k^* \mathbf{x}, B_k^{(a)1/2} M_k^* \mathbf{x} \right\rangle + \langle \mathscr{Q}_{k+1}\mathbf{x}, \mathbf{x} \rangle \tag{7.162}$$

$$= \left\| B_k^{(a)1/2} M_k^* \mathbf{x} \right\|^2 + \langle \mathscr{Q}_{k+1}\mathbf{x}, \mathbf{x} \rangle \geq c_{k+1} \|\mathbf{x}\|^2, \tag{7.163}$$

since $\|B_k^{(a)1/2} M_k^* \mathbf{x}\| \geq 0$ for all $\mathbf{x} \in \mathbf{X}$ and $\mathscr{Q}_{k+1} \in L(\mathbf{X})$ is strictly positive. Since $M_k, M_k^* \in L(\mathbf{X})$ and from (7.159) $B_k^{(a)} \in L(\mathbf{X})$ then from property (b) in Lemma 2.1.20 we have that $M_k B_k^{(a)} M_k^* \in L(\mathbf{X})$. Since $\mathscr{Q}_{k+1} \in L(\mathbf{X})$ and $M_k B_k^{(a)} M_k^* \in L(\mathbf{X})$ then from property (a) in Lemma 2.1.20 we have that $B_{k+1}^{(b)} = M_k B_k^{(a)} M_k^* + \mathscr{Q}_{k+1} \in L(\mathbf{X})$. Hence, $B_{k+1}^{(b)}$ is a strictly positive operator and there exists a constant $d_{k+1} > 0$, such that

$$d_{k+1}\|\mathbf{x}\|^2 \geq \left\langle B_{k+1}^{(b)}\mathbf{x}, \mathbf{x} \right\rangle \geq c_{k+1}\|\mathbf{x}\|^2. \tag{7.164}$$

From Lemma 2.1.31 we have that

$$\frac{1}{c_{k+1}}\|\mathbf{x}\|^2 \geq \left\langle B_{k+1}^{(b)-1}\mathbf{x}, \mathbf{x} \right\rangle \geq \frac{1}{d_{k+1}}\|\mathbf{x}\|^2, \tag{7.165}$$

Therefore, $B_{k+1}^{(b)-1}$ is strictly positive and from Theorem 2.1.32 there exists unique square roots $B_{k+1}^{(b)1/2}, B_{k+1}^{(b)-1/2} \in L(\mathbf{X})$. Hence by induction (7.142) is proved.

Now, if the model error covariance operator is uniformly strictly positive, then there exists a constant $c > 0$, such that

$$\langle \mathscr{Q}_k\mathbf{x}, \mathbf{x} \rangle \geq c\|\mathbf{x}\|^2, \tag{7.166}$$

for all $k \in \mathbb{N}_0$. We can substitute c_{k+1} in (7.163) for c so that

$$\left\langle B_{k+1}^{(b)}\mathbf{x}, \mathbf{x} \right\rangle = \left\| B_k^{(a)1/2} M_k^* \mathbf{x} \right\|^2 + \langle \mathscr{Q}_{k+1}\mathbf{x}, \mathbf{x} \rangle \geq c\|\mathbf{x}\|^2, \tag{7.167}$$

since $\mathscr{Q}_k$ is uniformly strictly positive for all time $k \in \mathbb{N}_0$. Applying Lemma 2.1.31 to (7.167) we have that

$$\frac{1}{c}\|\mathbf{x}\|^2 \geq \left\langle B_{k+1}^{(b)-1}\mathbf{x}, \mathbf{x} \right\rangle. \tag{7.168}$$

Then

$$\left\| B_{k+1}^{(b)-1/2}\mathbf{x} \right\|^2 = \left\langle B_{k+1}^{(b)-1/2}\mathbf{x}, B_{k+1}^{(b)-1/2}\mathbf{x} \right\rangle = \left\langle B_{k+1}^{(b)-1}\mathbf{x}, \mathbf{x} \right\rangle \leq \frac{1}{c}\|\mathbf{x}\|^2 \tag{7.169}$$

for all $\mathbf{x} \in \mathbf{X}$. Hence, there exists a positive real number $a^* \in \mathbb{R}^+$ such that (7.143) is satisfied, which completes the proof. □

We see that Lemma 7.3.6 is hugely important since it connects the Kalman filter in Definition 3.1.7 with (7.108) in Assumption 7.3.2. In Lemma 7.3.6 we assume that the observation error covariance operator $R_k \in L(\mathbf{Y})$, which is more general than required in our stability result in Theorem 7.3.4. If (7.109) holds then we show that a regularization parameter can be chosen in each assimilation step so that the Kalman filter is asymptotically stable. From (7.82) we see that reducing the regularization parameter has the effect of reducing the assumed observation uncertainty in the data assimilation scheme. This means that the filter trusts the observed data in each step leading to a stable analysis error in each step. Our result in Theorem 7.3.4 can be seen as an extension to the work of [74, Theorem 5.1]. Of course our result is dependent on a number of positivity conditions which we have seen. Furthermore, it was necessary to bound the analysis error by the condition number of the square root of the background error covariance operator and by the smallest regularization parameter chosen over time. This means that our worst case estimate is extremely unlikely to happen.

7.4 Summary

In this chapter, we have derived new theoretical results on the behaviour of the analysis error for linear dynamical systems. We have generalised many of the results from Chapter 6 and shown that for time-invariant and time-varying linear model dynamics, the stability of various cycled data assimilations can be achieved. We used ideas from Chapter 6 to split the state space in such a way to control the ill-posedness of the problem and expansive model dynamics. We also presented one numerical example for the Eady model using a realistic background error covariance matrix to weight the state space. Finally, we extended previous results and showed stability for a data assimilation scheme that employs an update to the background error covariance. We have shown that under a number of positivity assumptions that the Kalman filter from Chapter 3 produces unique square roots $B_k^{(b)1/2}, B_k^{(b)-1/2} \in L(\mathbf{X})$ for all time and satisfies the uniformity condition in (7.108). This means that if (7.109) holds

then under the conditions of Theorem 7.3.4 we would obtain an asymptotic stability result for the Kalman filter. In the next chapter we extend the results developed in this chapter to dynamical systems with nonlinear model dynamics and capture the behaviour of the analysis error in numerical experiments.

Chapter 8

Nonlinear model dynamics

In this chapter we develop new theoretical results for the stability of data assimilation schemes introduced in Chapter 3 for dynamical systems where the model dynamics are nonlinear and the observation operator is linear. This extends previous linear results from Chapter 7. We have published separately some of the results of this chapter in [60].

8.1 Time-varying nonlinear dynamics

We first return to Section 4.1 and rewrite the error evolution in its nonlinear form. We shall consider that the dynamical system is comprised of a nonlinear dynamical flow equation and a linear measurement equation. We let $\mathcal{M}_k^{(t)} : \mathbf{X} \to \mathbf{X}$ be a true nonlinear model operator which is a discrete-time process such that

$$\mathbf{x}_{k+1}^{(t)} = \mathcal{M}_k^{(t)} \left(\mathbf{x}_k^{(t)} \right), \tag{8.1}$$

for $\mathbf{x}_k^{(t)} \in \mathbf{X}$ for $k \in \mathbb{N}_0$. Again we use the notation $\mathbf{x}_k^{(t)}$, where t refers to the true state. We assume that we have a modelled nonlinear model operator $\mathcal{M}_k : \mathbf{X} \to \mathbf{X}$, such that

$$\mathcal{M}_k \left(\mathbf{x}_k^{(t)} \right) = \mathcal{M}_k^{(t)} \left(\mathbf{x}_k^{(t)} \right) + \boldsymbol{\zeta}_{k+1}, \tag{8.2}$$

where $\boldsymbol{\zeta}_k$ is some additive noise that we call *model error* for $k \in \mathbb{N}_0$. We require that the noise $\boldsymbol{\zeta}_k$ be bounded by some constant $\upsilon > 0$ for all time $k \in \mathbb{N}_0$. The observations and observation operator are assumed to take the same form as in (4.8) and (4.7) respectively. Therefore, from

$$\mathbf{x}_k^{(a)} = \mathcal{M}_{k-1} \mathbf{x}_{k-1}^{(a)} + \mathscr{R}_\alpha \left(\mathbf{y}_k - H \mathcal{M}_{k-1} \left(\mathbf{x}_{k-1}^{(a)} \right) \right), \tag{8.3}$$

where $\mathscr{R}_\alpha = (\alpha I + H^*H)^{-1}H^* \in L(\mathbf{Y}, \mathbf{X})$ we follow through the steps from (4.9) to (4.14) to derive an expression for the analysis error, such that

$$\mathbf{x}_k^{(a)} - \mathbf{x}_k^{(t)} = \mathcal{M}_{k-1}\left(\mathbf{x}_{k-1}^{(a)}\right) + \mathscr{R}_\alpha\left(\mathbf{y}_k - H_k\mathcal{M}_{k-1}\left(\mathbf{x}_{k-1}^{(a)}\right)\right) - \mathbf{x}_k^{(t)}, \tag{8.4}$$

$$\begin{aligned}
\mathbf{e}_k &= \mathcal{M}_{k-1}\left(\mathbf{x}_{k-1}^{(a)}\right) + \mathscr{R}_\alpha\left(\mathbf{y}_k^{(t)} + \eta_k - H_k\mathcal{M}_{k-1}\left(\mathbf{x}_{k-1}^{(a)}\right)\right) - \mathbf{x}_k^{(t)} && (8.5)\\
&= \mathcal{M}_{k-1}\left(\mathbf{x}_{k-1}^{(a)}\right) + \mathscr{R}_\alpha\left(H_k^{(t)}\mathbf{x}_k^{(t)} + \eta_k - H_k\mathcal{M}_{k-1}\left(\mathbf{x}_{k-1}^{(a)}\right)\right) - \mathbf{x}_k^{(t)} && (8.6)\\
&= \mathcal{M}_{k-1}\left(\mathbf{x}_{k-1}^{(a)}\right) - \mathcal{M}_{k-1}^{(t)}\left(\mathbf{x}_{k-1}^{(t)}\right) + \mathscr{R}_\alpha\left(\left(H_k^{(t)} - H_k\right)\mathbf{x}_k^{(t)} + \eta_k\right.\\
&\quad \left. + H_k\left(\mathcal{M}_{k-1}^{(t)}\left(\mathbf{x}_{k-1}^{(t)}\right) - \mathcal{M}_{k-1}\left(\mathbf{x}_{k-1}^{(a)}\right)\right)\right) && (8.7)\\
&= \mathcal{M}_{k-1}\left(\mathbf{x}_{k-1}^{(a)}\right) - \mathcal{M}_{k-1}\left(\mathbf{x}_{k-1}^{(t)}\right) + \boldsymbol{\zeta}_k\\
&\quad + \mathscr{R}_\alpha\left(-\boldsymbol{\omega}_k + \eta_k + H_k\left(\mathcal{M}_{k-1}\left(\mathbf{x}_{k-1}^{(t)}\right) - \boldsymbol{\zeta}_k - \mathcal{M}_{k-1}\left(\mathbf{x}_{k-1}^{(a)}\right)\right)\right) && (8.8)\\
&= \left(I - \mathscr{R}_\alpha H_k\right)\left(\mathcal{M}_{k-1}\left(\mathbf{x}_{k-1}^{(a)}\right) - \mathcal{M}_{k-1}\left(\mathbf{x}_{k-1}^{(t)}\right)\right)\\
&\quad + \left(I - \mathscr{R}_\alpha H_k\right)\boldsymbol{\zeta}_k + \mathscr{R}_\alpha\left(\eta_k - \boldsymbol{\omega}_k\right) && (8.9)\\
&= N_k\left(\mathcal{M}_{k-1}\left(\mathbf{x}_{k-1}^{(a)}\right) - \mathcal{M}_{k-1}\left(\mathbf{x}_{k-1}^{(t)}\right)\right) + N_k\boldsymbol{\zeta}_k + \mathscr{R}_\alpha\left(\boldsymbol{\eta}_k - \boldsymbol{\omega}_k\right), && (8.10)
\end{aligned}$$

where $\mathbf{e}_k := \mathbf{x}_k^{(a)} - \mathbf{x}_k^{(t)}$, $N_k := I - \mathscr{R}_\alpha H_k$ and the noise terms $\boldsymbol{\zeta}_k$, $\boldsymbol{\eta}_k$ and $\boldsymbol{\omega}_k$ are from (8.2), (4.8) and (4.7) respectively.

As a first attempt to examine the error behaviour we assume that the observation operator is time-invariant. We take norms on both sides and apply the triangle inequality and (c) in Lemma 2.1.20, such that

$$\|\mathbf{e}_k\| \leq \|N\| \cdot \left\|\mathcal{M}_{k-1}\left(\mathbf{x}_{k-1}^{(a)}\right) - \mathcal{M}_{k-1}\left(\mathbf{x}_{k-1}^{(t)}\right)\right\| + \|N\|\,\upsilon + \|\mathscr{R}_\alpha\|\left(\delta + \gamma\right), \tag{8.11}$$

where constants υ, δ and γ bound the noise on the model error, observations and observation operator respectively. For the Hilbert space $(\mathbf{X}, \|\cdot\|_{B^{-1}})$ this bound can be seen as a nonlinear extension to (7.2).

We now need some assumptions on the nonlinear map $\mathcal{M}_k$. It is natural to assume that the map is Lipschitz continuous. However, we will require that the map has a global Lipschitz constant for all time.

Assumption 8.1.1. *The nonlinear mapping $\mathcal{M}_k : \mathbf{X} \to \mathbf{X}$ is Lipschitz continuous with a global Lipschitz constant such that for all $\mathbf{a}, \mathbf{b} \in \mathbf{X}$ and $k \in \mathbb{N}$ there is K_k, independent of*

$\mathbf{a}, \mathbf{b}$ *such that*

$$\|\mathcal{M}_k(\mathbf{a}) - \mathcal{M}_k(\mathbf{b})\| \leq K_k \cdot \|\mathbf{a} - \mathbf{b}\|. \tag{8.12}$$

Furthermore, $\sup_k K_k =: K < \infty$. *We call* K *the global Lipschitz constant.*

If the system is time-invariant then of course, $K_k = K$ for all time. However, it is not necessary for the nonlinear system to be time-invariant. In this work we will refer to K without subscript as the global Lipschitz constant. Later in this chapter we show how this assumption can be relaxed.

Assuming Lipschitz continuity is a widespread approach for geophysical and meteorological applications, where it is well known that attractors exist within the dynamical models; see [78, p.196], [76, p.84], [53, p.97], [63, p.29] and [8, p.136]. In the case of weakly nonlinear model dynamics, it is possible to substitute the nonlinear dynamics with a first order Taylor expansion. Directly from (8.10) we can substitute the nonlinear terms $\mathcal{M}_{k-1}(\mathbf{x}_{k-1}^{(a)}) - \mathcal{M}_{k-1}(\mathbf{x}_{k-1}^{(t)})$ with the Fréchet derivative $\mathscr{M}_{k-1}$ of $\mathcal{M}_{k-1}$ at $\mathbf{x}_{k-1}^{(t)} \in \mathbf{X}$, such that

$$\mathbf{e}_k = N_k \mathscr{M}_{k-1} \mathbf{e}_{k-1} + N_k \mathbf{r}_{k-1} + N_k \boldsymbol{\zeta}_k + \mathscr{R}_\alpha \left(\boldsymbol{\eta}_k - \boldsymbol{\omega}_k \right), \tag{8.13}$$

where $\mathbf{r}_{k-1} = o\left(\mathbf{e}_{k-1}\right)$ is the error in the linear approximation, such that $\mathbf{r}_{k-1}$ is of a smaller order of magnitude than $\mathbf{e}_{k-1}$. Further details on the Fréchet derivative and the Taylor expansion can be found in [29, Chapter 11]. With this approach the nonlinear terms are removed from (8.13) and we are left with a linearised expression for the analysis error. Therefore, our theory in Chapter 7 would be then applicable to this scenario. However, this method of course depends on the higher order nonlinear terms in the Taylor expansion being negligible, which is not always true for nonlinear systems in NWP. This approach has been extensively studied in the literature as discussed in Chapter 4. Therefore, we instead focus our approach to nonlinear systems that satisfy Assumption 8.1.1.

Applying Assumption 8.1.1 we obtain from (8.11)

$$e_k \leq \nu \cdot e_{k-1} + \|N\| \, \upsilon + \|\mathscr{R}_\alpha\| \left(\delta + \gamma \right), \tag{8.14}$$

where $\nu := K\|N\|$ given the global Lipschitz constant K and $e_k := \|\mathbf{e}_k\|$ for $k \in \mathbb{N}_0$. Using Remark 6.2.2 we can bound (8.14) by

$$e_k \leq \nu \cdot e_{k-1} + \upsilon + \frac{\delta + \gamma}{2\sqrt{\alpha}}. \tag{8.15}$$

Since everything other than the analysis error is independent of time we can formulate the following result, which is the nonlinear extension of Theorem 7.2.1.

Theorem 8.1.2. *For the Hilbert space $(\mathbf{X}, \|\cdot\|_{B^{-1}})$, let Assumption 6.0.1 hold. If the nonlinear model operator $\mathcal{M}_k : \mathbf{X} \to \mathbf{X}$ is Lipschitz continuous and satisfies Assumption 8.1.1, then the error evolution in (8.14) and the error term $\mathbf{e}_k \in \mathbf{X}$ for $k \in \mathbb{N}_0$, where $\mathbf{e}_k := \mathbf{x}_k^{(a)} - \mathbf{x}_k^{(t)}$ is bounded by*

$$\|\mathbf{e}_k\| \leq \nu^k \|\mathbf{e}_0\| + \sum_{l=0}^{k-1} \nu^l \left(\upsilon + \frac{\delta + \gamma}{2\sqrt{\alpha}} \right), \tag{8.16}$$

for $k \in \mathbb{N}_0$. If $\nu \neq 1$ then

$$\|\mathbf{e}_k\| \leq \nu^k \|\mathbf{e}_0\| + \frac{1 - \nu^k}{1 - \nu} \left(\upsilon + \frac{\delta + \gamma}{2\sqrt{\alpha}} \right), \tag{8.17}$$

for $k \in \mathbb{N}_0$. If $\nu < 1$ then

$$\limsup_{k \to \infty} \|\mathbf{e}_k\| \leq \frac{\upsilon + \frac{\delta+\gamma}{2\sqrt{\alpha}}}{1 - \nu}. \tag{8.18}$$

Proof. We let $\nu := K\|N\|$, then (8.15) is similar to (6.13). Therefore, we can complete the proof using Theorem 6.1.3 for a different constant ν. □

We have described nonlinear error estimates for the analysis error of cycled data assimilation schemes in Theorem 8.1.2, which depends on Assumption 8.1.1. For the Hilbert space $(\mathbf{X}, \|\cdot\|_{B^{-1}})$, the sufficient condition to keep the analysis error bounded is that $\nu < 1$. Here the reconstruction error has to be strong enough so that, multiplied with the global Lipschitz constant K, ν is kept less than one. Now we explore how we can make $\|N\|$ small enough to ensure $\nu < 1$. We first explore a well-posed observation operator H.

Lemma 8.1.3. *Let $(\mathbf{X}, \|\cdot\|_{B^{-1}})$ be a Hilbert space with weighted norm and let H be an injective linear observation operator such that the operator equation is well-posed in accordance with Definition 2.3.1. Given a parameter $0 < \rho < 1$, then by choosing the regularization parameter $\alpha > 0$ sufficiently small we obtain $\nu \leq K\rho < 1$.*

Proof. We first prove the result for the infinite dimensional setting. This result is adapted from Lemma 6.1.4. Since the operator equation is well-posed, $G := H^*H$ has a complete orthonormal system $\varphi_{(1)}, \varphi_{(2)}, \ldots$ of eigenvectors with eigenvalues $\lambda_{(1)}, \lambda_{(2)}, \cdots > 0$. If $K > 1$

we choose ρ such that $\rho < 1/K$, otherwise we choose any $\rho < 1$. Then we choose an α such that

$$\alpha\left(\frac{1}{\rho} - 1\right) = \inf_{j=1,\ldots,\infty} \left|\lambda_{(j)}\right| > 0. \tag{8.19}$$

Then,

$$\begin{aligned}\nu = K\left\|N\right\| = K\left\|\left(I + \alpha^{-1}G\right)^{-1}\right\| &= K \sup_{j\in\{1,\ldots,\infty\}} \left|\frac{1}{1+\frac{\lambda_{(j)}}{\alpha}}\right| \\ &\leq \frac{K\alpha}{\alpha + \alpha\left(\frac{1}{\rho} - 1\right)} = K\rho < 1. \end{aligned} \tag{8.20}$$

For the finite dimensional case, the orthonormal system of eigenvectors and eigenvalues becomes finite and the proof is the same. □

It is clear from Lemma 8.1.3 that given any global Lipschitz constant $K > 0$, that is any model dynamics, we can always choose an $\alpha > 0$ sufficiently small so that $\nu \leq K\rho < 1$. The estimates in (8.20) are based on lower bounds for the spectrum of H^*H. In the large-scale or infinite dimensional case, our interest is with a compact observation operator H, where the spectrum decays to zero in the infinite dimensional setting. Here, to achieve a stable cycled scheme with an ill-posed observation operator, we now show that the Lipschitz constant has to be contractive with respect to higher spectral modes of H. We remark,

Remark 8.1.4. For the Hilbert space $(\mathbf{X}, \|\cdot\|_{B^{-1}})$, let Assumption 6.0.2 hold. Then (8.11) implies that in order to ensure stability the model operator $\mathcal{M}_k$ must be strictly damping, that is the global Lipschitz constant $K < 1$. This is apparent since for an infinite dimensional state space the norm of the reconstruction error $\|N\| = 1$.

Despite this, we will see that by splitting the state space $\mathbf{X}$ we are able to use the reconstruction error operator N to control the Lipschitz constant K over lower spectral modes. In considering lower and higher spectral modes separately we are able to obtain a stable cycled scheme for a wider class of systems. We will see that damping with respect to the observation operator H is required in the nonlinear map $\mathcal{M}_k$.

We define orthogonal projection operators, $P^{(1)}$ and $P^{(2)}$ from (7.5) with respect to the singular system of H. Then we can define the same subspaces $\mathbf{X}^{(1)}$ and $\mathbf{X}^{(2)}$ as in (7.6).

Returning to (8.10) we have,

$$\mathbf{e}_k = N\left(P^{(1)} + P^{(2)}\right)\left(\mathcal{M}_{k-1}\left(\mathbf{x}_{k-1}^{(a)}\right) - \mathcal{M}_{k-1}\left(\mathbf{x}_{k-1}^{(t)}\right)\right) + N\boldsymbol{\zeta}_k + \mathscr{R}_\alpha\left(\boldsymbol{\eta}_k - \boldsymbol{\omega}_k\right) \tag{8.21}$$

$$\begin{aligned} &= N|_{\mathbf{X}^{(1)}} P^{(1)}\left(\mathcal{M}_{k-1}\left(\mathbf{x}_{k-1}^{(a)}\right) - \mathcal{M}_{k-1}\left(\mathbf{x}_{k-1}^{(t)}\right)\right) + N\boldsymbol{\zeta}_k \\ &\quad + N|_{\mathbf{X}^{(2)}} P^{(2)}\left(\mathcal{M}_{k-1}\left(\mathbf{x}_{k-1}^{(a)}\right) - \mathcal{M}_{k-1}\left(\mathbf{x}_{k-1}^{(t)}\right)\right) + \mathscr{R}_\alpha\left(\boldsymbol{\eta}_k - \boldsymbol{\omega}_k\right). \end{aligned} \tag{8.22}$$

Now defining

$$\mathcal{M}_k^{(1)}(\cdot) := P^{(1)} \circ \mathcal{M}_k(\cdot) \text{ and } \mathcal{M}_k^{(2)}(\cdot) := P^{(2)} \circ \mathcal{M}_k(\cdot) \tag{8.23}$$

for all $k \in \mathbb{N}_0$, then we have

$$\begin{aligned} \mathbf{e}_k &= N|_{\mathbf{X}^{(1)}}\left(\mathcal{M}_{k-1}^{(1)}\left(\mathbf{x}_{k-1}^{(a)}\right) - \mathcal{M}_{k-1}^{(1)}\left(\mathbf{x}_{k-1}^{(t)}\right)\right) + N\boldsymbol{\zeta}_k \\ &\quad + N|_{\mathbf{X}^{(2)}}\left(\mathcal{M}_{k-1}^{(2)}\left(\mathbf{x}_{k-1}^{(a)}\right) - \mathcal{M}_{k-1}^{(2)}\left(\mathbf{x}_{k-1}^{(t)}\right)\right) + \mathscr{R}_\alpha\left(\boldsymbol{\eta}_k - \boldsymbol{\omega}_k\right), \end{aligned} \tag{8.24}$$

with restrictions according to $\mathbf{X}^{(1)}$ and $\mathbf{X}^{(2)}$ from (7.6). Using the triangle inequality and property (c) from Lemma 2.1.20 we can obtain a bound on this error, such that

$$\begin{aligned} \|\mathbf{e}_k\| &= \Big\| N|_{\mathbf{X}^{(1)}}\left(\mathcal{M}_{k-1}^{(1)}\left(\mathbf{x}_{k-1}^{(a)}\right) - \mathcal{M}_{k-1}^{(1)}\left(\mathbf{x}_{k-1}^{(t)}\right)\right) + N\boldsymbol{\zeta}_k \\ &\quad + N|_{\mathbf{X}^{(2)}}\left(\mathcal{M}_{k-1}^{(2)}\left(\mathbf{x}_{k-1}^{(a)}\right) - \mathcal{M}_{k-1}^{(2)}\left(\mathbf{x}_{k-1}^{(t)}\right)\right) + \mathscr{R}_\alpha\left(\boldsymbol{\eta}_k - \boldsymbol{\omega}_k\right)\Big\| \end{aligned} \tag{8.25}$$

$$\begin{aligned} &\leq \|N|_{\mathbf{X}^{(1)}}\| \cdot \left\|\mathcal{M}_{k-1}^{(1)}\left(\mathbf{x}_{k-1}^{(a)}\right) - \mathcal{M}_{k-1}^{(1)}\left(\mathbf{x}_{k-1}^{(t)}\right)\right\| \\ &\quad + \|N|_{\mathbf{X}^{(2)}}\| \cdot \left\|\mathcal{M}_{k-1}^{(2)}\left(\mathbf{x}_{k-1}^{(a)}\right) - \mathcal{M}_{k-1}^{(2)}\left(\mathbf{x}_{k-1}^{(t)}\right)\right\| \\ &\quad + \|N\boldsymbol{\zeta}_k\| + \|\mathscr{R}_\alpha\left(\boldsymbol{\eta}_k - \boldsymbol{\omega}_k\right)\| \end{aligned} \tag{8.26}$$

$$\begin{aligned} &\leq K_{k-1}^{(1)} \cdot \|N|_{\mathbf{X}^{(1)}}\| \cdot \left\|\mathbf{x}_{k-1}^{(a)} - \mathbf{x}_{k-1}^{(t)}\right\| \\ &\quad + K_{k-1}^{(2)} \cdot \|N|_{\mathbf{X}^{(2)}}\| \cdot \left\|\mathbf{x}_{k-1}^{(a)} - \mathbf{x}_{k-1}^{(t)}\right\| \\ &\quad + \|N\boldsymbol{\zeta}_k\| + \|\mathscr{R}_\alpha\left(\boldsymbol{\eta}_k - \boldsymbol{\omega}_k\right)\| \end{aligned} \tag{8.27}$$

$$\leq \left(\nu_{k-1}^{(1)} + \nu_{k-1}^{(2)}\right)\|\mathbf{e}_{k-1}\| + \|N\|\,\upsilon + \|\mathscr{R}_\alpha\|\left(\delta + \gamma\right), \tag{8.28}$$

where we have assumed Lipschitz continuity,

$$\left\|\mathcal{M}_{k-1}^{(j)}\left(\mathbf{x}_{k-1}^{(a)}\right) - \mathcal{M}_{k-1}^{(j)}\left(\mathbf{x}_{k-1}^{(t)}\right)\right\| \leq K_{k-1}^{(j)}\left\|\mathbf{x}_{k-1}^{(a)} - \mathbf{x}_{k-1}^{(t)}\right\| \tag{8.29}$$

for $j = 1, 2$, defining $\nu_{k-1}^{(1)} := K_{k-1}^{(1)} \cdot \|N|_{\mathbf{X}^{(1)}}\|$ and $\nu_{k-1}^{(2)} := K_{k-1}^{(2)} \cdot \|N|_{\mathbf{X}^{(2)}}\|$ with restrictions according to the singular system of H. Again, we now assume that the modelled nonlinear

operator $\mathcal{M}_k$ is globally Lipschitz continuous in accordance with Assumption 8.1.1, where $K_k^{(1)} \leq K^{(1)}$ and $K_k^{(2)} \leq K^{(2)}$ for all time k. Similar to Theorem 8.1.2 we can form the following result.

Theorem 8.1.5. *Let $(\mathbf{X}, \|\cdot\|_{B^{-1}})$ be a Hilbert space with weighted norm and let Assumption 6.0.1 hold. If the model operator $\mathcal{M}_k : \mathbf{X} \to \mathbf{X}$ is Lipschitz continuous and satisfies Assumption 8.1.1, then the analysis error $\mathbf{e}_k := \mathbf{x}_k^{(a)} - \mathbf{x}_k^{(t)}$ for $k \in \mathbb{N}_0$ is estimated by*

$$\|\mathbf{e}_k\| \leq \nu^k \|\mathbf{e}_0\| + \sum_{l=0}^{k-1} \nu^l \left(\upsilon + \frac{\delta + \gamma}{2\sqrt{\alpha}} \right), \tag{8.30}$$

where $\nu := \nu^{(1)} + \nu^{(2)}$, for $\nu^{(1)} := K^{(1)} \cdot \|N|_{\mathbf{X}^{(1)}}\|$ and $\nu^{(2)} := K^{(2)} \cdot \|N|_{\mathbf{X}^{(2)}}\|$ with restrictions according to the singular system of H. If $\nu \neq 1$ then

$$\|\mathbf{e}_k\| \leq \nu^k \|\mathbf{e}_0\| + \frac{1 - \nu^k}{1 - \nu} \left(\upsilon + \frac{\delta + \gamma}{2\sqrt{\alpha}} \right), \tag{8.31}$$

for $k \in \mathbb{N}_0$. If $\nu < 1$ then

$$\limsup_{k \to \infty} \|\mathbf{e}_k\| \leq \frac{\upsilon + \frac{\delta + \gamma}{2\sqrt{\alpha}}}{1 - \nu}. \tag{8.32}$$

Proof. The proof is the same as that of Theorem 7.2.1 for a different constant $\nu := \nu^{(1)} + \nu^{(2)}$, with restrictions according to the singular system of H. □

We see from Theorem 8.1.5 that the sufficient condition for stability of the cycled data assimilation scheme requires that $\nu := \nu^{(1)} + \nu^{(2)} < 1$. Applying the norm estimates in Lemma 8.1.3 and Lemma 7.1.3, we obtain

$$\nu = K^{(1)} \cdot \|N|_{\mathbf{X}^{(1)}}\| + K^{(2)} \cdot \|N|_{\mathbf{X}^{(2)}}\| \tag{8.33}$$

$$\leq K^{(1)} \cdot \rho + K^{(2)}, \tag{8.34}$$

given global Lipschitz constants $K^{(1)}$ and $K^{(2)}$ under Assumption 8.1.1 and a constant $0 < \rho < 1$. Here we directly see how the nonlinear growth in $\mathbf{X}^{(1)}$ can be controlled by the regularization parameter α. Furthermore, it is seen that the nonlinear system $\mathcal{M}_k$ has to be damping in $\mathbf{X}^{(2)}$ for all time in order to ensure stability. Therefore only if $\mathcal{M}_k$ is sufficiently damping on higher spectral modes of H will we be able to stabilise the cycled data assimilation scheme. We call this type of system dissipative with respect to H as summarised in the following definition.

Definition 8.1.6. A nonlinear system $\mathcal{M}_k$, $k \in \mathbb{N}_0$, is *dissipative with respect to* H if it is Lipschitz continuous and damping with respect to higher spectral modes of H, in the sense that $\mathcal{M}_k^{(2)}$ defined by (8.23) satisfies

$$\left\| \mathcal{M}_k^{(2)}(\mathbf{a}) - \mathcal{M}_k^{(2)}(\mathbf{b}) \right\| \leq K_k^{(2)} \cdot \|\mathbf{a} - \mathbf{b}\| \tag{8.35}$$

for $\mathbf{a}, \mathbf{b} \in \mathbf{X}$, where $K_k^{(2)} \leq K^{(2)} < 1$ uniformly for $k \in \mathbb{N}_0$.

Under this assumption that $\mathcal{M}_k$ is dissipative with respect to H, we can choose the regularization parameter $\alpha > 0$ small enough, such that

$$\rho < \frac{1 - K^{(2)}}{K^{(1)}}, \tag{8.36}$$

in order to make $\nu < 1$ and so achieve a stable cycled scheme. We are now able to summarise this result in the following theorem.

Theorem 8.1.7. *Let* $(\mathbf{X}, \|\cdot\|_{B^{-1}})$ *be a Hilbert space with weighted norm. Let the nonlinear system* $\mathcal{M}_k : \mathbf{X} \to \mathbf{X}$ *be Lipschitz continuous and dissipative with respect to higher spectral modes of* H *in accordance with Definition 8.1.6. Then, for regularization parameter* $\alpha > 0$ *sufficiently small we have* $\nu := K^{(1)}\|N|_{\mathbf{X}^{(1)}}\| + K^{(2)}\|N|_{\mathbf{X}^{(2)}}\| < 1$. *Under the conditions of Theorem 8.1.5 the analysis error is bounded over time by*

$$\limsup_{k \to \infty} \|\mathbf{e}_k\| \leq \frac{\upsilon + \frac{\delta + \gamma}{2\sqrt{\alpha}}}{1 - \nu}. \tag{8.37}$$

Proof. If $\mathcal{M}_k$ is Lipschitz continuous and dissipative with respect to H, we first show that we can achieve $\nu < 1$. From (8.34), the Lipschitz constants $K^{(1)}$ and $K^{(2)}$ determine our ability to achieve $\nu < 1$. Under the assumption that $\mathcal{M}_k$ is dissipative, then for the subspace $\mathbf{X}^{(2)}$ we have that $K^{(2)} < 1$.

We know that from Lemma 8.1.3 we can make ρ in (8.34) small enough so that (8.36) is satisfied. Then we obtain $\nu < 1$ from (8.34). The bound for the analysis error is then given by Theorem 8.1.5, which also provides the estimate in (8.37). The inequality completes the proof in accordance with Remark 6.2.2. □

We have seen that it is possible to keep the analysis error bounded for all time with a compact observation operator in a nonlinear infinite dimensional setting. This is due to the

model dynamics being dissipative with respect to higher spectral modes of the observation operator. In the case of time-invariant model dynamics the constant $K^{(2)}$ must be shown to be damping with respect to the subspace $\mathbf{X}^{(2)}$. This is analogous to the results in Chapter 7, where we split the state space so that there was a contraction in the error dynamics. For nonlinear model dynamics, the property exploited in the linear setting does not hold and therefore it is necessary to show this dissipative property for the model dynamics under consideration. The work of [7] was able to show local dissipativity for the incompressible two-dimensional Navier-Stokes equations where the model dynamics and the observation operator commute. An extension would be to show global dissipativity for a particular nonlinear dynamical system.

In the case of time-varying model dynamics then it must be shown that for all time k, the constants $K_k^{(2)} \leq K^{(2)} < 1$ and so obey the global property of Assumption 8.1.1 and are damping. This of course is a particular situation; however it is required for this theory to hold and must be shown for the model dynamics considered. We note that this global dissipativity property does not necessarily hold for many realistic models. An extension which would relax this assumption would be for the subspace $\mathbf{X}^{(2)}$ to be also dependent on time. Then in each assimilation step $\mathbf{X}^{(2)}$ could be chosen so that there is a contraction in the model dynamics with respect to the observation operator. In this case the regularization parameter would need to be chosen also in each assimilation step to allow for an expansion in the lower spectral modes in $\mathbf{X}^{(1)}$. This would lead to data assimilation schemes that update the background error covariance multiplicatively in the same way as seen in Section 7.2. We develop results for this in Section 8.2 and Section 8.3 after we explore the nonlinear behaviour of the analysis error numerically.

Now we explore the behaviour of the analysis error in the nonlinear setting using the Lorenz '63 model introduced in Chapter 5.

8.1.1 Numerical experiments

The theory that we have developed in Section 8.1 does not apply to the numerical experiments that are carried out in this section. This is because here we set-up experiments using the three dimensional Lorenz equations introduced in Chapter 5 and our main result in Theorem

8.1.7 is applicable to the infinite dimensional setting. Despite this, we will see interesting results that go further than our theoretical results. Previously in Chapter 6 and Chapter 7 we set-up numerical experiments for linear systems. In that case we were able to calculate the error equation explicitly using only the noise terms and an initial error. However, now we must set-up a complete data assimilation scheme to calculate the analysis error since we deal with nonlinear model dynamics. In this section we carry out a number of numerical experiments with two variations of the Lorenz '63 equations. Firstly we present results for the deterministic Lorenz equations from Chapter 5, which has been published in [60] and secondly we present results for the stochastic Lorenz equations. In the same way as Section 6.2.1 our approach is to use the same noise realisations when comparing experiments.

For the first experiment we omit model error and observation operator error to concentrate on the behaviour of the analysis error compared with the error in the observations in each assimilation step.

We set up a twin experiment, whereby we begin with an initial condition,

$$\left(x_0^{(t)}, y_0^{(t)}, z_0^{(t)}\right) = (-5.8696, -6.7824, 22.3356), \tag{8.38}$$

which was obtained using an initial reference point, $(0.001, 0.001, 2.001)$ that was spun-up for 1000 time-steps to obtain the initial condition $(x_0^{(t)}, y_0^{(t)}, z_0^{(t)})$. We run the model from this initial condition until time $t = 100$ with a step-size $h = 0.01$, which we call a *truth run*. Now using the truth run we create observations at every tenth time-step by adding random normally distributed noise with zero mean and standard deviation $\sigma_{(o)} = \sqrt{2}/40$. The background state is calculated in the same way at initial time t_0 with zero mean and standard deviation $\sigma_{(b)} = 1/400$ such that,

$$\left(x_0^{(b)}, y_0^{(b)}, z_0^{(b)}\right) = (-5.8674, -6.7860, 22.3338). \tag{8.39}$$

Now, ignoring the model error term and the observation operator error term in (8.10), we calculate the analysis error $\mathbf{e}_k$ for $k = 1, \ldots, 1000$. Assimilating only at every tenth time-step, we allow for the nonlinear model dynamics to play a role before we apply the data assimilation scheme. This means that every assimilation step k corresponds to 10 time-steps.

We saw in Theorem 3.1.13 that under weighted norms, 3DVar is equivalent to cycled Tikhonov-Phillips regularization for $\alpha = 1$. In this experiment we assume that the observation error covariance is modelled according to (6.68). However, we simulate a climatological

background error covariance. We calculate a sampled background error covariance between the background state and true state over the whole trajectory, such that

$$B = \begin{pmatrix} 117.6325 & 117.6374 & -2.3513 \\ 117.6374 & 152.6906 & -2.0838 \\ -2.3513 & -2.0838 & 110.8491 \end{pmatrix}. \tag{8.40}$$

Then we weight the state space with respect to the inverse of $B/\sigma^2_{(b)}$. Here $B/\sigma^2_{(b)}$ represents the correlation matrix C in the same way as in (7.37). By dividing B through by its variance $\sigma^2_{(b)}$, for regularization parameter $\alpha = \sigma^2_{(o)}/\sigma^2_{(b)}$ we connect cycled Tikhonov-Phillips regularization with 3DVar. We simulate the consequence of an ill-posed observation operator H with a random 3×3 matrix using the *rand* function in Matlab and set its last singular value $\mu_3 = 10^{-8}$ such that

$$H = \begin{pmatrix} 0.4267 & 0.5220 & 0.5059 \\ 0.8384 & -0.7453 & 1.6690 \\ 0.4105 & 1.6187 & 0.0610 \end{pmatrix}. \tag{8.41}$$

Therefore, H is strongly ill-conditioned with a condition number, $\kappa(H) \approx 2.1051 \times 10^8$.

Varying the regularization parameter α we can study the time-averaged error in the same way as in Chapter 6 and Chapter 7. In Figure 8.1 we plot the error integral against the regularization parameter for the Euclidean norm and the weighted norm in Figure 8.1(a) and Figure 8.1(b) respectively. Here we observe in both figures that α needs to be chosen small enough to keep the analysis error bounded, although if it is chosen too small it will lead to a large analysis error bound. Since the weight $\sigma^2_{(b)}B^{-1}$ is static in time the weighted norm acts as a rescaling in the vertical axis. This can be observed by comparing Figure 8.1(a) with Figure 8.1(b). We see that for a range of regularization parameters the analysis error is small. This is interesting since it demonstrates that the analysis error does not vary much for a small weight on the background. Only when the background term in (3.23) is weighted too much or too little, will the analysis error grow. Of course for each value of α the time-averaged error is different, which is difficult to see due to the scales in Figure 8.1(a) and Figure 8.1(b). However, we have confirmed this numerically by calculating the time-averaged error for this range of regularization parameters. We now plot some error evolutions and trajectories and weight the evolutions with respect to the Euclidean norm. It makes sense to weight the error

evolution with respect to the Euclidean norm since we want to associate the error evolutions with plots of the trajectories in state space.

We select the largest regularization parameter from the error integral plot in Figure 8.1. With this value of $\alpha = \sigma^2_{(o)}/\sigma^2_{(b)} = 200$ we connect 3DVar with cycled Tikhonov-Phillips. In Figure 8.2(a) we observe that the analysis error $\|\mathbf{e}_k^{(a)}\|_{\ell^2}$ fluctuates around the value of 20. Compared with the ℓ^2 norm of the difference between the true state in (8.38) and the background state in (8.39) which is 0.0046, the analysis error $\|\mathbf{e}_k^{(a)}\|_{\ell^2}$ is large. The analysis is not able to track the truth and this can seen in Figure 8.2(b), where we plot the truth and analysis in state space from assimilation time t_{200} until t_{220}. We observe over this time interval that the analysis does not stay on the same wing of the attractor as the truth. This is evident across the whole time interval, which we confirm in Figure 8.2(c) and Figure 8.2(d) where the truth and analysis are plotted in state space from assimilation time t_{774} until t_{805} and t_{858} until t_{895} respectively. In Figure 8.2(c) the analysis and truth are close together at assimilation time t_{774}. However over time the analysis fails to follow the truth onto the same wing of the attractor. This is also reflected in Figure 8.2(d) where the analysis spends most time on the wrong wing of the attractor compared to the truth.

Now we carry out an inflation to the background variance by choosing a smaller regularization parameter $\alpha = 2$, which corresponds to the parameter α where the error integral is smallest in Figure 8.1. Subsequently repeating with the same data, we observe in Figure 8.3(a) that the analysis error fluctuates around a much smaller value compared with Figure 8.2(a). This is reflected in Figure 8.3(b) where the analysis is now able to follow the trajectory of the truth better and remains for the assimilation time (t_{200} until t_{220}) on the same wing of the attractor as the truth.

In Figure 8.4(a) we inflate too much by choosing a regularization parameter $\alpha = 10^{-10}$ and observe that the analysis error becomes large again. This is due to the ill-conditioned observation operator leading to a large Tikhonov-Phillips inverse in norm. This of course means that the observation error $\boldsymbol{\eta}_k$ is amplified in each step leading to a large analysis error. The same behaviour has been observed in another numerical experiment in Section 6.3.1. For this choice of α we also plot the trajectories of the analysis and the truth in Figure 8.4(b). Here we observe that the analysis attempts to track the truth. However, the consequence of an ill-conditioned observation operator, leading to a large Tikhonov-Phillips inverse, forces

the analysis towards the observations which lie off the attractor. Since the scheme trusts the observations much more than the background, the analysis is forced towards the observations, hence the analysis error is smaller for all time in Figure 8.4(a) compared with Figure 8.2(a).

Here the numerical results support the theory developed in Section 8.1 that by choosing α small enough, we can reduce the analysis error of the cycled data assimilation scheme for all time. However if it is chosen too small the analysis error will be amplified for an ill-conditioned observation operator.

Here we have set-up observations that have additive noise which is drawn independently at every time-step from the Gaussian distribution. The corresponding error will be much better than the worst case error for which our estimates in Section 8.1 have been derived. However, we note that the worst case scenario is possible, though with very low probability. It is of the class of low-probability-high-risk-events, which are of particular importance for many environmental applications.

In order to demonstrate the bounds developed in Section 8.1, we repeat the experiment starting from the same random 3×3 matrix for the observation operator H. We increase μ_3 from 10^{-8} to 10^{-3}, which is necessary since we want to achieve $\|N\| < 1/K$. If μ_3 is chosen too small, that is H is very ill-conditioned, then we would need to choose α sufficiently small to obtain $\|N\| < 1/K$. Theoretically this is possible, however numerically, with such a small α, the matrix N then becomes close to singular. Therefore we choose $\mu_3 = 10^{-3}$ so that we have a different observation operator,

$$H = \begin{pmatrix} 0.4275 & 0.5218 & 0.5055 \\ 0.8381 & -0.7453 & 1.6692 \\ 0.4102 & 1.6188 & 0.0612 \end{pmatrix}, \tag{8.42}$$

with condition number, $\kappa(H) = 2.1051 \times 10^3$. We use the same initial condition, background state and error covariance matrix as before.

Since we are interested in the bound on the analysis error in (8.14) we need to compute the global Lipschitz constant for this experiment. Using the truth and background runs we can calculate a Lipschitz constant from (8.12) every 10 time-steps. Choosing the largest value over all time we obtain a global Lipschitz constant $K = 1.9837$ for this experiment. Therefore we choose a regularization parameter, $\alpha = 10^{-6}$ which is small enough so that

$\|N\| < 1/K$, leading to $\nu \approx 0.9918$ from (8.14). We calculate a bound on the observational noise with respect to the Euclidean norm and the weighted norm, so that $\delta = 0.1571$ and $\delta = 0.0034$ respectively.

In Figure 8.5 we plot the nonlinear analysis error from (8.10) and the bound on the analysis error in (8.14) for the Euclidean norm and a weighted norm in Figure 8.5(a) and Figure 8.5(b) respectively. As before in Figure 8.1 we see that the weighted norm has the effect of rescaling the error evolution in the vertical axis. Since we bound the analysis error by a linear update equation we observe the linear growth in our bound. For this choice of regularization parameter we observe large fluctuations in the nonlinear analysis error arising from a Tikhonov-Phillips inverse that is large in norm, which was discussed in the first experiment. Also in Figure 8.5 we plot the asymptotic limit of the analysis error from (8.37). From these numerical experiments we see that the numerical bound is not a very tight bound on the actual analysis error. This is of course expected since our approach is to use norm estimates, therefore we obtain a sufficient condition for a stable cycled scheme.

We have repeated this experiment with the same noise realisations for an observation operator $H : \mathbb{R}^3 \to \mathbb{R}^2$, such that

$$H = \begin{pmatrix} 1.1650 & 0.0751 & -0.6965 \\ 0.6268 & 0.3516 & 1.6961 \end{pmatrix}. \tag{8.43}$$

In the same way as before we can vary the regularization parameter α to study the time-averaged error. In Figure 8.6 we plot the error integral against the regularization parameter for the Euclidean norm and the weighted norm in Figure 8.6(a) and Figure 8.6(b) respectively. This experiment demonstrates that the same behaviour of the analysis error is present even when the observation operator does not have full rank. We will discuss this point further in Section 9.2.

We now carry out numerical experiments using the stochastic Lorenz equations introduced in Chapter 5. In this case we set-up an experiment for model equations that have additive Gaussian model error. We want to investigate the evolution of the analysis error where an additional error arises in the model equations. This type of model error represents the inaccuracy in modelling physical processes in the atmosphere. For simplicity we again assume that there is no noise on the observation operator such that our error evolution equation from

(8.10) becomes,

$$\mathbf{e}_k = N_k \left(\mathcal{M}_{k-1} \left(\mathbf{x}_{k-1}^{(a)} \right) - \mathcal{M}_{k-1} \left(\mathbf{x}_{k-1}^{(t)} \right) \right) + N_k \boldsymbol{\zeta}_k + \mathscr{R}_\alpha \boldsymbol{\eta}_k. \tag{8.44}$$

We again set-up a twin experiment, whereby we begin with an initial condition,

$$\left(x_0^{(t)}, y_0^{(t)}, z_0^{(t)} \right) = (-5.3661, -7.7303, 18.3983), \tag{8.45}$$

which was obtained using an initial reference point, $(0.001, 0.001, 2.001)$ that was spun-up for 1000 time-steps with the perfect model equations to obtain the initial condition $(x_0^{(t)}, y_0^{(t)}, z_0^{(t)})$. Here we remark that perfect model equations corresponds to $c^{(1)} = c^{(2)} = c^{(3)} = 0$ from the stochastic Lorenz '63 equations in Chapter 5. This means we assume that the deterministic model is true model $\mathcal{M}^{(t)}$ and the stochastic model is the wrong model $\mathcal{M}$. We produce a run of the system until time $t = 100$ with the perfect model equations and a step-size $h = 0.01$, which we call a *truth run*. Now using the truth run we create observations at every tenth time-step by adding random normally distributed noise with zero mean and standard deviation $\sigma_{(o)} = \sqrt{2}/40$. The background state is calculated in the same way at initial time t_0 with zero mean and standard deviation $\sigma_{(b)} = 1/400$ such that,

$$\left(x_0^{(b)}, y_0^{(b)}, z_0^{(b)} \right) = (-5.3636, -7.7289, 18.3970). \tag{8.46}$$

We set $c^{(1)} = c^{(2)} = c^{(3)} = 2$ for the modelled nonlinear model operator, such that there is a reasonable amount of stochastic noise added to the model equations. We calculate the analysis error $\mathbf{e}_k$ for $k = 1, \ldots, 1000$. Assimilating only at every tenth time-step, we allow for the nonlinear model dynamics to play a role before we apply the data assimilation scheme. We again assume that the observation error covariance is modelled according to (6.68) and simulate a climatological background error covariance. We calculate a sampled background error covariance between the background state and true state over the whole trajectory such that

$$B = \begin{pmatrix} 129.2075 & 127.4499 & 3.5113 \\ 127.4499 & 161.1427 & 1.7138 \\ 3.5113 & 1.7138 & 120.6357 \end{pmatrix}. \tag{8.47}$$

Then we weight the state space with respect to the inverse of $B/\sigma_{(b)}^2$ as before. We choose the same observation operator as before in (8.41).

Varying the regularization parameter α we can study the time-averaged error in the same way as in Chapter 6 and Chapter 7. In Figure 8.7 we plot the error integral against the regularization parameter for the Euclidean norm and the weighted norm in Figure 8.7(a) and Figure 8.7(b) respectively. We observe similar behaviour as the previous experiment for the Lorenz equations. We again plot some error evolutions and trajectories and weight the evolutions with respect to the Euclidean norm.

We connect 3DVar with cycled Tikhonov-Phillips regularization by choosing the largest regularization parameter from the error integral plot in Figure 8.7. With this value of $\alpha = \sigma^2_{(o)}/\sigma^2_{(b)} = 200$, in Figure 8.8(a) we observe that the analysis error $\|\mathbf{e}_k^{(a)}\|_{\ell^2}$ fluctuates around the value of 20. Compared with the ℓ^2 norm of the difference between the true state in (8.45) and the background state in (8.46) which is 0.0031, the analysis error $\|\mathbf{e}_k^{(a)}\|_{\ell^2}$ is large. We see the same behaviour in Figure 8.8(b) as seen previously in Figure 8.2(b) where the analysis fails to track the true state from assimilation time t_{200} until t_{220}. Similar to previously seen in Figure 8.2(c) and Figure 8.2(d) we see that in Figure 8.8(c) and Figure 8.8(d) that the analysis state is mostly on the wrong wing of the attractor compared with the truth.

Now we carry out an inflation to the background variance by choosing a smaller regularization parameter $\alpha = 10^{-4}$, which corresponds to the parameter α where the error integral is smallest in Figure 8.7. Subsequently repeating with the same data, we observe in Figure 8.9(a) that the analysis error fluctuates around a much smaller value compared with Figure 8.8(a). Again this behaviour has been seen previously in Figure 8.3(a) where we see in Figure 8.9(b) that the analysis tracks the true state as it switches between the different wings of the attractor.

In Figure 8.10(a) we inflate too much by choosing a regularization parameter $\alpha = 10^{-10}$ and observe that the analysis error becomes large again. This is the same behaviour as seen for the deterministic Lorenz equations. For this choice of α we can plot the trajectories of the analysis and the truth in Figure 8.10(b). Here we observe that despite there being significant model error, the analysis does a reasonable attempts to track the truth. Again however, an ill-conditioned observation operator means that the analysis is forced off the attractor due to the level of additive noise in the observations.

We have seen similar results for this extended set-up with the stochastic Lorenz equations compared with the previous experiment. We again explore the bounds developed in Section

8.1. Starting from the same random 3×3 matrix for the observation operator H. We increase μ_3 from 10^{-8} to 10^{-3}, which is necessary since we want to achieve $\|N\| < 1/K$. Thus we have the same observation operator as in (8.42).

Using the truth and background runs we can calculate a Lipschitz constant from (8.12) every 10 time-steps. Choosing the largest value over all time we obtain a global Lipschitz constant $K = 2.6456$ for this experiment. Therefore we choose a regularization parameter, $\alpha = 6 \times 10^{-7}$ which is small enough so that $\|N\| < 1/K$, leading to $\nu \approx 0.9921$ from (8.14). We calculate a bound on the observational noise with respect to the Euclidean norm and the weighted norm, so that $\delta = 0.1571$ and $\delta = 1.4906 \times 10^{-4}$ respectively. Using the truth run and (8.2) we can calculate the model error term $\boldsymbol{\zeta}_k$ and calculate the bound on the model error $\upsilon = 24.0089$ and $\upsilon = 0.0204$ for the Euclidean norm and the weighted norm respectively.

In Figure 8.11 we plot the nonlinear analysis error from (8.10) and the bound on the analysis error in (8.14) for the Euclidean norm and a weighted norm in Figure 8.11(a) and Figure 8.11(b) respectively. As before in Figure 8.7, we see that the weighted norm in Figure 8.11 has the effect of rescaling the error evolution in the vertical axis. We see very similar behaviour as in the last experiment with the deterministic Lorenz equations. Since we bound the analysis error by a linear update equation we observe the linear growth in our bound. For this choice of regularization parameter $\alpha = 6 \times 10^{-7}$ we observe large fluctuations in the nonlinear analysis error arising from a Tikhonov-Phillips inverse that is large in norm. We also plot the asymptotic limit of the analysis error from (8.37) in Figure 8.11. Again we see that the bound is not very tight, which is expected since we work with a sufficient condition for stability.

8.2 Nonlinear dynamics with a multiplicative update to the background error covariance

In this section we will provide a nonlinear extension to the results in Section 7.2 for the stability of cycled data assimilation schemes that employ a multiplicative update to the background error covariance operator. We will assume that the model dynamics are time-varying. However, the observation operator will remain an injective linear time-invariant

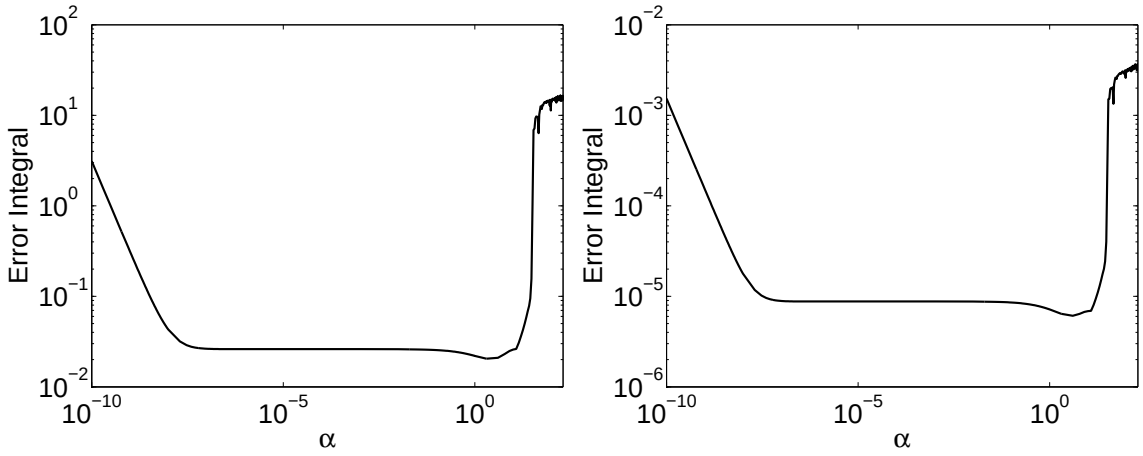

(a) (b)

Figure 8.1: (a) ℓ^2 norm of the time-averaged analysis error $\|\mathbf{e}_k\|_{\ell^2}$ integrated for all assimilation times $k = 1, \ldots, 1000$, varying the regularization parameter, α. (b) Weighted norm of the time-averaged analysis error $\|\mathbf{e}_k\|_{\sigma^2_{(b)}B^{-1}}$ integrated for all assimilation times $k = 1, \ldots, 1000$, varying the regularization parameter, α.

	8.2(b), 8.4(b), 8.8(b), 8.10(b)	8.2(c), 8.8(c)	8.2(d), 8.8(d)	8.3(b), 8.9(b)
Solid line (Truth)	$\mathbf{x}^{(t)}_{200:220}$	$\mathbf{x}^{(t)}_{774:805}$	$\mathbf{x}^{(t)}_{858:895}$	$\mathbf{x}^{(t)}_{200:220}$
Diamond (Truth)	$\mathbf{x}^{(t)}_{200}$	$\mathbf{x}^{(t)}_{774}$	$\mathbf{x}^{(t)}_{858}$	$\mathbf{x}^{(t)}_{200}$
Circle (Truth)	$\mathbf{x}^{(t)}_{201:220}$	$\mathbf{x}^{(t)}_{775:805}$	$\mathbf{x}^{(t)}_{859:895}$	$\mathbf{x}^{(t)}_{201:220}$
Square (Analysis)	$\mathbf{x}^{(a)}_{200}$	$\mathbf{x}^{(a)}_{774}$	$\mathbf{x}^{(a)}_{858}$	$\mathbf{x}^{(a)}_{200}$
Star (Analysis)	$\mathbf{x}^{(a)}_{201:220}$	$\mathbf{x}^{(a)}_{775:805}$	$\mathbf{x}^{(a)}_{859:895}$	$\mathbf{x}^{(a)}_{201:220}$
Dotted line (Analysis)	$\mathbf{x}^{(a)}_{200:220}$			

Table 8.1: Summary of the notation choices for Figure 8.2, Figure 8.3, Figure 8.4, Figure 8.8 Figure 8.9 and Figure 8.10.

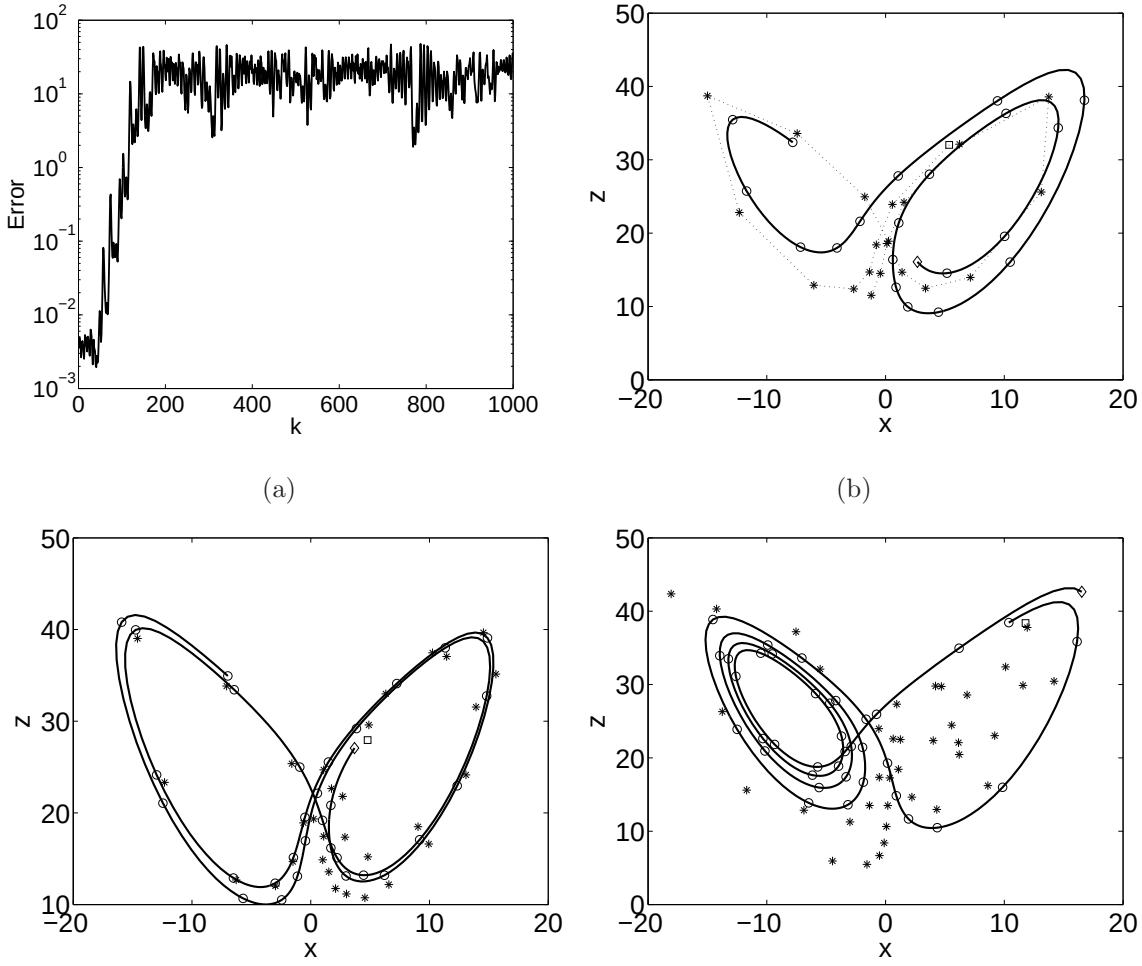

(a) (b)

(c) (d)

Figure 8.2: (a) ℓ^2 norm of the analysis error $\|\mathbf{e}_k\|_{\ell^2}$ as the scheme is cycled for index k, with regularization parameter $\alpha = 200$, which corresponds to 3DVar. (b), (c), (d) Trajectories, as described in Table 8.1.

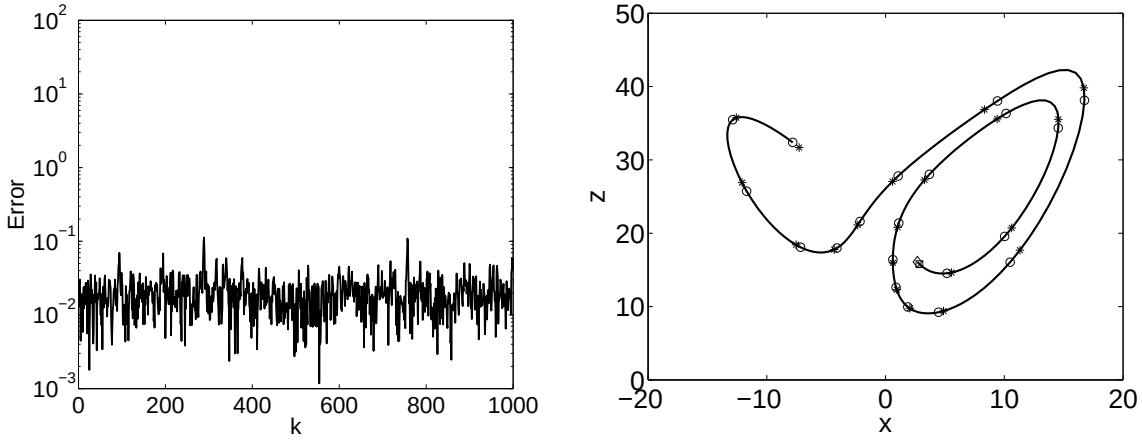

(a) (b)

Figure 8.3: (a) ℓ^2 norm of the analysis error $\|\mathbf{e}_k\|_{\ell^2}$ as the scheme is cycled for the index k, with regularization parameter $\alpha = 2$, an inflation in the background variance of 100%. (b) Trajectories, as described in Table 8.1.

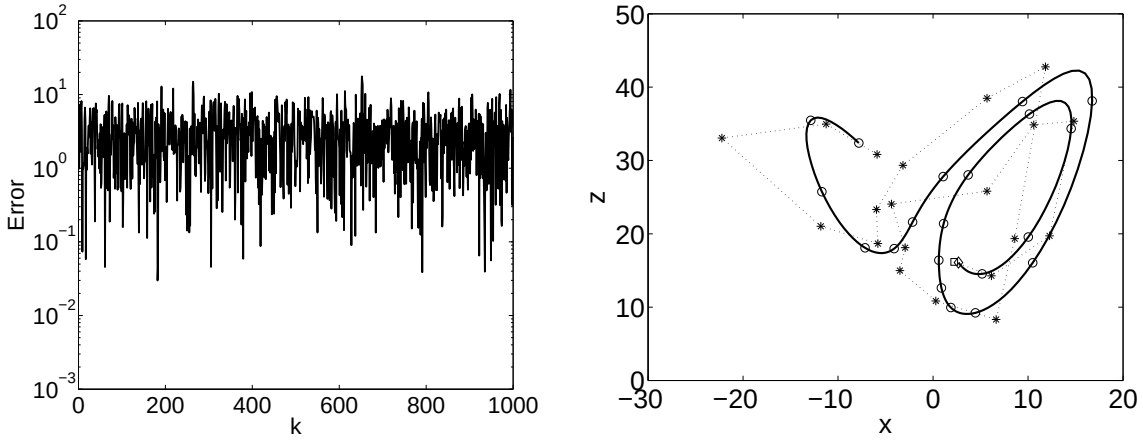

(a) (b)

Figure 8.4: (a) ℓ^2 norm of the analysis error $\|\mathbf{e}_k\|_{\ell^2}$ as the scheme is cycled for the index k, with regularization parameter $\alpha = 10^{-10}$, an inflation in the background variance of 2×10^{12}%. (b) Trajectories, as described in Table 8.1.

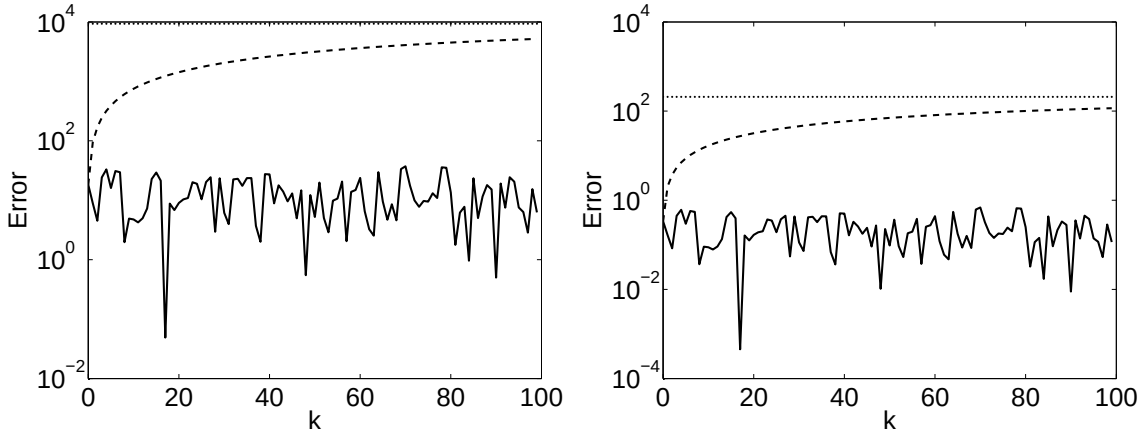

(a) (b)

Figure 8.5: (a) ℓ^2 norm of the analysis error, $\|\mathbf{e}_k\|_{\ell^2}$ as the scheme is cycled for the index k with regularization parameter, $\alpha = 10^{-6}$. (b) Weighted norm of the analysis error, $\|\mathbf{e}_k\|_{\sigma_{(b)}^2 B^{-1}}$ as the scheme is cycled for the index k with regularization parameter, $\alpha = 10^{-6}$. Solid line: Nonlinear analysis error. Dashed line: Linear bound. Dotted line: Asymptotic limit.

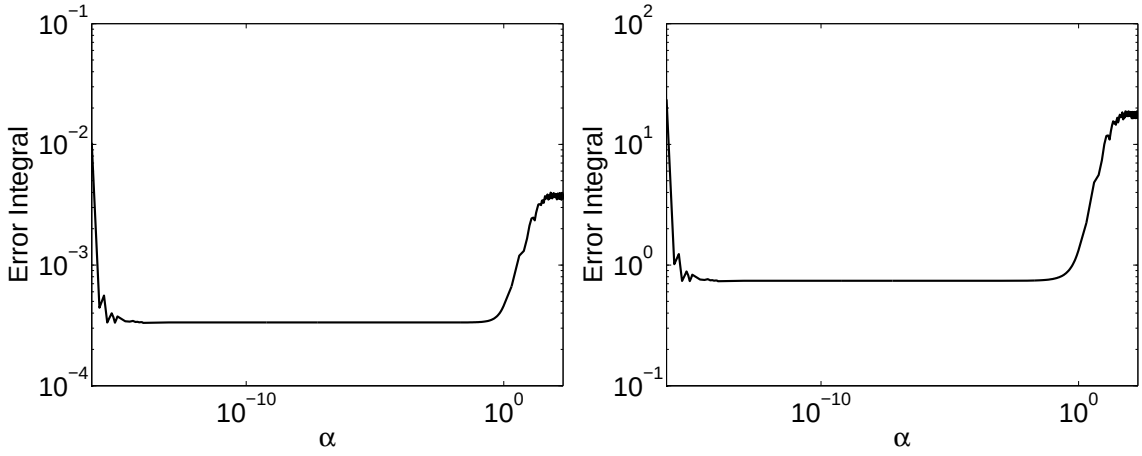

(a) (b)

Figure 8.6: (a) ℓ^2 norm of the time-averaged analysis error $\|\mathbf{e}_k\|_{\ell^2}$ integrated for all assimilation times $k = 1, \ldots, 1000$, varying the regularization parameter, α. (b) Weighted norm of the time-averaged analysis error $\|\mathbf{e}_k\|_{\sigma_{(b)}^2 B^{-1}}$ integrated for all assimilation times $k = 1, \ldots, 1000$, varying the regularization parameter, α.

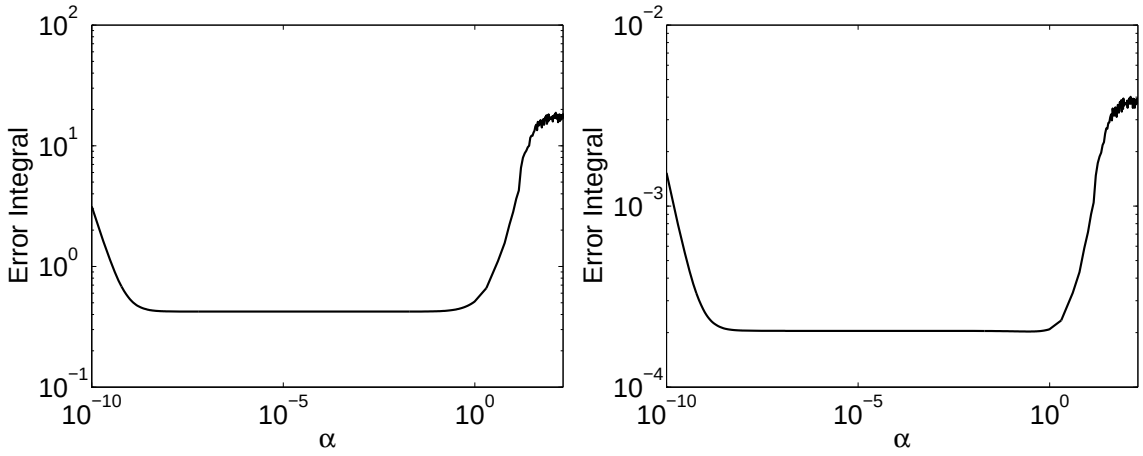

(a) (b)

Figure 8.7: (a) ℓ^2 norm of the time-averaged analysis error $\|\mathbf{e}_k\|_{\ell^2}$ integrated for all assimilation times $k = 1, \ldots, 1000$, varying the regularization parameter, α. (b) Weighted norm of the time-averaged analysis error $\|\mathbf{e}_k\|_{\sigma^2_{(b)}B^{-1}}$ integrated for all assimilation times $k = 1, \ldots, 1000$, varying the regularization parameter, α.

compact operator. Furthermore, we will consider a class of data assimilation schemes that perform an update to the background error covariance operator in the same way as in Section 7.2. Therefore, we shall assume a multiplicative update in the background variance, such that the Tikhonov-Phillips inverse becomes

$$\mathscr{R}_{\alpha_k} = (\alpha_k I + H^* H)^{-1} H^*. \tag{8.48}$$

As we will see, with the freedom to choose α_k in each assimilation step we will be able to derive a tighter bound to some degree on the nonlinear analysis error evolution compared with Section 8.1. In each cycled the bound on the nonlinear behaviour of the analysis error will become tighter. However, in order to seek the asymptotic result it is necessary to bound the analysis error by a lower bound on the sequence of regularization parameters over time.

From (8.10) we substitute $\mathscr{R}_\alpha$ for a time-dependent $\mathscr{R}_{\alpha_k}$ and substitute H_k for a time-invariant observation operator H, such that

$$\mathbf{e}_k = N_{\alpha_k}\left(\mathcal{M}_{k-1}\left(\mathbf{x}^{(a)}_{k-1}\right) - \mathcal{M}_{k-1}\left(\mathbf{x}^{(t)}_{k-1}\right)\right) + N_{\alpha_k}\boldsymbol{\zeta}_k + \mathscr{R}_{\alpha_k}\left(\boldsymbol{\eta}_k - \boldsymbol{\omega}_k\right), \tag{8.49}$$

where $N_{\alpha_k} := I - \mathscr{R}_{\alpha_k} H$. We define orthogonal projection operators, $P^{(1)}_{n_k}$ and $P^{(2)}_{n_k}$ from (7.49) with respect to the singular system of H. Then we can define the same subspaces $\mathbf{X}^{(1)}_{n_k}$

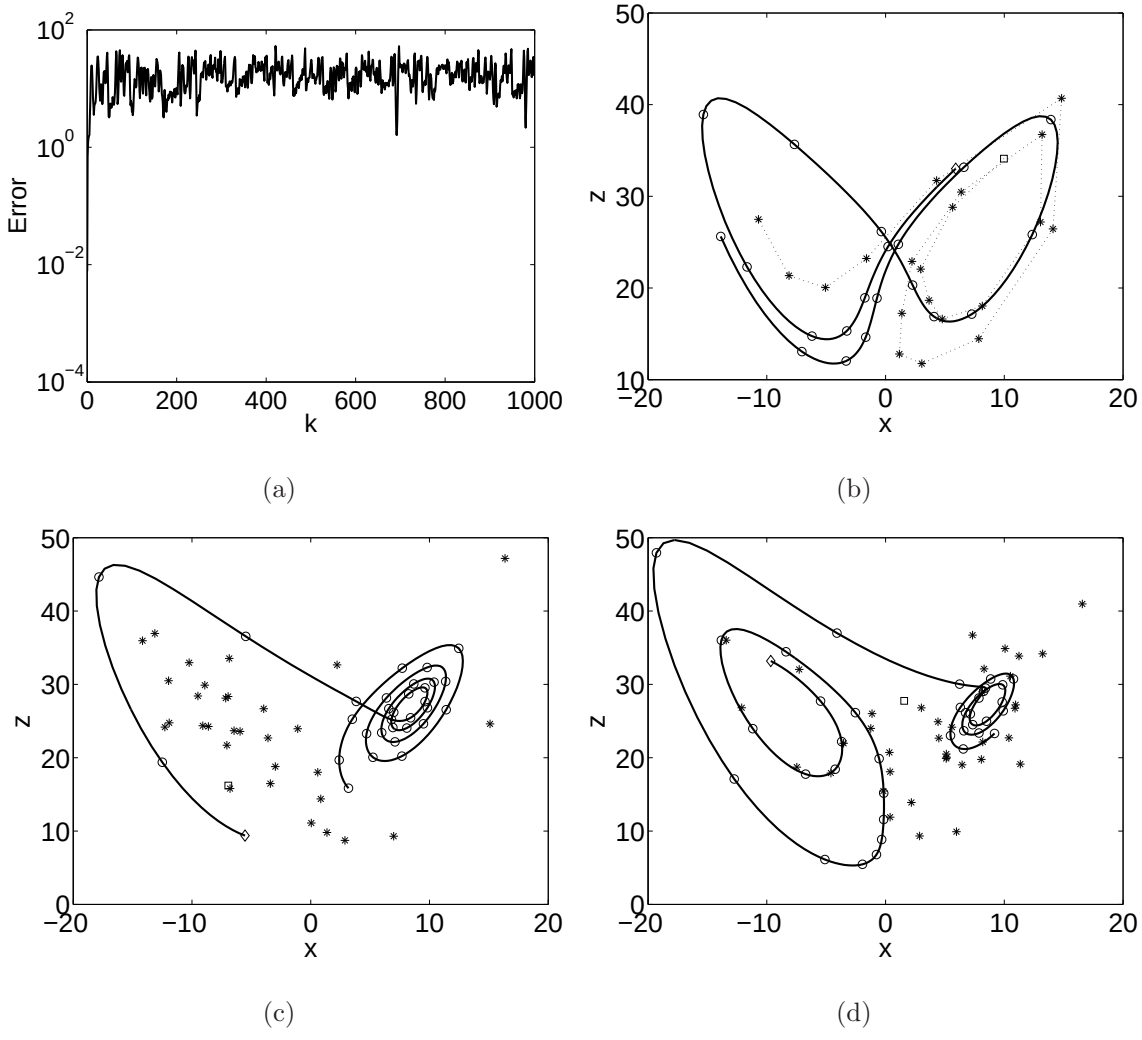

(a) (b)

(c) (d)

Figure 8.8: (a) ℓ^2 norm of the analysis error $\|\mathbf{e}_k\|_{\ell^2}$ as the scheme is cycled for index k, with regularization parameter $\alpha = 200$, which corresponds to 3DVar. (b), (c), (d) Trajectories, as described in Table 8.1.

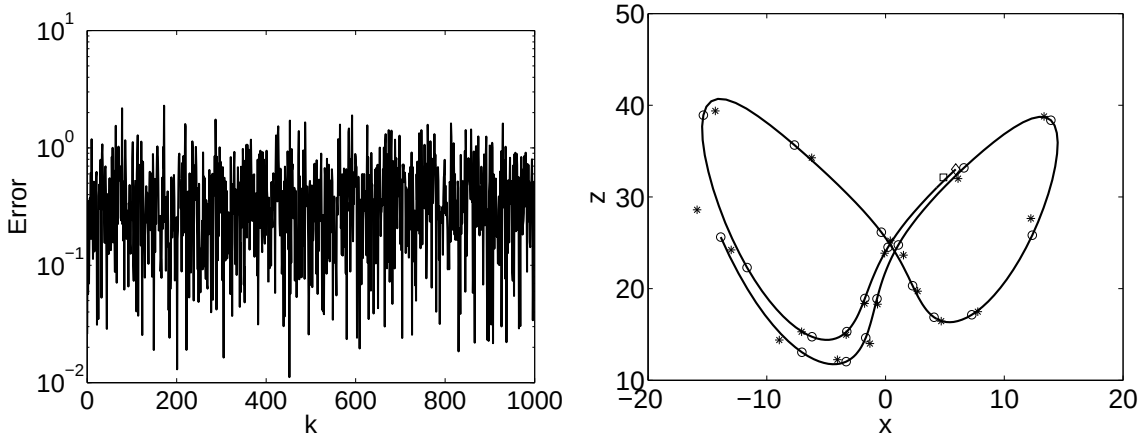

(a) (b)

Figure 8.9: (a) ℓ^2 norm of the analysis error $\|\mathbf{e}_k\|_{\ell^2}$ as the scheme is cycled for the index k, with regularization parameter $\alpha = 10^{-4}$, an inflation in the background variance of $2 \times 10^{6}\%$. (b) Trajectories, as described in Table 8.1.

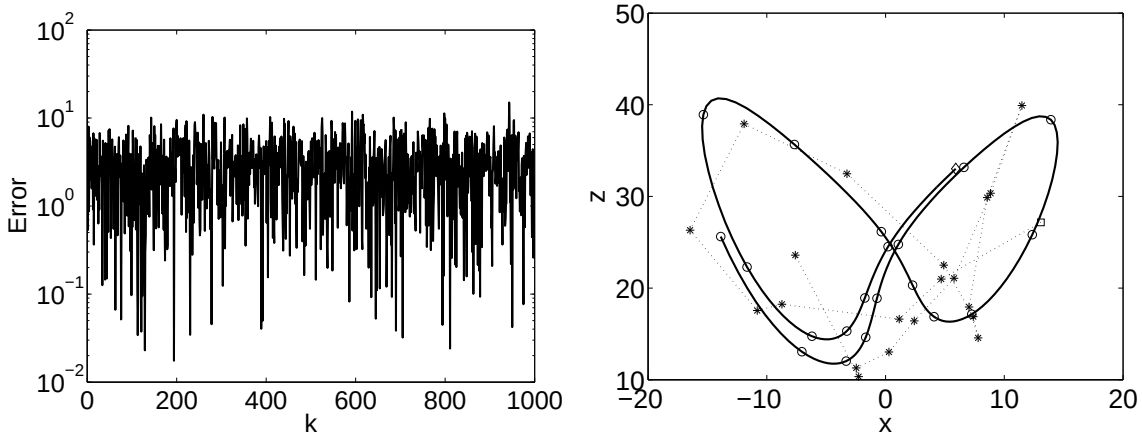

(a) (b)

Figure 8.10: (a) ℓ^2 norm of the analysis error $\|\mathbf{e}_k\|_{\ell^2}$ as the scheme is cycled for the index k, with regularization parameter $\alpha = 10^{-10}$, an inflation in the background variance of $2 \times 10^{12}\%$. (b) Trajectories, as described in Table 8.1.

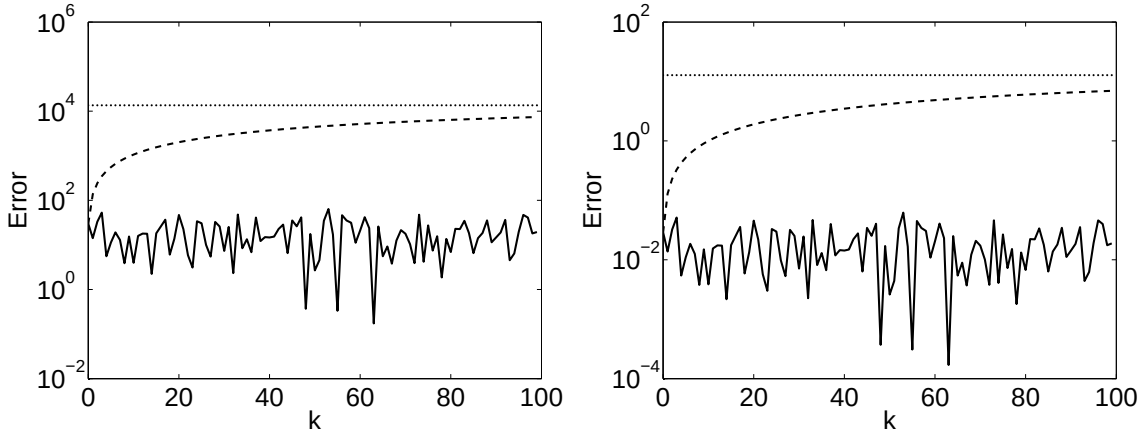

(a) (b)

Figure 8.11: (a) ℓ^2 norm of the analysis error, $\|\mathbf{e}_k\|_{\ell^2}$ as the scheme is cycled for the index k with regularization parameter, $\alpha = 6 \times 10^{-7}$. (b) Weighted norm of the analysis error, $\|\mathbf{e}_k\|_{\sigma^2_{(b)} B^{-1}}$ as the scheme is cycled for the index k with regularization parameter, $\alpha = 6 \times 10^{-7}$. Solid line: Nonlinear analysis error. Dashed line: Linear bound. Dotted line: Asymptotic limit.

and $\mathbf{X}^{(2)}_{n_k}$ as in (7.50). Returning to (8.49) and repeating the step from (8.21) to (8.22) and defining

$$\mathcal{M}^{(1)}_k(\cdot) := P^{(1)}_{n_k} \circ \mathcal{M}_k(\cdot) \;\text{ and }\; \mathcal{M}^{(2)}_k(\cdot) := P^{(2)}_{n_k} \circ \mathcal{M}_k(\cdot) \tag{8.50}$$

for all $k \in \mathbb{N}_0$, then

$$\begin{aligned} \mathbf{e}_k = {} & N_{\alpha_k}|_{\mathbf{X}^{(1)}_{n_k}} \left(\mathcal{M}^{(1)}_{k-1}\left(\mathbf{x}^{(a)}_{k-1}\right) - \mathcal{M}^{(1)}_{k-1}\left(\mathbf{x}^{(t)}_{k-1}\right)\right) + N_{\alpha_k}\boldsymbol{\zeta}_k \\ & + N_{\alpha_k}|_{\mathbf{X}^{(2)}_{n_k}} \left(\mathcal{M}^{(2)}_{k-1}\left(\mathbf{x}^{(a)}_{k-1}\right) - \mathcal{M}^{(2)}_{k-1}\left(\mathbf{x}^{(t)}_{k-1}\right)\right) + \mathscr{R}_{\alpha_k}\left(\boldsymbol{\eta}_k - \boldsymbol{\omega}_k\right). \end{aligned} \tag{8.51}$$

Now we are in a position to take norm estimates. Using the triangle inequality and property (c) from Lemma 2.1.20 we can repeat the steps from (8.25) through to (8.27), so that

$$\begin{aligned} \|\mathbf{e}_k\| \leq {} & K^{(1)}_{k-1} \cdot \left\| N_{\alpha_k}|_{\mathbf{X}^{(1)}_{n_k}} \right\| \cdot \left\| \mathbf{x}^{(a)}_{k-1} - \mathbf{x}^{(t)}_{k-1} \right\| \\ & + K^{(2)}_{k-1} \cdot \left\| N_{\alpha_k}|_{\mathbf{X}^{(2)}_{n_k}} \right\| \cdot \left\| \mathbf{x}^{(a)}_{k-1} - \mathbf{x}^{(t)}_{k-1} \right\| \\ & + \|N_{\alpha_k}\boldsymbol{\zeta}_k\| + \|\mathscr{R}_{\alpha_k}\left(\boldsymbol{\eta}_k - \boldsymbol{\omega}_k\right)\| \qquad (8.52) \\ \leq {} & \left(\nu^{(1)}_{k-1,\alpha_k} + \nu^{(2)}_{k-1,\alpha_k}\right) \|\mathbf{e}_k\| + \|N_{\alpha_k}\|\,\upsilon + \|\mathscr{R}_{\alpha_k}\|\,(\delta + \gamma)\,, \qquad (8.53) \end{aligned}$$

where we assume Lipschitz continuity from (8.29) and define $\nu^{(1)}_{k-1,\alpha_k} := K^{(1)}_{k-1} \cdot \|N_{\alpha_k}|_{\mathbf{X}^{(1)}_{n_k}}\|$ and $\nu^{(2)}_{k-1,\alpha_k} := K^{(2)}_{k-1} \cdot \|N_{\alpha_k}|_{\mathbf{X}^{(2)}_{n_k}}\|$. From Theorem 8.1.5 we know that for stability it is sufficient

to keep $\nu^{(1)}_{k-1,\alpha_k} + \nu^{(2)}_{k-1,\alpha_k} < 1$. We now show how this is possible to guarantee that the cycled data assimilation scheme remains stable. As we will see it is not necessary to bound the evolution of the analysis error by the global Lipschitz constant and therefore we can obtain a tighter bound on the nonlinear evolution of the analysis error in each step compared with Section 8.1.

Using Lemma 8.1.3 then there exists a constant $0 < \rho_k < 1$ we have that $\|N_{\alpha_k}|_{\mathbf{X}^{(1)}_{n_k}}\| < \rho_k$ on $\mathbf{X}^{(1)}_{n_k}$. Since the state space $\mathbf{X}^{(2)}_{n_k}$ has infinite dimension and the observation operator H is compact, then from Lemma 7.1.3 we have $\|N_{\alpha_k}|_{\mathbf{X}^{(2)}_{n_k}}\| = 1$ for any regularization parameter $\alpha_k > 0$. This leads to the following estimate,

$$\nu_{\alpha_k} := \nu^{(1)}_{k-1,\alpha_k} + \nu^{(2)}_{k-1,\alpha_k} = K^{(1)}_{k-1}\rho_k + K^{(2)}_{k-1}. \tag{8.54}$$

Therefore, we see directly in (8.54) that to keep $\nu_{\alpha_k} < 1$, $K^{(2)}_{k-1}$ must be strictly damping in each assimilation step k. This means that if the model dynamics are dissipative on some higher spectral modes of H, then we can arbitrarily choose $\mathbf{X}^{(1)}_{n_k}$ and $\mathbf{X}^{(2)}_{n_k}$ such that $K^{(2)}_{k-1} < 1$ in each step. This is a more general situation than before in (8.34) since we obtain a tighter bound on the nonlinear expansion in each step. Hence, on each assimilation step we change the space $\mathbf{X}^{(1)}_{n_k}$ so that there is a contraction in $\mathbf{X}^{(2)}_{n_k}$. Due to changing $\mathbf{X}^{(1)}_{n_k}$ we must choose a different regularization parameter α_k in each assimilation step, such that the constant ρ_k obeys

$$\rho_k < \frac{1 - K^{(2)}_{k-1}}{K^{(1)}_{k-1}}. \tag{8.55}$$

Before we present our stability result we must take a further bound on the analysis error evolution in (8.53). Therefore, we bound (8.53) by

$$\|\mathbf{e}_k\| \leq \nu_{\alpha_k} \|\mathbf{e}_k\| + \upsilon + \frac{\delta + \gamma}{2\sqrt{\alpha^*}}, \tag{8.56}$$

where $0 < \alpha^* \leq \inf_{k \in \mathbb{N}_0} \alpha_k$. This bound in (8.56) is similar to that in (7.47). Therefore, it is necessary to assume that the model dynamics restricted to $\mathbf{X}^{(1)}_{n_k}$ are bounded for all time. As discussed in Section 7.2 if we do not make this assumption then it might occur that $\alpha_k \to 0$ as $k \to \infty$, which cannot be allowed to happen. Hence, we must assume that Assumption 8.1.1 holds. Before we present our next stability result we must present the following definition, which is a nonlinear version of Definition 7.2.5.

Definition 8.2.1. Let $\mathcal{M}_k$, $k \in \mathbb{N}_0$ be a sequence of nonlinear operators on a Hilbert space $\mathbf{X}$ and let $\{\boldsymbol{\varphi}_i : i \in \mathbb{N}\}$ be a complete orthonormal system in $\mathbf{X}$. We call $\mathcal{M}_k$ a *uniformly dissipative sequence of Lipschitz continuous operators*, if for all $\mathbf{a}, \mathbf{b} \in \mathbf{X}$ and for every $0 < d < 1$ there is an $n_k \in \mathbb{N}$ such that

$$\left\| \mathcal{M}_{k-1}^{(2)}(\mathbf{a}) - \mathcal{M}_{k-1}^{(2)}(\mathbf{b}) \right\| = \left\| P_{n_k}^{(2)} \circ \mathcal{M}_{k-1}(\mathbf{a}) - P_{n_k}^{(2)} \circ \mathcal{M}_{k-1}(\mathbf{b}) \right\| \leq d \cdot \|\mathbf{a} - \mathbf{b}\|, \tag{8.57}$$

for all $k \in \mathbb{N}$ where $P_{n_k}^{(2)} : \mathbf{X} \to \operatorname{span}\{\boldsymbol{\varphi}_i, i > n_k\}$.

With both Assumption 8.1.1 and Definition 8.2.1 we can collect all parts of our analysis to present the following stability theorem for cycled data assimilation schemes.

Theorem 8.2.2. *Let $(\mathbf{X}, \|\cdot\|_{B^{-1}})$ be a Hilbert space with weighted norm. Let the nonlinear system $\mathcal{M}_k : \mathbf{X} \to \mathbf{X}$ be a uniformly dissipative sequence of Lipschitz continuous operators in accordance with Definition 8.2.1 that satisfies Assumption 8.1.1. Then for any constant $0 < d < 1$ there exists an $n_k \in \mathbb{N}$ in each assimilation step k in (8.3) such that*

$$\sup_{k \in \mathbb{N}} K_{k-1}^{(2)} = d. \tag{8.58}$$

Let Assumption 6.0.2 hold, then using the regularization parameter $\alpha_k > 0$ we can ensure for some constant $0 < \rho < 1$ that

$$\left\| N_{\alpha_k}|_{\mathbf{X}_{n_k}^{(1)}} \right\| \leq \frac{\rho - K_{k-1}^{(2)}}{K_{k-1}^{(1)}}, \tag{8.59}$$

for all $k \in \mathbb{N}$. Then under the conditions of Theorem 8.1.5, there exists a constant $0 < \chi < 1$, such that the analysis error is bounded over time by

$$\limsup_{k \to \infty} \|\mathbf{e}_k\| \leq \frac{\upsilon + \frac{\delta + \gamma}{2\sqrt{\alpha^*}}}{1 - \chi}, \tag{8.60}$$

where $0 < \alpha^* \leq \inf_{k \in \mathbb{N}_0} \alpha_k$.

Proof. If $\mathcal{M}_k$ is Lipschitz continuous and dissipative with respect to H, we first show that we can satisfy (8.58). From (8.54), the Lipschitz constants $K_{k-1}^{(1)}$ and $K_{k-1}^{(2)}$ determine our ability to achieve $\nu_{\alpha_k} < 1$ in each assimilation step k. Since $\mathcal{M}_k$ changes in each step and is uniformly dissipative with respect to higher modes of H, we change the subspace $\mathbf{X}_{n_k}^{(2)}$ so that there is a uniform contraction that satisfies (8.58). Now n_k is changing in each step k. Hence we must choose a regularization parameter $\alpha_k > 0$ in each step so that (8.59) holds. Since n_k

in (7.50) is finite this means that $\mathbf{X}_{n_k}^{(1)}$ is finite dimensional and we have the following norm estimate in each assimilation step k, such that

$$\left\| N_{\alpha_k}|_{\mathbf{X}_{n_k}^{(1)}} \right\| = \sup_{j\in\{1,\dots,n_k\}} \left| \frac{\alpha_k}{\alpha_k + \lambda_j} \right|, \tag{8.61}$$

where λ_j are the eigenvalues of the self-adjoint compact operator H^*H. We now show that we can choose a constant $0 < \alpha^* \leq \alpha_k$ for all $k \in \mathbb{N}_0$ so that

$$\sup_{j\in\{1,\dots,n_k\}} \left| \frac{\alpha^*}{\alpha^* + \lambda_j} \right| \leq \frac{\rho - K_{k-1}^{(2)}}{K_{k-1}^{(1)}}. \tag{8.62}$$

Since the eigenvalues of H^*H are assumed to be ordered then from (8.61) we have that

$$\sup_{j\in\{1,\dots,n_k\}} \left| \frac{\alpha_k}{\alpha_k + \lambda_j} \right| = \frac{\alpha_k}{\alpha_k + \lambda_{n_k}}. \tag{8.63}$$

Under Assumption 8.1.1 there exists a constant $c > 0$ such that $\sup_{k\in\mathbb{N}} K_{k-1}^{(1)} = c$. Since the model dynamics are assumed not to be globally damping then we have that $c \geq 1$. From (8.58) there exists a constant $0 < d < 1$ such that $\sup_{k\in\mathbb{N}} K_{k-1}^{(2)} = d$. Hence,

$$f := \frac{\rho - d}{c} \leq \frac{\rho - K_{k-1}^{(2)}}{K_{k-1}^{(1)}}. \tag{8.64}$$

We choose α^* such that

$$\alpha^* = \frac{\lambda^* f}{1 - f}, \tag{8.65}$$

where $\lambda^* := \inf_{k\in\mathbb{N}_0} \lambda_{n_k} > 0$ since n_k is finite. Then rearranging we have that

$$\frac{\alpha^*}{\alpha^* + \lambda^*} = f. \tag{8.66}$$

Therefore, we have found an $\alpha^* > 0$ such that (8.62) is satisfied, which means that there exists an $\alpha_k \geq \alpha^*$ in each step k such that (8.59) is satisfied. Then from (8.56) there exists a constant $0 < \chi < 1$ such that the bound for the analysis error is then given by

$$\|\mathbf{e}_k\| \leq \chi \|\mathbf{e}_k\| + \upsilon + \frac{\delta + \gamma}{2\sqrt{\alpha^*}}. \tag{8.67}$$

Then we can apply Theorem 8.1.5 to complete the proof by providing the estimate in (8.60).

□

This result has shown that an inflation in each assimilation step means that we can generalise the previous result in Section 8.1. We saw in (8.60) that our asymptotic result for the analysis error is dependent on a lower bound for the regularization parameter chosen over time. In order to obtain the bound on the evolution of the analysis error in (8.56) it was necessary to remove the time dependence in the noise term by using α^*. This is the same trade off as seen in Section 7.2. We now present the final theoretical result of this thesis, which is a nonlinear extension to Section 7.3.

8.3 Nonlinear dynamics with a general update to the background error covariance

In this section we present a nonlinear extension to the theoretical result in Section 7.3 for the stability of cycled data assimilation schemes that employ a general update to the background error covariance operator. Using (7.89), (7.83) and (8.49) we have the following evolution of the analysis error for nonlinear model dynamics,

$$\mathbf{e}_k = \hat{N}_{\alpha_k,k}\left(\mathcal{M}_{k-1}\left(\mathbf{x}_{k-1}^{(a)}\right) - \mathcal{M}_{k-1}\left(\mathbf{x}_{k-1}^{(t)}\right)\right) + \hat{N}_{\alpha_k,k}\boldsymbol{\zeta}_k + \mathscr{R}_{\alpha,k}\left(\boldsymbol{\eta}_k - \boldsymbol{\omega}_k\right), \tag{8.68}$$

where $\mathbf{e}_k := \mathbf{x}_k^{(a)} - \mathbf{x}_k^{(t)}$, $\hat{N}_{\alpha_k,k} := B_k^{1/2} N_{\alpha_k,k} B_k^{-1/2}$, $N_{\alpha_k,k} := (I + r^{-1}\alpha_k^{-1}\mathscr{G}_k^*\mathscr{G}_k)^{-1}$ where $\mathscr{G}_k := H_k B_k^{1/2}$ and $R_k = rI$ in accordance with (7.80) for all $k \in \mathbb{N}_0$. The noise terms $\boldsymbol{\zeta}_k$, $\boldsymbol{\eta}_k$ and $\boldsymbol{\omega}_k$ are the respective model error from (8.2), observation error from (4.8) and observation operator error from (4.7) for $k \in \mathbb{N}_0$. Using the projection operators $P_k^{(1)}$ and $P_k^{(2)}$ in (7.93) we split the state space to obtain the subspaces $\mathbf{X}_k^{(1)}$ and $\mathbf{X}_k^{(2)}$ as in (7.94). Then from (8.68) we have that

$$\begin{aligned}\mathbf{e}_k &= \hat{N}_{\alpha_k,k}\left(P_k^{(1)} + P_k^{(2)}\right)\left(\mathcal{M}_{k-1}\left(\mathbf{x}_{k-1}^{(a)}\right) - \mathcal{M}_{k-1}\left(\mathbf{x}_{k-1}^{(t)}\right)\right) + \hat{N}_{\alpha_k,k}\boldsymbol{\zeta}_k \\ &\quad + \mathscr{R}_{\alpha,k}\left(\boldsymbol{\eta}_k - \boldsymbol{\omega}_k\right) \qquad (8.69)\\ &= \hat{N}_{\alpha_k,k}|_{\mathbf{X}_k^{(1)}}\left(\mathcal{M}_{k,k-1}^{(1)}\left(\mathbf{x}_{k-1}^{(a)}\right) - \mathcal{M}_{k,k-1}^{(1)}\left(\mathbf{x}_{k-1}^{(t)}\right)\right) + \hat{N}_{\alpha_k,k}\boldsymbol{\zeta}_k \\ &\quad + \hat{N}_{\alpha_k,k}|_{\mathbf{X}_k^{(2)}}\left(\mathcal{M}_{k,k-1}^{(2)}\left(\mathbf{x}_{k-1}^{(a)}\right) - \mathcal{M}_{k,k-1}^{(2)}\left(\mathbf{x}_{k-1}^{(t)}\right)\right) + \mathscr{R}_{\alpha,k}\left(\boldsymbol{\eta}_k - \boldsymbol{\omega}_k\right) \qquad (8.70)\end{aligned}$$

where

$$\mathcal{M}_{k,k-1}^{(1)}(\cdot) := P_k^{(1)} \circ \mathcal{M}_{k-1}(\cdot) \text{ and } \mathcal{M}_{k,k-1}^{(2)}(\cdot) := P_k^{(2)} \circ \mathcal{M}_{k-1}(\cdot). \tag{8.71}$$

Using the triangle inequality and property (c) from Lemma 2.1.20 we can obtain a bound on this error as follows,

$$\begin{aligned}
\|\mathbf{e}_k\| &= \Big\| \hat{N}_{\alpha_k,k}|_{\mathbf{X}_k^{(1)}} \left(\mathcal{M}_{k,k-1}^{(1)} \left(\mathbf{x}_{k-1}^{(a)} \right) - \mathcal{M}_{k,k-1}^{(1)} \left(\mathbf{x}_{k-1}^{(t)} \right) \right) + \hat{N}_{\alpha_k,k} \boldsymbol{\zeta}_k \\
&\quad + \hat{N}_{\alpha_k,k}|_{\mathbf{X}_k^{(2)}} \left(\mathcal{M}_{k,k-1}^{(2)} \left(\mathbf{x}_{k-1}^{(a)} \right) - \mathcal{M}_{k,k-1}^{(2)} \left(\mathbf{x}_{k-1}^{(t)} \right) \right) + \mathscr{R}_{\alpha,k} \left(\boldsymbol{\eta}_k - \boldsymbol{\omega}_k \right) \Big\| \qquad (8.72) \\
&\leq \Big\| \hat{N}_{\alpha_k,k}|_{\mathbf{X}_k^{(1)}} \left(\mathcal{M}_{k,k-1}^{(1)} \left(\mathbf{x}_{k-1}^{(a)} \right) - \mathcal{M}_{k,k-1}^{(1)} \left(\mathbf{x}_{k-1}^{(t)} \right) \right) \Big\| \\
&\quad + \Big\| \hat{N}_{\alpha_k,k}|_{\mathbf{X}_k^{(2)}} \left(\mathcal{M}_{k,k-1}^{(2)} \left(\mathbf{x}_{k-1}^{(a)} \right) - \mathcal{M}_{k,k-1}^{(2)} \left(\mathbf{x}_{k-1}^{(t)} \right) \right) \Big\| \\
&\quad + \Big\| \hat{N}_{\alpha_k,k} \boldsymbol{\zeta}_k \Big\| + \| \mathscr{R}_{\alpha,k} \left(\boldsymbol{\eta}_k - \boldsymbol{\omega}_k \right) \| \qquad (8.73) \\
&\leq \kappa \left(B_k^{1/2}|_{\mathbf{X}_k^{(1)}} \right) \cdot \Big\| N_{\alpha_k,k}|_{\mathbf{X}_k^{(1)}} \left(\mathcal{M}_{k,k-1}^{(1)} \left(\mathbf{x}_{k-1}^{(a)} \right) - \mathcal{M}_{k,k-1}^{(1)} \left(\mathbf{x}_{k-1}^{(t)} \right) \right) \Big\| \\
&\quad + \kappa \left(B_k^{1/2}|_{\mathbf{X}_k^{(2)}} \right) \cdot \Big\| N_{\alpha_k,k}|_{\mathbf{X}_k^{(2)}} \left(\mathcal{M}_{k,k-1}^{(2)} \left(\mathbf{x}_{k-1}^{(a)} \right) - \mathcal{M}_{k,k-1}^{(2)} \left(\mathbf{x}_{k-1}^{(t)} \right) \right) \Big\| \\
&\quad + \kappa \left(B_k^{1/2} \right) \cdot \| N_{\alpha_k,k} \boldsymbol{\zeta}_k \| + \| \mathscr{R}_{\alpha,k} \left(\boldsymbol{\eta}_k - \boldsymbol{\omega}_k \right) \| . \qquad (8.74)
\end{aligned}$$

Using Assumption 8.12 we can further bound (8.74) by

$$\begin{aligned}
e_k &\leq \left(\kappa \left(B_k^{1/2}|_{\mathbf{X}_k^{(1)}} \right) \cdot K_{k-1}^{(1)} \cdot \Big\| N_{\alpha_k,k}|_{\mathbf{X}_k^{(1)}} \Big\| \right. \qquad (8.75) \\
&\quad \left. + \kappa \left(B_k^{1/2}|_{\mathbf{X}_k^{(2)}} \right) \cdot K_{k-1}^{(2)} \cdot \Big\| N_{\alpha_k,k}|_{\mathbf{X}_k^{(2)}} \Big\| \right) e_{k-1} \\
&\quad + \kappa \left(B_k^{1/2} \right) \cdot \| N_{\alpha_k,k} \| \, \upsilon + \| \mathscr{R}_{\alpha,k} \| \left(\delta + \gamma \right) , \qquad (8.76)
\end{aligned}$$

where $e_k := \|\mathbf{e}_k\|$, $K_{k-1}^{(1)}$ and $K_{k-1}^{(2)}$ are the Lipschitz constants on $\mathbf{X}_{k-1}^{(1)}$ and $\mathbf{X}_{k-1}^{(2)}$ respectively at time $k-1$ and υ, δ and γ are the bounds on the noise. Using Remark 7.3.1 and (7.102), (8.76) becomes

$$\begin{aligned}
e_k &\leq \left(\kappa \left(B_k^{1/2}|_{\mathbf{X}_k^{(1)}} \right) \cdot K_{k-1}^{(1)} \cdot \Big\| N_{\alpha_k,k}|_{\mathbf{X}_k^{(1)}} \Big\| + \kappa \left(B_k^{1/2}|_{\mathbf{X}_k^{(2)}} \right) \cdot K_{k-1}^{(2)} \right) e_{k-1} \\
&\quad + \kappa \left(B_k^{1/2} \right) \upsilon + \frac{\left\| B_k^{1/2} \right\| \left(\delta + \gamma \right)}{2\sqrt{r\alpha_k}}, \qquad (8.77)
\end{aligned}$$

If Assumption 7.3.2 holds then from (8.77)

$$\begin{aligned}
e_k &\leq \left(a^{(1)} b^{(1)} \cdot K_k^{(1)} \cdot \Big\| N_{\alpha_k,k}|_{\mathbf{X}_k^{(1)}} \Big\| + a^{(2)} b^{(2)} \cdot K_k^{(2)} \right) e_{k-1} \\
&\quad + ab\upsilon + \frac{b \left(\delta + \gamma \right)}{2\sqrt{r\alpha^*}}, \qquad (8.78)
\end{aligned}$$

where $0 < \alpha^* \leq \inf_{k \in N_0} \alpha_k$. We are now in a position to state the main result for nonlinear cycled data assimilation schemes that employ a general update to the background error covariance.

Theorem 8.3.1. *For the Hilbert space* $(\mathbf{X}, \|\cdot\|_{\ell^2})$*, let the nonlinear system* $\mathcal{M}_k : \mathbf{X} \to \mathbf{X}$ *be a uniformly dissipative sequence of Lipschitz continuous operators in accordance with Definition 8.2.1 that satisfies Assumption 8.1.1. Let Assumption 7.3.2 hold. Then for any constant* $0 < d < 1$ *there exists an* $n_k \in \mathbb{N}$ *in each assimilation step* k*, such that*

$$\sup_{k\in\mathbb{N}} K_{k-1}^{(2)} = \frac{d}{a^{(2)}b^{(2)}}, \tag{8.79}$$

with positive constants $a^{(2)}b^{(2)} \in \mathbb{R}^+$ *from (7.111). Let* $\mathscr{G}_k$ *be a uniform spectral sequence of injective linear compact operators in accordance with Definition 7.3.3. Then using the regularization parameter* $\alpha_k > 0$*, we can ensure for some constant* $0 < \rho < 1$ *that*

$$\left\| N_{\alpha_k,k}|_{\mathbf{X}_k^{(1)}} \right\| \leq \frac{\rho - a^{(2)}b^{(2)}K_{k-1}^{(2)}}{a^{(1)}b^{(1)}K_{k-1}^{(1)}}, \tag{8.80}$$

for all $k \in \mathbb{N}$ *and for positive constants* $a^{(1)}b^{(1)} \in \mathbb{R}^+$ *from (7.110). Under the conditions of Theorem 8.1.5, there exists a constant* $0 < \chi < 1$*, such that the analysis error is bounded over time by*

$$\limsup_{k\to\infty} \|\mathbf{e}_k\| \leq \frac{abv + \frac{b(\delta+\gamma)}{2\sqrt{r\alpha^*}}}{1-\chi}, \tag{8.81}$$

where $0 < \alpha^* \leq \inf_{k\in\mathbb{N}_0} \alpha_k$*.*

Proof. If $\mathcal{M}_{k-1}$ is Lipschitz continuous and dissipative with respect to higher spectral modes of the sequence of operators $\mathscr{G}_k$, we first show that we can achieve (8.79). Since $\mathcal{M}_k$ changes in each step and is assumed to be dissipative with respect to higher modes of $\mathscr{G}_k$ in each step, then we change the subspace $\mathbf{X}^{(2)}$ so that there is a uniform contraction that satisfies (8.79). Now n_k and the orthonormal system $\{\boldsymbol{\varphi}_{i,k} : i \in \mathbb{N}\}$ are changing in each step k. Hence we must choose a regularization parameter $\alpha_k > 0$ in each step so that (8.80) holds. Since n_k is finite this means that $\mathbf{X}_k^{(1)}$ from (7.93) is finite dimensional and we have the following norm estimate in each assimilation step k, such that

$$\left\| N_{\alpha_k,k}|_{\mathbf{X}_k^{(1)}} \right\| = \sup_{j\in\{1,\dots,n_k\}} \left| \frac{r\alpha_k}{r\alpha_k + \lambda_{j,k}} \right|, \tag{8.82}$$

where $\lambda_{j,k}$ are the eigenvalues of the sequence of self-adjoint compact operators $\mathscr{G}_k^*\mathscr{G}_k$ and r is in accordance with (7.80). We now show that we can choose a constant $0 < \alpha^* \leq \alpha_k$ for all $k \in \mathbb{N}_0$ so that

$$\sup_{j\in\{1,\dots,n_k\}} \left| \frac{r\alpha^*}{r\alpha^* + \lambda_{j,k}} \right| \leq \frac{\rho - a^{(2)}b^{(2)}K_{k-1}^{(2)}}{a^{(1)}b^{(1)}K_{k-1}^{(1)}}. \tag{8.83}$$

Since the eigenvalues of $\mathscr{G}_k^*\mathscr{G}_k$ are assumed to be ordered then from (8.82) we have that

$$\sup_{j\in\{1,\dots,n_k\}}\left|\frac{r\alpha_k}{r\alpha_k+\lambda_{j,k}}\right| = \frac{r\alpha_k}{r\alpha_k+\lambda_{n_k,k}}. \tag{8.84}$$

Under Assumption 8.1.1 there exists a constant $c>0$ such that $\sup_{k\in\mathbb{N}} K_{k-1}^{(1)} = c$. Since the model dynamics are assumed not to be globally damping then we have that $c \geq 1$. From (8.79) there exists a constant $0<d<1$ such that $\sup_{k\in\mathbb{N}} K_{k-1}^{(2)} = d/(a^{(2)}b^{(2)})$. Hence,

$$f := \frac{\rho-d}{a^{(1)}b^{(1)}c} \leq \frac{\rho-a^{(2)}b^{(2)}K_{k-1}^{(2)}}{a^{(1)}b^{(1)}K_{k-1}^{(1)}}. \tag{8.85}$$

From Definition 7.3.3 there exists a real positive constant $0<\lambda^*\leq\lambda_{n_k,k}$ for all $k\in\mathbb{N}_0$ such that we can choose α^* so that

$$\alpha^* = \frac{\lambda^* f}{r-rf}. \tag{8.86}$$

Then rearranging we have that

$$\frac{r\alpha^*}{r\alpha^*+\lambda^*} = f. \tag{8.87}$$

Therefore, we have found an $\alpha^*>0$ such that (8.83) is satisfied, which means that there exists an $\alpha_k\geq\alpha^*$ in each assimilation step k such that (8.80) is satisfied. Then from (8.78) there exists a constant $0<\chi<1$ such that the bound for the analysis error is then given by

$$e_k \leq \chi e_{k-1} + ab\upsilon + \frac{b\,(\delta+\gamma)}{2\sqrt{r\alpha^*}}. \tag{8.88}$$

This form is similar to (8.15) and we can use Theorem 8.1.2 to complete the proof. □

This result in Theorem 8.3.1 shows that it is possible to choose a regularization parameter in each assimilation step to stabilise the cycled data assimilation scheme. This was under the assumption that the nonlinear map $\mathcal{M}_{k-1}$ must be dissipative with respect to higher spectral modes of the operator $\mathscr{G}_k$ for all time. If this property can be shown for the nonlinear system then the result would give a tighter bound on the behaviour of the analysis error than previous in Theorem 8.1.7. This is because we can apply an update to the regularization parameter in each assimilation step which eliminates the need to bound the behaviour by the global Lipschitz constant. Also this result is dependent on the cycled data assimilation scheme producing unique square roots $B_k^{1/2}, B_k^{-1/2}\in L(\mathbf{X})$ for all time $k\in\mathbb{N}$ and uniformly bounded square root background error covariances in accordance with Assumption 7.3.2. In

Chapter 7 we showed under a number of conditions that the Kalman filter produces unique square roots $B_k^{1/2}, B_k^{-1/2} \in L(\mathbf{X})$ for all time and that (7.108) in Assumption 7.3.2 holds. An extension of this would be to show that Assumption 7.3.2 holds in the case of an extended Kalman filter in the nonlinear setting.

8.4 Summary

In this chapter, we have presented a nonlinear extension to the theoretical results developed in Chapter 7. We have shown that it is sufficient that the nonlinear model dynamics are dissipative on higher spectral modes of the observation operator in order to ensure stability of the cycled data assimilation scheme. Without this dissipative property then our stability results do not hold due to the ill-posedness of the problem. Firstly, we developed results for data assimilation scheme that employ static error covariances. Here we illustrated our theoretical results by showing a number of numerical experiments with the deterministic and stochastic Lorenz equations. Secondly, we investigated data assimilation schemes where there is a multiplicative update in the background error covariance. This was a direct extension to results from Section 7.2. Finally, we developed results for the case where there is a general update to the background error covariance in the same way as in Chapter 7. In the next chapter we produce conclusions to this work and discuss future extensions to the results developed in this thesis.

Chapter 9

Conclusions

In NWP advanced data assimilation techniques are applied to combine indirect noisy observational data, with a highly nonlinear complex numerical forecast model in order to generate an analysis. This analysis provides the best estimate to the state of the atmosphere. An initial guess which we call the background state is used to ensure the problem we solve is well-posed. This background state is calculated by forecasting the previous analysis to the current assimilation time. Data assimilation methods are then applied using the background state and current available observations. Currently, the process of cycling data assimilation schemes in operational NWP centres is dependent on the spatial scales. For example most operational NWP centres cycle their variational data assimilation schemes every six to twelve hours for their global system and cycle their variational data assimilation schemes every one to three hours for regional system.

In this thesis we have analysed the behaviour of the analysis error, which is defined as the difference between the analysis, obtained from the data assimilation scheme and the true state of the system. We have represented the evolution of the analysis error in an infinite dimensional setting. Despite all computational algorithms being finite dimensional, most numerical models used in NWP are discrete approximations to infinite dimensional linear and nonlinear partial differential equations. Therefore, working in an infinite dimensional setting means that we can tackle problems that exist in the finite dimensional setting in a general framework, which is mathematically consistent with our infinite dimensional dynamical system.

There are few theoretical and numerical results in the literature that are applicable to the behaviour of cycled data assimilation schemes in the infinite dimensional setting. Most results are relevant to finite dimensional linear (see Section 4.2 and in particular [54], [11], [40] and [21]) and nonlinear (see Section 4.3 and in particular [44], [82] and [77]) systems. Our approach in this thesis has involved investigating the behaviour of data assimilation schemes using norm estimates. Recently results have emerged in the literature using this approach for infinite dimensional linear (see Section 4.4 and in particular [57]) and nonlinear (see Section 4.5 and in particular [60] and [7]) systems.

9.1 Conclusions

In this thesis we have developed new theoretical results on the stability of cycled data assimilation schemes for a wide class of linear and nonlinear dynamical systems. In Chapter 2 we introduced tools from functional analysis that enabled us to analyse the evolution of the analysis error of the data assimilation schemes from Chapter 3.

In Chapter 3 we introduce three popular data assimilation schemes, 3DVar, 4DVar and the Kalman filter. We aligned each of these to cycled Tikhonov-Phillips regularization which we analysed in Chapter 6, Chapter 7 and Chapter 8.

In Chapter 4 we formulated an expression for the evolution of the analysis error for a cycled data assimilation scheme of the form introduced in Chapter 3. We found that our expression for the evolution of the analysis error linked with observer systems, which are popular in the field of control theory. We critically reviewed the literature regarding linear time-invariant, linear time-varying and nonlinear dynamical systems in the finite and infinite dimensional setting.

In Chapter 5 we introduced one linear model, the 2D Eady model and two versions (deterministic and stochastic) of the nonlinear Lorenz '63 model. These models were introduced so that they could be used in numerical experiments in Chapter 6, Chapter 7 and Chapter 8 to illustrate our theoretical results and the behaviour of the analysis error.

In Chapter 6 we presented new theoretical results on the stability of cycled 3DVar-type data assimilation schemes for constant and diagonal dynamical systems. We showed that we can choose a regularization parameter sufficiently small so that a cycled 3DVar scheme

introduced in Chapter 3 remains stable for all time. Moreover, if the regularization parameter was chosen too small then this made the analysis error worse by amplifying the error in the observations and observation operator. We found that it is necessary that the model dynamics are damping on higher spectral modes for our stability result to hold in the infinite dimensional setting. The dynamical systems which we considered in Chapter 6 were not applicable to realistic systems and therefore we used the set-up in Chapter 6 as a stepping stone to more advanced realistic dynamical systems in Chapter 7 and Chapter 8.

In Chapter 7 we derived new theoretical results on the stability of cycled data assimilation schemes for general linear dynamical systems. We showed for a class of compact operators, the Hilbert-Schmidt operator, we were able to split the state space so that there was a contraction in the error dynamics leading to a stable cycled data assimilation scheme for all time. We developed stability results for cycled 3DVar and 4DVar where the dynamical system comprised of a linear time-invariant model dynamics operator and a time-invariant observation operator. We illustrated this result for the 4DVar scheme using a dynamical system that was comprised of the 2D Eady model from Chapter 5 and a general injective linear time-invariant observation operator. We then extended this result and showed for a cycled data assimilation scheme that employs a multiplicative update in the background error covariance operator, that we could extend our stability results to dynamical systems with linear time-varying model dynamics. We showed that, given a perfect model Kalman filter and constant model dynamics, the inverse of the background error covariance is asymptotically unbounded. This result highlighted that the model error covariance operator is instrumental in keeping the evolving background error covariance operator stable. Finally, we demonstrated that if the square root of the background error covariance operator and its inverse exists and are bounded then our stability result holds for a cycled data assimilation scheme where there is a general update to the background error covariance operator. Moreover, we showed that for the Kalman filter if we can artificially inflate the background error covariance then we can show asymptotic stability in the infinite dimensional setting. Our result was under the following conditions:

1. the model dynamics are linear and bounded for all time;

2. the observation operator is an injective linear time-varying bounded operator;

3. the model error covariance operator is uniformly strictly positive for all time;

4. the initial background error covariance operator is strictly positive;

5. the observation error covariance operator is diagonal and static in time, see Section 7.3;

6. the square root background error covariance operator is uniformly bounded, such that (7.109) is satisfied.

We have seen that many of our conditions are similar to those in Kalman's work as discussed in Section 4.2.3. Similar to the results in the literature, we require that the model dynamics are bounded for all time and the initial background error covariance is strictly positive. However, our results are more restrictive due to our approach of norm estimates.

In Chapter 8 we provided a nonlinear extension to some of the linear results from Chapter 7. Here we considered a dynamical system comprised of a nonlinear model operator and a linear time-invariant observation operator. We showed that to achieve stability in the cycled data assimilation scheme it was necessary that the nonlinear dynamics be Lipschitz continuous and be dissipative on higher spectral modes. If the model dynamics satisfy Lipschitz continuity and dissipative behaviour then we demonstrated that a cycled 3DVar scheme is asymptotically stable. We illustrated the evolution of the analysis error for a cycled 3DVar scheme in numerical experiments using the deterministic and stochastic Lorenz '63 model. Then we showed that if a time-dependent regularization parameter is applied in each assimilation step to the cycled 3DVar scheme then the analysis error will remain bounded for all time. Finally, we demonstrated that if the model dynamics are dissipative with respect to higher spectral modes of the observation operator composed with the inverse square root of the background covariance operator, then the analysis error of a cycled data assimilation scheme that employs a general update in the background error covariance operator will be stable. In each of these cases it must be shown for the particular model dynamics operator that these dissipative properties hold. However, this is not necessarily true for many realistic models.

In conclusion, the results in this thesis have demonstrated that cycling data assimilation schemes in a high or infinite dimensional setting is a stable process for a wide range of

dynamical systems. Using the regularization parameter or equivalently inflating the variance of the background state, means that the analysis error can be kept bounded for all time.

9.2 Future work

In the derivation of our bounds on the analysis error for a variety of data assimilation schemes clearly many assumptions were made. We now discuss how many of these assumptions could be relaxed in future work and highlight the assumptions that are more difficult to relax.

In Chapter 7 we assumed that the square root background error covariance operator was uniformly bounded. If this can be shown to hold for the Kalman filter from Chapter 3 then our stability result in Section 7.3 would demonstrate stability for the Kalman filter in an infinite dimensional setting with a compact observation operator. This should be investigated further in future work by working through the proof of Lemma 7.3.6 to see under what conditions would (7.109) hold from Assumption 7.3.2.

One major assumption we have made in this work is that the observation operator is injective. We mentioned in Chapter 6 that this assumption was not necessary. However, in order to obtain the bound in (6.47) on the Tikhonov-Phillips inverse which is independent of the observation operator it was necessary to assume injectivity in H. It would be useful to the NWP community to relax this assumption since rank deficiency is a major problem when assimilating satellite data [71]. The work of [7] has shown that injectivity is not necessary to develop similar stability results for the Navier-Stokes system. As we saw in Section 2.3.1 if H is a compact operator then Tikhonov-Phillips regularization guarantees that the operator $\alpha I + H^*H$ is injective for $\alpha > 0$. Therefore, it is possible to assume that H is not injective, although one must take care of the nullspace of the observation operator. In Chapter 6, Chapter 7 and Chapter 8 we expressed elements spectrally therefore we would need to include the orthogonal projection operator $Q : \mathbf{X} \to \mathscr{N}(H)$ in our analysis.

In our work we have assumed throughout that the observation operator is linear. In the NWP community the observation operator might not be linear, especially when satellite data is assimilated [71]. We believe that nonlinearity in the observation operator would not change the phenomena seen in this work. We still think that a regularization parameter can be chosen to achieve a stable cycled data assimilation scheme. This is because our work

has shown that the analysis error is heavily influenced by the background error covariance. When solving a nonlinear operator equation it is highly likely that the problem is ill-posed in the classical sense. Therefore, the background state is necessary to ensure that we solve a well-posed problem. In the inverse problems community applying Tikhonov-Phillips regularization to nonlinear operator equations is popular, see [24] and [13]. Therefore, it would be interesting to analyse the behaviour of the analysis error for data assimilation schemes where the observation operator is nonlinear. In our work we have used Theorem 2.3.4 to guarantee a unique solution when we derived an expression for the evolution of the analysis error. However, we would have to take care of local minima, such that the minimiser to the nonlinear functional might not produce a unique global minimum in accordance with Theorem 2.3.4.

We have assumed for the majority of this work that the observation operator is time-invariant. We relaxed this assumption when we analysed the analysis error of cycled data assimilations schemes in Section 7.3 and Section 8.3 that employ a general update to the background error covariance operator. Further work could extend our results to time-varying observation operators for variational data assimilation schemes. Therefore, by allowing for a time-dependence one would need to describe the relationship between the properties of the observation operator over time in relation to the properties of the model dynamics.

In Chapter 7 for linear dynamical systems we have seen that our approach of norm estimates has led to a sufficient condition on the stability for cycled data assimilation schemes. We discussed in Chapter 4 that under conditions of observability and controllability, eigenvalues can be assigned to give a necessary and sufficient condition on the stability of time-invariant observer systems. Future research could investigate concepts of observability and controllability from infinite dimensional linear systems theory, leading to necessary and sufficient conditions on the behaviour of cycled data assimilation schemes, see [17, Chapter 14]. However, it is not clear from this thesis how one could extend linear theoretic results that rely on observability and controllability conditions to general nonlinear dynamical systems.

Our work has focused on deriving deterministic results for a variety of data assimilation schemes. Therefore, in this work we assumed that the noise on the observations, model and observation operator were bounded for all time. It would be possible to relax this assumption and carry through mean-square analysis with the assumption that the noise terms are mean

zero independent and identically distributed Gaussian variables. This stochastic direction could lead to some interesting results and should be considered in future work.

A key assumption that we made in this work is that the nonlinear model dynamics are Lipschitz continuous. As we have discussed in Chapter 8 the assumption of Lipschitz continuity is expected to hold locally in the field of geophysical and meteorological applications. For our theory to hold we would require global Lipschitz continuity. Without this assumption we think that it would be more difficult to carry out similar analysis for the behaviour of the analysis error of cycled data assimilation schemes.

Bibliography

[1] J.L. Anderson. An adaptive covariance inflation error correction algorithm for ensemble filters. *Tellus A*, 59(2):210–224, 2007.

[2] M. Arumugam and M. Ramamoorty. A dynamic observer for a synchronous machine. *International Journal of Control*, 15(6):1129–1136, 1972.

[3] G. Bachman and L. Narici. *Functional Analysis*. Academic Press Textbooks in Mathematics. Dover Books on Mathematics Series, 1966.

[4] S.P. Banks. A note on non-linear observers. *International Journal of Control*, 34(1):185–190, 1981.

[5] R.J. Barlow. *Statistics: A Guide to the Use of Statistical Methods in the Physical Sciences*. Manchester Physics Series. John Wiley & Sons, 1994.

[6] S. Barnett and R.G. Cameron. *Introduction to Mathematical Control Theory*. Oxford Applied Mathematics and Computing Science Series. Clarendon Press, 1985.

[7] C.E.A. Brett, K.F. Lam, K.J.H. Law, D.S. McCormick, M.R. Scott, and A.M. Stuart. Accuracy and stability of filters for dissipative PDEs. *Physica D: Nonlinear Phenomena*, 245(1):34 – 45, 2013.

[8] H.H.W. Broer, H. Broer, and F. Takens. *Dynamical Systems and Chaos*. Applied Mathematical Sciences. Springer New York, 2011.

[9] A.G. Butkovskii. *Theory of Optimal Control of Distributed Parameter Systems*. American Elsevier, 1969.

[10] M. Chen and C. Chen. Robust nonlinear observer for lipschitz nonlinear systems subject to disturbances. *Automatic Control, IEEE Transactions on*, 52(12):2365–2369, 2007.

[11] V. Cheng. A direct way to stabilize continuous-time and discrete-time linear time-varying systems. *IEEE Transactions on Automatic Control*, 24(4):641–643, 1979.

[12] S.E. Cohn and D.P. Dee. Observability of discretized partial differential equations. *SIAM Journal on Numerical Analysis*, 25(3):586–617, 1988.

[13] D. Colton and R. Kress. *Inverse Acoustic and Electromagnetic Scattering Theory*. Springer, second edition, 1997.

[14] J.B. Conway. *A Course in Functional Analysis*. Graduate Texts in Mathematics. Springer, 1990.

[15] M.J. Corless and A.E. Frazho. *Linear Systems and Control: An Operator Perspective*. Monographs and Textbooks in Pure and Applied Mathematics. CRC Press, 2003.

[16] P. Courtier, E. Andersson, W. Heckley, D. Vasiljevic, M. Hamrud, A. Hollingsworth, F. Rabier, M. Fisher, and J. Pailleux. The ECMWF implementation of three-dimensional variational assimilation (3d-var). i: Formulation. *Quarterly Journal of the Royal Meteorological Society*, 124(550):1783–1807, 1998.

[17] R.F. Curtain and A.J. Pritchard. *Functional Analysis in Modern Applied Mathematics*, volume 132. IMA, 1977.

[18] R.F. Curtain and A.J. Pritchard. *Infinite Dimensional Linear Systems Theory*. Lecture Notes in Control and Information Sciences. Springer-Verlag, 1978.

[19] R.F. Curtain and H. Zwart. *An Introduction to Infinite-Dimensional Linear Systems Theory*. Texts in Applied Mathematics. Springer, 1995.

[20] R. Daley. *Atmospheric Data Analysis*. Cambridge University Press, 1993.

[21] J. Deyst and C. Price. Conditions for asymptotic stability of the discrete minimum-variance linear estimator. *IEEE Transactions on Automatic Control*, 13(6):702–705, 1968.

[22] R.G. Douglas. *Banach Algebra Techniques in Operator Theory*. Graduate Texts in Mathematics. Springer, 1998.

[23] E.T. Eady. Long waves and cyclone waves. *Tellus*, 1:33–52, 1949.

[24] H.W. Engl, M. Hanke, and A. Neubauer. *Regularization of Inverse Problems*. Mathematics and its Applications. Kluwer Academic Publishers, 2000.

[25] M.J. Fabian. *Functional Analysis and Infinite-Dimensional Geometry*. CMS Books in Mathematics. Springer, 2001.

[26] M. Freitag and R.W.E. Potthast. Synergy of inverse problems and data assimilation techniques. In Press, 2013.

[27] S. Ghorpade and B.V. Limaye. *A Course in Calculus and Real Analysis*. Number 10 in Undergraduate Texts in Mathematics. Springer, 2006.

[28] G.H. Golub and C.H. Van Loan. *Matrix Computations*. The John Hopkins University Press, third edition, 1996.

[29] D.H. Griffel. *Applied Functional Analysis*. Dover Books on Mathematics Series. Dover, 2002.

[30] S.A. Haben. *Conditioning and Preconditioning of the Minimisation Problem in Variational Data Assimilation*. PhD thesis, Department of Mathematics and Statistics, University of Reading, 2011.

[31] J. Hadamard. *Lectures on Cauchy's Problem in Linear Partial Differential Equations*. Dover Phoenix Editions. Dover Publications, 2003.

[32] W.W. Hager and L.L. Horowitz. Convergence and stability properties of the discrete riccati operator equation and the associated optimal control and filtering problems. *SIAM Journal on Control and Optimization*, 14:295, 1976.

[33] A. Hannachi and K. Haines. Convergence of data assimilation by periodic updating in simple Hamiltonian and dissipative systems. *Tellus A*, 50(1):58–75, 1998.

[34] C. Heij, A.C.M. Ran, and F. Schagen. *Introduction to Mathematical Systems Theory: Linear Systems, Identification and Control*. Birkhäuser, 2007.

[35] A.H. Jazwinski. *Stochastic Processes and Filtering Theory*. Academic Press, 1970.

[36] C. Johnson. *Information Content of Observations in Variational Data Assimilation*. PhD thesis, Department of Meteorology, University of Reading, 2003.

[37] C. Johnson, B.J. Hoskins, and N.K. Nichols. A singular vector perspective of 4d-var: Filtering and interpolation. *Quarterly Journal of the Royal Meteorological Society*, 131:1–19, 2005.

[38] T. Kailath, A.H. Sayed, and B. Hassibi. *Linear Estimation*. Prentice-Hall Information and System Sciences Series. Prentice Hall, 2000.

[39] R.E. Kalman. Contributions to the theory of optimal control. *Boletinde la Sociedad Matematica Mexicana*, 5:102–119, 1960.

[40] R.E. Kalman and R.S. Bucy. New results in linear filtering and prediction theory. *Journal of Basic Engineering (ASME)*, 83D:95–108, 1961.

[41] M.H. Kalos and P.A. Whitlock. *Monte Carlo Methods*. Wiley, 2009.

[42] A. Kirsch. *An Introduction to the Mathematical Theory of Inverse Problems*. Applied Mathematical Sciences. Springer, 2011.

[43] P.E. Kloeden and E. Platen. *Numerical Solution of Stochastic Differential Equations*. Applications of Mathematics. Springer, 1999.

[44] S.R. Kou, D.L. Elliott, and T.J. Tarn. Exponential observers for nonlinear dynamic systems. *Information and Control*, 29(3):204–216, 1975.

[45] R. Kress. *Numerical Analysis*. Graduate Texts in Mathematics. Springer, 1998.

[46] R. Kress. *Linear Integral Equations*. Springer, 1999.

[47] J.M. Lewis, S. Lakshmivarahan, and S. Dhall. *Dynamic Data Assimilation: A Least Squares Approach*. Cambridge University Press, 2006.

[48] J.L. Lions. *Optimal Control of Systems Governed by Partial Differential Equations*. Springer, 1971.

[49] K.N. Liou. *An Introduction to Atmospheric Radiation*. International Geophysics Series. Academic Press, 2002.

[50] A.C. Lorenc. Analysis methods for numerical weather prediction. *Quarterly Journal of the Royal Meteorological Society*, 112(474):1177–1194, 1986.

[51] A.C. Lorenc, S.P. Ballard, R.S. Bell, N.B. Ingleby, P.L.F. Andrews, D.M. Barker, J.R. Bray, A.M. Clayton, T. Dalby, D. Li, et al. The Met. Office global three-dimensional variational data assimilation scheme. *Quarterly Journal of the Royal Meteorological Society*, 126(570):2991–3012, 2000.

[52] E.N. Lorenz. Deterministic nonperiodic flow. *Journal of the Atmospheric Sciences*, 20(2):130–141, 1963.

[53] E.N. Lorenz. *The Essence of Chaos*. University of Washington Press, 1993.

[54] D.G. Luenberger. Observing the state of a linear system. *IEEE Transactions on Military Electronics*, 8(2):74 –80, 1964.

[55] D.G. Luenberger. Observers for multivariable systems. *IEEE Transactions on Automatic Control*, 11(2):190 – 197, 1966.

[56] B.A. Marx. *Dynamic Magnetic Tomography*. PhD thesis, Mathematisches Institut, Georg-August Universität Göttingen, 2011.

[57] B.A. Marx and R.W.E. Potthast. On instabilities in data assimilation algorithms. *GEM-International Journal on Geomathematics*, 3:253–278, 2012.

[58] R.B. Messaoud, Z. Nadia, and K. Mekki. Local state observers for nonlinear systems. In *2011 International Conference on Communications, Computing and Control Applications (CCCA)*, pages 1–5. IEEE, 2011.

[59] T. Miyoshi. The Gaussian approach to adaptive covariance inflation and its implementation with the local ensemble transform Kalman filter. *Monthly Weather Review*, 139(5):1519–1535, 2011.

[60] A.J.F. Moodey, A.S. Lawless, R.W.E. Potthast, and P.J. van Leeuwen. Nonlinear error dynamics for cycled data assimilation methods. *Inverse Problems*, 29(2):025002, 2013.

[61] J.B. Moore and B.D.O. Anderson. Coping with singular transition matrices in estimation and control stability theory. *International Journal of Control*, 31(3):571–586, 1980.

[62] K.W. Morton and D.F. Mayers. *Numerical Solution of Partial Differential Equations: An Introduction*. Numerical Solution of Partial Differential Equations: An Introduction. Cambridge University Press, 2005.

[63] A.H. Nayfeh and B. Balachandran. *Applied Nonlinear Dynamics: Analytical, Computational, and Experimental Methods*. Wiley-VCH Verlag GmbH, 2007.

[64] J. O'Reilly. *Observers for Linear Systems*. Mathematics in Science and Engineering. Academic Press, 1983.

[65] V. N. Phat. *Constrained Control Problems Of Discrete Processes*. Series on Advances in Mathematics for Applied Sciences. World Scientific Publishing Company, 1996.

[66] S. Ponnusamy. *Foundations of Mathematical Analysis*. Birkhäuser Boston, 2011.

[67] R.W.E. Potthast, A.J.F. Moodey, A.S. Lawless, and P.J. van Leeuwen. On error dynamics and instability in data assimilation. In Press, 2012. Preprint available: MPS-2012-05 http://www.reading.ac.uk/maths-and-stats/research/maths-preprints.aspx.

[68] F. Rabier, H. Järvinen, E. Klinker, J.F. Mahfouf, and A. Simmons. The ECMWF operational implementation of four-dimensional variational assimilation. i: Experimental results with simplified physics. *Quarterly Journal of the Royal Meteorological Society*, 126(564):1143–1170, 2000.

[69] F. Rawlins, S.P. Ballard, K.J. Bovis, A.M. Clayton, D. Li, G.W. Inverarity, A.C. Lorenc, and T.J. Payne. The Met. Office global four-dimensional variational data assimilation scheme. *Quarterly Journal of the Royal Meteorological Society*, 133(623):347–362, 2007.

[70] J.D. Riley. Solving systems of linear equations with a positive definite, symmetric, but possibly ill-conditioned matrix. *Mathematical Tables and Other Aids to Computation*, 9(51):96–101, 1955.

[71] C.D. Rodgers. *Inverse Methods for Atmospheric Sounding: Theory and Practice*. Series on Atmospheric, Oceanic and Planetary Physics. World Scientific, 2000.

[72] W.J. Rugh. *Linear System Theory*. Prentice-Hall Information and System Sciences Series. Prentice Hall, 1996.

[73] B.P. Rynne and M.A. Youngson. *Linear Functional Analysis*. Springer Undergraduate Mathematics Series. Springer, 2007.

[74] M.K. Schneider and A.S. Willsky. A Lyapunov method for establishing strong and weak stability of infinite-dimensional Kalman filters for space-time estimation. 2007. Preprint available: http://ssg.mit.edu/group/alumni/mikesch/lyapunov.pdf.

[75] Y. Shen, Y. Huang, and J. Gu. Global finite-time observers for Lipschitz nonlinear systems. *Automatic Control, IEEE Transactions on*, 56(2):418–424, 2011.

[76] H.N. Shirer. *Nonlinear Hydrodynamic Modeling: A Mathematical Introduction*. Lecture Notes in Physics. Springer-Verlag, 1987.

[77] Y. Song and J.W. Grizzle. The extended Kalman filter as a local asymptotic observer for discrete-time nonlinear systems. *Journal of Mathematical Systems, Estimation and Control*, 5(1):59–78, 1995.

[78] C. Sparrow. *The Lorenz Equations: Bifurcations, Chaos, and Strange Attractors*. Applied Mathematical Sciences. Springer-Verlag, 1982.

[79] A.M. Stuart. Inverse problems: a Bayesian perspective. *Acta Numerica*, 19:451–559, 2010.

[80] A.M. Stuart and A.R. Humphries. *Dynamical Systems and Numerical Analysis*. Cambridge Monographs on Applied and Computational Mathematics. Cambridge University Press, 1998.

[81] O. Talagrand. On the mathematics of data assimilation. *Tellus*, 33(4):321–339, 1981.

[82] T.J. Tarn and Y. Rasis. Observers for nonlinear stochastic systems. *IEEE Transactions on Automatic Control*, 21(4):441–448, 1976.

[83] P.J. van Leeuwen. Particle filtering in geophysical systems. *Monthly Weather Review*, 137(12):4089–4114, 2009.

[84] P.J. van Leeuwen. Nonlinear data assimilation in geosciences: an extremely efficient particle filter. *Quarterly Journal of the Royal Meteorological Society*, 136(653):1991–1999, 2010.

[85] M.T. Vaughn. *Introduction to Mathematical Physics*. Wiley-VCH, 2008.